Characterization of the avian designer cells AGE1.CR and AGE1.CR.pIX considering growth, metabolism and production of influenza virus and Modified Vaccinia Virus Ankara (MVA)

Dissertation

zur Erlangung des akademischen Grades

Doktoringenieurin
(Dr.-Ing.)

von Dipl.-Biotechnol. Verena Lohr
geb. am 06.12.1983 in Gifhorn

genehmigt durch die Fakultät für Verfahrens- und Systemtechnik
der Otto-von-Guericke-Universität Magdeburg

Promotionskommission: Prof. Dr.-Ing. Andreas Seidel-Morgenstern (Vorsitz)
Prof. Dr.-Ing. Udo Reichl (Gutachter)
Dr. rer. nat. Ingo Jordan (Gutachter)
Prof. Dr.-Ing. Ralf Pörtner (Gutachter)

eingereicht am: 27.06.2014

Promotionskolloquium am: 25.11.2014

Kurzfassung

Für die Produktion von rekombinanten Proteinen wie Wachstumsfaktoren, Hormonen und therapeutischen Antikörpern ist die Zellkultivierung eine etablierte Technologie. In der Herstellung von Virusimpfstoffen werden embryonierte Hühnereier, primäre Hühnerembryofibroblasten, diploide Zellen (z.B. MRC-5 Zellen) und adhärent oder in Suspension wachsende immortalisierte Zelllinien, z.B. Vero, MDCK oder BHK-21 Zellen, verwendet. Neue Suspensionszelllinien, die in chemisch-definierten Medien proliferieren (und damit serumfrei wachsen), wurden in den letzten Jahren entwickelt.

Zwei sogenannte Designerzelllinien, AGE1.CR und AGE1.CR.pIX, entwickelt von ProBiogen AG, wurden in Hinblick auf eine Verwendung zur Produktion des modifizierten Vaccinia Ankara Virus (MVA) als Impfstamm oder viralem Vektor entwickelt. Ursprung dieser Zellen war embryotisches Material der Moschusente (*Caririna moschata*). Immortalisierung wurde durch das Einbringen der adenoviralen Gene E1A und E1B erreicht. Die AGE1.CR.pIX Zelllinie exprimiert zudem das adeonvirale Gen pIX. Um robuste Prozesse zu etablieren und schließlich die Zulassung als Zellsubstrat für die Herstellung humaner Impfstoffe zu erlangen, ist eine umfassende Charakterisierung dieser neuen Zelllinien nötig. In der vorliegenden Arbeit wurde das Wachstumsverhalten und der Stoffwechsel von AGE1.CR und AGE1.CR.pIX Zellen untersucht. Zudem wurde die Eignung dieser Zellen für die Produktion von MVA und Influenzaviren evaluiert.

Bei der Batch-Kultivierung beider Zelllinien im Labormaßstab (bis 1 L Bioreaktoren, Rührkessel und Wave) wurden Zellkonzentrationen von bis zu $1x10^7$ Zellen/mL erreicht. Aus den erhaltenen Wachstumskurven wurden spezifische Wachstumsraten und Aufnahme- bzw. Produktionsraten der Hauptmetabolite (z.B. Glucose, Glutamin, Lactat) und Aminosäuren berechnet. Diese wurden in einer Stoffflussanalyse verwendet, um eine intrazelluläre Flussverteilung in der exponentiellen Wachstumsphase der AGE1.CR.pIX Zellen zu erhalten. Es zeigte sich ein Überflussstoffwechsel von Glucose in Richtung Laktat und Alanin, der auch für andere immortalisierte Zellen wie MDCK oder CHO beschrieben ist. Allerdings zeigten Ergebnisse der Stoffflussanalyse und gemessene maximale Enzymaktivitäten, dass bei den AGE1.CR.pIX Zellen die Glutaminolyse als Energielieferant eine geringe Rolle spielt. Statt Glutamin wurden andere Aminosäuren (u.a. Leucin und Asparagin) verstoffwechselt, um den Zitronensäurezyklus „anzukurbeln“. Die in diesen Studien erlangten Kenntnisse zu Wachstum und Stoffwechsel waren Grundlage für die Entwicklung von kontinuierlichen und

Perfusionsprozessen zur Herstellung von Influenzaviren bzw. MVA bei hohen Zellkonzentrationen.
Infektionsparameter für MVA, Influenzavirus A/PR/8/34 (H1N1) und zwei kaltadaptierte Stämme (A/Singapore/1/57 (H1N1) und B/Vienna/1/1999/37) wurden zunächst in kleinem Maßstab (u.a. Schüttelkolben) optimiert. Mithilfe dieser Versuche konnten Prozesse für die Produktion von MVA und Influenzaviren etabliert werden. Diese wurden anschließend auf 1 L Rührkessel- und Wave-Reaktoren skaliert. Mit den gewählten Parametern konnten MVA-Titer von 10^7–10^8 Viren/mL und Influenzavirustiter von 10^6–10^9 Viren/mL (je nach Virusstamm) erreicht werden. Diese Titer sind vergleichbar mit Ausbeuten aus etablierten Prozessen bei denen embryonierte Hühnereier, Hühnerembryofibroblasten oder MDCK Zellen verwendet werden. Mit AGE1.CR Zellen konnten höhere Influenzavirustiter erreicht werden als mit AGE1.CR.pIX Zellen. Dagegen wurden deutlich höhere MVA-Titer mit AGE1.CR.pIX Zellen erzielt. Es wurde zudem untersucht, ob über einer bestimmten kritischen Zellkonzentration zum Zeitpunkt der Infektion ein durch sinkende zellspezifische Ausbeuten darstellender Zelldichteeffekt auftritt. Für MVA und die kaltadaptierte Influenzaviren wurden kritische maximale Zellkonzentrationen von 4–5x10^6 Zellen/mL identifiziert. Zur Aufklärung dieses Zelldichteeffektes, wurden (mit Focus auf den MVA-Prozess) durchflusszytometrische Methoden zur Bestimmung der Zellzyklusverteilung und des apoptotischen Status der Zellpopulation entwickelt. Es konnten keine deutlichen Veränderungen in der Zellphysiologie (veränderte Zellzyklusverteilung der Zellpopulation oder deutlich erhöhte Anteil apoptosicher Zellen) bei höheren Zellkonzentrationen zum Zeitpunkt der Infektion beobachtet werden, die verminderte Ausbeuten erklären könnten. Akkumulierende Stoffwechselprodukte oder verbrauchte Medienbestandteile scheinen daher die wahrscheinlichste Ursache für den Rückgang der zellspezifischen Ausbeute zu sein. In zukünftigen Studien sollte ermittelt werden, ob Perfusions- oder Fed-Batch-Strategien den Zelldichteeffekt vermindern könnten.

In dieser Arbeit wurden Prozesse entwickelt, mit denen hohe Titer von MVA und Influenzaviren erreicht wurden. Die Eignung der Zelllinien AGE1.CR und AGE1.CR.pIX für die Produktion dieser Viren wurde damit gezeigt. Generell können die durchgeführten Arbeiten zu Wachstum, Stoffwechsel und Virusproduktion als Basis für Folgestudien und Projekte zur Zulassung dieser Zelllinien für die Produktion von Veterinär- und Humanimpfstoffen dienen.

Abstract

Cell culture technology is an established technology for production of therapeutic antibodies. For manufacturing of human viral vaccines, embryonated chicken eggs, primary chicken embryo fibroblasts, diploid cells (e.g. MRC-5 cells) or immortalized cell lines such as MDCK, Vero or BHK-21 (growing adherently or in suspension) are used. New host cell lines growing in suspension and in chemically-defined media (that means also serum-free) have been designed over the last years.

Two such new candidate cell substrates are the avian designer cell lines AGE1.CR and AGE1.CR.pIX. They have been designed by ProBioGen AG for production of Modified Vaccinia Virus Ankara (MVA) as a vaccine or as a viral vector. They originate from embryonic cell material of the Muscovy duck (*Cairina moschata*) and have been immortalized by stable insertion of adenoviral E1A and E1B genes. The AGE1.CR.pIX cell line in addition expresses the adenoviral protein pIX. For process optimization and approval, such new cell lines and their characteristics have to be thoroughly evaluated so that robust processes can be set up and the cell lines might be approved for vaccine manufacturing. In this work, growth characteristics and metabolism of AGE1.CR and AGE1.CR.pIX cells were studied. Furthermore, their suitability to propagate MVA as well as influenza virus was evaluated.

Both cell lines were found to proliferate to up to $1x10^7$ cells/mL in small-scale systems (e.g. shaker flasks) as well as 1 L lab-scale bioreactors (stirred-tank and Wave). Specific growth rates and exchange rates of main metabolites (for example glucose, glutamine and lactate) and amino acids were calculated from batch cultivations. Those rates were used for metabolic flux analysis to derive a flux distribution of AGE1.CR.pIX cells in the exponential growth phase. An overflow metabolism from glucose towards lactate and alanine was observed as reported for other immortalized cell lines such as MDCK and CHO. Flux analysis and measurement of maximum enzyme activities, however, showed that glutaminolysis plays only a minor role in energy metabolism of AGE1.CR.pIX cells. Instead of glutamine, rather other amino acids (e.g. leucine and asparagine) were catabolized to feed the TCA cycle. Generated data and knowledge in this work considering growth and metabolism of the avian designer cells could be used in follow-up studies where a continuous and perfusion process were developed for production of MVA and influenza viruses at high cell concentrations.

In scouting infection experiments with Modified Vaccinia Virus Ankara, the influenza virus strain A/PR/8/34 (H1N1), and two cold-adapted influenza virus strains

(A/Singapore/1/57 (H1N1) and B/Vienna/1/1999/37), infection parameters were optimized. For MVA and influenza virus, production processes were established and scaled to 1 L Wave and stirred-tank bioreactor. With the chosen process parameters, MVA titers of $1x10^7$–$1x10^8$ viruses/mL and influenza virus titers of 10^6–10^9 viruses/mL (depending on virus strain) were achieved. These are competitive titers in comparison to established production systems like embryonated chicken eggs, chicken embryo fibroblast cultures or MDCK cells. AGE1.CR cells supported higher influenza virus titers compared to AGE1.CR.pIX cells, whereas AGE1.CR.pIX cell supported higher MVA titers. In addition, it was evaluated whether virus yields decrease when using high cell concentrations at time of infection (the so-called cell-density effect) and if this might correlate with cell physiology changes. For MVA as well as cold-adapted influenza virus strains, critical cell concentrations at which cells can be infected without yield losses were found to be 4–$5x10^6$ cells/mL. To examine the reasons for the cell density effect (focusing on the MVA process), flow cytometric assays were established to follow the cell cycle distribution and apoptotic status of the cell population before and after infection. Considerable changes in cell physiology (altered cell cycle distribution of the cell population or a clearly increased percentage of apoptotic cells) that might explain decreasing virus yields could not be found in infection experiments using high cell concentrations. Accumulated or depleted medium components thus seem to be the most likely reason for the cell-density effect. Further studies should evaluate whether perfusion or fed-batch strategies might overcome or weaken this effect.

In summary, in this work production processes for MVA and influenza virus propagation were established that yield high titers. The suitability of AGE1.CR and AGE1.CR.pIX cells for production of those viruses was therewith shown. Generally, the characterization of growth, metabolism and virus production done in this work can be a basis for further studies and projects towards approval of these cell lines for human or veterinary vaccine manufacturing.

Danksagung

Herrn Prof. Dr.-Ing. Udo Reichl danke ich fur die Möglichkeit, die vorliegende Arbeit in seiner Arbeitsgruppe anzufertigen, für die guten Forschungsbedingungen, die Diskussion der Ergebnisse und für die Möglichkeit, während der Promotion eine Zeit als Gastwissenschaftler in Montréal arbeiten zu dürfen. Vor allem die Möglichkeit, an Konferenzen teilzunehmen habe ich sehr genossen.

Dr. rer. nat. Ingo Jordan und Prof. Dr.-Ing. Ralf Pörtner danke ich dafür, dass sie trotz vieler anderer Verpflichtungen die Gutachterfunktion übernommen haben.

Frau PD Dr. rer. nat. Yvonne Genzel danke ich fur die Betreuung der Arbeit, ihre Diskussionsbereitschaft, ihre Unterstützung dabei mich weiterzuentwickeln und Chancen zu ergreifen und für ihre Motivationsfähigkeit.

Bei Dr. Steffen Klamt und vor allem Oliver Hädicke möchte ich mich für eine produktives Kooperationsprojekt und viele Diskussionen bedanken.

Ebenfalls möchte ich Ingo Jordan, Volker Sandig, Amine Kamen und Timo Frensing danken, die die Arbeit oder Teile der Arbeit möglich gemacht, mit verfolgt, mit betreut und mit diskutiert haben.

Besonders danken möchte ich Anne-Kareen Blechert, Daniel Vazquez, Suzana Djeljadini und Stefan Mahr danken, die durch ihre Bachelor- und Masterarbeiten unter großem Einsatz wesentliche Teile der vorliegenden Arbeit mitentwickelt und generiert haben.

Für die Gesellschaft in langen Enzym-Nächten, jede Menge Hilfe und Unterstützung, aber auch Ablenkung während und nach der Doktorarbeit möchte ich Anne-Kareen Blechert ausdrücklich danken.

Einen ausdrücklichen Dank verdient auch Annegret Frauendienst, die viele Hürden kleiner und weniger aufwendig gemacht hat und immer ein offenes Ohr bei Schwierigkeiten hatte.

Auserdem möchte ich mich bei den TAs der Gruppe Bioprozesstechnik, Claudia Best, Nancy Wynserski, Ilona Behrendt, Susanne König, Corina Siewert, Carmen Ziemann und Felicitas Hasewinkel bedanken, die immer eine oder mehrere helfende Hände frei hatten und eine große Unterstützung waren.

Ebenfalls danke an die Kollegen in Berlin, die bis zur Verteidigung der Arbeit mit mir gefiebert haben.

Ein sehr herzliches Dankeschön gilt den Doktoranden, die mit im gleichen Promotionsboot saßen. Vor allem Alexander Rath, Susann Freund, Matthias Meininger, Stefan Heldt, Markus Rehberg, Britta Isken, Andreas Bock, Christian Riedele, Josef Schulze-Horsel, Joachim Ritter, Regina Samaga und Diana Vester. Danke für die fachlichen Diskussionen, den (schwarzen) Humor und die vielen gemeinsamen Unternehmungen. Mit Euch zusammen habe ich die Promotionszeit in Magdeburg sehr genossen!

Ein besonders großer Dank gilt meinen Eltern, meiner Schwester und meinem Bruder plus Familien, die mich in allem jederzeit unterstützt, mich oft aufgefangen und vor allem immer motiviert haben.

Content

Symbols

Symbol	Meaning	Unit
α	significance level	-
c	concentration of a metabolite	µM or mM
μ	maximum specific growth rate, determined during exponential growth phase of cells	1/h or h^{-1}
CCI	cell concentration at time of infection	cells/mL
C_{RBC}	red blood cell concentration (used in hemagglutination assay)	cells/mL
C_{TP}	total virus particle concentration (by hemagglutination assay)	virus particles/mL
$C_{Trypsin}$	trypsin activity that shall be used	U/cell
$C_{Trypsinstock}$	trypsin activity of stock solution	U/mL
$C_{V,max}$	maximum virus titer	viruses/mL
$C_{VP,max}$	maximum virus particle concentration	virus particles/mL
DO	dissolved oxygen	%
gDW	gram dry weight, biomass	gDW
hpi	hours post infection	h
moi	multiplicity of infection	viruses/cell
ν	uptake or release rate (metabolites)	µmol/gDW/h
n	number, e.g. number of experiments or number of chromosomal sets	-
rpm	rounds per minute or rocks per minute	-
t, t_0	time, start time point	h
$TCID_{50(SV)}$	seed virus titer	viruses/mL
toi	time of infection	h
V_c	culture volume	L, mL, µL
V_{SV}	seed virus volume	L, mL, µL
X, X_V	biomass, viable cell concentration	cells/mL or gDW
Y_{CSP}	cell-specific virus particle yield (determined by hemagglutination assay)	virus particles/cell
Y_{CSV}	cell-specific virus yield	viruses/cell
$Y_{Lac/Glc}$, $Y_{Amm/Gln}$	yield coefficients product/substrate	-
$Y_{Xv/Glc}$, $Y_{Xv/Gln}$	yield coefficients viable cells/substrate	-

Abbreviations

Abbreviation	Meaning	Abbreviation	Meaning
7-AAD	7-aminoactinomycin D	F6P	fructose 6-phosphate
AcCoA	acetyl-coenzyme A	FAD/$FADH_2$	flavin adenine dinucleotide
AEM	Adenovirus Expression Medium	FBP	fructose 1,6-bisphosphate
αKG	α-ketoglutarate	FDA	Food and Drug Administration
Ala	alanine	Fum	fumarate
Amm	ammonium	G2M	gap II or mitosis phase in cell cycle
apo	apoptotic fraction of a cell population	G0G1	quiescent (G0) or gap I phase in cell cycle
Arg	arginine	G6P	glucose 6-phosphate
Asn	asparagine	GAP	glyceraldehyde 3-phosphate
Asp	aspartate	GC	gas chromatography
ATP	adenosine-triphosphate	GDH	glutamate dehydrogenase
BCA	bicinchoninic acid	gDW	gram dry weight (specific cell dry weight in [pg])
BHK-21	baby hamster kidney cell line	Glc	glucose
ca	cold-adapted	Gln	glutamine
CD-U2	chemically-defined proliferation medium	GLNase	glutaminase
CD-VP4	chemically-defined virus production medium	Glu	glutamate
CEF	chicken embryo fibroblasts	Gly	glycin
CEV	cell-associated enveloped virus (MVA)	GS	glutamine synthetase
CHO	Chinese hamster ovary cell line	HA/HAU	heamagglutination/ hemagglutination units
Cit	citrate	HEK293	human embryonic kidney cell line
CR	duck cell line (full name: AGE1.CR)	HeLa	human cancer cell line
CR.pIX	duck cell line modified with adenoviral pIX protein (full name: AGE1.CR.pIX)	His	histidine
Cys	cysteine	HIV	Human Immunodeficiency Virus
DHAP	dihydroxyacetone phosphate	HPLC	high-performance liquid chromatography
DNA	deoxyribonucleic acid	ICH	International Conferences on Harmonization of Technical Requirements for Registration of Pharmaceuticals for Human use
EEV	extracellular enveloped virus (MVA)	IEV	intracellular enveloped virus (MVA)
EGFP	enhanced green fluorescent protein	Ile	isoleucine
EMA	European Medicines Agency	Lac	lactate

Abbreviation	Meaning	Abbreviation	Meaning
LAIV	live-attenuated influenza virus	PS	phosphatidylserine
Mal	malate	Pyr	pyruvate
MDCK	Madine Darby Canine Kidney cells	r	reaction
Met	methionine	R5P	ribose-5-phosphate
MVA	Modified Vaccinia Virus Ankara	RNA	ribonucleic acid
MVAegfp	MVA containing egfp insert	S	synthesis phase in cell cycle
MVAmcherry	MVA containing mcherry insert	Ser	serine
MVAwt	MVA wildtype	SOP	standard operating procedure
NAD/NADH	Nicotinamide adenine dinucleotide	STR	stirred-tank reactor
OAA	oxaloacetic acid	subG0G1	fraction of cells containing less than one genome
oxPhos	oxidative phosphorylation	SuccCoA	succinyl-coenzyme A
PC	pyruvate carboxylase	TCA	tricarboxylic acid cycle
PDH	pyruvate dehydrogenase	$TCID_{50}$	tissue culture infectious dose 50
PE	phycoerythrine	Thr	threonine
PEP	phosphoenolpyruvic acid	Trp	tryptophan
PFA	paraformaldehyde	Tyr	tyrosine
PG	phosphoglyceric acid	Val	valine
Phe	phenylalanine	WHO	World Health Organization
PI	propidiumiodide	wt	wildtype
Pro	proline		

List of Figures

List of Tables

1 Motivation

Vaccines had and have a tremendously positive impact on public health. The history of vaccines began at the end of the 18th century with vaccination against smallpox. Since then, vaccines against many viral and bacterial infectious diseases have been developed. Today, vaccines are an inherent part of public health care, and indispensable for early protection of children as wells as for protection when travelling to other geographical regions.

The evolution of vaccines is a perfect example of technological innovation, diversification and increasing safety demands [1]. In the beginning of vaccine usage, people empirically found that exposure with material of infected persons or animals can protect against infection. First vaccines (mostly harvested from lymph drain of animals) against diseases like cholera, smallpox and rabies were produced. After this first innovation leap in the late 19th century – vaccine availability itself – distribution and storage of vaccines was improved. Freeze-dry techniques led to stable vaccines that could be shipped to other countries and used for several weeks. This allowed worldwide vaccination campaigns against smallpox, tuberculosis and polio. The strive was successful and occurrence of several diseases were drastically diminished or even erased as smallpox [2]. The next step of technology improvement was taken to increase safety standards and thus reduce negative side effects of vaccination. This was of particular importance to persuade vaccinees – healthy people in contrast to patients with acute infections – to accept vaccines. The development of live-attenuated virus strains improved safety, e.g. for smallpox or influenza virus vaccines [3, 4]. In parallel, production techniques were improved towards more defined systems, i.e. from animals or organs to tissues, primary cells or even diploid and immortalized cell lines. Together with improved purification processes, purity standards were drastically increased. Also, innovations and improvements in cell culture technology and process technology were made. With this, today it is possible to culture a vast quantity of cells in one reactor [5].

The amount of available vaccines increases steadily and various products are in the pipeline for testing or approval. Moreover, new vaccine types evolve steadily. Molecular technology as well as advances in immunology fueled the development of new vaccine types (e.g. recombinant or DNA vaccines, virus-like particles), more effective formulation or new routes of delivery [6]. Viral vectors today play a huge role in research and development for new vaccines, e.g. against Human Immunodeficiency Virus (HIV) whose worldwide spread is still not under control [7, 8]. Thereby, two viral systems are most promising (reflected by the amount of publications and clinical trials that are conducted) – adenovirus and Modified Vaccinia Virus Ankara (MVA), a live-attenuated vaccinia virus. Both are able to transfer

genetic material efficiently to the host and thus lead to expression of antigens by the host cell. This triggers the immune system so that a protective effect is developed. One classical vaccine that still plays an important role protects against influenza disease. The influenza virus is a highly adaptable virus causes seasonal epidemics with great impact on global health. Pandemics which might occur at every time might be devastating and thus, influenza virus vaccine development still strives to keep pace with virus evolution [9].

Besides all improvements and innovations, the full potential of technology that is currently available for vaccine production is by far not exploited and does not always fit the need of safer and more immunogenic vaccines. One issue is that using diploid or immortalized cell lines instead of using eggs or primary cell cultures for the production of vaccines only slowly becomes accepted. In contrast to the biggest branch of animal cell-based biopharmaceutical production, the production of therapeutic antibodies, where chinese hamster ovary (CHO) cells dominate the field, a variety of other cell lines are historically used for vaccine production. If not eggs or primary material were used, mainly four cell lines have been of importance so far: MDCK, Vero, WI-38 and MRC-5 cells [5, 10]. All those cell lines are well-characterized and approved for production of several vaccines, i.e. influenza virus, polio virus or rabies virus. However, their use comes with certain disadvantages, e.g. adherent cell growth limiting scalability. More established cell lines such as BHK-21 and HEK293 cells have already been used for veterinary vaccine production [11], but might be difficult to be approved for human vaccine manufacturing [12]. In the last ten years, several new cell substrates were developed that fulfill modern regulatory standards. As BHK-21 and HEK293 cells, they proliferate in suspension and thus offer an easier scalability. Also, most of them can be cultivated in chemically-defined media, containing neither animal sera nor unknown hydrolysates. Advantages that are presumably connected with this are higher consistency, improved process robustness, higher safety due to less impurities, and, probably most important in future, easier transfer to production facilities in other countries with less developed industrial infrastructure. From those new so-called designer cell lines, PER.C6 (human) [13], EB66 (duck) [14], CAP (human) [15], and AGE1.CR or AGE1.CR.pIX (duck), respectively [16], are most promising. All cell lines are currently evaluated for various applications and shown to be productive for influenza virus, MVA or adenoviral vectors and poliovirus [5, 17].

For market approval, a thorough characterization of the cell substrate as well as the produced virus is demanded. Testing the cell substrate upon contaminations, adventitious agents and its genetic stability needs to be done as well as demonstration of GMP compliant development and documentation [12]. Also, the production process itself must be known profoundly in order to avoid production losses, product inconsistencies or contaminations. Knowing cell-based parameters such as growth rate, metabolic behavior, cell physiology and

expectable yields thus usually can help to control and improve a process. In the last years, the two initiatives, Quality by Design (QbD) and Process Analytical Technology (PAT), further boosted the aim to control and monitor the process and product. For this, suitable methods for monitoring crucial parameters need to be chosen or have to be developed [6].

In this work, the AGE1.CR and AGE1.CR.pIX cell lines were evaluated as vaccine producer cells. They will be abbreviated throughout this work as CR and CR.pIX. Both cell lines are of avian origin, offering the opportunity to produce avian-susceptible viruses such as MVA that can be used as a viral vector. In addition, influenza virus (human as well as avian strains) can be produced with these cell lines [18, 19]. Both model viruses were used in this project.

One part of this evaluation aimed at characterization of cell growth and metabolism to record cell-specific parameters such as growth rate and growth behavior as well as to get more insights into the metabolism of the cells. This was thought to be helpful in process development as no other immortalized avian cell line has been used in such a biotechnological application before. Optimizing medium and cultivation parameters, however, is only possible if nutrient requirements and metabolic behavior of the cell lines is known. For this, growth curves, spent media analyses and metabolic flux analysis should be applied. Furthermore, analysis of generated data considering significance of observed findings should be addressed when analyzing parallel and repetition experiments. Metabolic studies were done as collaboration project together with the group for Analysis and Redesign of Biological Networks of Dr. Steffen Klamt at the MPI Magdeburg.

Suitability of CR and CR.pIX cells as an alternative to primary cell material like chicken embryo fibroblasts for MVA production should be evaluated. In order to maximize virus yields, optimization of infection parameters was required. In combination with this, infections at high cell concentrations were interesting to cultivate more producer cells. However, the cell density effect that has been described as productivity loss at high cell concentrations had to be kept in mind [20, 21]. Thus, we intended to monitor cell physiology, e.g. apoptosis. Using a recombinant MVA strain expressing the enhanced green fluorescent protein, EGFP, we also tried to follow the infection in the cultured cell population by flow cytometric analysis. In a further approach, cells should be tested as host cells for influenza virus production. A comparison of achievable titers to those obtained with commonly used cell substrates such as MDCK or Vero cells should show general applicability. Thereby, the common influenza virus strain A/PR/8/34 that has and is used as backbone for many seasonal inactivated influenza virus vaccine strains was used. Furthermore, we were interested in producing live-attenuated influenza virus strains that are on the rise for seasonal influenza vaccines [22]. Again, infection parameters should be examined and optimized aiming at maximal virus yields and better understanding of this new host cell line.

2 Background

To provide a basis for discussion, the relevant topics of this work will be addressed in the following four sub-sections. At the beginning, general information about vaccines and their production is given (chapter 2.1.1 and 2.1.2). In conjunction, cell-based vaccine production is introduced, including suitable cell lines that can be used (chapter 2.1.3). In more detail, the origin and development of the cell lines CR and CR.pIX is explained. Cell-based topics that were studied in this work are then addressed in chapter 2.1.4: cell metabolism and methods to characterize it as well as relevance and measurement of cell cycle and apoptotic status of cells. Further, MVA and influenza viruses, the two viruses that were studied in this work are introduced (chapter 2.2 and 2.3, respectively). This includes an explanation of their current production processes. Finally, parameters that can or need to be optimized or monitored when developing a new process are explained.

2.1 Vaccines and viral vaccine production

Major threat and cause for premature deaths are infectious diseases. Although difficult to count, 17 million deaths have been assigned to infectious diseases in 2003 [23]. With vaccines, one fortunately has an extraordinary effective measure for prevention at hand for some of these diseases. Vaccines save millions of lives every year and their success rates are remarkable. Cases of measles, polio, mumps, pertussis or diphteria have all been dramatically been reduced in countries where broadscale vaccination programs exist. And development of improved vaccines or vaccines against emerging diseases is ongoing with an enormous amount of money, effort and manpower. This work studies new cell lines for the production of viral vaccines. Thus, the history of vaccines and their production as well as vaccine types that are in use or under development, will be given as background information. Thereby, the focus is on human vaccines against viral diseases.

2.1.1 Vaccine history

Viruses, bacteria and parasites exist longer than mankind and have evolved to infect all kinds of living systems, i.e. plants, bacteria, fungi, all kinds of animals and therefore also humans. Most of them do not harm their hosts, but those that infect and sicken animals and humans have always threatened mankind.

Already in the 10th century, measles, smallpox, diphtheria, cholera and pertussis epidemics have been reported. First comprehensive and detailed descriptions date from the 16th and 17th century. At that time, the cause of these diseases and especially the existence of viruses was not known. The fight against them with the help of vaccines started with people who empirically found for smallpox that transmission of infectious material in small amounts to a non-infected person can prevent an infection. This principle quickly spread around the world. In 1777, the US army as a first institution established a mandatory so-called variolation or inoculation against smallpox. At the same time, Edward Jenner, an English physicist, started experiments with cows infected with the smallpox-related cowpox. From these studies, he learned that lymph drain from infected cows protected humans against smallpox infection upon exposure, but did not induce as severe adverse effects as when using smallpox material from infected persons. Finally, in 1796 he successfully vaccinated a boy, James Phipps, against smallpox with material isolated from calf lymph. His treatment is today honored as the first vaccination in history against smallpox. In parallel, huge scientific efforts were made in basic virology: 1757 Thomas Francis found for example that the measles are caused by an infectious agent which is smaller than one could observe by eye. When more infectious diseases were identified as such (e.g. rabies, diphtheria, rubella and cholera), scientific efforts to understand infectious diseases and their causative agents were increased. They resulted in several medical breakthroughs with the outcome of a couple of vaccines during the 19th century (chronically depicted in Figure 2.1). After World War II, three decades with important innovations started. In 1945, the first influenza virus vaccine developed by Jonas Salk and Thomas Francis was approved and vaccines against tuberculosis, polio, measles and rubella followed until 1971. With the availability of vaccines, international immunization programs against tuberculosis, polio and smallpox were planned and executed between 1947 and 1988. These programs dramatically reduced the occurrence and expansion of several diseases, but only smallpox could officially be declared as eradicated in 1980 [2]. Vaccines against more complex or less abundant diseases like Japanese encephalitis followed in the 80s and 90s [1, 24]. Also at that time, 1980, the first cell culture-based vaccine was approved – a rabies vaccine produced in human diploid MRC-5 cells.

Today, the vaccine market value accounts for approximately 25 billion US dollars and is estimated to increase to 100 billion US dollars in 2025. Although this makes up only 2–3% of the global pharmaceutical market, its success rate is higher than for other pharmaceuticals as it faces an above-average growth rate of 10–15% per year. In comparison, the pharmaceutical market growth is estimated to be 5–7% [25]. At the moment, human vaccines covering 25–30 diseases are on the market. Many of them are included in the

routine vaccination schedule for children and adults. Another 120 plus new products are in the pipeline.

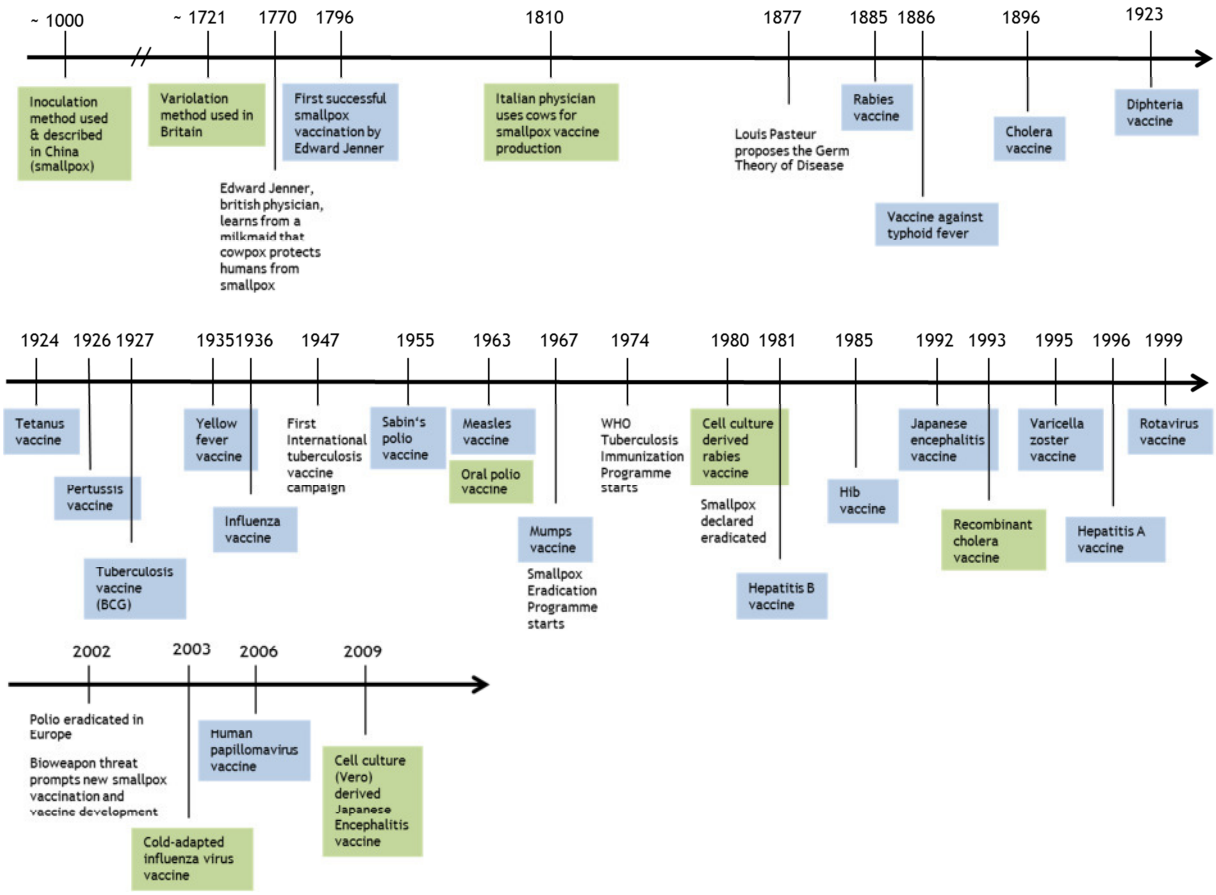

Figure 2.1: Chronology of milestones in human vaccine research, development and application. Blue colored boxes indicate development of new vaccines. Uncolored boxes show milestones in basic research or worldwide programmes against infectious diseases. Green boxes indicate milestones in vaccine process development, e.g. the first use of a cell culture-based vaccine. Figure based on [24].

In the late 20th century until now, three strategies have been followed in vaccine development and research: first is to produce better vaccines which means more efficient and more safe. Second is the enormous effort that is being made to develop vaccines against so-called emerging viruses and highly complex viral diseases (e.g. against the persisting HIV). Third, vaccines against diseases that are not induced by viruses or bacteria (cancer, diabetes) move into the focus of vaccine research. Generally, closing the so-called north-south gap – 80% of the world population lives in developing countries, but make up only 20% of the vaccine market – is one high priority goal. To achieve this, new vaccines, but above all, new processes are needed that enable on-site vaccine production.

2.1.2 Viral vaccine types

Vaccines vary in their characteristics. For example, whole virus particles can be used for the vaccine or only virus particle parts or antigens. Also, inactivated or live-attenuated vaccines can be distinguished. Thus, several vaccine types can be produced, fitting the particular application (Figure 2.2 illustrates some vaccine types focusing on the main content or priciniple of the vaccine, not regarding adjuvants and formulation buffers) [23].

Inactivated whole virus vaccines, generated by harvesting active whole virus particles and their subsequent chemical or physical inactivation, make up the largest part of available vaccines. The seasonal influenza vaccine, for example, is often produced in such a way. Other viruses are fragmented before vaccine formulation, yielding so-called subunit or split vaccines. Thereby, either the whole particle is broken down to parts or a fragmentation into surface proteins is done so that only immunoactive parts of the virus will be administered with the vaccine. One example of this vaccine type is the Hepatitis B virus vaccine that only contains the surface proteins of the Hepatitis B virus. Other inactive subunit vaccines are virus-like particles. For their production, virus proteins are expressed in a recombinant host. The expression of these proteins then induces a self-assembly of virus-like structures. Such vaccines (e.g. the Human Papilloma virus vaccine) thus contain viral proteins, but no viral genes.

Two related vaccine types are recombinant vaccines and vector vaccines. Both use genetically modified viruses, mainly modified by insertion of genes that serve as vaccine strain. The difference is the origin of the gene that has been inserted. Recombinant viruses mostly are viruses that are somehow genetically modified in order to improve immune response or production yields. Influenza vaccines, for example, usually contain genetically modified so-called reassortant virus strains. They contain antigens from the virus strain that is targeted by the vaccine and antigens from virus strains that have beneficial properties for production. On the other hand, viral vector vaccines are viruses that only serve as a carrier for foreign antigens. MVA is such a vector that can be used to introduce antigens from other pathogens, e.g. HIV, into host cells so that an immune response against HIV can be induced in the vaccinated person.

Recently, DNA vaccines have been developed. Such a vaccine does not contain a viral vector that delivers genes coding for antigens, but only contains the DNA itself. When transferred into human cells, expression of viral genes starts and viral proteins are produced. Some cells of the immune system will recognize the proteins and start defeating viral proteins and the cells expressing them. If later the person is infected by the respective pathogen, the immune system remembers the previous challenge and can efficiently attack the virus. So far, however, DNA vaccination is still in a developmental stage.

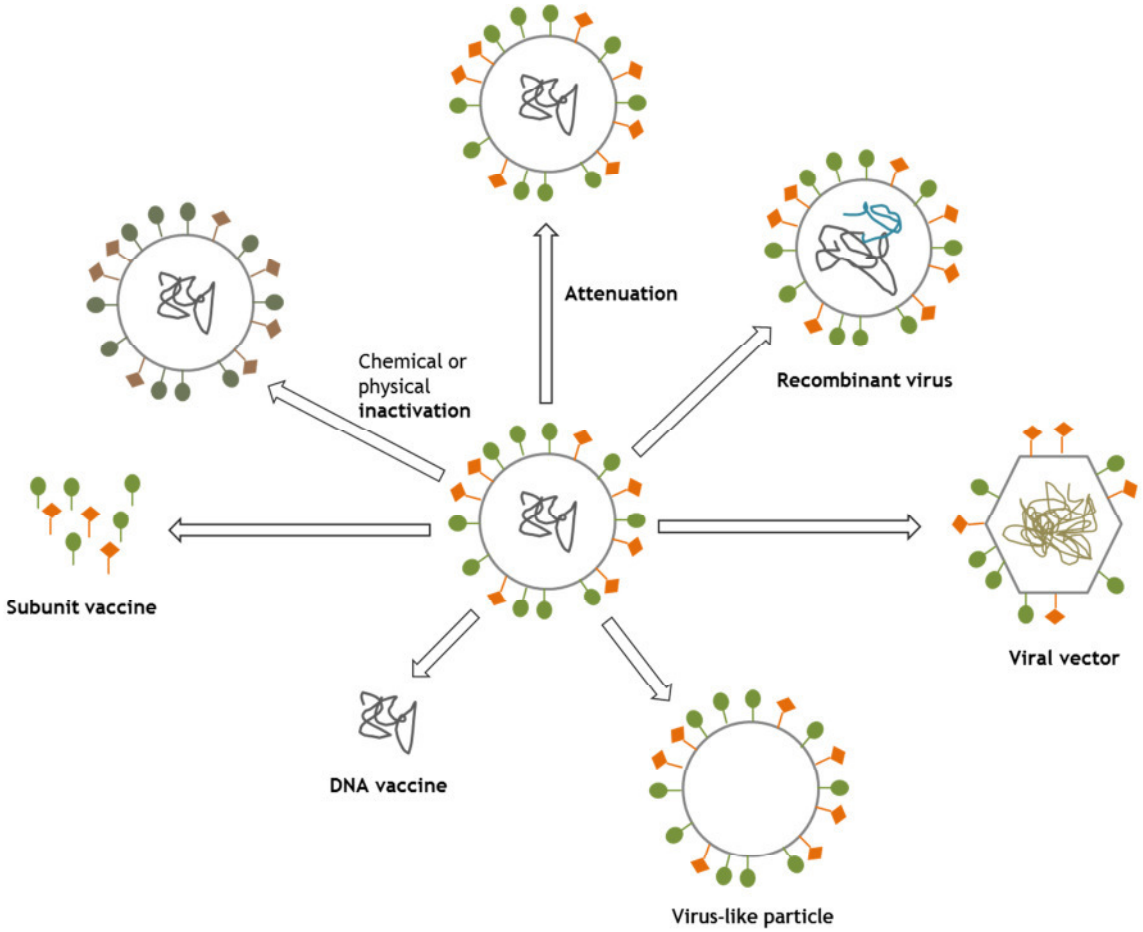

Figure 2.2: Common vaccine types. Based on a model virus, several vaccine types can possibly be developed. One distinguishes inactivated or live vaccines (mostly attenuated) and the way they have been produced. Whole virus particles are the most complex form (in a biological sense, not in a process sense). Less complex forms can be virus-like particles, subunit vaccines or DNA vaccines. Recombinant and viral vector vaccines both are genetically modified viruses that serve as a vaccine.

Live-attenuated vaccines are derived from wild type pathogens which were attenuated by genomic or physical selection, for example by adaptation to lower temperatures. Whole "living" viruses are then administered into the vaccinee where - due to their attenuation – they induce an immunogenic response, but no disease. Two examples of such live-attenuated vaccines will be topic of this work. One is MVA, which has an attenuated phenotype for mammalian species. Its attenuation is a result of several mutations that occurred during passaging in avian hosts over a long time [26, 27]. Other examples are the live-attenuated influenza virus strains that first have been developed in the 70s. Their attenuation was achieved by propagation over several passages at 25–33°C [28]. By this, genomic modifications occurred, leading to a loss of their ability to vividly spread at higher temperatures, i.e. body temperature [29]. Both viruses will be discussed in more detail in the respective introductory sections (2.2 for MVA, 2.3 for influenza).

Many vaccines are produced in eggs, tissues or primary cell cultures [11, 30]. Since 1980 when a cell culture-based rabies vaccine was developed and used, cell lines as production systems are on the rise. Immortalized cell lines (also termed transformed or continuous cell lines) bring the advantage of unlimited cell division. With this, the continuous supply with primary material is superfluous, being an ethical and a logistic advantage. The next section will introduce cell culture-based vaccine production and cell lines that have studied or used for this application. Thereby, the focus will be on cell lines suitable for vaccinia viruses or influenza virus production as these viruses have been used in this work. Regulatory aspects that are today important to consider in terms of approval for the production of human virus vaccines, are briefly addressed as well.

2.1.3 Cell culture-based virus vaccine production

This section shall introduce the cells and cell lines used or evaluated at the moment for MVA and influenza virus industrial production and the pros and cons for them. Afterwards, some aspects of cell culture processes are introduced. As a first aspect, cell growth and metabolism as well as methods to characterize metabolism are explained generally (section 2.1.3.1). Second, changes in cell physiology during cultivation and infection that might occur during virus infection are introduced (section 2.1.3.2 and 2.1.3.3).

2.1.3.1 Cells and cell lines for production of MVA and influenza virus vaccines

The manufacturing capacity for viral vaccines produced in embryonated hen's eggs and conventional primary cultures such as CEF, is limited [31]. This constraint may be overcome by using other existing cell substrates such as Madin Darby Canine Kidney (MDCK), Vero cells, BHK-21 cells or, as an alternative, introduce new cell substrates of human or avian origin. Some cell lines relevant for production of MVA or influenza virus vaccines with their advantageous and disadvantageous characteristics (see Table 2.1) are introduced in this section.

Approval of cell lines for human vaccine production, however, is difficult. Several institutions are involved in guidance and approval, amongst others the World Health Organization (WHO), the United States Food and Drug Administration (FDA), the European Medicines Agency (EMA) and the International Conferences on Harmonization of Technical Requirements for Registration of Pharmaceuticals for Human use (ICH). Guidelines are available, but there is no standardized classification or approval procedure [12, 32]. Thus, often case-to-case decisions are made based on cell line characteristics and vaccine demand.

Table 2.1: Cell lines that have been evaluated for production of MVA or influenza virus vaccines and are or could be approved for industrial manufacturing.

Name	Original organism/ tissue	Advantages/Disadvantages	Refe-rences
		Spontaneous transformation process	
BHK-21	Hamster/ kidney	+ Used since decades for veterinary rabies vaccine production; growth in suspension - Approval for human vaccines questionable	[33, 34]
MDCK	Dog/ kidney	+ Used since decades in vaccine research and production; adherent or suspension growth possible; 1st cell line that was approved for influenza vaccine production; gold-standard for influenza virus propagation - often only approved to be used for 20 passages	[5, 35, 36]
MDBK	Cow/ kidney	+ Often used in veterinary vaccine research and production - Approval for human vaccines questionable	[37, 38]
Vero	Monkey/ kidney	+ Used since decades for vaccine research and production (e.g. rabies and polio virus vaccine) - often only approved to be used for 20 passages, only adherently growing cultures productive	[5, 35, 39]
EB14	Chicken/ embryonic cells	+ avian origin, susceptible for influenza and MVA, growth in suspension - Retroviruses have been found	[40]
EB66	Duck/ embryonic cells	+ avian origin, susceptible for influenza and MVA, growth in suspension; in Japan currently in New Drug Application (NDA) Phase for influenza virus vaccine production - not much data available until now	[14, 41]
		Defined transformation process	
HEK293	Human/ kidney	+ well-known cell line, growth in suspension - human cell line – not first choice for human virus vaccine production; not susceptible for MVA	[42, 43]
PER.C6	Human/ neuro…	+ suspension growth; PER.C6-derived tuberculosis vaccine currently in clinical trial - human cell line - not first choice for human virus vaccine production; not susceptible for MVA	[13, 44]
CAP	Human/ neuro…	+ suspension growth, susceptible for various viruses - human cell line - for human vaccine production not first choice; not much data available until now; not susceptible for MVA	[15, 45]
CR CR.pIX	Duck/ embryonic cells	+ avian origin, susceptible for e.g. influenza and MVA, growth in suspension; CR.pIX-derived tuberculosis vaccine currently in clinical trial - not much data available until now	[18, 19, 46]

A continuous producer cell line suitable for modern MVA and influenza virus production should in any case be

- permissive for MVA and influenza virus, respectively
- acceptable in terms of regulatory issues (origin documented, fully characterized, stable, at best non-tumorigenic)

and optimally

- proliferates in suspension to simplify scalability
- proliferates and produces virus in a medium not containing any animal-derived components
- yields competitive virus titers (target values are $\geq 10^8$ $TCID_{50}$/mL for MVA, about 3 log HA units/100 µL for inactivated influenza virus vaccine, and approximately 10^7 $TCID_{50}$/mL for live-attenuated influenza virus)

Cell lines that have been shown to be able to either produce influenza virus or MVA will later be used as a reference to evaluate the suitability of CR and CR.pIX cells for vaccine production. As CR and CR.pIX cells, respectively, were exclusively used in this work, they will be introduced in more detail in the next section.

2.1.3.2 CR and CR.pIX cells

The CR and CR.pIX cell lines have been generated specifically for production of modern vaccines. Different aspects of these cell lines have been examined in this work – growth, metabolism and their suitability to produce MVA as well as influenza virus. Thus, although publications and a comprehensive review about their development have been published [16, 18], their history and specific characteristics will be introduced in this paragraph.
For the generation of CR and CR.pIX cells, respectively, explants from duck embryos were dissected and retinal cell material (presumably neuronal) was chosen to be the basis for cell line development. Embryonic, presumably neuronal, cells harvested from this material were transformed using adenoviral type 5 genes for immortalization. E1A and E1B genes were chosen therefore as their effects have been well-studied with HEK293 and, recently, also PER.C6 cells that both are immortalized using these genes as well [13, 47, 48]. The outcome of this manipulation was the CR cell line. One clone was further modified to improve its ability to produce MVA. Therefore, the capsid protein pIX from adenovirus type 5 was introduced into the cell genome [49]. Both cells (CR and the further modified CR.pIX) were subsequently adapted to growth in suspension and serum-free media. The final cell lines are named CR and CR.pIX. As potential cell substrates for vaccine production, all manipulations (including passaging) were performed in clean room areas and have been documented

following GMP guidelines. Several characteristics and safety testings were performed with the cell products.
In these tests

- no adventitious agents (avian, bovine or porcine viruses, mycoplasma or other bacteria) could be detected
- no cytopathic effects on various sentinel cell lines were observed
- no signs of infection or antibody responses were observed in different animals
- no endo- or exogeneous retroviral contamination was determined by measuring reverse transcriptase activity
- genetic stability for >90 passages was confirmed.

Early experiments also proved susceptibility towards MVA, and – later - MVA-based vaccine vectors and influenza virus [19, 50]. However, setting up production processes might require a more detailed understanding of the behavior of CR and CR.pIX cells. One aim therefore was to characterize proliferation and metabolism in more detail. After a brief introduction of cell cultivation methods, those cell-based aspects are addressed in the next chapters.

2.1.4 Cell cultivation and cell physiology

Several cultivation systems can be used for growth of suspension cells and have successfully been tested for industrial applications (for an overview see for example [51-53]). They differ in complexity and the degree they can control cultivation parameters and the cellular environment. For small-scale cultivations, usually uncontrolled systems are used. T-flasks or shaker flasks are placed in an incubator so that constant temperature and CO_2 supply are ensured. In these systems, the pH or the oxygen supply, can, however, not be controlled and thus the pH will drop during cultivation (mainly due to lactate that is produced by the cells and acidifies the medium). For long-term cultivations and to provide a more stable cellular environment, bioreactors are used. Here, various types and models are available with each having its advantages and disadvantages. Today, two systems are widely used: stirred tank reactors and wave agitated bioreactors (also called Wave bioreactor). Those rocked bioreactors are widely used since beginning of the trend towards single-use bioreactors in industrial manufacturing. However, disposable STR are today available from various suppliers as well. Both systems (STR and Wave bioreactor) have both been shown to be suitable for cultivation of cells, but especially differ in their way to aerate and agitate the cell suspension.

Besides the choice of different cultivation systems, the cultivation strategy also needs to be chosen for the respective application [51]. The easiest way is to perform a batch cultivation. Here, cells are inoculated in the bioreactor and after several days, cell cultivation is stopped and/or harvested. Using this strategy, cells usually run through several characteristic growth phases. After a lag phase following inoculation, cells start dividing and thus, an exponential increase in cell concentration can be observed. If nutrients are spent and in parallel, toxic waste products accumulate, some cells stop dividing so that altogether, the cell concentration only increases slowly. This is called the decline phase which then turns into the stationary phase of cell growth. Finally, if more cells die than are produced, the cell population enters the death phase.
For the virus production phase that usually follows a short growth phase, batch mode is used in most of the cases. However, also other strategies are applicable. In case, a longer cultivation time is requested, fed-batch processes can be applied where cells are feeded with fresh medium during growth and/or virus production phase. If a continuous harvest of either product or medium is necessary, one can choose a continuous cultivation strategy. During the whole cultivation, material (cells, product and old medium) is continuously harvested from the reactor and balanced by a continuous inflow of fresh medium. A variant of a continuous cultivation, but with cell retention, is the perfusion strategy.

2.1.4.1 Metabolism

Cultured cells do not show growth characteristics typically found in their original tissue or organ. They more show characteristics of cancer cells regarding metabolism and cell physiology [54, 55]. This paragraph will introduce principal aspects of the general metabolism that is found for such cells and implications one can gain from knowledge of metabolism for process development and monitoring.
A generalized scheme of the central metabolism of cultured cells usually contains the main parts glycolysis, pentose phosphate pathway (PPP), tricarboxylic acid cycle (TCA), amino acid catabolism (often towards intermediates of the TCA) and the oxidative phosphorylation transferring electrons from NADH, NADPH and FADH to oxygen to generate the high-energy molecule ATP (Figure 2.3). Growing and dividing cells need to generate several compounds as nucleotides, fatty acids and proteins. Therefore they need precursors, reducing equivalents and energy in form of molecules as NADH and ATP. The main arteries of energy generation are glycolysis, TCA cycle and pentose phosphate pathway. The glycolytic pathway degrades glucose into pyruvate, whereby NADH and ATP molecules are produced. The pentose phosphate pathway yields ribose sugars for nucleotide synthesis. After glycolysis, pyruvate-derived acetyl-CoA is oxidized and recycled in the TCA. This pathway

yields the highest amounts of reduction equivalents that again can be converted to ATP via oxidative phosphorylation. However, the interplay of glycolysis and TCA has been found to be impeded for transformed cells, i.e. tumor cells but also most immortalized cell lines in biopharmaceutical production. They mainly convert glucose into lactate so that pyruvate is not available in large amounts. The TCA thus cannot be fed “from top to bottom” via pyruvate, but needs to be fed otherwise. To overcome this obstacle, cells pursue the way of amino acid catabolism feeding the TCA “from the side” via several TCA intermediates. A major role for transformed cells plays glutaminolysis: glutamine is converted into glutamate and subsequently into α-ketoglutarate (αKG), thus providing an intermediate of the TCA. During this and other deamination reactions of amino acid catabolism, ammonia is built as a side product.

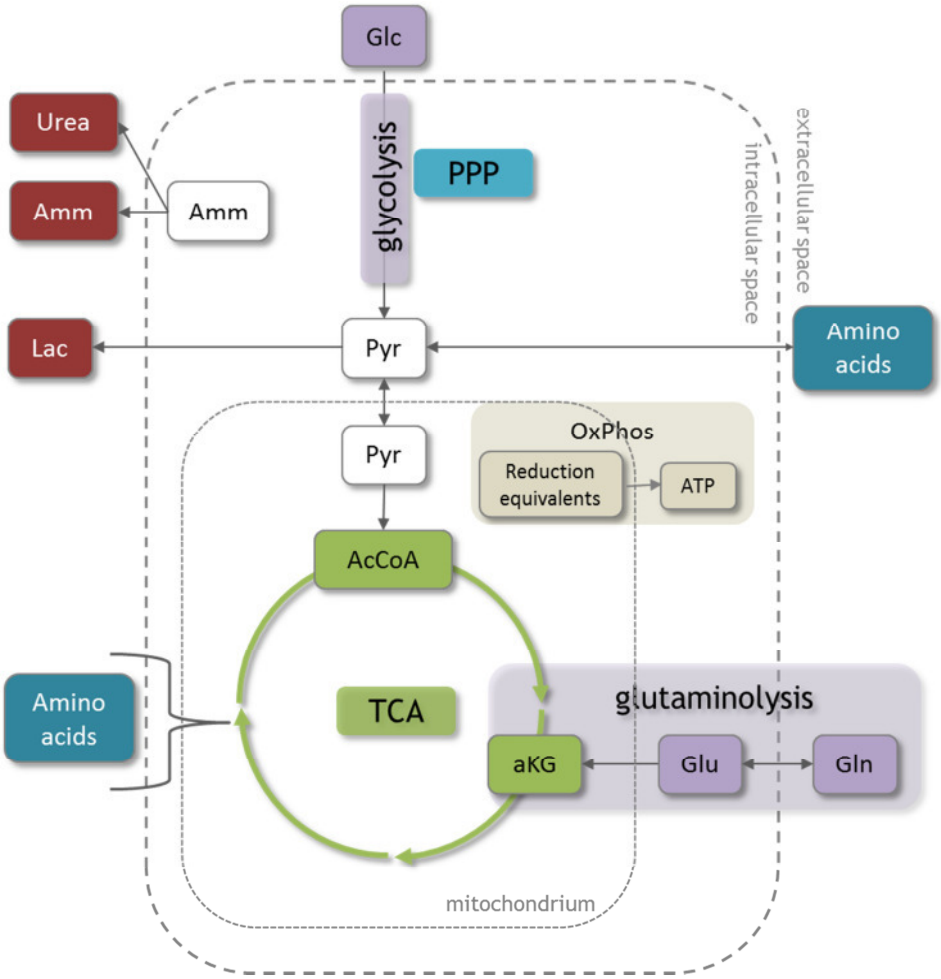

Figure 2.3: Main pathways in the central metabolism of cells. Glucose as the main energy supply is metabolized in glycolysis and the TCA cycle. Besides glucose, amino acids and especially glutamine feed the TCA cycle. Reducing equivalents that are produced in glycolysis and TCA cycle are regenerated via the electron transport chain. ATP is mainly generated by oxidative phosphorylation. For transformed cells, ammonia and lactate have been found to be the main waste products that are derived by glucose and glutamine consumption.

To summarize this, cells need carbohydrates (e.g. glucose), glutamine and other amino acids to generate precursors for biomass production and enough energy for maintenance, proliferation and product formation. Therefrom, several waste products result. Mainly, ammonia and lactate are built and excreted in siginifcant amounts. They have been shown to be responsible for viability and fitness decreases in cell cultures due to toxicity (ammonia) or reduction of extracellular pH (lactate) (see for example [56, 57]). Knowledge of metabolism and nutrient requirements of the respective cells can help with two implications: medium development and cultivation strategy.

As described above, cells mainly use glucose, glutamine and other amino acids to gain energy. These nutrients need to be provided by the medium that is used for cell cultivation. Usually, complex media are used in cell culture technology that provide these nutrients together with salts, vitamins, trace elements and sometimes precursors for lipid biosynthesis, e.g. ethanolamine. Hundreds of different formulations have been developed and tested and nearly for every cell line specialized media have been established. One prominent example of a basal medium that has been varied innumberable times is Dulbecco's Modified Eagle's Medium (DMEM), a medium developed in the 60s containing 32 compounds. Supplements like fetal bovine serum or plant hydrolysates are often used in addition as they contain growth supporting molecules as peptides or proteins like growth factors. Their exact complex composition, however, cannot be measured. On the one hand, this results in lot-to-lot inconsistencies impeding robust processes. On the other hand, modern processes ask for a profound knowledge of every part of the process, including the applied raw materials. Therefore, most companies try to culture cells in serum-free media or, even better, media free of any non-characterized and animal derived substances. This development is also demanded and supported by the FDA. Today, many so-called chemically-defined media are on the market. They contain significantly more compounds to substitute serum or hydrolysates. The use of a well-balanced and well-designed medium is thus one important parameter to yield a fast, but robust process. Its development only comes with the understanding of the cells' metabolism and demands. Another implication for metabolic studies is developing a process with minimized production or presence of waste products. Lactate and ammonia naturally accumulate in the medium during cell cultivation. However, high concentrations of both waste products have been shown to reduce cell viability and thus culture longevity. Strategies to reduce their concentration can include modified media (with e.g. reduced glucose concentrations or substitution of glucose by other sugars), altered process strategies (fed-batch processes or continuous cultivations where old medium is diluted or replaced by fresh medium thus bleeding waste products) or even genetic modification of metabolic pathways that lead to waste product formation [58].

The relevance of studies concerning cell metabolism is thus clear. How metabolism is studied can vary in methods and complexity. Some methods will be shortly introduced here as they were applied in this project.

One simple way is to perform spent media analyses. This can help to optimize nutrient supply and to identify limiting nutrients or inhibiting substances. Therefore, samples are taken after a certain cultivation time and one measures the nutrient concentrations that are present in the medium. Usually, concentrations of the main metabolites lactate, glucose, ammonia, glutamate, glutamine and potentially amino acids are determined. Based on the experimental data, further characterstics, e.g. netto bilances of all spent or excreted amino acids, can be determined. Relating the waste product with its main source can give information about medium balancing. Yield coefficients like $Y_{Lac/Glc}$ (lactate production from glucose uptake) or $Y_{Amm/Gln}$ are commonly used to characterize the status of a cell culture. If values from the whole timecourse of cultivation are available, exchange rates (uptake or release) can be calculated. Mostly this is done by balancing concentration differences over time during the exponential growth phase, taking into account cell growth/biomass formation. Section 3.2.4 of materials and methods will give a more detailed explanation on rate calculation.

Characterization of metabolism or cell performance in general can be done by comparing specific growth rates and exchange rates of metbaolites derived from cultivation under condition x compared to condition y. However, such analyses need a careful consideration of errors. Analytical errors, variations due to heterogeneity of cell culture or raw materials, and variances due to heterogeneity of pre-cultures have to be mentioned. A thorough analysis including statistical significance testing of derived growth and exchange rates when comparing stirred-tank reactor (STR) and Wave bioreactor cultivations will be discussed in chapter 4.1.3.2.

Still, netto balances, yields and exchange rates cannot elucidate how the metabolic pathways within the cell are used. Therefore, either intracellular metabolite concentrations or conversions need to be measured (e.g. as in [59]) or mathematical modeling approaches based on metabolic networks need to be used. Different methods have been developed and comprehensive reviews on applied methodologies and their benefits for mammalian cell culture research are available [60, 61]. Here, only some techniques with the focus on applicability and required prerequisites (summarized in Figure 2.4) will be introduced generally.

One of the most common mathematical approaches is the mass balancing method Metabolic Flux Analysis (MFA) that has long been used to describe bacteria metabolism. Over the last 20-25 years, scientists tried to apply MFA also for the description of (the more complex) metabolism of eukaryotic cells, e.g. transformed mammalian cell lines. In continuous

cultivations or the exponential growth phase during batch cultivations, this method can evaluate possible intracellular flux distributions based on calculated exchange fluxes.

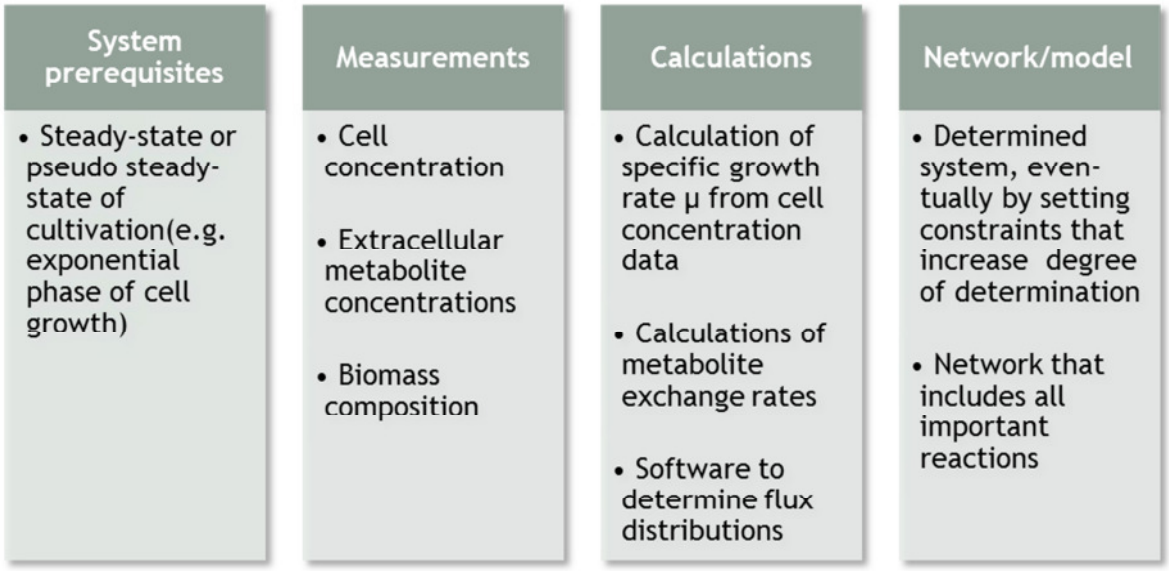

Figure 2.4: Prerequisites and parameters needed for performing Metabolic Flux Analysis.

When having set up a network model describing the metabolic pathways one is interested in, one key prerequisite for calculating a unique flux distribution is that the network is determined. This means that enough fluxes are known (experimentally determined exchange rates) to fully resolve all fluxes within the network. Depending on the number of metabolites that can be measured and the size of the network, sometimes the network is underdetermined and further assumptions or constraints need to be implemented. To avoid overinterpretation of a particular flux distribution due to wrong assumptions, a variant of MFA, the so-called Flux Variability Analysis (FVA), can be used. FVA enables one to calculate flux ranges instead of specific flux distributions for underdetermined systems [62]. With both methods (MFA and FVA) one can calculate intracellular flux ranges from measured extracellular rates. Software tools such as the *CellNetAnalyzer* toolbox help with calculations [63]. There are more ways to study the metabolism of cells, e.g. ^{13}C analysis with which one can follow the intracellular conversion of special metabolites. However, such experiments are costly and more difficult to measure and analyze than experiments for MFA or FVA and were therefore not included or explained in detail in this work.

One aim of this work was to evaluate metabolism of avian CR and CR.pIX cells with the help of MFA and FVA techniques. Available background information for metabolic studies on these cells was rare as no avian cell line had been studied in detail before. Only feeding studies of chicken or turkey have been published, regarding the whole organism or, e.g. the

liver, giving at least hints towards some specific characteristics of avian cell metabolism [64, 65].

2.1.4.2 Cell cycle distribution, apoptosis and necrosis

Cell cycle and apoptotic status affect cell growth as well as productivity (see for example [66, 67]). Therefore, monitoring those cell characteristics can give important implications for process development.

When proliferating, cells constantly run through the cell cycle (Figure 2.5). After cell division, cells being in the G1 phase have one set of chromosomes (1n). At this time, they can pursue two ways: either they stop dividing by entering the arrest phase G0, or they move on in proliferation and start synthesizing their genome by replication of the DNA (S phase, 1n→2n). At the end of the S phase, two identical sets of chromosomes are present in the cell (2n) and the cells prepare for division during the so-called G2 phase. During the following mitosis (M phase), division takes place so that finally two identical daughter cells are formed. Usually, eukaryotic cells need 20-30 h for one cycle, whereby mitosis only takes approximately 1 h and DNA replication (S phase) only about 8 h. The rest of the time, cells prepare either for synthesis or for mitosis by a complex interplay of several proteins (cyclins and cyclin-dependent kinases) ensuring that only cells with an intact set of chromosomes can divide [68].

Knowing the cell cycle distribution of the cell population during cell growth phase and virus production phase gives interesting hints for culture fitness and productivity. During cell growth and for production of therapeutic proteins or viruses, a high percentage of dividing cells has been found to be beneficial [21, 67, 69]. A high growth rate can be sustained when cells are cycling quickly through the cell cycle without being arrested in the G0 phase. Also, virus production has been shown in some studies to be dependent on the host cell and thus on cell physiology with proliferating cells being more productive [70]. Choosing the time of infection determines in which cell cycle distribution cells are infected. Therefore, cell cycle status has also been appointed as cause of the cell density effect that is often observed when cell concentrations above a certain “critical” concentration are present at time of infection (critical concentration probably depending on cell, virus as well as medium). This effect will later be discussed in more detail (section 2.2.4).

There are different methods available to measure the cell cycle status of the cell population, reviewed for example by Uzbekov et al. [71]. Mostly, molecules that intercalate in the DNA of the cell during replication and division, e.g. propidiumiodide (PI) or bromodeoxyuridine (BrdU), are used. Determination of the amount of this molecule in the

cells thus can be correlated with the amount of chromosomal DNA and therefore with the cell cycle phase.

For a cell, there are mainly two ways to die (see Figure 2.6 for a schematic overview). Upon physical injury, cells undergo necrosis, the so-called acute cell death. After necrosis has been induced, the membrane integrity is lost and cellular structures (organelles, cytoskeleton, DNA) are destroyed. At the end of this process, the membrane ruptures and all cellular parts are spilled out into the extracellular medium.

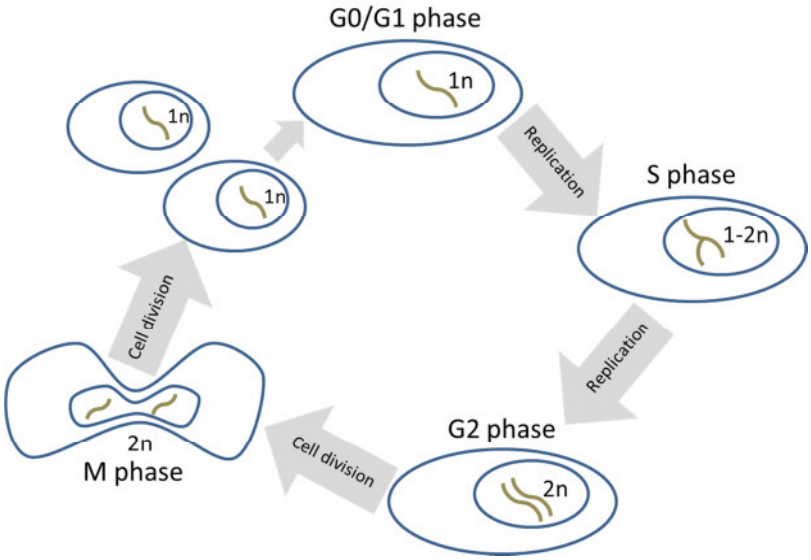

Figure 2.5: Cell cycle progression. Before cell division by mitosis, the cell genome has to be duplicated. Preparation of this happens during the gap phase 1 (G1). Afterwards, DNA is replicated in the so-called synthesis (S) phase. At this time, the number of chromosome sets thus increases from 1 to 2. After division, two daughter cells are present with each having one identical set of chromosomes. Quiescent cells that are in the gap phase 0 (G0) do not proliferate anymore, but can re-enter the G1 phase upon environmental stimuli.

The second way of cell death is triggered by stress signals, e.g. nutrient deprivation [72] or infection with virus, e.g. poxvirus and influenza virus [73-75]. If cellular receptors register such stress signals, the so-called programmed cell death, apoptosis, is induced. During apoptosis, cells pass different stages, each one induced and accompanied by specific molecular processes. One of the first events is the loss of mitochondrial membrane integrity, followed by a signaling pathway including specific proteases – caspases – that trigger every part of the apoptotic pathway. Initiator caspases (caspases 8, 10, 9 and 2) are responsible for cleaving effector caspases (caspases 3, 7 and 6). Those finally digest cytosolic compounds like the cytoskeleton. Chromatin in the nucleus condensates, then DNA fragmentates. Finally, vesicles form, so-called apoptotic bodies, that portion the cell parts such that neighbor cells can phagocytose the cell remainings [76].

A variety of methods for the detection of necrotic and apoptotic cells have been developed for flow cytometry [77]. Detection of necrotic and (late) apoptotic cells is for example

possible by incubating the cell suspension with staining solutions including trypan blue, PI, or 7-aminoactinomycin (7-AAD). Due to their size, these staining moecules can only enter the cell if the plasma membrane is permeabilized due to damage or treatment. Then, trypan blue stains intracellular proteins so that the cells appear blue. PI and 7-AAD intercalate in the DNA. With all three staining procedures alone, dead cells can thus be detected without the differentiation of necrotic and apoptotic cells. Detecting specifically apoptotic cells can be done by immunohistological detection of the signaling proteins. Antibodies against all known caspases have been generated and can be used in flow cytometry. Another method is to analyze the DNA fragmentation using assays like the TUNEL assay. With this assay, DNA strand breaks are visualized by fluorescing nucleotides that bind to the end of the DNA strand. The higher the DNA fragmentation degree, the higher the fluorescence signal. Another mehod is to detect phosphatidylserine of the plasma membrane that is not accessible in intact cells as it is present at the cytosolic side of the membrane. Upon apoptosis, membrane integrity is impaired and phosphatidylserine molecules flip to the outer side of the membrane [78]. Then, it can be detected by using annexin V, a protein with high affinity towards phosphytidylserine [79].

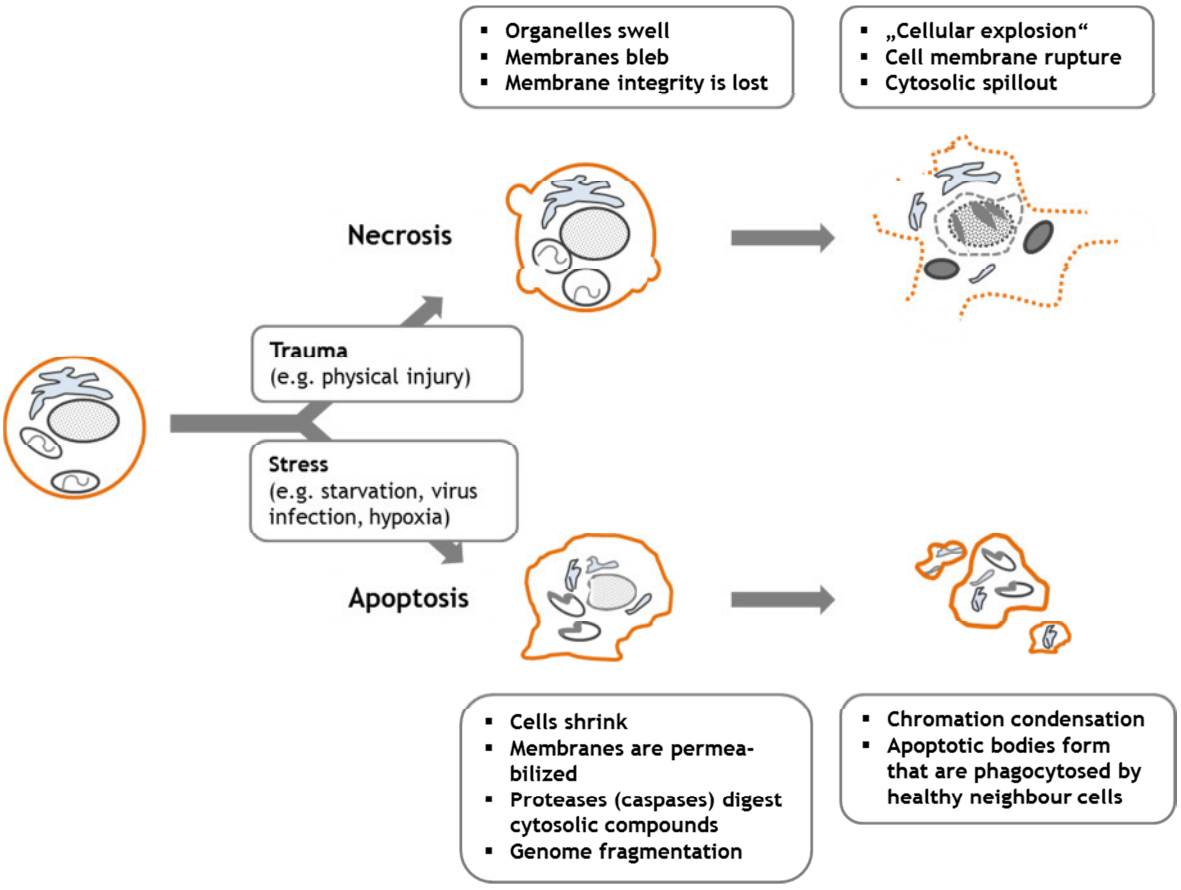

Figure 2.6: Consequences of cell death via necrosis and apotosis. Changes in cell morphology are depicted together with main macromolecular and morphological characteristics. Adapted from [80] and [81].

Reducing the amount of cells that undergo cell death during growth phase elongates the exponential and stationary growth phase. With this, higher cell concentrations can be achieved as well as an increased culture longevity. Necrosis can be reduced by avoiding stimuli like shear stress. Especially for recombinant protein production processes, efforts have been made to reduce apoptosis. Among others, expression of anti-apoptotic genes such as Bcl-2 have been found to be efficient [66, 82]. Cells usually induce apoptosis when infected by a virus in order to decelerate virus spread in the tissue [83, 84]. Viruses on the other hand antagonize this principle by suppressing apoptosis. For example, the adenoviral genes E1A and E1B in conjunction have early been found to be responsible for apoptosis suppression and growth stimulation. Since then, those genes are commonly used for targeted immortalization of cell lines, amongst others HEK293, PER.C6 and CR cells. Reduction of apoptosis thus has two outcomes: increased culture longevity and cell fitness as well as a fostered virus spread in the cell population which is beneficial for virus production processes – more healthy cells can synthesize more virus particles. One other reason for the aim of a low apoptotic status in the cultivated cell population is that during apoptosis, cellular DNA is released into the medium. Reducing the amount of apoptotic cells thus also reduces the amount of host cell DNA in the medium which substantially facilitates purification of the vaccine product and helps to meet the criteria for residential host cell DNA concentration. Characterizing the cell culture regarding cell physiology is therefore interesting for process development.

2.2 MVA and its relevance as a vaccine

The production of MVA was evaluated in this work. Therefore, the virus and its characteristics will be introduced here. MVA is an attenuated strain of vaccinia virus and was developed in 1975. As a vaccine against smallpox, but even more as vaccine vector, MVA has become vitally important and today is utilized in several vaccines on the market or in clinical trials. The following sections introduce its history (chapter 2.2.1 and 2.2.2), application fields (chapter 2.2.3) and production (chapter 2.2.4). Thereby, virus characteristics that can influence the development of a robust and productive cell culture-based MVA production process will be addressed.

2.2.1 Vaccinia viruses

Vaccinia viruses belong to the genus *Orthopoxviridae*. All vaccinia viruses are enveloped viruses that carry a linear double-stranded DNA genome (schematic structure shown in Figure 2.7).

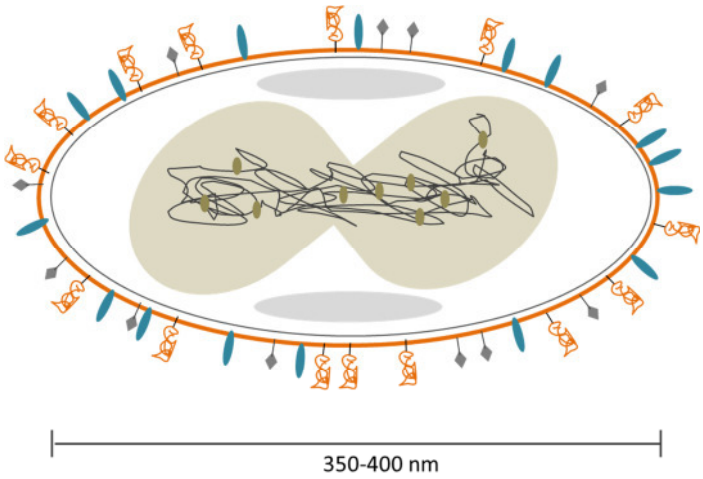

Figure 2.7: Schematic structure of a vaccinia virus. In the center of the virus particle, the bone-shaped core structure with the packaged double-stranded DNA genome is arranged. Also, some proteins are packaged in the core (spots). Together with the core, elliptic lateral bodies are wrapped in a viral envelope. At the surface of the virus particle, different proteins have been found. Their composition and abundance change during virus maturation.

In the core, the viral genome is packed with structural proteins and enzymes that are needed for viral gene transcription. Core and proteinaceous lateral bodies (with today unknown function) are wrapped together into an envelope that can differ during maturation in its composition. Vaccinia viruses are one of the biggest viruses - in terms of physical size (200-400 nm in diameter), but also in terms of genome size (~200 kbp).

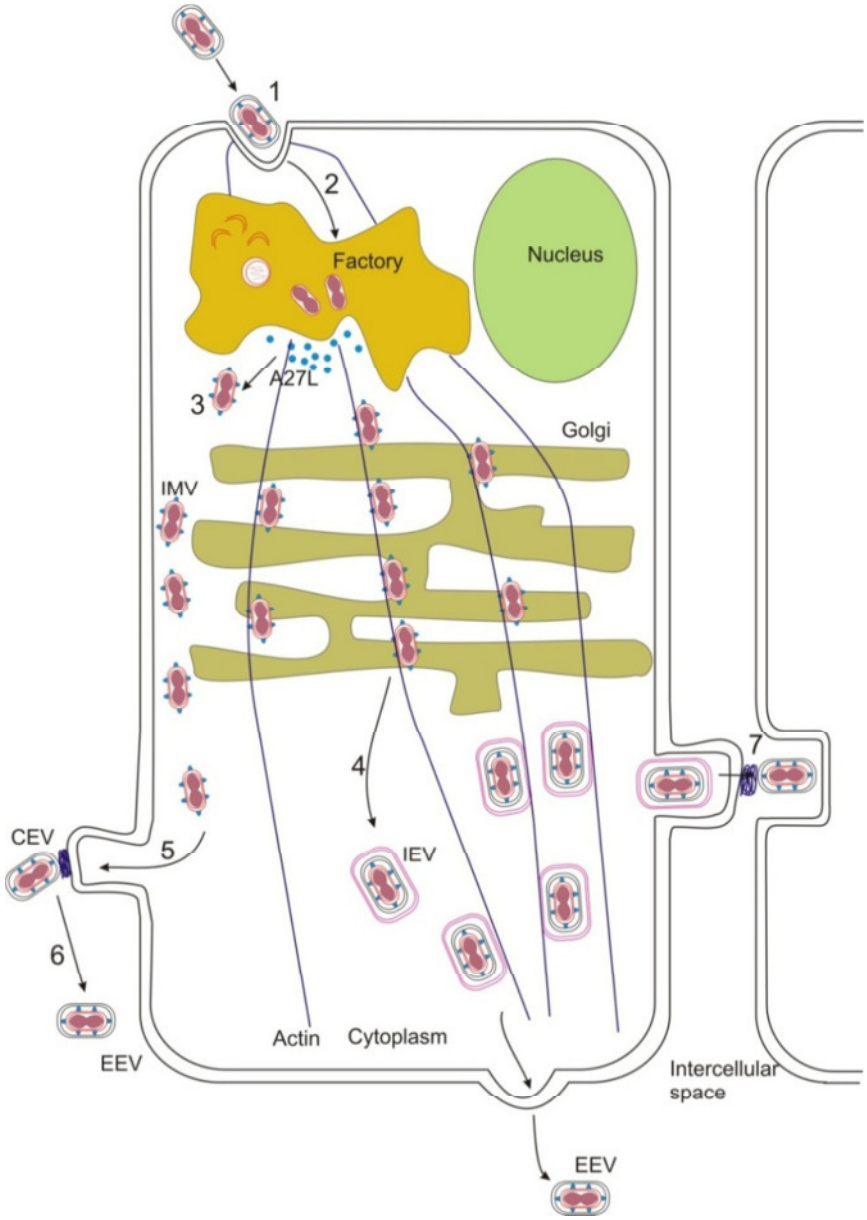

Figure 2.8: Replication cycle of MVA in a host cell. Infection of a host cell starts with 1) the internalization of the virus particle. 2) After unpacking the DNA, replication and translation start in so-called viral factories in the cytoplasma. 3) First intracellular mature virions (IMV) occur at the site of viral factories and can be 4) either transported through the Golgi system where they acquire an additional membrane and now are called intracellular enveloped virions, IEV, 5) or transported directly to the cell membrane where they are released from the cell as extracellular enveloped virions, EEV (6). Also, IEV can be exported and (like IMV) can stay attached to the outer surface of the cell membrane as cell-associated enveloped virions (CEV) before being entirely released from the cell. From [85].

Within the genome, approximately 200 open reading frames have been identified. Whether all open reading frames are coding for specific proteins or not, is yet not known for many of them. There are, however, several proteins for which a unique role in viral infection, maturation and transmission could be identified. One can distinguish three regions within the genome. A central region (~100 kbp) encodes conserved proteins between different vaccinia virus strains which are mostly structural proteins or otherwise essential for virus

replication. Left and right terminal regions are more variable and encode proteins that are mainly non-essential for virus replication, but affect viral host range, virulence and interactions with the host immune system. Regarding the sequence of virus maturation steps after infection, one can categorize genes and encoded proteins as early, middle or late [86]. The replication cycle of vaccinia viruses is schematically shown in Figure 2.8. Infection starts with the attachment to a cell triggering internalization of the virus particle (step 1). Different internalization ways have been suggested in literature, for example receptor-mediated fusion in a pH-dependent manner and receptor-mediated endocytosis [87]. The corresponding receptors, however, have not been identified yet. By internalization, viral DNA is released into the cytoplasm of the cell. Recruitment of cellular membrane structures leads to the formation of distinct local areas, so-called viral factories, where early gene replication and translation of first proteins take place already minutes after infection (step 2) as for example nicely shown by Stiefel et al. using cell and single virus infection experiments [88]. Viral enzymes for DNA replication and mRNA synthesis belong to the first transcribed genes, but also several viral factors that block the innate immune response are produced at this time. Parallel to DNA replication, late transcription factors (intermediate genes) and structural proteins are transcribed approximately 5–6 h post infection (hpi). In this phase, the first immature particles occur as crescent-shaped structures in the cytoplasm.

At the end of this process, several proteins, especially the D13 protein trigger the formation of the typical brick-shaped structure. Now, first mature virus particles can be observed, named intracellular mature virions (IMVs, step 3). IMVs can be distinguished from other virus particles due to their characteristic surface proteins, e.g. the A27L protein.

Part of the IMVs are then actively transported by recruited cellular microtubules through the trans-Golgi network and thereby receive a lipid membrane (step 4). Such intracellular enveloped virions (IEV) are destined to exit the cell. Therefore, they are further transported to the cell membrane [89]. By fusion of the outer viral membrane with the cell membrane, both intracellular forms, IMVs and IEVs, can exit the cell (step 5 or 7), whereby not all IMVs leave the host cell. Also, virions must not be released entirely from the cell, but are able to induce the formation of cellular actin tails which bind the particles to the outer membrane of the cell (see step 7). This virion form is called cell-associated enveloped virus (CEV). With the help of those actin tails, CEVs can also be propelled away from the cell towards surrounding cells and are thus responsibe for middle-distance virus spread. For long-distance spread, CEVs can be released completely from the cell surface (step 6). As so-called extracellular enveloped virions (EEVs), such virions can diffuse through the extracellular space and infect host cells further away [90]. Release of CEVs is mediated by characteristic

proteins with the most abundant ones being A34R, B5R and A33R. These proteins determine the long-distance spread of vaccinia virus in a tissue or cell population.

Several virus genera and species within the family of *Poxviridae* are responsible for infections in different hosts, e.g. fowlpox and canarypox in birds, cowpox in cows or smallpox in humans. The responsible strain for worldwide human smallpox epidemics that in particular occurred in the 18th and 19th century, is the highly infectious variola virus strain. Two principal forms were clinically differentiated: Variola major which caused high case-fatality rates of about 30% and Variola minor causing a milder form of smallpox with only approximately 1% fatal cases. Human-to-human transmission of smallpox infection is mediated by aerosols and droplets or through close contact with contaminated clothes or bedding. After infection and an incubation period of 10–14 days, first symptoms can be observed. At first, influenza-like symptoms including high fever, malaise and headache typically set in. Next, lesions erupt in the throat and the mouth and directly thereafter the characteristic rash appears on hands, forearms and on the face. Eventually, the rash spreads over the entire body. Only at this stage, infected persons can transmit smallpox to others. The typical skin lesions often become pustules that leave behind extensive scars. This and other frequent long-term symptoms like encephalitis, blindness and secondary bacterial infections complicate the patients' recovery.

2.2.2 Smallpox vaccines

Smallpox has been known since ancient times and its spread was humungous leading to about 400,000 deaths in Europe during the 18th century. Combatting this disease was an early aim of scientists, physicists and politicians around the world. It is therefore probably not surprising that the first treatment of an infectious disease by vaccination was a vaccination against smallpox (conducted by Edward Jenner in 1796). Since then, several different vaccines have been developed [1]. Their evolution is a fine example how improved techniques, process development and quality demands influence vaccine types and production methods (Table 2.2).

The vaccine and vaccination method developed by Jenner in the late years of the 18th century can be seen as zero generation. He used material from cowpox lesions or calf-lymph as live virus vaccine [91]. With the next generation of vaccines, the innovation of freeze-dried formulation was introduced. This methodology helped to prolong the shelf life and thus allowed transportation to all regions in the world. Therefore, 1st generation vaccines with DryVax® from Wyeth being the most prominent product, were applied during the ambitious global smallpox eradication campaign that was started by the WHO in 1967. Its success became clear in 1980, when the WHO officially announced the eradication of

smallpox from the world. It is so far the only time a human disease could be extinguished by vaccination. Although live vaccinia viruses of 1st generation vaccines were used successfully, they all had an imperfect safety record. Therefore, in parallel, vaccine development moved on to ensure post-eradication demand and at the same time reduce the long list of adverse effects and contraindications that were mainly ascribed to the low purity of calf lymph-derived vaccine. One important step towards safer vaccines was changing the production system from animals to tissue cultures or cell lines. In the following, chicken eggs, human MRC-5 cells or Vero cells were used to produce 2nd generation vaccines based on different virus strains. Prominent products within this generation are for example ACAM1000® and ACAM2000®, produced by Acambis/Sanofi [92]. The latter is produced from microcarrier cultures of Vero cells and is approved for the market since 2007.

Table 2.2: Selected smallpox vaccines that have been developed until today.

Name	Strain	Production system	Further details
		Zero generation	
Jenner vaccine	Cowpox	Cows and calves	Administered by inoculation: transfer of infectious material from pustules or calf lymph into the skin of the vaccinee
		1st generation	
SPSV	NYCBH strain#	Lymph from infected calves	Frozen liquid formulation
DryVax®	NYCBH strain	Lymph from infected calves	Wyeth vaccine, freeze-dried, not produced and approved anymore
Lister	Lister strain	chorioantallois membrane of hen's eggs	Freeze-dried
		2nd generation	
ACAM1000® & ACAM2000®	NYCBH strain	MRC-5 cells & Vero cells	Acambis/Sanofi vaccine, cell culture-based
Elstree BN	Lister/Elstree strain	Chicken embryonic fibroblasts (CEF)	Bavarian Nordic vaccine
		3rd generation	
LC16m8	Lister strain	Mostly produced in CEF	Deletion in B5R gene
NYVAC	Copenhagen strain	Mostly produced in CEF	Deletions in 18 immunomodulatory genes
MVA*	Ankara strain	Mostly produced in CEF	Deletion of 15% of genome by serial passaging on CEF cells
ACAM3000®	MVA-based	Cell culture-based production	By Acambis/Sanofi
IMVAMUNE®	MVA-based	Cell culture-based production	By Bavarian Nordic, approved since 2013

Several vaccinia virus strains and production systems have been used. Zero, 1st and 2nd generation vaccines were live virus vaccines, whereas 3rd generation vaccines contain live-attenuated vaccine strains [93].

NYCBH: vaccinia virus strain isolated and propagated by the New York City Board of Health

* MVA: Modified Vaccinia Virus Ankara, a live-attenuated strain derived from the Ankara strain

Despite the innovation of a cell culture-based manufacturing process, the 2nd generation vaccines are still live virus vaccines sometimes inducing serious side effects like myocarditis. Already during the eradication program, this problem was tackled. First, chemically or physically inactivated virus vaccines were developed and studied, but failed to induce immune protection. Therefore, attenuated virus strains with a diminished virulence were developed as 3rd generation vaccines based on several vaccinia virus strains (e.g. Lister or Ankara) [94, 95]. They only induced mild and seldom adverse side effects so that safety was dramatically increased. Also, they were all shown to be efficient and to induce the same level of immune response as live virus vaccines [96, 97].

By now, the most promising attenuated strain is MVA that has been used in this work. The following paragraph will point out its relevance as vaccine and viral vector vaccine strain.

2.2.3 MVA as vaccine and vaccine vector

Although smallpox was officially declared eradicated in 1980, vaccinia virus vaccines are still stockpiled by several countries. By quick vaccination, fast limitation of new recurrences that might easily infect the now naïve population, shall be assured. In addition, a potent vaccine could also be a quick measure against bioterroristic attacks. Production of vaccinia viruses or MVA as one attenuated derivative is therefore still a subject for vaccine industry. Just in 2013, a new MVA-based smallpox vaccine (IMVAMUNE® from Bavarian Nordic) has been approved by the FDA.

Development of MVA started in 1958 when Anton Mayr in Munich began long-time passaging of the vaccinia virus Ankara strain on CEF cultures [26]. After 370 passages, he examined the virus population and found a significantly reduced or even missing virulence in rabbits, mice and several different cell cultures or tissues. He pursued the passaging on CEF cultures and 12 years later finally plaque-purified the 570th passage. Again, a reduced or missing virulence in various animal models and cultures was observed. Only CEF cultures seemed to be susceptible by the strain now called MVA. Various intense studies of the genotype and phenotype of MVA followed in order to characterize the new virus strain.

Sequencing revealed that the virus had lost 15% of its genome now containing only 178 kbp (in contrast, the vaccinia virus Copenhagen strain contains 192 kbp). Within these 178 kbp, 193 open reading frames (ORFs) have been identified coding for 177 genes [98, 99]. Interestingly, 25–30 genes are truncated versions, many ORFs are re-organized and some genes are not present in the MVA genome at all – always compared to other vaccinia virus strains such as Lister or Copenhagen. Figure 2.9 shows the main modifications in the genome of MVA. Most of the genes that are unfunctional or missing in the MVA genome served as

host range factors (e.g. K1L and C7L), virulence factors (e.g. A36R) and factors for immune evasion (e.g. A39R, A40R). Those factors are mainly associated with the left terminal region of the genome. Interestingly, three fragmented and several truncated genes were found in the conserved central region as well. For several of them, functions have not been elucidated yet, but for some involvement in virus structure and stability (like the F3L envelope protein or the D3R structure protein) has been shown.

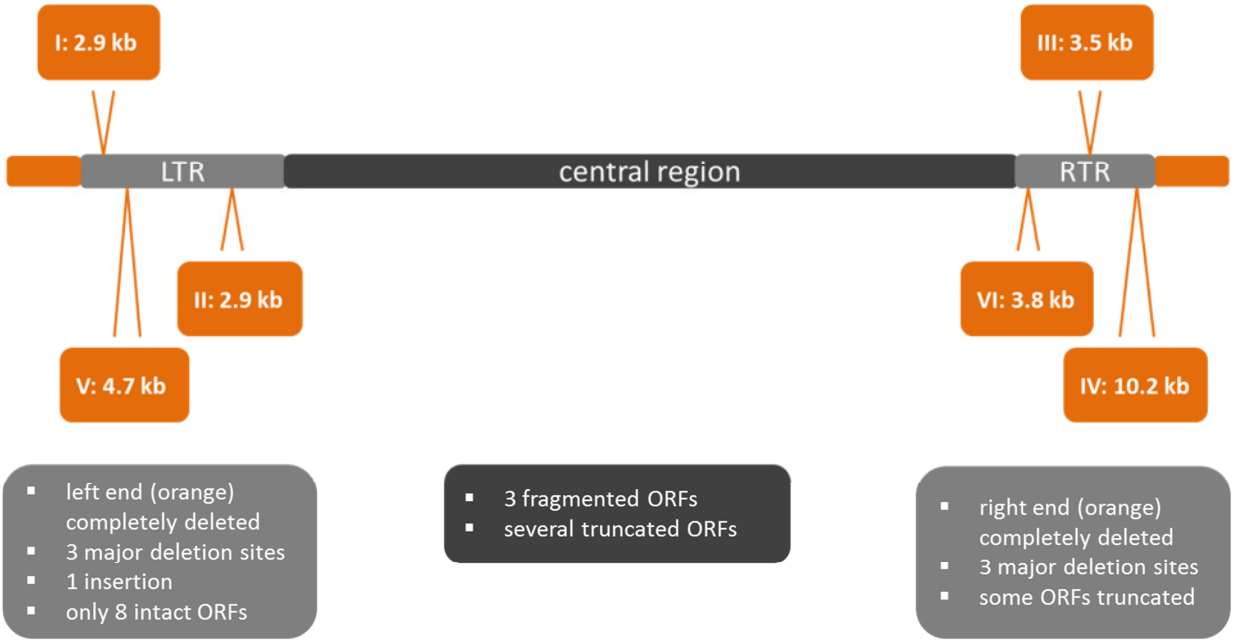

Figure 2.9: Organization of the MVA genome with localization of large deletion sites compared to parenteral strains. For each genomic region (central region, left terminal region (LTR), right terminal region (RTR)), the main mutations or deletions are listed. Orange bars and boxes indicate large regions that disappeared during the process of attenuation. Numbers have been assigned to deletion sites and located according to [27]. Note that bar lengths do not correlate with size of the respective genomic part.

Through the genomic rearrangements and deletions, the phenotype of MVA is significantly altered in comparison to the parenteral vaccinia virus strain. The most striking modification is the limited host specificity of MVA. Long-time passaging on CEF cultures resulted in a virus that is fully infective only for cell material from chickens or, presumably, avian species in general. Several studies have shown that most primary and continuous cells of mammalian origin are not propagating MVA with very few exceptions (e.g. hamster BHK-21 cells and monkey MA104 cells) [34]. Actually, MVA can infect mammalian cells, but its assembly then is blocked at the stage of immature virions [100, 101]. Probably due to its modified genetic equipment, MVA also has an excellent immune-boosting ability and has shown to stimulate T-cell responses [102] as well as T-lymphocytes [103].

In addition to its use as smallpox vaccine, MVA can be used as a vector vaccine that delivers antigens from other pathogens or diseases against which protective immunity is needed.

Besides the immune triggering functions of MVA, its genomic size makes it one of the most promising candidates for vectored vaccines. One, or several, large genetic inserts of up to 25 kbp can be cloned into the MVA genome. One common method is to introduce the gene or genes of interest into deletion site III [104]. Antigens from other pathogens or diseases can thus be delivered by MVA into cells to trigger an immune response against the respective antigen. After several years of extensive research and development, various different MVA-based vector vaccines are now on the market or in clinical trials (as of 07.02.2014, www.clinicaltrials.gov lists 185 studies). Thereby, different diseases have been targeted. First, targets can be viral pathogens. MVA-based vectors carrying antigens from Hepatitis C virus, Human Papillomavirus, Japanese Encephalitis Virus, Respiratory Synctical Virus and Influenza Virus have been developed and phase I and phase II clinical trials are ongoing [93]. Also, the enormous effort to find an efficient vaccine against HIV includes research with MVA as a vector vaccine. Several HIV antigens (usually env, gag, pol) have been cloned into MVA in order to induce an adequate immune response as a vaccine itself or as an immune booster before vaccination with other constructs [105, 106]. The aim is to either help the patient's immune system to deal with virus infection or – better – to prevent infection. A second target group are bacterial pathogens. One vaccine against tuberculosis (containing the antigen 85A from *Mycobacterium tuberculosis* [107]) and one vaccine against malaria (containing the gene encoding for the adhesion protein ME-TRAP of *Plasmodium falciparum* [108]) is right now tested in phase I and phase II clinical trials, respectively. A third group which might be fought with MVA as a vector is the huge group of cancer diseases. Vaccines against various cancer forms have been developed and today are tested in terms of efficiency and efficacy. Those vaccine candidates include MVA-based vectors against colorectal and breast cancer [109, 110].

In summary, MVA is considered not only as a vaccine against smallpox, but as a vector either alone, or as a booster vaccine that precedes a virus or DNA vaccine. Its established production processes as well as indications for possible production optimization will be addressed in the next section.

2.2.4 MVA production processes

For a virus production process, the cell substrate that is chosen to propagate the virus significantly influences yields. Therefore, host cells that have or can be used for production of MVA are introduced first in this section.

Due to the origin and acquired host specificity of MVA, two systems are most suitable as substrates: the chorioallantoic membrane of chicken eggs and primary CEF cultures. These systems are convenient and sufficient for the generation of small bulks of MVA that are

usually needed for research or clinical trials, but also have been and are used for industrial production of MVA. MVA is perfectly adapted to CEF cells and titers around $1x10^8$ pfu/mL are usually achieved [111, 112]. With this, approximately 0.2–1 dose of vaccine can be prepared from 1 mL culture broth, depending on the complexity of the purification process and associated product losses. However, utilizing primary host cells does not fulfill all requirements of a robust and modern process. CEF cultures can only be cultivated as adherent cells and the surface they require for growth limits scalability of the production system. Also for primary cell cultures, sterile eggs from special flocks need to be constantly supplied. Another disadvantage of adherent primary cultures is that they usually cannot proliferate without serum, which with its changing quality and animal origin today is considered highly problematic. Alternatives, however, are rare. As mentioned before, some mammalian cell lines are permissive for MVA [112]. Probably most suitable are BHK-21 cells. In direct comparison studies from Carroll and Moss as well as Hornemann et al., they yielded slightly lower titers than CEF cells of approximately $1x10^7$ pfu/mL [111, 112]. However, as BHK-21 cells have not been approved for use in human vaccine manufacturing so far, probably due to their spontaneous immortalization and exposure to polyoma virus [113]. Therefore, BHK-21 cells might not be a vital option for manufacturing of MVA-based vaccines. In order to provide a well-known cell susbtrate for vaccine production, a MVA strain adapted to growth in Vero cells has been developed by long-time passaging [114]. For whatever reason, this MVA strain though has not been studied further.

Four immortalized avian cell lines have been described to date for use in MVA propagation and production: i) chicken DF-1, ii) quail QT5, iii) duck EB66 and iv) CR.pIX. DF-1 cells are derived from CEF by spontaneous immortalization and provide similar titers as their progenitor CEF [115]. These cells proliferate in adherence and need serum-containing medium. One step forward was made with the other three cell lines. They all are adapted to growth in suspension and chemically-defined media. One, the duck EB66 cell line, was developed by Vivalis, and provides titers similar to CEF cultures. AS DF-1, it has been immortalized spontaneously, but with duck embryonic stem cells as origin [14]. Few years ago, Baxter, on the other hand, has presented the QT5 cell line, derived from quail embryonic tissue which was immortalized by UV light treatment. It was shown to propagate MVA and recombinant MVA strains up to $1x10^9$ pfu/mL [116]. Recently, the avian designer cell lines CR and CR.pIX have been developed for use in MVA or MVA-based vaccine production (developed by ProBioGen AG in cooperation with IDT Biologika GmbH). They have been derived and developed from duck embryonic material [16, 18]. As they are the host cells used and characterized in this work, a more detailed description is given in section 2.4.2.

Concerning the MVA production process itself and its development, relatively little has been achieved over the last years. On the one hand, MVA usually is used in virology for medical studies or basic research to understand virus replication and immunogenicity. On the other hand, suspension cell lines for large scale production of MVA and MVA-based products have only been developed in the last years and mostly are proprietary so that process development studies are not accessible to the scientific community. Nevertheless, the following process steps and parameters need to be considered when developing a suspension process with MVA as a product (illustrated in Figure 2.10). (Note: purification and formulation of the product will not be addressed here, because in this work only the upstream process was considered.)

Before setting up a process, all raw materials need to be chosen and prepared. From a master seed virus (which can for example be purchased from culture collections such as the American Type Culture Collection (ATCC)), a working seed virus needs to be generated. MVA master seeds will usually be virus stocks that have been propagated in eggs or CEF cultures. An adaptation to the host cell line that is used in the process could therefore be necessary (box no. 1 in Figure 2.10). However, MVA is said to be genetically stable [3] and thus, it is probably not necessary to adapt the virus over several passages to the new host cell. In parallel, host cells need to be cultivated so that enough viable cells are avaible to propagate the virus (box no. 2 in Figure 2.10). Decisions on the medium that is provided and on the used cultivation system therefore have to be taken.

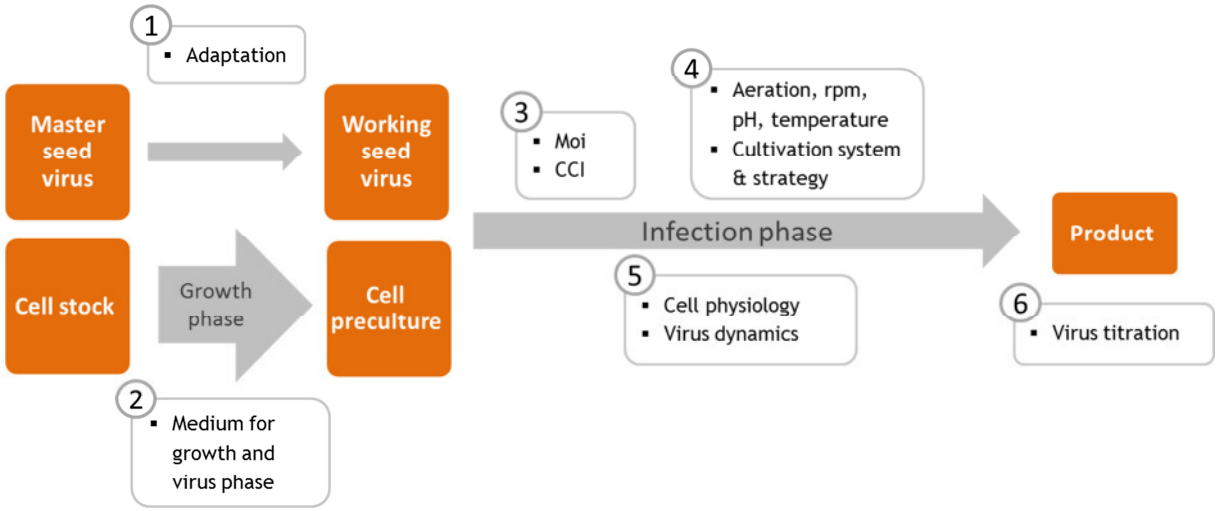

Figure 2.10: Schematic MVA production process. Generally, the process can be divided into seed virus production, cell growth phase and infection phase until the virus product has been produced. For each phase, parameters that have to be evaluated or monitored are listed in white boxes above or below the process steps. Moi: Multiplicity of infection, CCI: Cell concentration at time of infection.

Bioreactor systems control parameters like pH and dissolved oxygen (DO) and thus can be beneficial for establishment of a robust process. However, the cell growth phase usually

takes only 2–4 days. Therefore, using non-controlled systems (e.g. T-flasks or shaker flasks) might be sufficient. The time of infection (toi) also needs to be chosen carefully, taking into account three parameters: i) viability of cells which should be high as the cells need to synthesize virus particles, ii) all required nutrients should be present, but no inhibiting substances should have been accumulated, and iii) the cell concentration at time of infection (CCI). The latter has been reported to be important for adenovirus, baculovirus and influenza virus production [42, 117-119], but was not studied for MVA. These studies demonstrated that above a certain CCI, the cell-specific virus yield drops substantially, called the "cell density effect". Studies related to this topic indicate that the reasons for the cell density effect are highly dependent on the production system (virus species, host cell line and medium) and thus cannot be generalized. Explanations for this effect include depletion of nutrients or accumulation of inhibiting substances [119]. Also, activity or availability of host cell factors required for virus replication may change with the cell cycle [21] or with metabolic shifts at higher cell densities [117]. As an example, for production of influenza virus typically 1–2x10^6 cells/mL are used, but with fed-batch or perfusion strategies, exhaustion of medium components and influence of inhibiting substances can be avoided and high-yield infections of 1x10^7 cells/mL have been demonstrated [120, 121]. The aim of overcoming the cell density effect is to maintain or even increase the cell-specific productivity in order to improve process yield, i.e. to increase the vaccine doses per reactor volume. A break-even point between space-time yield and cell density effect thus has to be identified during process development.

Upon infection, the multiplicity of infection (moi) has to be chosen (box no. 3 in Figure 2.10). The moi is the ratio between the number of active virus particles that are added to the cell culture as seed virus and the cell number. Several optimization studies have been done in CEF, BHK-21 and other cells and found an optimal moi between 0.01 and 0.1 [34, 112]. This means that the cell culture is infected with 1 or 10 infectious viruses per 100 cells. Finally, one has to decide whether a medium exchange or medium feed is necessary at time of infection. This decision usually depends on the medium composition and the duration of the cell growth phase. If the growth medium hinders virus infection in any way or nutrients do not suffice for growth and infection phase, a feeding or exchange strategy might be necessary. Now, virus seed can be added to the cell preculture and the infection phase starts. Upon infection, cultivation parameters might be changed (box no. 4 in Figure 2.10). A reduced temperature for example might be chosen in order to reduce temperature-triggered degradation of active virus particles. Control of the pH in this phase can be crucial as very low or very high pH conditions (<6 or >8) might destroy virus surface proteins and the viral envelope. During process development, identification of an pH optimum or an optimal range might thus be required.

During the infection phase, the process can be monitored at different levels. Using controlled systems, cultivation parameters pH, temperature, DO, agitation rate (e.g. given in rounds per minute, rpm) and aeration are usually monitored. Also, the monitoring of several cell-related parameters might be interesting. Cell concentration and viability, cell metabolism, morphology and generally cell physiology might be of interest. In this project, cell physiology means cell cycle and apoptotic status as well as infection status of a cultured cell population. Knowing these parameters might allow to gain insights into the interaction between virus and host cell and give indications for process bottlenecks. Of highest importance to judge the process success is to follow the increase of virus titer and of course the final virus yield (box no. 5 and 6, respectively, in Figure 2.10). This will also determine the harvest time which for the system MVA/CEF is usally between 48 and 72 hpi, but can be dependent on the host cell line. Virus titration is done by $TCID_{50}$ or plaque assays which determine the concentration of active virus particles in a sample [122]. Although they are time-consuming and prone to various errors [123], their application is indispensable to determine virus infectivity and therefore product quantity and quality. Another possibility to follow the spread of virus in the culture is to measure the amount of viral genomes for example via PCR. In contrast to titration methods, these assays estimate the total amount of virus particles in a sample. Dosage of MVA as live-attenuated vaccine, however, is adjusted by infectious virus units per dose and thus, the $TCID_{50}$ (or plaque) assay is more important than PCR methods for product quantification.

With MVA, one process specificity needs to be considered. As seen in Figure 2.8, different MVA virion forms can exist in the cells (IMVs and IEVs), attached to the cells (CEVs), or outside of the cells (EEVs). To harvest the maximal amount of infectious virions, cells should be disrupted in freeze-thaw and sonification steps before quantification and downstream processing.

2.3 Influenza virus and influenza virus vaccine production

Each winter season, influenza epidemics occur across the globe. These seasonal influenza epidemics are estimated to annually cause 3–5 million cases of severe illness and between 0.25 and 1 million deaths worldwide [124]. Of even greater economic impact, however, are the large numbers of mild to moderate cases resulting in productivity losses, absenteeism and costs on the health services. Economic losses are difficult to calculate. One study estimates, for example, that influenza epidemics directly and indirectly account for losses of approximately 10 billion US dollars per annum – only in the United States [125]. Furthermore, if a new virus strain with efficient abilities to transmit from human-to-human meets a naïve population, a pandemic might occur. So far, human mankind has suffered from three devastating influenza pandemics: the Spanish flu 1918, the Asian flu 1957 and the Hongkong flu 1968. In 2009, the most recent pandemic, the so-called swine flu, occurred which was not as fatal as the ones before. In addition, from 2003 until today, avian influenza H5N1 has caused 641 confirmed infections of humans mainly in Southeast Asia and Africa. Therefrom, 380 were lethal [126]. It is not clear when and how threatening the next pandemic will be and which subtype will be involved, but enormous efforts are on the way to be prepared and to prevent the projected millions of deaths that a devastating pandemic could cause today [9]. With such numbers and perspectives, the significance of measures against influenza infections becomes clear. Typically, soon after infection with influenza virus, patients suffer from fever, aching muscles, headache, cough and a running nose. With an influenza infection, there is a significant risk to develop severe complications like bronchitis, pneumonia or the development or worsening of a chronic congestive heart failure. Besides antiviral drugs, vaccines are the most effective measure against influenza epidemics as well as pandemics.

In this section, the influenza virus will be introduced first (chapter 2.3.1). Then, influenza vaccines and their current egg-based production process will be described before the possible improvement of timelines and production capacity with cell culture-based production is addressed (chapter 2.3.2). Therein, process parameters that need to be considered when developing a new process are introduced.

2.3.1 Influenza virus

All information given in this chapter are based on basic virology books and reviews that are referenced here, if not stated otherwise [127, 128].

Structure and classification

Influenzavirus A, influenzavirus B and *influenzavirus C* are three genera within the family of *Orthomyxoviridae*. In humans, only influenza A and B viruses are of epidemiological interest. Therefore, influenza C viruses are not considered here.

Influenza virions are pleomorphic particles (mainly spherical or filamanteous) with 80–120 nm in diameter – one fourth of MVA virions. They are enveloped viruses with a segmented genome. Eight segments of single-stranded negative-sense RNA, varying in size from 890 to 2,341 nucleotides, encode for 14 known proteins (Table 2.3). Some of them are splice variants and are presumably not produced regularly.

Table 2.3: Influenza virus proteins: nomenclature, segment localization and functions.

Protein	Segment	Known or putative functions
Polymerase B1 protein, PB2	1	Together form the RNA polymerase, which is responsible for replication and transcription
Polymerase B2 protein, PB1 *Splice variants: N40 & PB1-F2*	2	
Polymerase A protein, PA *Splice variant: PA-X*	3	
Haemagglutinin, HA	4	Receptor binding; mediates membrane fusion of cell and virus and thus induces infection and release of progeny viruses; major antigen
Nucleocapsid protein, NP	5	Principal component of the nucleocapsid, induces host cell immune response
Neuraminidase, NA	6	Cleaves cellular neuraminic acid, prevents virus aggregation, ensures release of newly synthesized virus particles
Matrix protein 1, M1	7	Forms the matrix, helps in packaging nucleocapsids into emerging virus particles
Matrix protein 2, M2 *Splice variant: M42*	7	Acts as proton channel, thus regulates pH
Non-structural protein 1, NS1	8	Post-transcriptional RNA control, affects cellular antiviral defense as virulence factor
Non-structural protein 2, NS2 (also named nuclear export protein, NEP)	8	Responsible for transport of new nucleocapsids from nucleus to the cytoplasm

The genome is covered by a matrix consisting of M1 proteins, which itself is wrapped by a host cell-derived lipid membrane. Prominent projections on the membrane are formed by HA and NA proteins (Figure 2.11).

As surface glycoproteins, HA and NA proteins are the main antigenic determinants. Based on both antigens, influenza A viruses are subdivided into subtypes, determined by 18 H (H1-H18) and 11 N (N1-N11) variants. Several combinations occur in nature with H1N1 and H3N2 being the subtypes circulating in humans at the moment. Other exotic subtypes have only been found recently in their natural host, for example a H17N10 virus which was found 2012 in fruit bats [129] or a H18N11 virus found in Peru in bats as well [130]. HA or NA variants are not present in influenza B viruses. Influenza viruses are connotated with the type (A or

B), the host species (not indicated if human), the geographical site the isolate has been found, a serial number, the year of isolation, and the H and N variants in brackets. One example would be: A/PuertoRico/8/34 (H1N1).

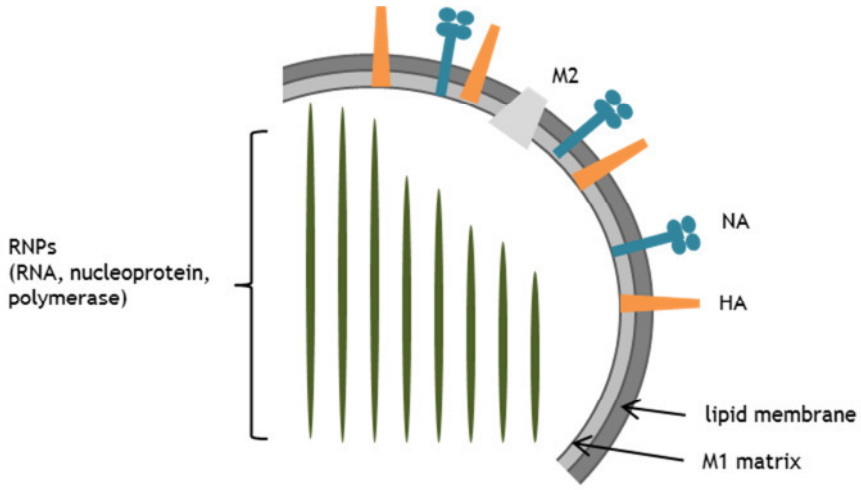

Figure 2.11: Schematic structure of an influenza A virus. The eight RNA segments are arranged together with viral polymerase and nucleoproteins as ribonucleoproteins (RNPs). They are surrounded by an envelope consisting of M1 proteins and a host cell-derived lipid membrane. Surface proteins are matrix protein 2 (M2 which acts as a proton channel) and the main antigens heamagglutinin (HA) and neuraminidase (NA) that define the virus subtype.

Replication cycle

Influenza viruses bind to sialic acid residues on cellular glycolipids and glycoproteins via the HA protein. The way those sialic acids are bound to the penultimate galactose of the glycostructures thereby determines host specificity. Viruses that are able to recognize α-2,6 linkage are able to infect humans, viruses recognizing α-2,3 linked sialic acids are able to infect birds. After attachment, viruses are internalized by endocytosis. Several molecular processes then follow, ending in the release of viral ribonucleoproteins (consisting of viral RNA, the nucleoprotein NP and viral polymerase) into the cytoplasm. Approximately 20–30 min after attachment, RNPs are transported into the nucleus. Here, viral RNA is transcribed into viral mRNA that is transported back into the cytoplasma to be translated by the cellular ribosomal machinery. After processing in the endoplasmatic reticulum and the Golgi apparatus, the now glycosylated viral proteins are delivered to the cell membrane. In parallel, positive sense cRNA is made from negative sense viral RNA so that cRNA can serve as template for replication of vRNA copies. New ribonucleoprotein complexes are built, and assemble with the viral proteins at the cell membrane. Finally, the release of particles from the cell is mediated by the NA protein. In total, approximately 6 h elapse from entry of one virus particle to release of first progeny particles.

Transmission and evolution

Influenza viruses occur in many species – amongst others birds, domestic animals and humans. Generally, influenza virus subtypes are highly species-specific (because of the different sialic acid linkages at their cellular receptors). Transmission of avian influenza viruses to humans, for example, has only been observed for four subtypes H5N1, H7N3, H7N7 and H9N2 [126]. To allow for interspecies transmission, mutations must occur in viruses travelling between birds and humans, e.g. the H5N1 virus subtype. Influenza viruses are evolutionary dynamic viruses with high mutagenic rates. A missing proofreading function of the RNA polymerase and thus misincorporation of nucleotides can result in virus evolution called antigenic drift. This drift is the molecular explanation for the seasonal epidemics and consequently explains the necessity of new seasonal vaccines ever year. If the viral genome is reassorted by a co-infection of one host with two different virus strains and haphazard segment exchange, this is called antigenic shift. For example, the H1 can thus be replaced by H3 (this is also possible for the NA of course). Eventually, viruses then evolve that replicate more efficiently or which show a faster transmission. The principle of reassortment of viral segments is also used in vaccine production to generate highly propagative strains. By using the HA and NA segments from circulating strains and the other segments from a well-propagating strain (often A/PuertoRico/8/34 H1N1), so-called high-growth reassortants are created. Those strains show the desired antigenicity, but are also propagating quickly in eggs or cell substrates to high titers so that vaccine production is accelerated.

If altered viruses in nature hit a population that is not pre-immunized by cross-protection or earlier epidemics and if these viruses also acquire high transmission rates, a pandemic is likely to occur. Overcrowded cities, high mobility and globalization additionally facilitate a rapid spread of influenza virus. Besides the use of antiviral drugs which is a possibility to treat the disease itself, vaccines are the most efficient measure against influenza epidemics and pandemics. Influenza virus vaccines and their production will be explained in the next sections.

2.3.2 Influenza virus vaccines and their production

The permanent mutations of influenza viruses due to antigenic shift and drift demands a year-round surveillance of circulating strains. Clinical specimen are collected throughout the influenza season and characterized antigenically and genetically. New strains or variants that are suggested for use in the seasonal vaccine are then produced in eggs. In few specialized labs, high growth reassortants are produced from those egg isolates (usually by

reassorting the HA and NA genes of the isolate with the other 6 segments from the H1N1 strain A/PR/8/34). Only after the vaccine strain candidates have been evaluated and released by regulatory agencies, vaccine manufacturers can begin to develop a vaccine production process [131].

2.3.2.1 Current vaccines and their egg-based production

In the last decades, trivalent vaccines were produced. They combine three virus strains in one vaccine, mostly one H1N1 strain, one H3N2 strain and one B strain. In 2013/14 for example, the vaccine comprised an A/California/7/2009 H1N1 strain (pandemic 2009-like), an A/Victoria/361/2011-like H3N2 strain and a B/Massachusetts/2/2012-like strain (B/Yamagata lineage). A quadrivalent vaccine was approved for the first time in 2013, additionally including a B/Brisbane/60/2008-like strain (B/Victoria lineage). Each influenza vaccine contains 15 µg of HA antigen per strain. Mostly, inactivated vaccines (whole virus, subunit or split vaccines) are used so far, which are administered by intramuscular injection. Although inactivated vaccines have shown to be safe and well tolerated with an efficacy of 60–95% [132], they mediate only low levels of cellular immunity and cross-protection [133]. To improve the immune response, the addition of adjuvants has been tested and, for example the adjuvant MF59 has been used in Novartis' pandemic vaccine of 2009/2010. However, risks are or might be associated with adjuvants and thus the more feasible way is to improve the antigenicity of the vaccine itself. One approach to achieve this is to use live-attenuated virus strains in the vaccine.

Live-attenuated influenza vaccines (LAIVs) contain cold-adapted, temperature-sensitive influenza virus strains (usually three as in trivalent inactivated vaccines) and are administered through a nasal spray. Cold-adaptation allows those strains to replicate at temperatures below body temperature. Temperature-sensitivity inhibits replication at temperatures at or above body temperature. In the upper respiratory tract, virus strains can replicate to a minimal degree and thus mimick a natural infection with influenza viruses. Most likely due to this, LAIVs induce not only strain-specific immunity, but also T cell responses that may be cross-reactive and thus contribute to protection against a wider spectrum of influenza A and B strains [134-136]. In the lower respiratory tract, however, the temperature-sensitive viruses cannot replicate. Downstream processing requirements are less stringent and thus less expensive for mucosal LAIVs. Moreover, as the vaccine is not administered intramuscular or intradermal, no sterile needles or trained staff is required for vaccination, which greatly simplifies distribution and application. LAIVs have been developed and used since the 70s and are now approved as vaccines in US, Canada, Russia and Europe. Today, FluMist® (MedImmune) and related vaccines are used to an extent of

about 9% in the US [132]. Since 2011, the European analogue Fluenz® is also on the market. So far, all LAIVs are produced in egg-based processes [22]. In the next years, however, an increase of LAIV use is expected with the WHO encouraging this development as part of the global pandemic influenza action plan [31].

Cold-adaptation is usually achieved by passaging the virus in cell cultures or eggs that are incubated at 25°C [137, 138]. After several passages, temperature-sensitivity is tested by temperature challenge studies (incubation at higher temperatures). In addition, genome analyses are carried out in order to identify temperature-sensitive markers that seem to be an indication for temperature-sensitivity [29, 139, 140]. Otherwise, LAIV strains are generated like inactivated vaccines – by genetic reassortment of circulating strains with a master donor strain. Thus, not every circulating strain needs to be adapted to low temperatures. Like the A/PR/8/34 strain for inactivated vaccines, usually the same cold-adapted and temperature-sensitive master donor strains are used as backbone (Table 2.4) [28, 141].

Table 2.4: Cold-adapted master donor strains used for industrial production of LAIV.

Strain	Subtype	cold-adaptation by
A/AnnArbor/6/60	H2N2	passaging at 25°C in primary chicken kidney cells
B/AnnArbor/1/66	-	passaging at 25°C in primary chicken kidney cells
A/Leningrad/134/17/57	H2N2	~50 passages at 25°C in chicken eggs
A/Leningrad/134/47/57	H2N2	~50 passages at 25°C in chicken eggs
B/USSR/60/69	-	~50 passages at 25°C in chicken eggs

The majority of live-attenuated as well as inactivated influenza vaccines are still produced in eggs. However, egg-based influenza vaccine production involves several problems. One problem ist that in case of a pandemic or surprising epidemics egg supply from the specialized flocks might be problematic or take too many time. Usually 4-6 months pass with classical egg-based vaccine production from the decision that a certain virus strain shall become a vaccine strain until the release of the first vaccine batch. Long timelines also limit production capacities. The number of vaccine doses produced in the season 2011/2012 was 1 billion. Projected for 2015/2016 are 1.7 billion doses that will be produced worldwide. These numbers might sound comfortable. However, taking into account approximately 7 billion people worldwide, a critical shortage in vaccine supply in case of a pandemic is obvious, especially because seasonal vaccine production already uses manufacturer's full capacities [9]. A production process with shortened timelines would reduce the time without vaccine protection between an upcoming epidemic or pandemic and the availability of a vaccine and is thus currently the biggest aim. Cell culture-based production does not rely on egg-supply and could help to overcome limitations that are

connected with egg-based production. Some are immense logistics, possible allergic reactions, shortages in vaccine supply in case of an avian influenza epidemic, possible contamination with adventitious agents and long start-up times for a process. The next section introduces the approach of cell culture-based influenza vaccine production that has been enforced in the last years.

2.3.2.2 Cell culture-based influenza virus vaccine processes

The above mentioned limitations of egg-based production might be overcome by cell culture-based processes. Ideally, such a process will be optimized in terms of process time and yield, costs (raw materials, purification), approval (cells and conditions that fit regulatory requirements) and feasibility of production also in developing countries.
Like for MVA production, the cell line used as substrate must be carefully chosen at first. Adherent cell cultures have been used since decades for influenza vaccine production development and are thus well understood. Common cell lines are adherently growing MDCK or Vero cells, cultivated in either static sytems or in reactors with the help of microcarriers as attachment substrate. However, the necessity to use microcarriers impairs scalability. Suspension cell cultures are therefore considered as the more promising substrate for future cell culture-based manufacturing. Suspension MDCK [142-144] and Vero cells [145, 146], PER.C6 cells [13], HEK293 cells [42] and EB66 cells [14] are available. The feasibility of all those cell lines to produce sufficient virus amounts in high quality has been proven.
After having chosen a cell line, process parameters and modes have to be evaluated and optimized with the aim to set up a process yielding high titers in short time. Most parameters already played a role in MVA production (see Figure 2.10) and are thus not repeated here. However, some issues only need to be considered in influenza virus vaccine production. Those are addressed in this paragraph.
Master seed viruses produced in eggs can be obtained for example from the National Institute for Biological Standards and Control (NIBSC). Due to their high host cell specificity, the adaptation of master seed virus to the used host cell line is crucial for influenza virus production [147]. In this work, MDCK-derived seed viruses were used so that an adaptation from MDCK towards CR or CR.pIX cells had to be performed. The number of passages that are needed to adapt the virus can take 1 to 10 passages. During adaptation, virus titers and virus dynamics are monitored in order to ensure the generation of a highly active seed virus which spreads fast in the cell population. For the growth phase, the same parameters as for MVA production play a role. A cell density effect has been described for influenza virus propagation [42, 119]. As for suspension cells high CCI can be used, the critical CCI is at best identified already during initial process development. For overcoming this effect or in

general for increasing space-time yield, different process strategies besides batch processes have been evaluated showing that perfusion processes are a vital option to improve virus yields [119-121].

For optimization of an influenza production process, one parameter adds to the list for MVA production optimization: trypsin addition (needs to be added to box 3 in Figure 2.10). Release of influenza particles from a cell and thus the ability to infect neighbour cells depends on the HA protein. This function, however, only works if the HA protein is cleaved. Addition of a protease (usually trypsin) to the cell/virus suspension provokes HA cleavage and also interferes with the antiviral defense of the host cell [148, 149]. Thus, trypsin enables influenza virus spread in the culture. The time of trypsin addition, addition regime (once or several times in intervals), and the amount of trypsin (i.e. trypsin activity) that is added, must be optimized [150]. Thereby, the optimum has shown to depend on the host cell which might release protease inhibitors and thus impair trypsin activity [151].

In contrast to MVA, for influenza virus often very low moi between 0.0001 and 0.05 are chosen. Again, this parameter needs to be re-tested for every influenza virus strain as shown by Aggarwal et al. using LAIV [152], but also for A/PR/8/34-based reassortants [75, 153]. Process optimization needs to be supported by assays. Thereby, it is most important to measure the product concentration. i.e. infective virus particles and total number of virus particles. Influenza viruses (like MVA) can be quantified by $TCID_{50}$, plaque assays or PCR methods. One method, however, which is less complicated, can be used in addition. In the so-called heamagglutination assay (HA assay), virus sample dilutions are mixed with erythrocytes. Due to the capability of the HA protein to agglutinate red blood cells, the agglutination power of the sample dilutions can be used to estimate the number of virions in a sample. This assay only takes few hours and thus considerably facilitates monitoring of the virus concentration during the process.

When having optimized or tested the parameters listed in this chapter, it should be possible to set up a reproducible production process for influenza virus.

3 Materials and methods

All materials and methods used to generate the results of this project are explained in this chapter. Detailed information about the devices and materials that were used can be found in the Appendix (Tables A1). Used SOPs from the Bioprocess Engineering group at the MPI Magdeburg are either given in detail in the Appendix or listed in Appendix A6.
Four sub-sections will describe how CR and CR.pIX cells were cultivated (chapter 3.1), which analytics and methods were used to analyze cell physiology and metabolism (chapter 3.2 and 3.3), how infection experiments with MVA were done and analyzed (chapter 3.4) and finally, how influenza infection experiments were performed and analyzed (chapter 3.5).

3.1 Cultivation of CR and CR.pIX cells

This first sub-section of materials and methods lists the cell stocks and media used for proliferation of CR and CR.pIX cells and how cultivations in different cultivation systems (T-flasks, shaker flasks, STR and Wave bioreactor) were performed.

3.1.1 Cell growth media

At the beginning, CR and CR.pIX cells were grown in AEM, a serum-free medium originally developed for growth of HEK293 cells which was freshly supplemented with 4 mM glutamine before usage. Later, a chemically-defined medium CD-U2 was available and replaced AEM. In order to cultivate the cells as done by ProBioGen, which used Glutamax (a stable dipeptide of glutamine and alanine, which however cannot be measured in the first 12–48 h of the cultivation), CD-U2 was supplemented with 2 mM glutamine and 2 mM alanine separately. In addition, 10 ng/mL Long-R3 IGF were added.

3.1.2 Working cell bank

CR and CR.pIX cultures from a cell bank of ProBioGen were cultured, and working cell banks were established and stored in liquid nitrogen or its gas phase (-196°C or -155°C, respectively). During the whole project, several passages were frozen and stored, namely passage numbers 15, 23 and 24 (starting with cell bank from ProBioGen as 1st passage). Cell

concentrations of 1–2x10^7 cells/mL were therefore aliquoted in fresh medium containing 10% DMSO in cryo tubes and frozen at -20°C for 2 h. Then, cells were transferred to a -80 °C freezer and at the next day stored in liquid nitrogen.

Thawing of cells was done by quick thawing in a water bath, mixing the cryo content with 15 mL medium and subsequent centrifugation (150xg, 7 min) to remove remaining DMSO. The cell pellet was re-suspended in 6 mL fresh medium and cell suspension was pipetted into a T25 flask and incubated under standard conditions. After 1 or 2 days, cells were counted and transferred to a bigger flasks or a shaker flask by either dilution or re-suspension (after centrifugation) in fresh medium.

3.1.3 T-flask and shaker flask cultivation

For back-up cultures, pre-cultures and small-scale experiments, cells were cultivated in either T-flasks or baffled shaker flasks. T-flasks were incubated at 37°C and 5% CO_2 in a static incubator. Baffled shaker flasks were agitated at 185 rpm in an Infors orbital shaker with 5 cm amplitude. Cells in shaker flasks were also incubated at 37°C with 5% CO_2. For some experiments, the temperature was varied, but this will be indicated at the respective experiment. Inoculation of a new passage was always done with a start cell concentration of 8x10^5 cells/mL. If the necessary splitting ratio was higher than 1:5, cell suspension was mixed with fresh medium to achieve the desired cultivation volume and cell concentration. For lower split ratios, cell suspension was centrifuged and cells were re-suspended in fresh medium. Passaging of the cells was performed until passage number 100 as the cells had been proven to be stable until this passage number. Different volumes and incubation parameters were used for different flask sizes (Table 3.1).

Table 3.1: Parameters used for cultivation of CR and CR.pIX cells in T-flasks and shaker flasks.

Vessel	T25	T75	T175	Small shaker	Big shaker
Nominal capacity [mL]	50	250	550	125	250
Working volume [mL]	6	15	50	50	150
Shaking frequency (rpm)	-	-	-	185	185

3.1.4 Cultivation in 1 L stirred-tank bioreactor

As inoculum, cells from 3–4 day old shaker flask pre-cultures were taken after centrifugation (200xg, 10 min) and re-suspension in fresh CD-U2 medium. The stirred-tank reactor (STR) was filled with this cell suspension (as in small-scale systems, the starting cell concentration was 8x10^5 cells/mL) and started. Monitoring and control of cultivation parameters were

carried out with the cellferm-pro® system (DasGip AG). Bioreactors were equipped with pitched-blade stirrers and the stirring speed was always constant at 120 rpm. Cultures were aerated by pulsed submers aeration with air enriched with a variable content of O_2 and CO_2. Together with 1M Na_2CO_3, this allowed a two-sided control of pH via CO_2 or base addition. The DO set-point of 50% was controlled via O_2 addition. The pH value was allowed to drop from 7.4 to 7.0 during the first 72 h of cell growth and controlled at pH 7.0 afterwards. During cell growth, the temperature was set to 37°C. Only for infection experiments using cold-adapted influenza virus strains, the temperature was reduced at time of infection to 33°C. In the Appendix, Table A2 gives more information about the controller settings.

3.1.5 Cultivation in 1 L Wave bioreactor

The inoculum for starting a Wave bioreactor was prepared as for the STR reactor. 2 L Wave bags (Sartorius, working volume 1 L) were used which are pre-sterilized and contain all necessary ports for aeration and sampling. Two bags could be incubated simultaneously on the reactor platform. It is important to note that pH and DO could not be controlled in the Wave bioreactor. Only addition of air, CO_2 and O_2 could be set to a certain value. An aeration unit was used to provide the cells via headspace aeration with 220 mL/min air enriched with 21% O_2 and a variable content of CO_2, which was dependent on the pH of the cell suspension. At the beginning of the cultivation, when pH was between 7.3 and 7.5, CO_2 fraction was set to 7.5%. When pH decreased during cultivation, it was adjusted to 5% or even 2.5%. The Wave bioreactor was agitated using a rocking speed of 15 rpm and an angle of 8%. Due to a temperature sensor below the bags, a temperature of 37°C could be constantly held during cell growth. For some experiments concerning the propagation of cold-adapted influenza strains, the temperature was reduced to 33°C after growth phase.

3.2 Measurement of physiological cell parameters

Measurement of cell concentration is crucial as this parameter is needed for example to determine the inoculation volume, to calculate growth rates as well as uptake and release rates of metabolites and finally to determine the correct moi in virus infection experiments. Therefore, measurement of cell concentration (always measured in conjunction with cell viability) is the main method described here. Furthermore, cell physiology during cell proliferation and after infection with virus was analyzed by using flow cytometric methods that determine the cell cycle and apoptotic status of the cell population. These methods are also described in this subsection.

3.2.1 Measurement of cell concentration

Cell concentration, viability and average cell diameter of CR and CR.pIX cells were determined using the ViCellXR device (BeckmanCoulter). This device stains the cells with trypan blue, takes 100 pictures of the sample while passing through the flow cell, and analyzes pictures with image analysis software. Several parameters like minimum cell diameter or minimum circularity have to be carefully adjusted to find the most suitable way to count and analyze each cell line. After carefully choosing those parameters and a validation, a protocol "Entenzellen" (for protocol and validations see Appendix A3) was established with which the measurement precision was validated to be 5% in maximum. Samples from bioreactor experiments were counted in triplicates, whereas samples from T-flasks or shaker flasks were only measured once due to to volume limitations.

3.2.2 Measurement of cell cycle status by flow cytometry

The cell cycle phases correlate directly with the DNA content of a cell. Therefore, one can distinguish different phases by staining cells with PI that intercalates into the cell DNA.
In this work, approximately $1x10^6$ cells from a growing or infected culture were fixed in ethanol overnight (then stable for up to 6 months) and subsequently stained with PI. With this procedure, cells in apoptosis that contain less than one chromosome set (subG0G1 cells), resting cells in G0/G1 phase with one chromosome set, cells in synthesis phase S with 1-2 chromosome sets and resting cells in G2/M phase with 2 chromosome sets can be distinguished.

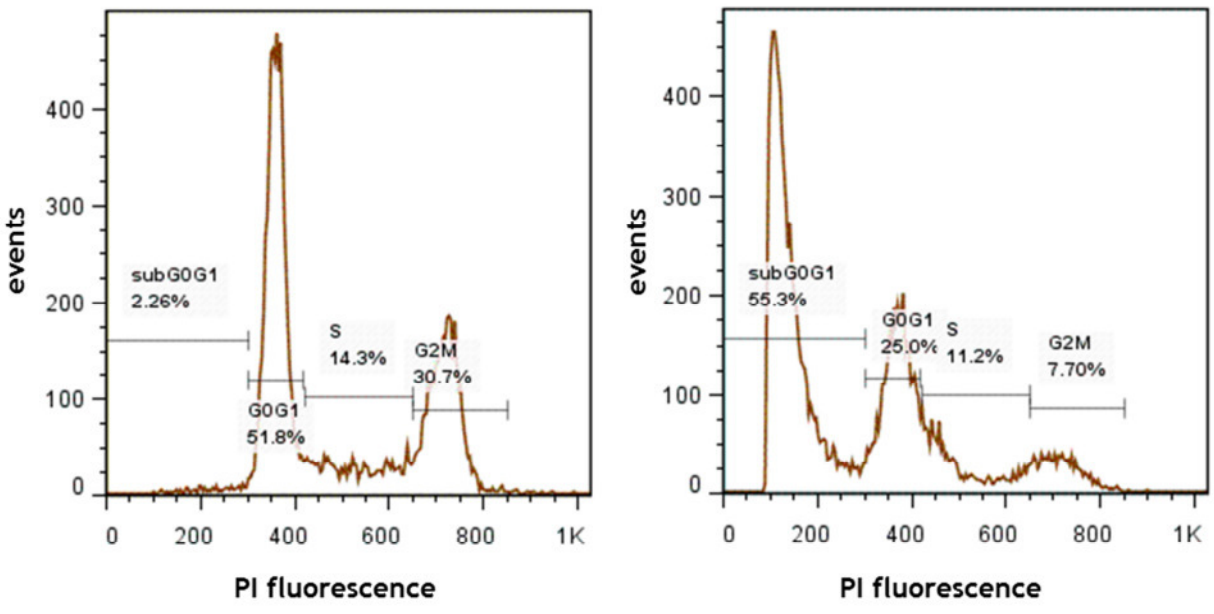

Figure 3.1: Cell cycle histograms of CR.pIX cells. Left: Healthy cells from exponential growth phase (60 h after inoculation); right: cells that have been incubated for 24 h with 1 µM staurosporine to induce apotosis.

Measurement was done with the flow cytometer EpicsXL (BeckmanCoulter) and generated data was analyzed using the FlowJo software (TreeStar Inc., version 7.6.3). Details on staining and analysis procedure are described in the respective SOP (Appendix A4). In preliminary experiments, the apoptosis inducing agent staurosporine in different concentrations was used as a control for gate-setting. Generally, cell cycle distribution histograms look like the examples given in Figure 3.1.

3.2.3 Measurement of apoptotic status by flow cytometry

The apoptotic status of the cells is of interest in particular during infection and was analyzed with the GuavaNexin Reagent. It detects phosphatidylserine at the outer membrane by binding of annexin V, which is labeled itself with phycoerythrine (PE). Cells showing PS at the outer side of the membrane are defined to be early apoptotic as they already induced membrane permeabilization. A second marker in the GuavaNexin assay is 7-AAD that (like trypan blue) enters dead or necrotic cells that already lost their membrane integrity. Overall, four cell populations can be distinguished with this reagent: i) viable cells (not stained), ii) early apoptotic cells (only stained with the orange-fluorescing annexin-PE, iii) late apoptotic or necrotic cells (stained with annexin-PE and red-fluorescing 7-AAD) and iv) cell debris (stained with 7-AAD). Examplary plots of these four populations are shown in Figure 3.2.

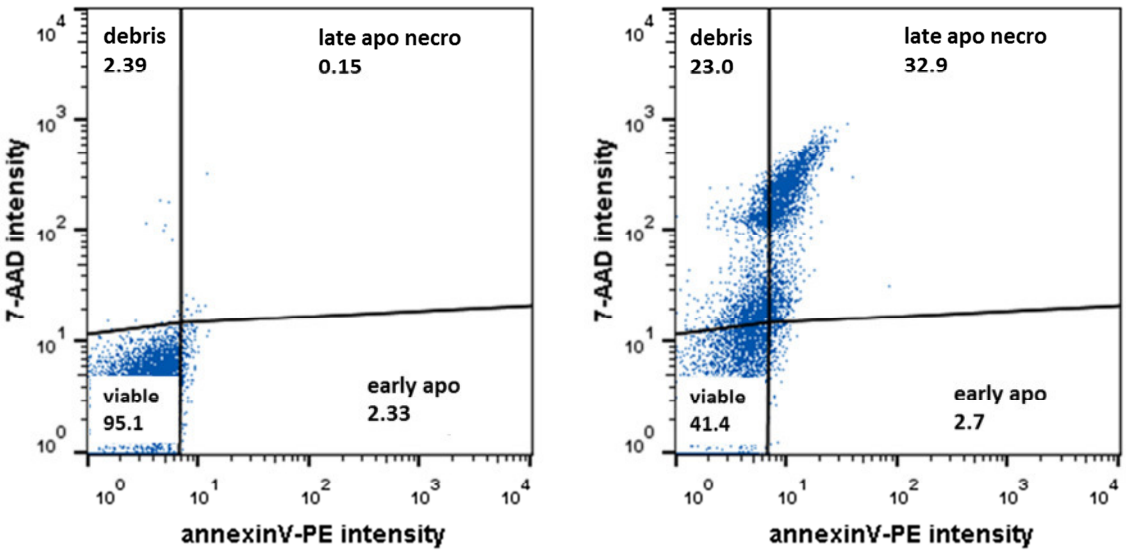

Figure 3.2: Flow cytometric analyses of cell samples stained with 7-AAD and annexinV-PE (GuavaNexin kit). Left: Unstained sample of CR.pIX cells infected with MVAegfp for 120 h; Right: Stained sample of CR.pIX cells infected with MVAegfp for 120 h. Gates had been set with unstained sample taken directly before infection.

When establishing this assay, cells were incubated with staurosporine, valinomycin and MVA to induce apoptosis and to generate controls for gate setting. For every sample, an unlabeled negative control was prepared and measured in parallel. When analyzing cells that were infected with the virus strain MVAegfp (a recombinant MVA leading to the production and accumulation of EGFP protein in infected cells), compensation was done for flow cytometry to account for signal overlapping of EGFP and PE fluorescence. The plots derived from such a sample are shown as example in Figure 3.2B. The complete procedure is given in the SOP shown in Appendix A5.

3.3 Materials and methods used for metabolic studies

All methods and procedures that were needed to characterize the growth performance and the metabolism of CR and CR.pIX cells, are described in this section. The analytics used to determine biomass composition and extracellular metabolite concentration provide the basis for MFA (chapter 4.1.3.3). As this analysis method was not developed in this work, the focus will be on the general principle and application of this method.

3.3.1 Measurement of metabolite concentrations

Different methods and devices were used to measure extracellular metabolite concentrations. Glucose, lactate, glutamine, glutamate and ammonia concentrations were measured using the BioProfile 100plus (Nova Biochemicals) that determines sample concentrations enzymatically (SOP see list Appendix A6). Concentrations of amino acids were quantified via anion exchange HPLC [154]. Only for cultivations used for MFA, amino acid concentrations were additionally quantified in the cell culture group of Prof. Noll at the University of Bielefeld. There, amino acid concentrations were measured with a HPLC device after derivatization [155]. Pyruvate concentrations were determined using another HPLC method [156], and uric acid concentrations were detected with a commercially available enzymatic assay (Uric Acid Assay Kit, BioVision, method not validated). Table 3.2 summarizes the methods for metabolite concentration measurement and the standard deviations that were obtained from method validations.

Table 3.2: Standard deviations of the method as derived from validation of methods to measure metabolite concentrations.

Metabolite	Standard deviation of the method	Device
Glucose	0.39 mM[b]	BioProfile100plus (Nova Biomedicals)
Lactate	0.30 mM[b]	
Glutamine	12.8%[a]	
Ammonium	4.5%[a]	
Glutamate	0.03 mM[b]	
Pyruvate	2.1%[a]	HPLC (DX-320, Dionex)
Alanine	8.6%[a]	HPLC (ICS-5000, Dionex)
Arginine	3.2%[a]	
Asparagine	0.44 mM[b]	
Aspartate	0.55 mM[b]	
Cysteine	0.09 mM[b]	
Glycine	2.7%[a]	
Histidine	0.54 mM[b]	
Isoleucine	0.64 mM[b]	
Leucine	0.56 mM[b]	
Methionine	0.33 mM[b]	
Phenylalanine	0.13 mM[b]	
Threonine	0.11 mM[b]	
Tryptophane	0.22 mM[b]	
Tyrosine	0.32 mM[b]	
Valine	0.82 mM[b]	
Uric acid	-	enzymatic assay

[a]relative standard deviations of the method were taken for parameters that have shown an inhomogeneity of variances
[b]absolute standard deviations of the method were taken for parameters that have shown homogeneous variances

3.3.2 Determination of biomass composition

Cell dry weight and biomass composition of CR and CR.pIX cells were determined from samples of exponentially grown cells in order to generate information needed for a profound MFA. Generally, for each of those assays, three biological replicates and at least three measurements were done per sample. If present, outliers were excluded for calculation of averages and standard deviations.

Measurement of cell dry weight was done by weighing a defined amount of cells in fresh medium against fresh medium without cells after drying the samples at 60°C. The elemental composition was determined externally (Labor Pascher, Remagen). Cellular protein content was analyzed using the BCA assay (Pierce/ThermoScientific). Therefore, the cell lysate from a defined amount of cells was prepared. Amino acid content of whole cell protein was determined with the HPLC device used for amino acid quantification after acidic hydrolysis in HCl. DNA and protein contents of the cells were determined using cell lysate from a defined amount of cells after purification of DNA and RNA. The QIAamp DNA Blood Mini kit

(Qiagen) and the NucleoSpin RNAII kit (Macherey-Nagel) were used therefore. DNA and RNA concentrations were determined by absorption measurement of the samples. A more detailed description of the sample preparation and measurement principles can be found elsewhere [157]. Standard deviations for cell dry weight as well as RNA, DNA and protein concentration measurements were not determined by method validation, but by measuring replicates from independent samples.

3.3.3 Determination of maximum *in vitro* enzyme activities

Maximum activities of four enzymes were determined in vitro in order to support results of MFA: pyruvate dehydrogenase (PDH, EC 1.2.4.1), pyruvate carboxylase (PC, EC 6.4.1.1), glutaminase (GLNase, EC 3.5.1.2) and glutamine synthetase (GS, EC 6.3.1.2). Therefore, assays described by Janke et al. were used [158]. The measured samples were generated by harvesting exponentially growing cells (72 h after inoculation), washing them in 0.8% NaCl and storing the pellet at -80°C until analysis. The parameters pH, dilution of sample and (for GS and GLNase) incubation time were varied and optimized. The respective SOPs are listed in Appendix A6.

3.3.4 Calculation of specific growth rate, substrate yields, metabolic uptake and release rates

It has to be noted that all calculated rates (growth rate, uptake and release rates) are specific rates, but will be referred to as rates.
The growth rate μ was estimated via linear regression of the logarithm of the cell concentrations in the exponential growth phase:

$$X(t) = X(t_0) \cdot e^{(\mu \cdot t)} \quad (1)$$

$X(t_0)$ thereby is the biomass that was present at start of the exponential growth phase, whereas X(t) is the biomass at a distinct cultivation time during the exponential growth phase. The biomass (X) can be either viable cell concentration (X_v) or – for MFA – dry cell weight DW, which was calculated from viable cell concentration and cell-specific dry weight. The cell death rate of cells was not considered in this work as only the exponential growth phase was analyzed. To describe cell metabolism and to compare different cultivations with each other, yield coefficients are often used. In this work, five yields are used and discussed. First of all, the four most important metabolites glucose, lactate, glutamine and ammonia can be put into relation by the yield coefficients $Y_{Lac/Glc}$ and $Y_{Amm/Gln}$:

$$Y_{Lac/Glc} = \frac{[Lac]_{t1} - [Lac]_{t0}}{[Glc]_{t0} - [Glc]_{t1}} \quad \text{and} \quad Y_{Amm/G\ln} = \frac{[Amm]_{t1} - [Amm]_{t0}}{[G\ln]_{t0} - [G\ln]_{t1}}. \tag{2}$$

The time t1 is the cultivation time where the highest viable cell concentration was achieved. $[Glc]_{t0}$ and $[Glc]_{t1}$ are glucose concentrations at the beginning of the cultivation (or exponential growth phase) and at the time point of maximum viable cell concentration.
Furthermore, the biomass (in this case as viable cell concentration) per substrate yields $Y_{XV/Glc}$ and $Y_{XV/Gln}$ were calculated to describe the utilization efficiency of main substrates glucose and glutamine:

$$Y_{X_V/Glc} = \frac{X_{V,t1} - X_{V,t0}}{[Glc]_{t0} - [Glc]_{t1}} \quad \text{and} \quad Y_{X_V/G\ln} = \frac{X_{V,t1} - X_{V,t0}}{[G\ln]_{t0} - [G\ln]_{t1}}. \tag{3}$$

Uptake or release rates of extracellular metabolites were determined via curve fitting (by least square estimation) of the concentration data to:

$$c_i(t) = c_i(t_0) + v_i \cdot \frac{DW(t_0)}{\mu} \cdot e^{(\mu \cdot t)-1} \tag{4}$$

Concentrations of metabolite i at starting time point (t_0) and the calculated specific growth rate μ from equation (1) were set as fixed parameters.
With this, the uptake or release rate v_i of each metabolite can be calculated. To avoid overestimation of glutamine uptake rates, this parameter was corrected afterwards to take into account spontaneous glutamine deamination. For determination of the glutamine degradation rate, STRs (n=3) were filled with CD-U2 medium (supplemented with the standard glutamine concentration of 2 mM) and run exactly under the same conditions as cell cultivations, but without adding cells. Over several days, samples were taken and the glutamine concentration was measured. From this time course of concentration, a glutamine degradation rate k_{Gln} of 0.0032 h^{-1} in CD-U2 medium could be obtained by linear regression of $\log[Gln]_t/[Gln]_0$ plotted over time.

3.3.5 Metabolic network and flux analysis

Data and flux analysis were both done within a collaboration project with Oliver Hädicke and Dr. Steffen Klamt from the group Analysis and Redesign of Biological Network of the MPI Magdeburg.

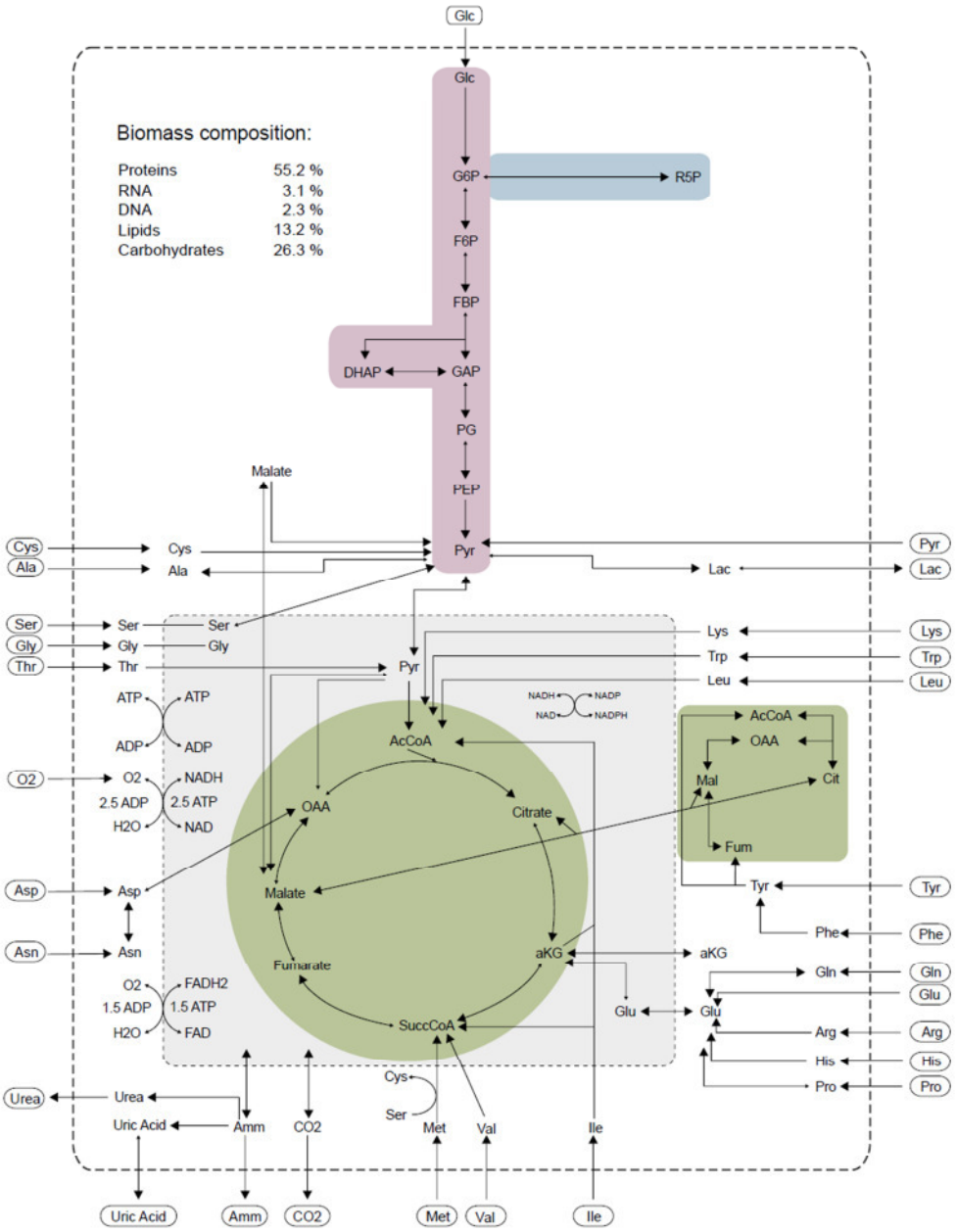

Figure 3.3: Scheme of the metabolic network used for characterization of the metabolism of avian CR and CR.pIX cells. The mitochondrial space is indicated with a grey background. Rosé: glycolysis, blue: pentose phosphate pathway branch, green: TCA cycle (cytosolic and mitochondrial), extracellular metabolites indicated with an oval border. Dashed lines illustrate membranes (cell membrane and mitochondrial membrane within). Arrows indicate defined reaction directions. Thereby, a small arrow head displays a possible, but unlikely reaction direction (e.g. PEP◄► PG).

A stoichiometric network model describing the central metabolism of CR.pIX cells was developed based on several metabolic networks described for mammalian and insect cell lines, entries in the KEGG database from *Gallus gallus* (chicken), *Meleagris gallopavo* (turkey) and *Taeniopygia guttata* (zebra finch), and based on literature dealing with metabolism of birds [64, 159, 160]. It consists of 97 reactions including 72 metabolites and describes the central carbon and nitrogen metabolism. It comprises uptake and release of substrates and waste products, glycolysis, TCA cycle, oxidative phosphorylation, transport

reactions, anaplerotics, catabolism of amino acids and synthesis of macromolecules (biomass). Schematically, the network is shown in Figure 3.3.

All reactions that are included are also listed in the Appendix (Table A7). This network as well as the biomass composition of CR.pIX cells and calculated exchange rates were implemented in the CellNetAnalyzer software [63]. The network can be downloaded there (www.mpi-magdeburg.mpg.de/projects/cna/cna.html).

Uptake and release rates were calculated as described before (section 3.3.4). To adequately account for analytical errors, a MonteCarlo analysis was performed using rates and their respective measurement errors (Table 3.2). Thus, 100,000 sample data sets were randomly generated. With this, extracellular rate ranges could be obtained that were imported into the CellNetAnalyzer. Only some uptake and release rates that were known beforehand to be inactive due to measurements were set to zero, e.g. alanine uptake, uric acid release and urea release. For flux variability analysis, no further constraints were set. The derived flux distribution with ranges (rate value plus/minus corresponding standard deviation as upper/lower boundaries for the rate) for every flux will later be discussed as “scenario 1”.

For some fluxes, further constraints had to be set after a first estimation in order to gain a determined system. Exchange rates were set as fixed constraints and additionally, the pyruvate-carboxylase (catalyzing reaction r46) was assumed to be inactive, as supported by enzyme activity measurement (see section 3.3.3). With these few constraints, the network was over-determined and a unique flux distribution could be computed. This flux distribution will later be referred to as “scenario 2”.

More detailed information on the metabolic network and the application of MFA and FVA can be found in the recent publication on this study [157].

3.4 Materials and methods used for MVA infection experiments

This sub-section lists materials and methods used for MVA infection experiments. First, MVA strains that were used to infect CR and CR.pIX cells are listed. Then, the infection procedure is described before two assays are introduced that were used to evaluate a successful infection: the $TCID_{50}$ assay to quantify active MVA particle concentrations and the infection status measurement via flow cytometry that was developed for cell populations that were infected with MVAegfp. Finally, calculations that were done in order to determine virus yields, are introduced.

3.4.1 Virus strains

To characterize the avian cell lines CR and CR.pIX as substrates for the production of MVA, two strains were used in infection experiments: the MVA wildtype (MVAwt) and a recombinant virus strain with an egfp gene insert (with the enhanced green fluorescent protein EGFP as a product). MVAwt starting material were working seed virus banks generated and filled at ProBioGen. MVAegfp seed virus that was genetically engineered based on MVAwt was obtained from the group of Prof. Sutter at the LMU Munich (Table 3.3).

Table 3.3: MVA seed viruses obtained as starting material for this project.

Virus strain	Derived/ obtained from	$TCID_{50}$ [viruses/mL]
Wildtype MVA	ATCC/LGC #VR-1508	$1.0x10^7$
Wildtype MVA	Working seed ProBioGen from 31.10.2007	$2.0x10^7$
Wildtype MVA	Working seed ProBioGen from 31.10.2007	$5.0x10^7$
MVAegfp*	Working seed LMU Munich, derived from MVA wildtype of A. Mayr	$1.0x10^8$

*more details on how this strain was constructed can be found in Appendix A8

3.4.2 Infection procedure

Before infection with MVA, cells were cultivated in CD-U2 until they reached a certain cell concentration. In contrast to the standard CCI of $2x10^6$ cells/mL for influenza infection, cells were routinely cultured until a cell concentration of $4x10^6$ cells/mL was obtained. Then, a 1:2 dilution with virus propagation medium was done. At the beginning of the project, when cells were cultivated in AEM medium, the virus production medium was MegaVir (HyClone). Later, after switch to CD-U2 proliferation medium, the chemically-defined virus production medium CD-VP4 (Biochrom) was used. Due to dilution, a final CCI of $2x10^6$ cells/mL was adjusted. For some experiments, the CCI was chosen even higher. Cells were then infected with using a desired moi with a seed virus volume (V_{sv}) that was calculated as follows:

$$V_{SV} = \frac{X_V \times V_c \times moi}{TCID_{50(SV)}} \tag{5}$$

with X_V as the viable CCI, V_C as the culture volume and $TCID_{50(SV)}$ as the titer of the used seed virus. If not indicated otherwise, a moi of 0.05 was used. Sampling was done as described previously. It has to be noted that the addition of virus medium results in a significant increase in culture osmolality, which leads to an aggregation of cells. The formed aggregates can comprise up to 50 cells, which are not identifiable as single cells anymore (see for example [161]). Therefore, ViCell measurements of cell concentrations and cell

viability had to be interpreted carefully. As an indication for a successful infection, cell viability was chosen.

As active MVA virions occur intra- and extracellularly, $TCID_{50}$ samples were subjected to a three-fold freeze/thaw procedure after sampling, sonicated for 1 min in a sonication water bath and finally centrifuged 10 min at 1500xg to remove cell debris (Fig. 3.4). Supernatants were then stored at -80°C until analysis of all samples belonging to the same experiment.

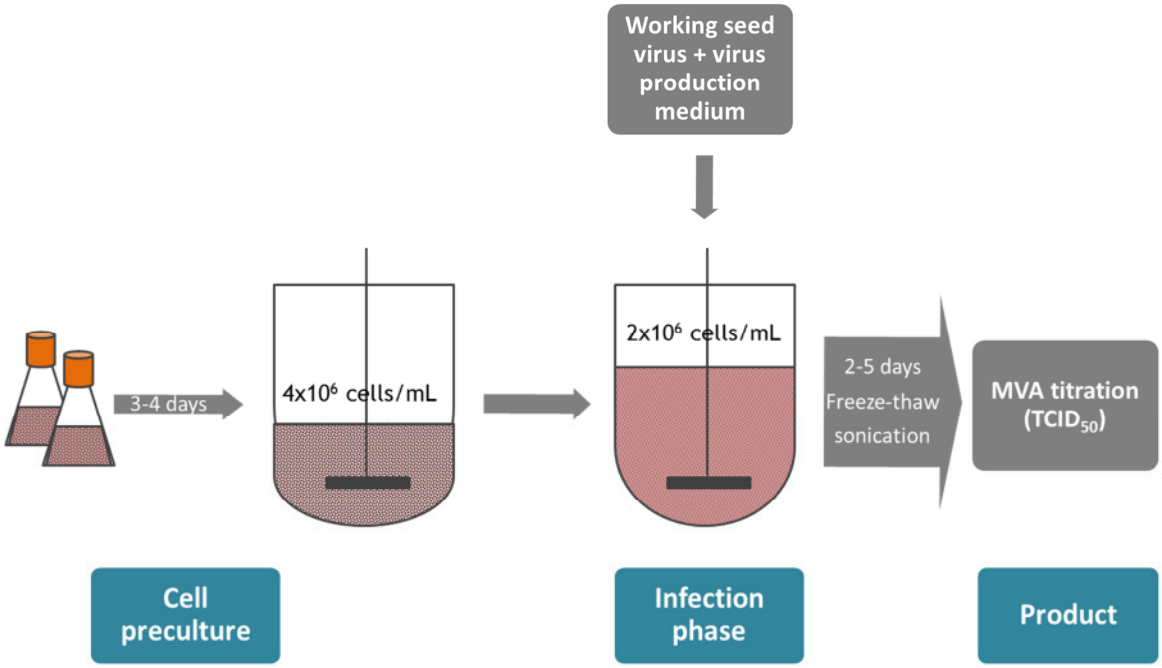

Figure 3.4: Process scheme of cell growth and infection procedure of CR or CR.pIX cells with MVA. Cells are grown up to a specific cell concentration (usually $4x10^6$ cells/mL) and then infected with MVA. Thereby, the cell suspension is diluted with virus production medium. After infection, samples can be taken to analyze virus titer. In order to harvest all MVA virions (intra-or extracellular), freeze-thaw and sonication steps are required.

3.4.3 Adaptation and seed virus production

Starting with virus material from ProBioGen or the LMU Munich (see Table 3.3), a seed virus production with CR.pIX cells was performed. No passaging was performed for adaptation of MVA to CR.pIX cells as for MVAwt the starting material was already derived from a CR.pIX culture or (for MVAegfp) from primary CEF cultures. Thus, the former host was an avian species in either way and thus no improvement was expected when passaging MVA for several passages in CR.pIX cells. As it was known that MVA replicates better in CR.pIX cells, no parallel seed viruses from CR cell cultures were produced. Cells were infected with a moi of 0.05 at the standard CCI of $2x10^6$ cells/mL (after dilution with virus production medium). Every 12 h, samples were taken to measure viability and cell concentration. When viability dropped below 80%, the culture was harvested and prepared for titration by freeze-thaw

cycles and sonication as described in section 3.5.2. Samples were then stored at -80°C and titrated. Harvests with highest titers were chosen as working seed viruses.

3.4.4 $TCID_{50}$ assay for the quantification of active virus particles

Quantification of infectious MVA virions was done via $TCID_{50}$ assay using adherent Vero cells. Before titration, samples were freeze-thawed three times and subsequently treated for 1 min in a sonication water bath in order to lyse the cells and release intracellular virions into the supernatant. After pelleting cells and cell debris, supernatants were used as samples for titration. A three-step staining was performed after infection of Vero cells with serial dilutions of the samples. First, cells were treated with a rabbit antibody against vaccinia virus (Quartett), second an anti-rabbit antibody coupled to horseradish peroxidase was added to bind to the first antibody and third, a solution containing 3-aminoethyl-carbozol and hydrogen peroxide was applied to stain cells with bound antibody. Red stained cells could be observed with a light microscope. Titers were calculated from titration by method of Spearman and Kärber as for influenza virus titrations. The detailed assay procedure can be found elsewhere [18] and in the corresponding SOP (listed in Appendix A6). MVA titers measured with this assay will be given in [viruses/mL].

3.4.5 Infection status of MVAegfp infected cultures

Cells infected with MVAegfp virus accumulate EGFP proteins in their cytoplasm as a side-effect of virus genome replication, transcription and translation. Accumulation of EGFP showed to be a good approach to determine the infection status of a cell population. To detect infected cells by flow cytometry, the cells need to be treated with paraformaldehyde leading to aggregation and cross-linkage of proteins. With this treatment, a stable fluorescent signal can be detected, because EGFP proteins cannot leak through the cell membrane. Several pre-tests were performed to establish a feasible assay procedure with a subsequent flow cytometry analysis. An excitation wavelength of 488 nm was used and signal was followed in the FL1 channel detecting emission at 505–545 nm. For more details see Appendix A9. A fixation time of 0.5–24 h resulted in a stable signal pattern and stable mean intensities (Figure 3.5). Final output of this assay is the percentage of infected cells in the examined cell population. Distinguishing “uninfected” from “infected” cells was done by measurement of either a mock-infected sample or a sample taken at 0 hpi. With such control samples, a gate for infected cells was set to 1% (false-positive rate). Samples from one experiment were measured with so-derived gate settings.

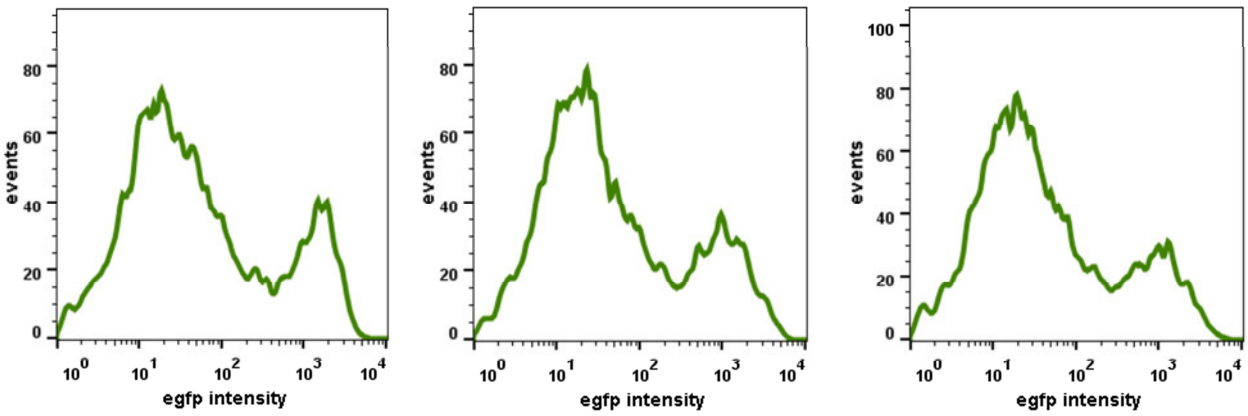

Figure 3.5: Fluorescence signals of MVAegfp infected CR.pIX cells fixed for 2 h (A), 24 h (B) and 48 h (C). CR.pIX cells infected with MVAegfp in a shaker flask were harvested 50 hpi and fixed with paraformaldehyde at 4°C. After this incubation time, samples were measured by flow cytometry in order to identify critical fixation time. Histograms showed the same distribution and mean intensities.

3.4.6 Calculation of cell-specific virus production yield

To calculate a yield from each infection experiment, $X_{V,max}$ (which in MVA infection experiments is CCI) will be used in relation to the maximum virus concentration ($C_{V,max}$). With this, the cell-specific virus yield Y_{CSV} based on the $TCID_{50}$ assay results can be calculated.

$$Y_{CSV} = \frac{C_{V,\max}}{X_{V,\max}} \tag{6}$$

Note that only infectious viruses could be quantified for MVA infection experiments and thus cell-specific yields from MVA infection experiments always refer to infectious virus concentrations.

3.5 Materials and methods used for influenza virus infection experiments

This sub-section lists materials and methods used for influenza virus infection experiments. First, influenza virus strains that were used are given and adaptation and infection procedures are explained. Afterwards, analytics to quantify total virus particles (hemagglutination (HA) assay) and active virus particles ($TCID_{50}$ assay) are described, as well as calculations of cell-specific virus yields.

3.5.1 Virus strains

Four different virus strains were used in this work (Table 3.4). The human influenza virus strain A/PR/8/34 (H1N1), obtained from the Robert-Koch-Institute (ampoule no. 3138), was used as a reference strain and in optimization experiments. This strain will later be referred to as A/PR/8. Three LAIV strains (live-attenuated influenza virus, cold-adated (*ca*), Vero-adapted) were kindly provided by the Polymun Scientific GmbH (D. Katinger).

Table 3.4: Starting material of influenza virus strains used in this project.

Virus strain	Cold-adapted?	$TCID_{50}$ [viruses/mL]
A/PR/8/34 (H1N1) MDCK-adapted	no	$3.2x10^9$
A/Singapore1/57 *ca* x A/Singapore/2339/2000 (H1N1) Vero-adapted	yes*	$3.2x10^7$
A/Switzerland *ca* x A/Vienna (H3N2) Vero-adapted	yes*	$1.0x10^5$
B/Vienna/1/1999/37 *ca* x B/Singapore/548/2000 Vero-adapted	yes*	$1.0x10^7$

* cold-adapted (*ca*) virus strains were generated by Polymun AG as described by Romanova et al. [162]; at first place, the *ca* backbone (donor) strain is given

3.5.2 Infection procedure

Cells were grown in T-flasks, shaker flasks or bioreactors up to a certain cell concentration. The standard CCI was $2x10^6$ cells/mL. For some experiments, however, a higher cell concentration was chosen. Cells were infected using a moi of 0.001 (if not stated otherwise; calculation is described in section 3.4.2). Trypsin needs to be added when infecting cells with influenza virus to help the virus spread in the population. The volume $V_{TrypsinStock}$ that was added to the cell suspension at time of infection, was calculated as follows:

$$V_{TrypsinStock} = \frac{X_V \times V_c \times C_{Trypsin}}{C_{TrypsinStock}} \tag{7}$$

Here, $C_{Trypsin}$ is the trypsin activity [units/cell] required for infection. If not stated otherwise, a standard trypsin activity of $1x10^{-6}$ units/cell was used. The activity of the trypsin stock solution $C_{TrypsinStock}$ was 500 units/mL for small scale infection experiments and 5000 units/mL for bioreactor experiments.

Usually, infection took place directly in the cell suspension after reaching the desired cell concentration in cell growth medium. Only for some experiments, a complete medium exchange was performed. Therefore, the whole culture was centrifuged at 150xg for 10 min to collect cells prior to re-suspension in fresh CD-U2 medium. For a partial medium exchange, half of the culture volume was centrifuged, re-suspended in fresh medium and

subsequently pooled with the remaining non-centrifuged culture. After infection, cultures were sampled once or twice per day to immediately determine the cell concentration and viability and to collect samples for determination of virus titers ($TCID_{50}$ titers and HA values). These samples were stored at -80°C until analysis of all samples belonging to the same experiment.

3.5.3 Adaptation and seed virus production

Adaptation of each virus strain to CR.pIX cells was performed with the starting material shown in Table 3.4. Therefore, cells were infected with a moi of 0.001 and samples were taken every 12 or 24 h to measure cell concentration and HA value. At the time point, a HA value of ≥ 0.5 log HA units/100µL was detected, several cryo tubes were filled with the virus containing culture and stored at -80°C. In parallel, a new flask was inoculated with 1 mL of this culture (thus without knowing the moi). This was done several times so that 1–5 passages of virus propagated in CR.pIX cells were available. Subsequently, HA values and $TCID_{50}$ titers of each passage were determined and the harvest with the highest $TCID_{50}$ titer was chosen as seed virus.
Adaptation of the A/PR/8 strain was done at 37°C, whereas adaptation of LAIV strains was done at a reduced temperature of 33°C. CR.pIX-adapted working virus seeds were stored as a working virus bank in aliquots at -80°C for all further experiments.

3.5.4 HA assay for the quantification of virus particles

The antigen load during influenza virus infection experiments was followed by the HA assay. This assay is based on the ability of the viral HA protein to bind to proteins on red blood cells. A mixture of HA-carrying particles and red blood cells thus results in an agglutinated cell/particle network that prevents red blood cells to settle out of a suspension. By serially diluting a virus sample in a round-bottom 96well plate and adding a consistent amount of red blood cells, the amount of HA-carrying particles in the sample can be estimated. Thereby, it has to be noted that active and inactive HA-carrying virus particles are detected by the HA test. Samples as well as a standard sample used to compensate variations caused by different lots of chicken erythrocytes were analyzed as described in the respective SOP (see Appendix A6). The read-out of this method is log10 HA units/100 µL which will be written as log HAU/100 µL or HA value in the text. The HA assay was validated with a maximum error of 0.3 log HAU/100 µL [163].

3.5.5 $TCID_{50}$ assay for the quantification of infectious virus particles

Infectious titers were measured by titration of supernatants on MDCK monolayers (SOP listed in Appendix A6). Samples from A/PR/8 experiments were analyzed at 37°C, whereas samples from LAIV strains were analyzed at 33°C. Antibodies against the HA protein were purchased from NIBSC institute, namely anti-A/PR/8 (NIBSC code #03/242), anti-A/Brisbane/59/2007 (NIBSC code #08/112) for detection of the A/Singapore strain and anti-B/Yamagata/16/88 (NIBSC code #92/582) for detection of the B/Vienna strain. All primary antibodies were used in a 1:200 dilution. As a secondary antibody, a donkey anti-sheep Alexa488 IgG (Invitrogen) was used in a 1:500 dilution. $TCID_{50}$ titers (read-out: viruses/mL) were calculated according to Spearman and Kärber [122].

3.5.6 Calculation of cell-specific virus yields

Using the assumption that every virus particle binds one red blood cell, one can calculate the total concentration of virus particles in a sample (C_{TP}) from HA values using the formula

$$C_{TP} = C_{RBC} \times 10^{\log HAunits/100\mu L}. \quad (8)$$

Here, C_{RBC} is the concentration of red blood cells in [cells/mL] that was used for the assay. The total influenza virus particle concentration measured by HA assay is given in [particles/mL]. To discriminate virus titers determined by $TCID_{50}$ assay, these infectious virus particle concentrations will be given in [viruses/mL] throughout the text. In contrast to MVA experiments, where only infectious particles were measured, influenza infection experiments thus produce two yields – the cell-specific particle yield Y_{CSP} based on the HA assay results and the cell-specific virus yield Y_{CSV} based on $TCID_{50}$ assay results:

$$Y_{CSP} = \frac{C_{VP,\max}}{X_{V,\max}};\ Y_{CSV} = \frac{C_{V,\max}}{X_{V,\max}}. \quad (9)$$

For influenza virus infection experiments, cell concentrations after infection could be measured and in most cases, the viable cell concentration increased even after infection. Thus, the $X_{v,max}$ chosen for calculation can be the concentration measured at or after time of infection.

4 Results and discussion

4.1 Cell characteristics, growth and metabolism

Characterization of a cell line at first hand includes the evaluation of cell morphology as well as biochemical characteristics such as elemental and biomass composition. Also, the latter parameters are useful for further analyses, such as MFA. To estimate the potential of a cell line as a producer cell line for vaccine manufacturing, growth characteristics like maximum achievable cell concentrations, culture longevity and cell growth rate are then the next features that need to be studied. At best, cell proliferation is fast enough to allow for short process periods with high cell concentrations that allow for high product yields.
The following chapter gives results concerning cell characteristics with regard to two objectives: First, to provide parameters needed for metabolic studies (cell weight, biomass composition, growth rate) and second to bring cell growth properties of CR and CR.pIX cells into relation with other cells used in biopharmaceutical production. Parts of this chapter were published [157, 164].

4.1.1 Cell morphology and biomass composition

Both cell lines used in this study proliferate as single cells in suspension. Only small aggregates form during cell growth – mainly duplets that most likely are parent and daughter cells in the process of cell division (Figure 4.1.1).

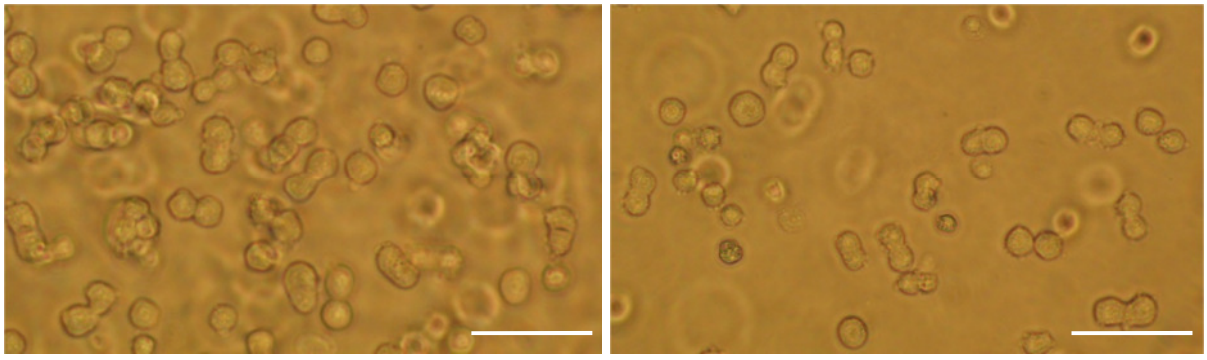

Figure 4.1.1: Light microscopy images of CR (left) and CR.pIX (right) cells after three days growth in shaker flasks in serum-free AEM medium. White bars indicate a length of 50 µm.

Cell diameters ranged between 11 and 15 µm with bigger diameters in the exponential growth phase. CR and CR.pIX cells are thus relatively small compared to other cells, e.g. MDCK cells with up to 20 µm in diameter [165, 166] or CHO cells with 15–18 µm [167].

Biomass composition of CR and CR.pIX cells was analyzed in order to obtain parameters for the later applied MFA (see chapter 4.1.3.3). Although data about macromolecular composition and protein composition of various cell lines is available in literature, no avian cell line had been studied in detail before. Thus, CR and CR.pIX cell samples were analyzed according to the description given in section 3.3.2 in order to derive the following values:

- Cell-specific dry cell weight
- Elemental composition
- Protein content (fraction of whole biomass)
- DNA content (fraction of whole biomass)
- RNA content (fraction of whole biomass)
- Amino acid content (fraction of whole cell protein)

It is well known that cell volume and weight as well as protein and RNA contents change with culture duration [168]. However, only the exponential growth phase was of interest in this project for metabolic flux analysis, and hence only samples from this cultivation phase (72 h after inoculation) were taken for analyses. Averages from all measurements with CR and CR.pIX cells were calculated as significant differences were neither expected nor observed between both cell lines. Three measurements were done for each cell line so that final values are an average of five or six measurements (biological replica from independent cultures and sample preparations with varying numbers of technical replica; outliers were removed if present). The results in conjunction with other published data of eukaryotic cells are summarized in Table 4.1.1.

The measured specific cell dry weight of 314 pg/cell is a rather low value compared to other published values, but plausible as CR and CR.pIX cells are smaller than e.g. Sf9 or AGE1.HN cells with an average cell diameter of 15–18 µm [167, 169]. DNA and RNA contents are also similar to other published values of eukaryotic cells. Higher RNA than DNA values were expected as the cell contains a certain stock of different RNAs including tRNAs, rRNAs, snRNAs and mRNAs so that the overall amount is normally higher than the amount of genomic DNA. A relatively low fraction of protein (54%) was measured for CR and CR.pIX cells. This is considerably lower than e.g. the 80-100% that were measured for AGE1.HN cells. Only one publication describes a similar value of 60% for mouse hybridome cells [170]. As a comparison, yeast cells were described to consist of only 37% protein [171].

Table 4.1.1: Biomass composition of CR and CR.pIX cells and published data from other eukaryotic cell lines.

	CR & CR.pIX	Mouse hybridoma	Sf9	AGE1.HN	CHO	Pichia pastoris
Cell weight [pg/cell]	314±47[a]	250/470/250	612	475	315	-
DNA content [%]	2.3±0.7	1.4/1.4/10.8	5.0	-	1.9	0.1
RNA content [%]	3.0±0.3	3.8/5.8/5.6	13.0	3.0	5.8	6.6
Protein content [%]	53.7 ±6.4	72.9/70.6/60.1	-[c]	80-100	70.6	37
Asn	4.5[b]	4.4	5.9	9.3[d]	5.4	8.8[d]
Asp	5.5 ± 0.4	4.7	5.9		4.3	
Glu	4.7 ± 0.3	5.0	7.0	12.8[d]	4.9	18.6[d]
Gln	6.0[b]	6.2	7.0		5.9	
Ala	16.3 ± 1.1	8.3	7.0	8.1	8.7	10.7
Arg	11.2 ± 2.1	5.9	8.0	5.2	4.9	6.7
Cys	2.0[b]	2.8	-	2.8[b]	1.8	~0
Gly	11.1 ± 0.8	8.5	5.4	9.5	8.1	7.1
His	3.0[b]	2.2	3.1	2.2	2.0	1.8
Ile	2.9[b]	4.2	5.9	4.5	4.8	4.1
Leu	7.4 ± 0.4	8.1	8.7	8.7	8.5	7.0
Lys	8.0[b]	6.8	9	7.5	8.5	6.3
Met	1.4 ± 0.3	2.2	3.7	1.7[b]	2.2	0.8
Phe	2.5 ± 0.3	3.2	5.5	3.6	3.5	3.0
Pro	2.2 ± 0.2	5.3	5.3	4.0	5.3	3.7
Ser	3.3 ± 0.3	6.9	4.6	6.2	6.3	6.4
Thr	2.5 ± 0.4	5.7	4.8	4.9	5.5	5.8
Trp	2.0[b]	1.1	2.6	1.1[b]	0.6	1.4
Tyr	3.0 ± 0.9	2.6	4.6	1.9	2.6	2.1
Val	2.3 ± 0.2	6.0	6.6	6.1	6.1	5.6
References	[157]	[172]/[173]/[174]	[175]	[160, 168]	[176]/ [177]	[171]

[a]average values and standard deviations are derived from n=5 or n=6 measurements.
[b]values estimated from data of other eukaryotic cells
[c]no value given or measured
[d]the sum of glutamate/glutamine and aspartate/asparagine, respectively, is given, because deamination during protein hydrolysis was not determined so that a differentiation between both was not possible

Regarding the amino acid content, it has to be noted that cysteine as well as tryptophan are known to decompose during acidic hydrolysis so that these values could not be analyzed. Furthermore, asparagine and glutamine are converted at least partially into their acidic equivalents aspartate and glutamate. To account for this, 47.5% of measured glutamate and

aspartate were considered to be derived from glutamine and asparagine [178]. Although some amino acids were measured with slightly higher (alanine, arginine and glycine) or lower (isoleucine, proline, threonine and valine) amounts than in other cells, no striking differences could be identified. As high method errors can occur during acidic hydrolysis and sound conclusions about a biological meaning would only be speculation, the protein composition was considered to be similar to other transformed cell lines.

Although lipid and carbohydrate fractions make up a considerable amount in cells, they were not measured in this project due to two reasons. First, available analytical methods are laborious and error-prone so that results from those methods were expected to be unreliable. Second, a sensitivity analysis of MFA, testing how different fractions influence the calculation result, showed only a minor impact (data not shown). According to Sheikh et al., the ratio between lipid and carbohydrate fractions is 1:2 [179]. The residual biomass of CR and CR.pIX cells thus was finally assumed to consist of 13.2% lipid and 26.3% carbohydrate. These chosen values are in agreement with literature data (9–20% reported for lipid content and 3.5–37% reported for carbohydrate content [170, 172, 174, 178, 180].

Finally, the elemental composition of CR cells was determined to be $C_1H_{1.838}N_{0.237}O_{0.392}S_{0.006}$ - a very similar result to other eukaryotic cells as CHO and yeasts like *pichia pastoris* [171, 173, 181]. This similarity was expected as the elemental composition is a conserved characteristic of cells that can only vary within small margins.

In summary, the macromolecular and protein composition as well as the elemental composition of CR and CR.pIX cells were determined as accurate as possible and were similar to published data on eukaryotic cells. These cell-specific values could be used for implementation into the later applied metabolic model.

4.1.2 Cell growth characteristics

To evaluate whether the avian cell lines CR and CR.pIX are competitive substrates useful for biopharmaceutical (in particular vaccine) production, cell growth characteristics are one major parameter. At best, the cells proliferate to high cell concentrations at high viability and show long culture longevities. Both, cell viability and cell concentrations should be known before starting infection experiments so that the time point of infection can be chosen appropriately. Finding a proper proliferation medium is tightly connected with these objectives. The chosen medium should provide enough substrates for biomass formation and – for a modern robust process – should be animal component-free or, at best, chemically-defined.

In this study, growth curves of CR and CR.pIX cells were recorded in different commonly used cultivation systems, namely T-flasks, shaker flasks, 1 L STR and 1 L Wave bioreactor to

characterize cell growth. The serum-free medium AEM and the chemically-defined medium CD-U2 were used. Maximal cell concentrations, longevity of cultures (the time until cell death phase) and the growth rate μ were extracted from these experiments and will be discussed in the following chapter.

Cell growth in serum-free AEM medium

At the beginning of the project, CR and CR.pIX cells were cultivated in the commercially available serum-free medium AEM. However, as the priority was on the cultivation in chemically-defined medium CD-U2, only main parameters derived from AEM growth curves are shown and discussed here (Table 4.1.2). Some experiments were scouting experiments involving infection of cells with influenza or vaccinia virus after approximately 100 h. Thus, no maximal cell concentrations or culture longevities were identified for those cultures. For this reason, the number of experiments from which maximal cell concentrations and growth rates were derived, can vary.

Table 4.1.2: Growth characteristics of CR and CR.pIX cells in serum-free AEM medium. Maximal cell concentrations, growth rates and culture longevities derived from growth experiments in different cultivation systems are shown. All experiments were inoculated with the same starting cell concentration ($8x10^5$ cells/mL).

cell line	cultivation system	X_v max[b] [$x10^6$ cells/mL]	average maximum X_v [$x10^6$ cells/mL]	μ[c] [1/h]	average μ[c] [1/h]	average culture longevity[d] [h]
CR	T175 (2)[a]	6.0–7.3	6.7	0.0211–0.0222	0.0217	132
	Shaker (3)	7.8–9.3	8.7	0.0279–0.0293	0.0284	108
	Wave (1)	5.3	5.3	0.0232	0.0232	168
	STR (4/2)	5.8–6.0	5.9	0.0195–0.0251	0.0230	168
CR.pIX	T175 (1)	7.1	7.1	0.0237	0.0237	144
	Shaker (3)	4.8–5.1	5.0	0.0233–0.0271	0.0252	96
	Wave (1)	7.2	7.2	0.0255	0.0255	108
	STR (0)	-	-	-	-	-

[a]number of experiments from which maximum cell concentration could be determined is given in brackets; if number of experiments from which a growth rate could be determined is lower, this is indicated at second place
[b]maximum viable cell concentrations; if data from different experiments are available, minimum and maximum values are given
[c]growth rates were determined by linear regression of logarithm of viable cell concentrations measured in the exponential growth phase. The time window therefore was 20–100 h if the growth curves were not shifted substantially towards lower or higher cultivation times. 3–9 values were used for determination of μ; if data from different experiments are available, minimum and maximum values are given
[d]cultivation time at which onset of cell death (decreasing cell viability) was observed

Maximum cell concentrations did not differ significantly between the different cultivation systems with the exception of shaker flask cultures where highest maximal cell

concentrations of 8–9x10^6 cells/mL could be reached for CR and lowest for CR.pIX cells (5x10^6 cells/mL). No large differences could be observed for the other three cultivation systems with regard to cell growth dynamics, maximal cell concentrations, and growth rates when comparing CR and CR.pIX cells. Also, culture viabilities were usually between 85 and 95% showing no trend towards higher viabilities in bioreactor or shaker flasks (data not shown).

Long-term monitoring of cell concentration and viability during passaging in AEM (Appendix A10) occasionally showed drastic break-downs of culture viability. This was also observed by ProBioGen in parallel experiments and pointed towards a non-optimal composition of AEM for the avian cell lines. The fact that bioreactor experiments yielded comparably low cell concentrations supported the hypothesis of a sub-optimal medium composition. In order to improve process robustness and performance in bioreactors, the process was changed towards use of CD-U2, a tailor-made chemically-defined medium for proliferation of CR and CR.pIX cells.

Cell growth in chemically-defined CD-U2 medium

CD-U2 was developed by ProBioGen in cooperation with the University of Bielefeld with the goal to improve CR.pIX cell growth. In particular, long-time passaging showed higher viabilities for CR.pIX cells after switch to CD-U2 medium (see Appendix A11). Representative growth curves of CR and CR.pIX cells grown in CD-U2 medium are shown in Figure 4.1.2 in conjunction with cell viability and pH values.

A lag phase with only slow increases in viable cell concentration was observed for approximately 24 h after inoculation for both cell lines and in all cultivation systems except shaker flasks. In shaker flasks, the exponential growth phase started directly after inoculation and lasted until 96–108 h. A pronounced stationary growth phase was not observed, but a rather immediate onset of cell death. At this time point, a low pH (6.5) was present in the uncontrolled shaker flasks which most likely inhibited cell growth and triggered the onset of cell death. Cells in T-flasks proliferated slower and pH values below 6.5 were reached 1–2 days later than in shaker flask cultures. Correlated with this, the onset of cell death in T-flasks started only between 168 h (CR) and 192 h (CR.pIX). In Wave cultures (also without pH control), low pH values also correlated with the onset of cell death at 216 h (CR) and 168 h (CR.pIX). The delay of pH drop and cell death compared to shaker flask cultures is most likely due to the manual adjustment of CO_2 in the air flow which was applied in Wave cultivations that was probably lagging behind cellular requirements. In the STR system where the pH (as well as DO) could be controlled, cell growth was prolonged until 240 h (Figure 4.1.2B). Of course, culture longevity is also

dependent on substrate availability and depletion which will be addressed again in chapter 4.1.3.

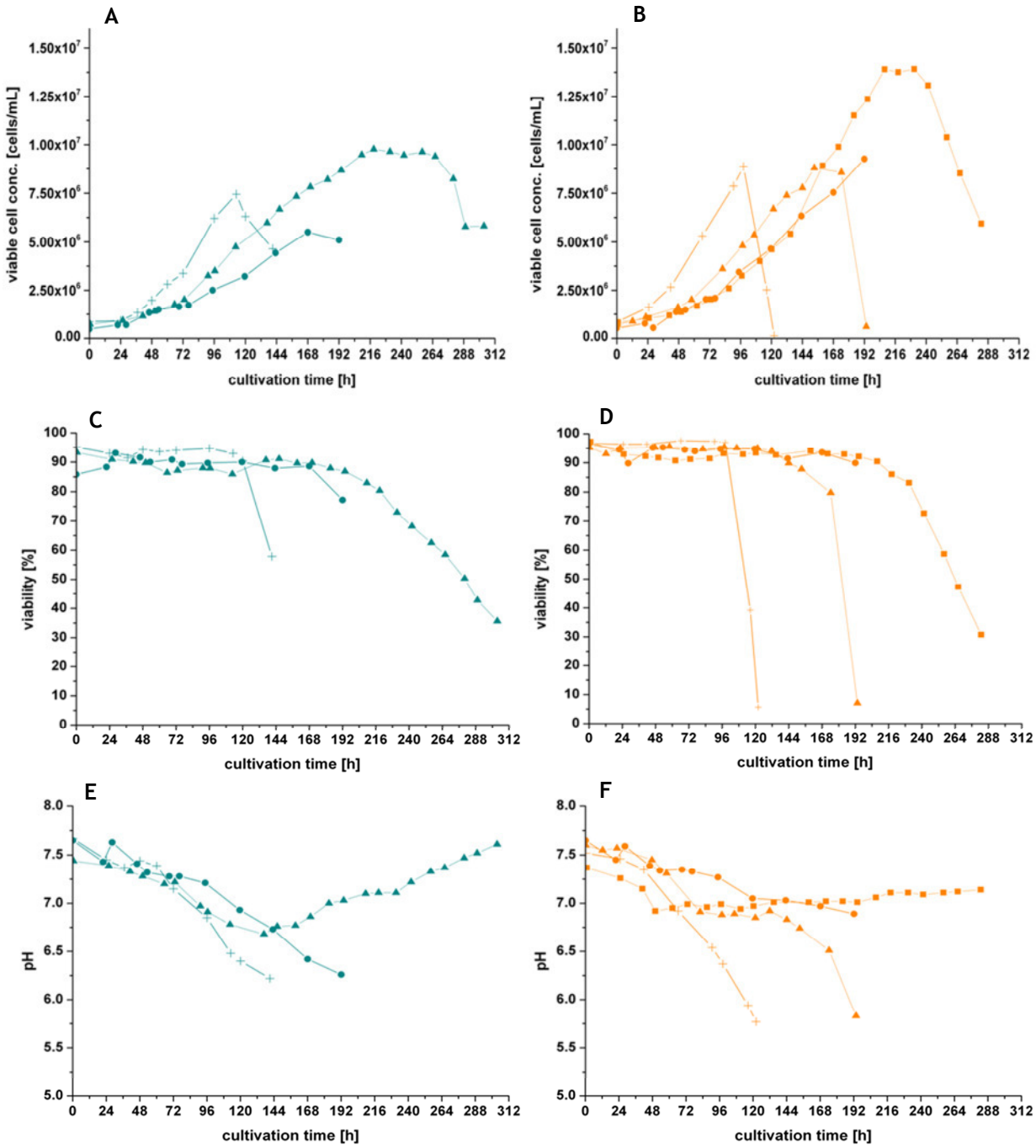

Figure 4.1.2: Cultivation of CR (left column) and CR.pIX (right column) in CD-U2 medium using different cultivation systems. Time courses of viable cell concentration (A and B), viability (C and D) and pH values (E and F) are shown for cells grown in T-flasks (●), shaker flasks (+), Wave bioreactor (▲) and STR (■).

Overall, culture longevity was best in STR or Wave cultivations. Both systems supported cell growth with slight advantages for the controlled STR where highest cell concentrations could be observed (Table 4.1.3). This influence on cell growth was expected due to

different aeration, agitation and pH control principles as they create a substantially different environment for the cells. To investigate if not only growth curves but also cell physiology is affected, the cell cycle distribution of cells cultured in Wave and STR was analyzed (Figure 4.1.3) in addition.

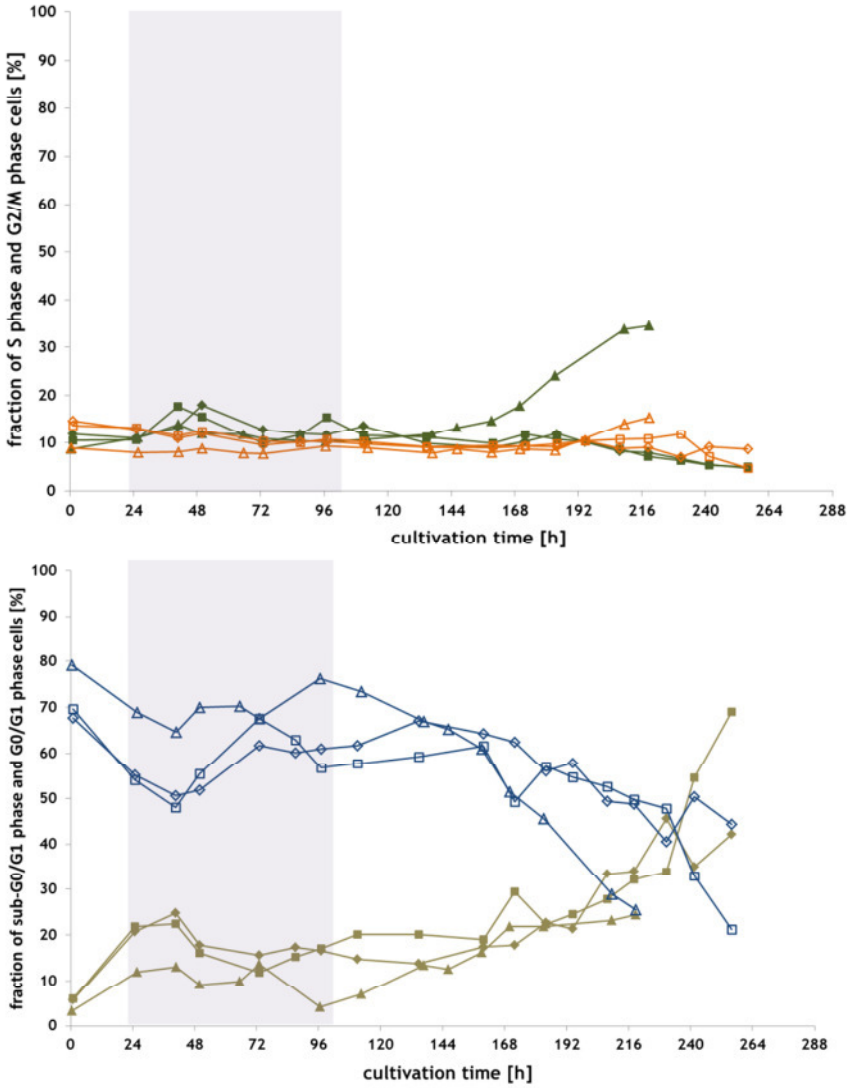

Figure 4.1.3: Cell cycle fractions of CR.pIX cells grown in CD-U2 medium in either Wave bioreactor (▲) or STR (■ and ◆, two independent experiments). Cells in four phases can be distinguished. Top: replicating cells in S phase (closed symbols) and resting cells after mitosis in G2/M phase (open symbols); Bottom: apoptotic or necrotic cells in subG0/G1 phase (closed symbols) and resting cells before mitosis in G0/G1 phase (open symbols). Exponential growth phase is indicated by a grey background. To facilitate interpretation of data, the measurement error of 5% (generally determined for flow-cytometric measurements) is not depicted with the curves.

Especially during the exponential growth phase (grey background in Figure 4.1.3), fractions of cells in the different cell cycle phases did not vary significantly. Only at the end of the exponential growth phase, an increase of subG0/G1 phase cells could be observed in conjunction with a loss of G0/G1 cells. This is a result of starting cell death. Also, the increase of S phase cells at the end of the Wave cultivation can be assigned to an onset of

cell death, i.e. cells that were in the G2/M phase while DNA degradation starts were classified as S phase cells. Interestingly, only small fractions of cells (approximately 10%) were in the S phase, even in the exponential growth phase. This is a relatively low value compared to e.g. adherent MDCK cells where 25% S phase cells during exponential growth were measured [182] or NS0 cells with 20–40% S phase cells [183]. As this is obviously not a result of poor cell proliferation of CR.pIX or CR cells (as they proliferate with normal growth rates to relatively high cell concentrations), this could be an artifact related to true suspension growth, high growth rates and/or high cell concentrations. As the cell concentration is high and cells fast dividing and not surface-limited, the population might show a high heterogeneity and a lower fraction of S phase cells.
Maximum cell concentrations and growth rates from all growth curves recorded in CD-U2 medium are summarized in Table 4.1.3. With these values, a comparison to other cell lines is possible in order to evaluate the potential of CR and CR.pIX cells for biopharmaceutical production.

The achieved cell concentrations of up to $14x10^6$ cells/mL are at the top edge (when regarding batch cultivations) of reported maximum cell concentrations in literature. With adherent cell lines that are often used for vaccine production, cell concentrations of $1–3x10^6$ cells/mL are reported for batch cultivations applying 1–5 g/L microcarrier [121, 184]. Using suspension cell lines, expansion of the culture is easier as no surface limitation is present and thus cultures of suspension Vero, BHK-21, PER.C6 or CHO cells are reported to even achieve $2–5x10^6$ cells/mL [146, 185-187]. Higher cell concentrations of $7–30x10^6$ cells/mL were for most cell lines only possible when changing to fed-batch or perfusion mode. This has been shown for example several times for CHO cells in fed-batch mode or HEK293 and PER.C6 cells in perfusion mode [120, 186, 188]. With CR and CR.pIX cells, even batch cultivations resulted in such high concentrations of around $10x10^6$ cells/mL. Follow-up studies using these cells in high cell density cultivations (e.g. achieved by fed-batch strategies or perfusion systems such as the ATF system) are thus likely to yield even higher cell concentrations. As the growth rate calculation is sensitive towards the chosen time interval, values cannot be compared with its distinct values, but the range of growth rates reported for transformed mammalian cells is 0.01–0.03 h^{-1} [44, 51, 189, 190], and thus in the same range as growth rates found for CR and CR.pIX cells. These characteristics should be beneficial not only for studies at very high cell concentrations, but also for setting up continuous cultures. As has been shown recently, indeed CR cells could be cultivated at a constant cell concentration of $4x10^6$ cells/mL in a bioreactor [45].
Taking together, two results seem important. First of all, in shaker flasks high cell concentrations can be reached in a short period of time. Thus, this system is most

appropriate to carry out pre-cultures or scouting experiments with several parallel cultures. STR and Wave cultures both yielded high cell concentrations with no significant differences in cell cycle distribution. However, the STR system supported higher culture longevity and offers the advantage of a fully controlled system so that long-term experiments or studies at high cell concentrations are best carried out in STR. Second, growth experiments showed that the proliferation medium CD-U2 matches the demands of these cell lines and that the cells have a clear potential to be used in high cell density cultivations.

Table 4.1.3: Growth characteristics of CR and CR.pIX cells in chemically-defined CD-U2 medium. Maximum cell concentrations, growth rates and culture longevities derived from growth experiments in different cultivation systems are shown. All experiments were inoculated with the same starting cell concentration ($8x10^5$ cells/mL).

cell line	cultivation system	X_v max[b] [$x10^6$ cells/mL]	average maximum X_v [$x10^6$ cells/mL]	μ[c] [1/h]	average μ[c] [1/h]	average culture longevity[d] [h]
CR	T175 (2)	5.5–8.6	7.0	0.0181–0.0191	0.0186	168
	Shaker (6)	6-0–10.3	7.7	0.0237–0.0264	0.0247	108
	Wave (2)	9.8–10.3	10.0	0.0190–0.0217	0.0204	168
	STR (0)	-	-	-	-	-
CR.pIX	T175 (2)	6.8–9.3	8.0	0.0196–0.0227	0.0212	192
	Shaker (7)	5.0–10.9	6.7	0.0202–0.0245	0.0228	108
	Wave (4/2)	8.4–8.8	8.6	0.0194–0.0230	0.0207	156
	STR (14/5)	5.1–13.9	10.1	0.0160–0.0253	0.0196	216

[a]number of experiments from which maximum cell concentration could be determined is given in brackets; if number of experiments from which a growth rate could be determined is lower, this is indicated at second place
[b]maximum viable cell concentrations; if data from different experiments are available, minimum and maximum values are given
[c]growth rates were determined by linear regression of logarithm of viable cell concentrations measured in the exponential growth phase. The time window therefore was 20–100 h if the growth curves were not shifted substantially towards lower or higher cultivation times. 3–9 values were used for determination of μ; if data from different experiments are available, minimum and maximum values are given
[d]cultivation time at which onset of cell death (decreasing cell viability) was observed

4.1.3 Cell metabolism

In the first section of this chapter (4.1.3.1), the general metabolism of CR and CR.pIX cells regarding main metabolites that are usually monitored in cell cultures will be discussed based on concentration time courses and yield coefficients. In section 4.1.3.2, reproducibility of such processes is addressed. Therefrom, conclusions were derived regarding the interpretation of technical or biological replicates with indications for the design of comparative studies. In the last section 4.1.3.3, flux distribution of CR.pIX cells derived by MFA will be discussed.

4.1.3.1 Metabolism regarding main extracellular metabolites

In this section an overview about the production and consumption of extracellular main metabolites shall be given. These are usually monitored in cell cultures and thus were investigated first in this project with two objectives. On the one hand to exclude the possibility that growth limitations or limitations during virus production occur due to substrate depletion. On the other hand, the metabolism of a producer cell should be known so that for example accumulation of lactate and ammonia to toxic concentrations can be prevented or feeding strategies for high cell cultivations can be developed. In this section, only cultivations in CD-U2 medium will be shown and discussed as experiments in this medium were investigated further with MFA and were also mainly used for virus production experiments.

Glucose and pyruvate are the two main energy and carbon sources in CD-U2 medium. Galactose is present only in negligible amounts (2% of the whole carbon pool) and was not considered. All amino acids are included in the medium with asparagine, aspartate, arginine and glycin as the main pools. (Unfortunately, measurements of amino acid concentrations were biased by a matrix effect of this medium which prevented the use of the method established at the Bioprocess Engineering group at the MPI Magdeburg [154]. Therefore, measured values showed high variability and are not reliable in detail. Thus, time courses of amino acid concentrations are not shown and discussed in this chapter. However, at the end of the project, measurements could be done using a derivatization method established at the Cell Culture Technology group of Prof. Thomas Noll at the University of Bielefeld [155]. Those values were later used for MFA, see chapter 4.1.3.3.) Figure 4.1.4 shows representative concentration profiles of main metabolites that were obtained from cultivations of CR and CR.pIX cells in different cultivation systems.

The main substrate glucose was taken up by both cell lines and in all cultivation systems in a very similar way (3.1.4C and D). The steady decrease in glucose ended in depletion for bioreactor cultures after 168–240 h. A correlation between the time points of glucose depletion and beginning cell death is clearly observable, showing that growth seems to be mainly glucose-dependent as commonly found for all cultured cells [54]. In shaker flask cultivations, glucose depletion was not reached as the cells died before - most likely due to critical pH values (see section 4.1.2). Although glucose uptake was very similar for all cultivations, lactate profiles differed (end concentrations between 25 mM and 50 mM). Degradation reactions of serine, cysteine and pyruvate as a second carbon source are probable to account as well for lactate production (see metabolic network, Figure 3.4). Yet, their influence will be discussed later (section 4.1.3.3).

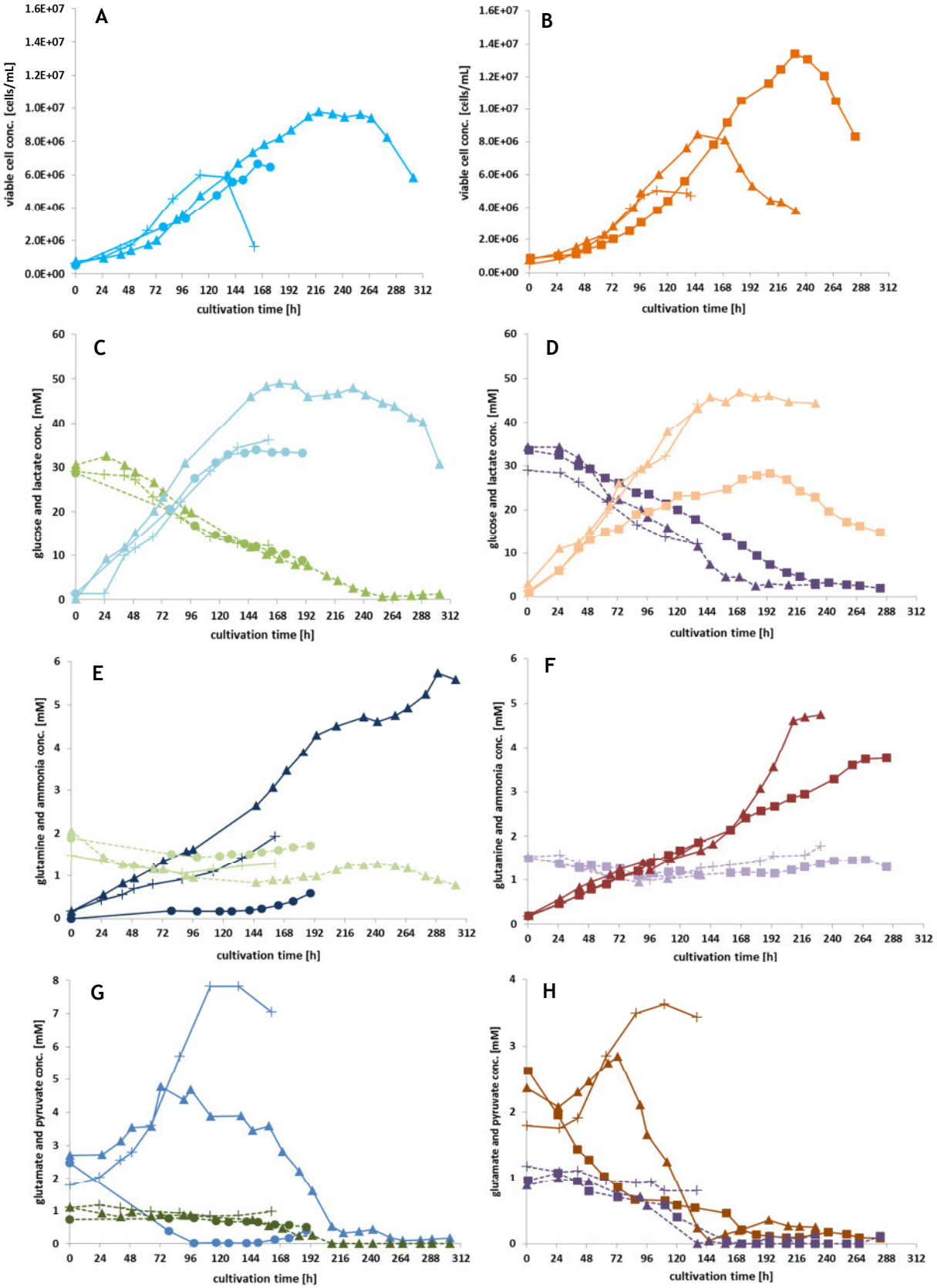

Figure 4.1.4: Time courses of viable cell and main metabolite concentrations during cultivation of CR (left column) and CR.pIX (right column) cells in CD-U2 medium. Data from cultivations in shaker flasks (+), T-flasks (●), Wave bioreactor (▲) and STR (■) are shown. A and B: viable cell concentrations, C and D: glucose (dashed lines) and lactate (solid lines) concentrations, E and F: glutamine (dashed lines) and ammonia (solid lines) concentrations, G and H: glutamate (dashed lines) and pyruvate (solid lines) concentrations.

Glutamine time profiles (Figure 4.1.4E and F) were rather constant. Hardly any uptake was observed as the slight decrease of concentration can be ascribed to glutamine deamination. As this was studied in more detail using MFA, more discussion on glutamine metabolism of CR.pIX cells can be found in chapter 4.1.3.3. In opposite to glutamine, glutamate was taken up by the cells (slowly, but steadily) until depletion after 144 h in reactor cultures (Figure 4.1.4G and H). However, glutamate concentration is only 0.8 mM at the beginning and thus, rather low amounts are provided even when taken up completely. Ammonium curves only show concentrations above 2 mM in reactor cultures at late cultivation times (>144 h), namely 5 mM in Wave reactor and 4 mM in STR. That are much higher concentrations than expected from glutamine and glutamate degradation reactions.

A substantial amount of ammonium thus seems to be derived from degradation of other amino acids. The observed concentrations between 2 and 5 mM are rather low when compared to maximum concentrations between 3 and 8 mM that are reported to reduce cell fitness or induce cell death during batch cultivation of other cells [56, 57].
Interesting time profiles were observed for pyruvate (Figure 4.1.4G and H). As a second carbon source, we expected to see pyruvate decrease for all cultures. However, an immediate uptake of pyruvate was only observed in STR cultures. In Wave cultures, uptake was delayed with both cell lines. Here, pyruvate concentration stayed constant or even increased until mid of the exponential growth phase. After reaching a maximum concentration, pyruvate was taken up rapidly and was depleted simultaneously with glucose. For shaker flask cultures the concentration profile was even more unexpected as the pyruvate concentration increased during the whole cultivation time until end of the culture. At this time, 4–8 mM pyruvate (depending on the cell line) had been accumulated in the medium which means that cells released a substantial amount of this carbon source. This rather counterintuitive behavior might be explained by some studies that showed cells to deliberately release pyruvate in order to build a protection wall against oxygen radicals [191, 192]. Experiments triggering hypoxia or hyperoxia might be therefore interesting in order to test this hypothesis. However, in this project no further tests towards this were performed, but the observation should encourage a more detailed analysis of the metabolism of avian cells. In particular, experiments with ^{13}C-labelled glucose could give more information.
Due to problems with quantification of amino acid concentrations when using CD-U2 medium, no time courses are shown here. However, no amino acid was deprived before glucose was taken up completely so that an inhibiting effect due to missing amino acids could not be found (data not shown).

From concentration measurements, yield coefficients like $Y_{Lac/Glc}$ or $Y_{Gln/Amm}$ can be calculated and are often reported in literature to discuss the metabolic behavior of cells [54]. However, calculation of these yields for CR and CR.pIX experiments revealed that a meaningful interpretation of such yields is not possible due to two reasons. First, the biological variability from experiment to experiment was large so that even when comparing only shaker flask or STR cultivations of one cell line in one medium, yields differ largely. The second and more important reason why these yields are not interpreted further in this study is the fact that the production of ammonia and lactate is not correlated only to glucose and glutamine uptake as was already described.

Other yields that can be helpful to describe the metabolism or metabolic efficiency of cells, and to compare it to other studies, are the yield coefficients $Y_{Xv/Glc}$ and $Y_{Xv/Gln}$. For cultivation of CR cells, $Y_{Xv/Glc}$ yields were 4–8x10^8 cells/mmol. Yields for CR.pIX cells were slightly lower (3–5x10^8 cells/mmol). Such values were also described for other cell lines. Siegwart et al., for example, found yields of 7x10^8 cells/mmol during batch cultivation of HEK293 cells and similar values were reported for mouse hybridoma cells (1–10x10^8 cells/mmol) [193, 194]. A trend of higher yields for shaker and STR cultures was observed in comparison to Wave cultures, although it has to be noted that the overall difference of the values was not large. However, if one assumes that a higher yield means more efficient glucose utilization, shaker and STR cultures were superior to Wave cultures. Glutamine yields, $Y_{Xv/Gln}$, were higher than $Y_{Xv/Glc}$ yields with 0.7–3.1x10^{10} cells/mmol for CR cells and 1.0-3.4x10^{10} cells/mmol for CR.pIX cells. Some cultivations even yielded a negative value reflecting low glutamine starting concentrations (2 mM glutamine vs. 30 mM glucose) and neglectable glutamine uptake (see for example shaker and STR cultivations in Figure 4.1.4F). Reported values for $Y_{Xv/Gln}$ in literature are usually smaller, e.g. 1–10x10^8 cells/mmol for hybridoma cells and 0.4x10^8 cells/mmol for HEK293 [193, 194]. This can be explained with higher start concentrations of glutamine that were used and a clear glutamine uptake that is usually observed for these cells. This observation of more abundant "outliers" for $Y_{Xv/Gln}$ together with the observed insensitivity towards cell line and cultivation system, formed the hypothesis that glutamine does not play an important role for the energy metabolism of CR and CR.pIX cells (this topic will be revisited in chapter 4.1.3.3).

Two findings were followed-up. First of all, regarding experiments in different cultivation systems, a more thorough comparison of STR and Wave bioreactor cultivations might help to evaluate which system is superior in terms of production processes with CR or CR.pIX cell lines. As, however, varying starting concentrations and variable cell growth were already observed before, an analysis of variability when performing independent experiments should

be done before in order to prevent misinterpretation of results and thus to prevent deriving untenable conclusions. For this purpose, the next paragraph shows an inter-experimental comparison of CR.pIX cultivations. Second, the interesting observations on pyruvate and glutamine metabolism (i.e. the non-consumption in case of glutamine) in particular demanded a more detailed metabolic analysis for CR.pIX cells. Therefore, MFA was performed and revealed interesting insights into metabolism of avian cells.

4.1.3.2 Impact of biological variability on experimental planning

Inter-experimental variability in data can be influenced by many parameters, among others:

- raw material quality and lots ([195, 196])
- pre-culture heterogeneity and history ([197, 198])
- starting conditions (inoculation cell and metabolite concentrations)
- biological variation (to some extent shown in [199])
- measurement errors ([200])

Pre-culture heterogeneity and raw material quality were not analyzed within this project. However, they are anavoidable. Using different medium lots, for example, cannot be circumvented during a long-term project and also during production. Here, the three factors measurement errors, variability in starting conditions, and biological variation will be discussed. CR.pIX cells grown in CD-U2 medium were used for this analysis as most experiments were performed with this medium, and as this process is relevant for production of vaccines.

The first variability that occurs when performing several experiments that are to be compared among each other, is the variability in starting concentrations. Inoculation cell concentration as well as the starting concentrations of the main metabolites glucose, glutamine, glutamate and pyruvate of all CR.pIX cultures varied to some extent (Table 4.1.4). The inoculation cell concentration showed a standard deviation of 5.0–9.4% around the set-point of $8x10^5$ cells/mL. With pre-culture processing including a centrifugation step, this seems a fairly low deviation. Starting concentrations of metabolites showed standard deviations of 0.1–21%. This can be ascribed to carry-over of medium from the pre-culture and measurement errors. Also, different media lots might show deviating metabolite concentrations. It has to be noted that the large relative variation of glutamate and pyruvate also is a result of low concentrations for which a small deviation already results in high relative variation. Generally, it is possible that starting condition variations might lead

to differences in cell growth curves and metabolite concentration time courses between one cultivation and the other.

Table 4.1.4: Average starting concentrations of viable cells and main metabolites with standard deviations and relative errors that have been measured for several experiments.

	Xv[a] [x10^5 cells/mL]	Glc conc.[b] [mM]	Gln conc.[b] [mM]	Glu conc.[b] [mM]	Pyr conc.[b] [mM]	N=[c]
Wave cultivations	7.8 ± 0.7 9.4%	34.2 ± 0.1 0.1%	1.57 ± 0.1 2.3%	0.9 ± 0.1 2.3%	2.8 ± 0.6 20.9%	2[c]
STR cultivations	8.0 ± 0.4 5.0%	31.0 ± 4.5 14.5%	1.59 ± 0.2 11.7%	0.8 ± 0.2 20.5%	2.6 ± 0.1 3.6%	10 (7[d])

[a]viable cell concentrations measured at time of inoculation
[b]concentration measured directly after inoculation
[c]number of experiments; average calculation from two experiments should normally not be done, but could not be avoided as for additionally performed Wave experiments using CD-U2, different viable cell concentrations were used for inoculation which hampers comparability
[d]pyruvate concentration was not determined in all experiments resulting in a reduced number of experiments (given in brackets) for this metabolite

To further address technical and inter-experimental variability, time courses need to be considered. Four independent STR growth experiments were included in the following comparison, each comprising of two parallel reactor runs inoculated with the same pre-culture. Parallel reactor runs were used to assess the "technical" variation, whereas independent runs were used to assess the "inter-experimental" variation. Overall, data of eight STR runs could be compared against two independent Wave growth experiments (Figure 4.1.5). Differences in time profiles directly transfer to different uptake or release rates so that these parameters together with the growth rate can be analyzed and discussed. The calculated rates of each single bioreactor run are given in Table 4.1.5. One can deduce from Figure 4.1.5 and Table 4.1.5 that reactor runs inoculated with the same pre-culture (e.g. STR 2a vs. STR 2b) result in very similar time courses of viable cell and metabolite concentrations and thus show only negligible differences in rates. It was thus concluded that parallel reactor runs cannot be analyzed as two independent experiments, but should be considered as technical replica. If two parallel runs are performed, an average of both parallel runs can be used for comparison to other experiments.

The second variability that has to be considered is the measurement error that already was part of the above mentioned variances in starting cell concentrations and time courses. To account for this error in rate calculation, the standard deviations for the method derived from assay validation (see Table 3.2) were used for a MonteCarlo simulation. 100,000 random data sets were generated and for each set the corresponding rates were calculated. From this set of rates, the respective empirical standard deviation was derived and is given in Table 4.1.6 for the four (averaged) STR and two single Wave cultivations.

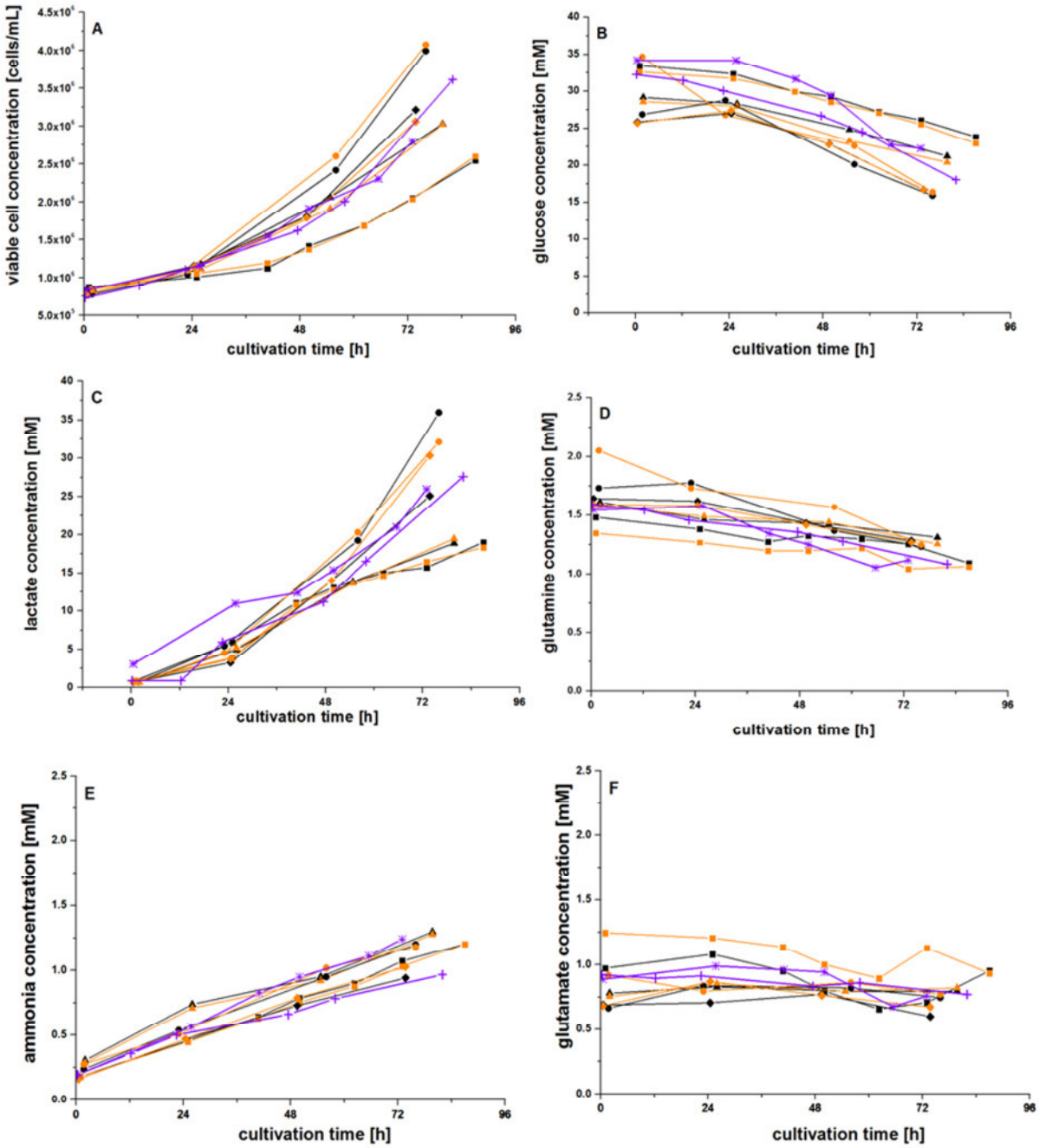

Figure 4.1.5: Time courses of viable cell and main metabolite concentrations during cultivation of CR.pIX cells cultivated in STR (black and orange) and Wave bioreactor (violet stars and crosses). Concentrations of A: viable cells, B: glucose, C: lactate, D: glutamine, E: ammonia, F: glutamate. Two parallel STR cultivations are shown, indicated by same symbols, but in orange and black. Overall, 8 STR runs are shown (4 experiments with 2 parallel runs each) and 2 independent Wave bioreactor runs.

Considering growth rates, glucose uptake and ammonia as well as lactate release rates, relative standard deviations of 3.2–12.5% were derived. These values are in the same range than the relative standard deviations in starting concentrations which were between 0.1–13.5% (see Table 4.1.4). Moreover, such deviations have also be observed in other studies calculating rate or flux errors [201, 202]. Only uptake rates for glutamine and glutamate deviated to a large extent (11.7–157.9%). This can be assigned to a high sensitivity of rate

calculation with those metabolites that stay nearly constant over the considered time interval.

Table 4.1.5: Growth rates, uptake and release rates from single cultivations of CR.pIX cells in STR and Wave bioreactor. Four STR experiments were performed (1–4) with two parallel reactor runs for each experiment (a and b).

	μ [1/h]	Glc[a]	Lac[a]	Gln[a]	Amm[a]	Glu[a]
1a	0.0161	-205.65[b]	293.18	-6.22	18.70	-14.96
1b	0.0161	-217.42	323.91	-5.74	18.80	-7.03
2a	0.0169	-207.11	399.80	-4.52	16.52	-0.83
2b	0.0185	-198.83	374.72	-6.57	15.37	-0.69
3a	0.0252	-255.96	614.66	-10.77	13.28	-1.83
3b	0.0239	-225.61	594.70	-10.56	14.44	-0.52
4a	0.0208	-220.58	523.44	-5.84	8.12	-1.31
4b	0.0215	-217.23	525.49	-6.26	9.23	-2.91
Wave1	0.0186	-290.80	390.33	-8.41	15.62	-5.96
Wave2	0.0220	-238.99	434.06	-7.57	9.19	-2.54

[a]uptake or release rates in [μmol/gDW/h]
[b]negative rates indicate uptake of the metabolite

Opposed to the small differences seen for technical replica (e.g. STR1a vs STR1b), one could observe rather high inter-experimental differences (Table 4.1.6, e.g. STR1 vs STR3). The growth rate for example varied between 0.016 and 0.025 h^{-1} between the STR runs, whereas rates calculated from parallel runs were nearly identical. For uptake and release rates this discrepancy was even higher, and, in particular, clear for the lactate release rate. While the difference between technical replica was 31 μmol/gDW/h in maximum (STR1a vs STR1b), a difference of even 296 μmol/gDW/h between experiments (STR1 vs STR3). For interpretation of Wave versus STR performance, it is obvious that rates from a single STR run compared to a single Wave experiment differed considerably. For STR1 for example a glucose uptake rate of 211.5 μmol/gDW/h was found, whereas for Wave1 a higher rate of 290.8 μmol/gDW/h was calculated (an increase of 37%). Such large differences support the hypothesis that there are significant differences between both cultivation systems.
Also, clear differences between average rates over all STR and Wave cultivations were observable (see Table 4.1.6 lower part). For example glucose uptake rates differed considerably to 46.4 μmol/gDW/h (21%). Only the growth rate was found to be nearly identical with 0.020 and 0.021 h^{-1} for STR and Wave, respectively.

Table 4.1.6: Average growth rates, uptake and release rates from independent STR and Wave cultivations. Average rates and corresponding standard deviations from parallel STR runs are given (upper part) as well as average rates and standard deviations over all STR and all Wave runs.

	μ [1/h]	Glc	Lac	Gln	Amm	Glu
	0.016	-211.5	308.5	-6.0	18.8	-11.0
1[a]	6.0E-04	14.5	15.3	4.7	1.5	1.3
	3.7%	6.9%	5.0%	78.6%	8.0%	11.5%
	0.018	-203.0	387.3	-5.5	15.9	-0.8
2[a]	7.5E-04	17.9	21.0	7.0	2.0	1.2
	4.2%	8.8%	5.4%	126.2%	12.5%	157.9%
	0.025	-240.8	604.7	-10.7	13.9	-1.2
3[a]	8.9E-04	16.7	31.4	5.7	1.4	0.9
	3.6%	6.9%	5.2%	53.4%	10.1%	76.6%
	0.021	-218.9	524.5	-6.1	8.7	-2.1
4[a]	6.7E-04	12.8	25.3	3.4	0.9	0.6
	3.2%	5.8%	4.8%	56.2%	10.4%	28.4%
	0.020	-217.5	466.1	-7.0	14.0	-2.5
STR[b]	3.8E-03	16.2	133.2	2.4	4.3	4.9
	18.7%	7.4%	28.6%	34.5%	30.5%	195.8%
	0.021	-251.9	423.1	-7.8	10.8	-3.4
Wave[b]	2.4E-03	36.6	30.9	0.6	4.6	2.4
	11.4%	14.5%	7.3%	7.6%	42.1%	71.2%

[a]absolute rate values are given as first value [μmol/gDW/h], subsequently absolute standard deviations and, finally, relative standard deviations [%]
[b]averages of all STR runs and all Wave runs, respectively

The inter-experimental standard deviation, calculated from average rates of all STR and all Wave cultivations, respectively, varied between 7.3% (lactate release) and 42.1% (ammonia release) and was higher than 50% for glutamate uptake. As these values are higher than measurement errors and deviations from technical replica, one can conclude that the inter-experimental variance is likely to be the major contributor to the overall variance. Finding such large differences even when regarding only STR runs performed under the same conditions, it was questionable whether there is a statistically relevant difference between both cultivation systems. The statistical analysis that was applied to answer this question was also used to address a second question, namely how many experiments would be needed in order to mathematically assign statistical significance when including all known errors for analysis? Detailed information on the applied statistical methods to approach these questions can be found in the publication about this part of the project [164] or in standard books or reviews on statstics, e.g. by Fitzner et al. [203]. Here, only the most relevant results will be presented and discussed.

Statistical analysis

For the statistical analysis of rates derived from STR and Wave cultivations, a two-sided t-test for two independent samples with a significance level of α=0.05 was performed. The null hypothesis (H_0) that the rates are equal in both cultivation systems was tested against the alternative hypothesis (H_1) that the rates differ significantly. Two scenarios were considered. On the one hand, only standard deviations from measurement errors were assumed to play a role in rate calculation. On the other hand, a fixed overall standard deviation of 25% was applied. This value was chosen as it is within the interval for inter-experimental variances that has been found.

At first, rates from Wave and STR cultivations were compared one to one, e.g. Wave 1 vs STR 3 or Wave 2 vs STR 1 – altogether 36 comparisons. Using only the measurement error, 12 out of 36 tests identified a significant difference between rates. 9 out of 18 tests that compared STR values with each other, however, showed significant differences as well. It is thus very likely that false-positive results were obtained. When applying the standard deviation of 25%, which is a more realisitic value as it includes measurement error and inter-experimental variability, only 3 out of 36 tests showed a significant difference between STR and Wave. Second, we tested averaged STR rates against Wave rates. Now, all possible tests showed no significant difference. Therefore, the null hypothesis cannot be rejected and – contrary to the anticipated outcome – one must assume that CR.pIX cells perform equivalently in both cultivation systems.

It must be emphasized here that if only the standard deviation of a multiple measurement per sample would have been used as error as done by many studies [160, 201], we would have wrongly concluded that many rates differ significantly between STR and Wave cultures.

Implementing the observed variances into experimental planning, we computed the number of experiments that are needed to identify a significant difference of 50% between rates found in both cultivation systems, e.g. glucose uptake rate of 150 µmol/gDW/h in STR and 75 µmol/gDW/h in Wave cultivation. With a relative rate measurement error of 10%, which is a realistic value for most methods, one would need four biologically independent experiments for each cultivation system. Only if the rate difference is as high as 100% between both cultivations (150 µmol/gDW/h in STR and 300 µmol/gDW/h in Wave bioreactor), two experiments would be sufficient to identify a significant rate difference.

It is clear that typically four independent cell culture experiments for each set-up will not be performed due to costs and time-limitations. However, using less experiments will probably generate statistically insignificant data. Also, changing the significance level towards less stringent values than α=0.05 will increase the probability to identify significantly different rates.

Four effects were analyzed in this part of the project: starting conditions, measurement errors, "technical" variations when performing parallel cultivations and inter-experimental variations. Starting conditions did vary to a certain extent, but as it cannot be ruled out how this correlates to uptake, release or growth rates, this parameter could not be analyzed further. Measurement errors (meaning errors derived by method validation, not repeated measurements of one sample) should be known for rate calculation as they can account for up to 12.8% in data variation (see Table 3.2). Minimization of measurement errors could only be done by improving the measurement techniques or assays. "Technical" variation or process variance (as the variance between two parallel cultivations inoculated with the same pre-culture at the same day) was shown to be only a minor contributor to the overall variance (12.5% in maximum when neglecting glutamine and glutamate uptake rates). In contrast, the inter-experimental variance was shown to be a major source of variation in the calculated metabolic rates (42.1% in maximum, again neglecting values for glutamine and glutamate uptake). This effect should be taken into account when comparing two systems to get an unbiased interpretation of experimental results.
There are four main outcomes of this part of metabolic study:

- cultivation of CR.pIX cells in STR and Wave bioreactor did not result in significantly different rate values
- validated methods for measuring cell and metabolite concentrations are crucial in order to evaluate the impact of assay errors on rate calculation
- analyzing experiments using parallel runs might lead to a high rate of false-positive assignments; however, they can provide experimental confidence when testing new parameters
- inter-experimental variation accounts for the main part of variance and, in reverse, a high number of biologically-independent experiments would be needed to mathematically demonstrate significant differences between two set-ups; this does not mean that trends that have been observed when changing parameter x or y are not true – although probably cannot be shown statistically

4.1.3.3 Flux distribution obtained by flux analysis

FVA and MFA were used to study the metabolism of CR.pIX cells in more detail. In particular, the intracellular fluxes related to glutaminolysis were of special interest (as glutamine uptake was not observed, see Figure 4.1.4F). Also, as no avian transformed cell line had been studied before in detail, the metabolic behavior in comparison to other commonly used transformed cell lines was of interest.

All shaker flask cultivations that were performed throughout the project could not be analyzed by MFA due to problems closing C and N balances. This scrutinized the idea of finding hints explaining pyruvate increases in shaker flasks that had been observed for CR and CR.pIX cells. Wave cultivations were not analyzed as there was no significant performance difference between Wave and STR cultures and the chemical glutamine degradation rate was determined in STR runs. Finally, only STR run was chosen for calculation the general flux distribution of CR.pIX cells (C and N balance closure >85%). For this experiment, amino acid concentrations were measured using the derivation method as described in section 3.3.1.

Extracellular rates for the considered STR cultivation

Growth rate and uptake and release of metabolites were calculated (Table 4.1.7) and compared to rates found for other transformed cell lines. Overall, we chose six data sets where equal units were given or could be calculated for comparison, namely three publications on the metabolism of human AGE1.HN cells [160, 201, 204] and one publication each on HEK293 [178] and MDCK cells [159, 205]. For most of the metabolites, the measured exchange rates during CR.pIX cultivation have the same direction (uptake or release) and are in the same range compared to those found for other cell lines. Larger differences in rates in CR.pIX cell cultivations were observed for only few metabolites.

First, glutamine uptake was zero with CR.pIX cells with the whole glutamine concentration decrease as a result of glutamine hydrolysis as addressed before. Associated with this, only low amounts of ammonia were released into the medium (≤1.4 mM at the end of the exponential phase) with a significantly lower rate (12.6 µmol/gDW/h) than those observed for other cells (48.5–91.7 µmol/gDW/h). For production of cell culture-derived products this is a beneficial characteristic as high ammonia concentrations are known to be toxic with negative impact on cell growth and product formation [206]. Transformed mammalian cells have been described to gain 30–65% of energy from glutaminolysis, but reduce this proportion when high glucose concentrations are present in the medium [207]. For CR.pIX cells, glutamine appears not to be essential as the high glucose uptake rate and several amino acids complement energy supply. The second difference was a slightly higher release rate of alanine in CR.pIX cells (31.6 µmol/gDW/h) in comparison to other cell lines. Release of alanine is (in conjunction with lactate release) considered an indication for overflow glycolytic or glutaminolytic metabolism and is often observed for immortalized cell lines like hybridoma or CHO cells [208-210]. Interestingly, with MDCK cells no alanine accumulation was observed during exponential growth phase, although high uptake rates of glucose and glutamine were observed for this cell line [205].

Table 4.1.7: Extracellular fluxes for cultivation of CR.pIX cultures in comparison with literature data.

	CR.pIX STR[a]	AGE1.HN Shaker[b]	AGE1.HN Tube[c]	AGE1.HN Tube[d]	HEK293 STR[e,g]	MDCK STR[f,g]
Time frame [h]	24–97	18–90	72–169	0–74	0–72	16–80
Initial glc [mM]	33	20-25	30	30	15	30
Initial gln [mM]	1.5	5	2	4	1	2
Glc	-211.2 ± 10.8	-123.0	-126.9	-429.2	-395.5	-1108.7
Lac	297.6 ± 8.8	263.3	87.6	639.8	439.0	2108.0
Pyr	-30.1 ± 0.8	-28.7	-2.9	-76.5	-	0.0
Gln	-0.1 ± 0.1	-37.1	-41.2	-95.5	-66.5	-70.9
Amm	12.6 ± 0.9	-[h]	-	91.7	48.5	51.8
Glu	-1.4 ± 1.1	4.0	0.9	17.0	-1.4	-42.1
Ala	31.6 ± 4.9	17.5	8.0	20.6	11.8	-49.4
Arg	-9.9 ± 2.8	-8.2	-4.4	-12.4	-15.3	-11.7
Asn	-17.1 ± 8.5	-2.9	-2.0	-7.3	-4.6	-1.9
Asp	-17.8 ± 3.2	-14.1	-8.9	-16.2	-0.2	-2.0
Cys	0.0	0.2	-1.1	-0.2	-	-2.4
Gly	-4.8 ± 4.8	2.6	-0.8	6.8	17.0	2.3
His	-2.3 ± 0.4	-1.7	-0.7	-3.2	-3.5	-2.8
Ile	-6.2 ± 4.4	-8.1	-1.4	-14.7	-21.8	-12.3
Leu	-7.9 ± 3.2	-11.5	-3.2	-23.8	-24.7	-23.5
Lys	-5.5 ± 0.3	-6.9	-3.5	-16.6	-12.6	-22.9
Met	-4.1 ± 2.0	-3.1	-1.2	-6.6	-4.9	-6.4
Phe	-2.5 ± 1.0	-3.3	-1.5	-6.3	-5.4	-8.9
Pro	-0.1 ± 0.1	7.1	13.1	13.4	0.8	6.7
Ser	-8.3 ± 8.3	-12.2	-5.7	-33.4	-17.7	-16.8
Thr	-3.4 ± 1.9	-4.9	-2.0	-8.0	-9.5	-14.9
Trp	-1.5 ± 0.2	-0.9	-0.4	-0.8	-[h]	-5.2
Tyr	-1.8 ± 1.8	-2.8	-1.4	-5.5	-4.6	-5.0
Val	-4.3 ± 2.8	-8.4	-1.8	-14.2	-19.1	-17.0
Uric acid	0.0	-	-	-	-	-

All rates are given in µmol/gDW/h

[a]standard deviations in this column are derived from MonteCarlo sampling of measured or estimated rates using validated standard deviations of the methods as boundaries

[b]from [160]; [c]from [204], cultivation in bioreactor tubes; [d]from [201]; [e]from [178]; [f]from [159, 205]

[g]these fluxes were re-calculated to [µmol/gDW/h] with the given fluxes and cell dry weights

[h]no values published

Third, glycine was taken up by CR.pIX cells, but released by other cell lines. Although the uptake rate is not high and the calculated interval entails zero, this is an interesting observation as glycine is reported to be an essential amino acid for birds. It is therefore plausible that glycine is taken up and needs to be provided for CR.pIX cells by the medium [64]. The fourth finding is that asparagine and aspartate were consumed by CR.pIX cells in higher amounts or at least at high rates. They are both precursors of oxaloacetate and can

thus be channeled into the TCA cycle (see Figure 2.4 or Figure 3.4). One could speculate that CR.pIX cells compensate a low glutaminolysis rate with these amino acids.

Flux distribution & enzyme activity measurements

The calculated exchange rates were used to calculate intracellular flux distributions. In scenario 1, we applied FVA and used the flux rate values plus/minus their corresponding standard deviations as upper/lower boundaries. Since this system is underdetermined, only flux ranges can be calculated. However, some conclusions can already be drawn from these calculated flux ranges. With scenario 2, a unique flux distribution was calculated via MFA. For this, mean extracellular rate values from scenario 1 were used and the flux through the pyruvate carboxylase (PC) was assumed to be inactive (resulting in an over-determined system). Measured uptake rates for the essential amino acids histidine, lysine and tryptophan were slightly below their minimal requirements for biomass formation with the determined growth rate. For the determination of the intracellular flux distribution via FVA and MFA, we therefore allowed for slightly higher *in silico* upper boundaries for the respective rates to fit the minimal stoichiometric demands for the measured specific growth rate. Selected fluxes from both calculations (scenarios 1 and 2) are shown in Figure 4.1.6 and fully listed in Appendix A7. Short names for the reactions are also defined there. Percentages that are given in the following discussion are the proportion of the considered flux on the sum of all fluxes for this metabolite.

Glycolysis and pyruvate metabolism

For most rates of glycolysis, relatively small limits can be calculated in scenario 1 as they only depend on the glucose uptake rate that was given by the measurement of extracellular glucose (Figure 4.1.6A). When setting the constraints of scenario 2, all fluxes are uniquely resolved.

Glucose is taken up with high rates (211 µmol/gDW/h) - at least comparable to other reported cell culture experiments - and then processed via glycolytic reactions to pyruvate. Only 1% of the glucose is fed into the pentose phosphate pathway for nucleotide synthesis. Such low pentose phosphate influxes were also observed in other studies with transformed cells, e.g. 1.5% and 2.9% in human AGE1.HN cells [160, 204].

Pyruvate is taken up in lower amounts than glucose (Pyr); the rest of the cytoplasmic pyruvate is mainly derived from glycolysis (92%) and in small parts from cysteine degradation and the malic enzyme reaction (together 1%). Similar to other transformed cells, cytosolic pyruvate is mainly converted to lactate (73%) or alanine (9%). The rest (17%) is transported to the mitochondrium where it is converted to acetyl-CoA and further oxidized. Overall, the flux distribution at the pyruvate node shows that the majority of the

glucose-associated metabolism of CR.pIX cells is used to generate ATP and reducing equivalents in the glycolysis (Figure 4.1.6C).

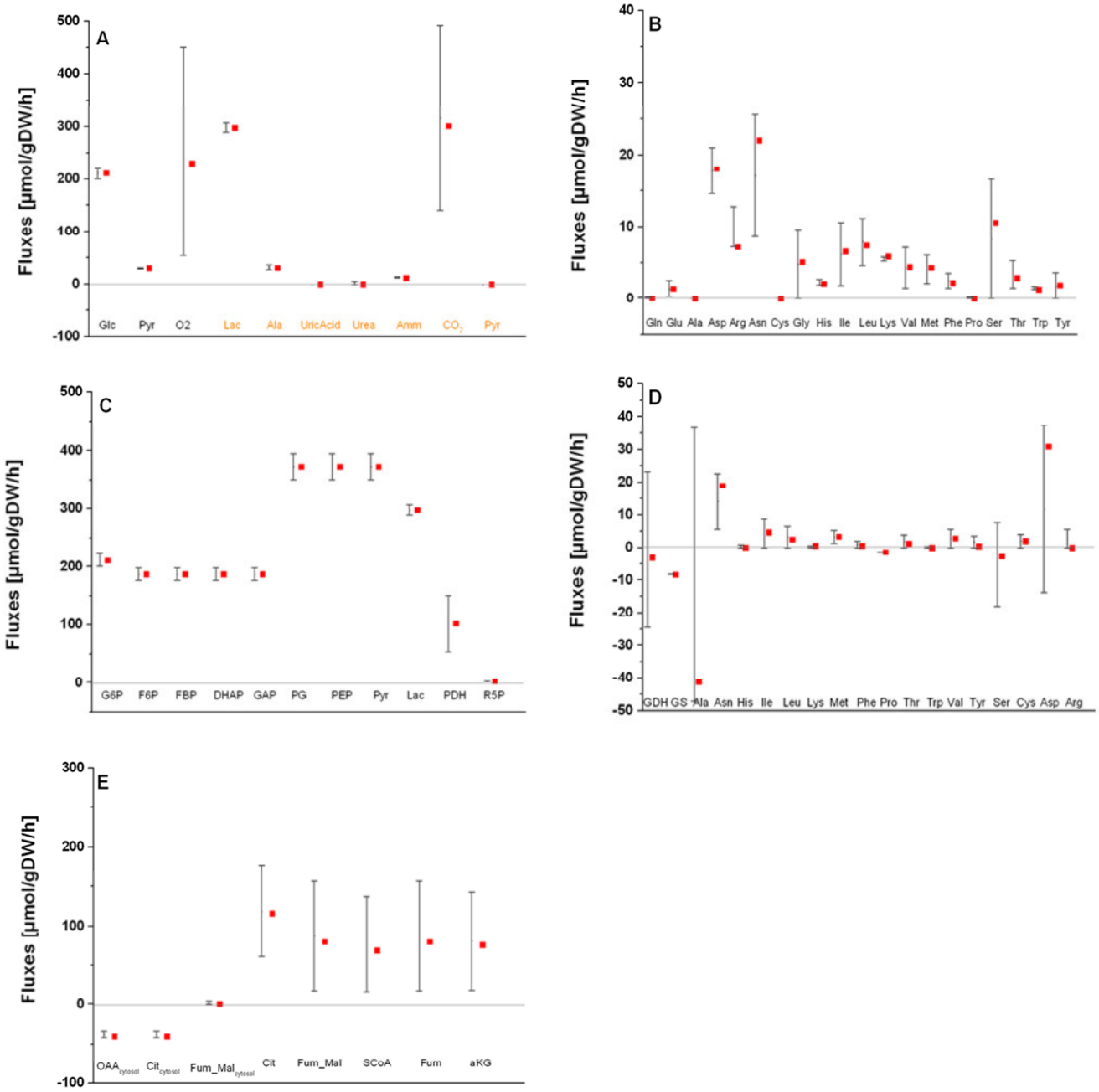

Figure 4.1.6: Extra- and intracellular fluxes calculated for cultivation of CR.pIX cells in 1 L STR. Black bars indicate fluxes or flux ranges from scenario 1, red squares indicate fluxes derived from scenario 2. A: uptake and release of metabolites except amino acids (Glc, Pyr and O_2 uptake rates, the other rates (orange labels) are release rates), B: uptake and release of amino acids, C: glycolysis (labeling indicates product of the respective reaction, only the reaction Pyr to AcCoA catalyzed by PDH is indicated with enzyme name), D: amino acid catabolism (reactions from Gln to Glu and from Glu to Gln, respectively, are indicated by their enzyme names GDH and GS), E: TCA cycle. Labels below the corresponding bars are defined in the network model (see Appendix A7).

The generally known Warburg effect or aerobic glycolysis, leading mostly to lactate, can thus also be observed in transformed cells from avian origin. Only a minority of the cytosolic pyruvate is transported into the mitochondrium. Other studies have shown with enzyme activity measurements that several transformed cell lines show low activities of the three enzymes pyruvate dehydrogenase (PDH), pyruvate decarboxylase (PC) and phosphoenolpyruvate carboxykinase (PEPCK) that serve as connectors between glycolysis and TCA cycle [211, 212]. For our cells, a PDH activity was calculated (since the lower boundary of this reaction is strictly positive), but the non-resolvable PC reaction is not obligatory as its flux range also includes zero. From this and the low net shuttle fluxes for pyruvate, we inferred that glycolysis is only weakly connected to the TCA cycle. Supporting this hypothesis, maximum activities of PC and PDH were only 0.2 nmol/10^6cells/min, which is similar to what was found for MDCK cells [213]. These values support the used constraint of a missing anaplerotic reaction towards OAA. However, the measured low PDH activity seems to contradict the calculated flux of 102 µmol/gDW/h. One possible explanation is given by the significantly smaller calculated lower boundary of this flux when fewer and less stringent assumptions in scenario 1 are applied. However, at least a basal activity is required even for scenario 1 as the lower boundary is strictly positive.

TCA cycle

Applying the constraints of scenario 1, the fluxes for the TCA cycle are weakly determined as they show high ranges and sometimes also include zero as a solution (Figure 4.1.6E). Only for scenario 2, the TCA cycle fluxes can be resolved to distinct positive values, meaning that the fluxes of the TCA cycle circulate in the oxidative direction as expected so that reduction equivalents are produced. Calculated TCA fluxes for CR.pIX cells were around 75 µmol/gDW/h. This is at the upper range than has been calculated by metabolic flux analysis for AGE1.hn, MDCK and CHO cells. For those cell lines, TCA fluxes of 9–78 µmol/gDW/h were described (summarized in [160]).

The reaction catalyzed by pyruvate dehydrogenase to acetyl-CoA generates 88% of mitochondrial acetyl-CoA. Other influxes towards this TCA precursor come from amino acids, namely isoleucine (4%) and leucine (7%), tryptophan and lysine (together 1%). The following reactions of the TCA cycle are fed from other catabolic reactions: α-ketoglutarate from cytosolic influx and succinyl-CoA from isoleucine, valine, serine and methionine degradation. This again shows the high dependency of the TCA cycle activity on relatively high amino acid uptake and catabolic rates in CR.pIX cells. The two anaplerotic reactions towards malate and oxaloacetate are not uniquely resolvable. However, when assuming in scenario 2 that the pyruvate carboxylase is inactive [211, 212], the flux towards malate can be uniquely calculated to 35 µmol/gDW/h.

Oxidative phosphorylation & ATP balance

The oxidation of NADH and $FADH_2$ in the mitochondrium leading to the generation of ATP takes place in large quantities: fluxes of 177 µmol/gDW/h for the NADH oxidation and 46 µmol/gDW/h for $FADH_2$ oxidation were calculated. A minor flux for the transport reaction shifting reducing equivalents from the mitochondrium to the cytosol was calculated to be 30 µmol/gDW/h.

As for example observed for mouse hybridoma and CHO cells [214, 215], reducing equivalents make up a large pool for ATP generation in CR.pIX cells. The highest fraction is derived from TCA cycle: together with the electron transport chain this makes up 74% of the generated ATP. The rest is derived from glycolysis (26%). In other studies, the TCA cycle is also described to be responsible for 60–80% of ATP generation [214, 215]. Although considerable ATP amounts are needed for lipid synthesis, amino acid transporters, upper glycolysis and biomass, the high (unspecific) ATP consumption through the maintenance reaction (966 µmol/gDW/h) indicates that there is an ATP overload, which is either used by CR.pIX cells for certain maintenance reactions or passed through futile cycles.

Amino acid and nitrogen metabolism

When applying the underdetermined scenario 1, most fluxes for amino acid uptake and catabolism (Figure 4.1.6A and D) have a determined direction and are constrained to a relatively small range (e.g. for catabolism of valine and cysteine). No uric acid synthesis could be found experimentally and thus the uric acid synthesis flux was thus set to zero. Although this reaction is known to take place in avian cells, this is not a fully unexpected finding. Uric acid was detected in livers and kidneys of chicken and turkey, but not in all bird tissues [64]. CR.pIX cells, as other transformed cells, use ammonia as a sink and release the excess cytosolic ammonia (that is produced by deamination reactions of amino acids) into the medium (r82) where it accumulates. However, due to low glutamine exploitation, the ammonium concentration stays at a low level so that probably toxic concentrations of ≥ 5 mM are not reached.

When applying the determined scenario 2, all fluxes of amino acid catabolism can be uniquely resolved. Catabolic rates of some amino acids, e.g. tryptophan and histidine, are low, indicating that the uptake of these amino acids is matching the anabolic demand of the cell. This can be taken as indication that the medium is well balanced. Interestingly, the fluxes through the glutamine synthetase (GS, i.e. in the direction of glutamate synthesis) are negative as glutamine uptake was not sufficient for biomass synthesis and glutamine therefore has to be synthesized from the glutamate pool. Glutamate itself is mainly derived from degradation reactions of isoleucine, valine and aspartate. Especially aspartate is taken up in large parts and converted mainly to glutamate. Other amino acids that could

compensate for glutamine conversion to glutamate, are arginine, histidine and proline. However, only arginine is taken up by the cells in considerable amounts by CR.pIX cells. Via the glutamate dehydrogenase reaction, the generated glutamate is normally converted to α-ketoglutarate and thus distributed into the TCA cycle. In CR.pIX, however, we found only a very low flux (4.1 µmol/gDW/h) which indicates that glutamate is not fed directly into the TCA cycle. Thus, one could speculate that the path from glutamate to α-ketoglutarate is generally not used extensively by the CR.pIX cells. The classical dependency on glutamine is then not valid for CR.pIX cells.

This hypothesis of low glutamine-dependency was supported by further growth experiments and enzyme activity measurements. First, the maximal enzyme activities of GLNase and GS were measured in order to obtain an impression of the potential to convert glutamine to glutamate (GLNase) and glutamate to glutamine (GS). Flux variability analysis predicted no conversion from glutamine to glutamate. The measurement of the corresponding enzyme activity showed a maximum activity of 0.1 nmol/10^6cells/min, which is an even lower value than the measured 1.5–7.4 nmol/10^6cells/min for MDCK cells [158, 213]. The flux from glutamate to glutamine (GS) was predicted to be active towards glutamine so that glutamine can be used for biomass formation. The measured enzyme activity showed a maximal activity of 5.9 nmol/10^6cells/min. This value is on the one hand significantly higher than the value for the reverse reaction and on the other hand at the upper boundary of reported values for MDCK cells (0.6–6.5 nmol/10^6cells/min, [158, 213]). Thus, this enzyme activity supports the calculated flux distribution towards glutamine and the low level of glutamine utilization. Finally, cells were cultured in glutamine-free medium. After three passages during which the cells were adapted to this medium, an equal cell growth in terms of maximum cell concentrations was observed [157], ultimately showing the low glutamine-dependency of CR.pIX cells.

FVA and MFA were applied to CR.pIX cells in order to get more insights into the metabolism of these avain designer cell lines. Overflow metabolism as usually observed for transformed cell lines was found, converting nearly all taken up glucose to lactate and alanine. When closely studying CR.pIX cell metabolism, low glutamine dependency was found which led to the conclusion that glutamine supplementation is not essential for CR.pIX cell proliferation. Based on the performed analyses and the developed metabolic network model, optimization of medium and feed requirements might be facilitated.

4.1.4 Chapter summary and outlook

CR and CR.pIX cell growth in serum free AEM as well as in chemically-defined CD-U2 medium was characterized. Best growth performance of CR.pIX cells was obtained in CD-U2 medium: Faster cell growth which manifestated in higher growth rates as well as an increased culture longevity. Growth rates around 0.02 h^{-1} were achieved, showing that CR and CR.pIX cells proliferate as well as other pharmaceutically relevant cell lines such as CHO or MDCK. Achievable maximum cell concentrations were dependent on the cultivation system. Shaker flasks experiments led to high cell concentrations (up to $1x10^7$ cells/mL), but early cell death. Bioreactor runs led to slightly higher maximum cell concentrations (up to $1.4x10^7$ cells/mL in STR) and, more importantly, an increased culture longevity.

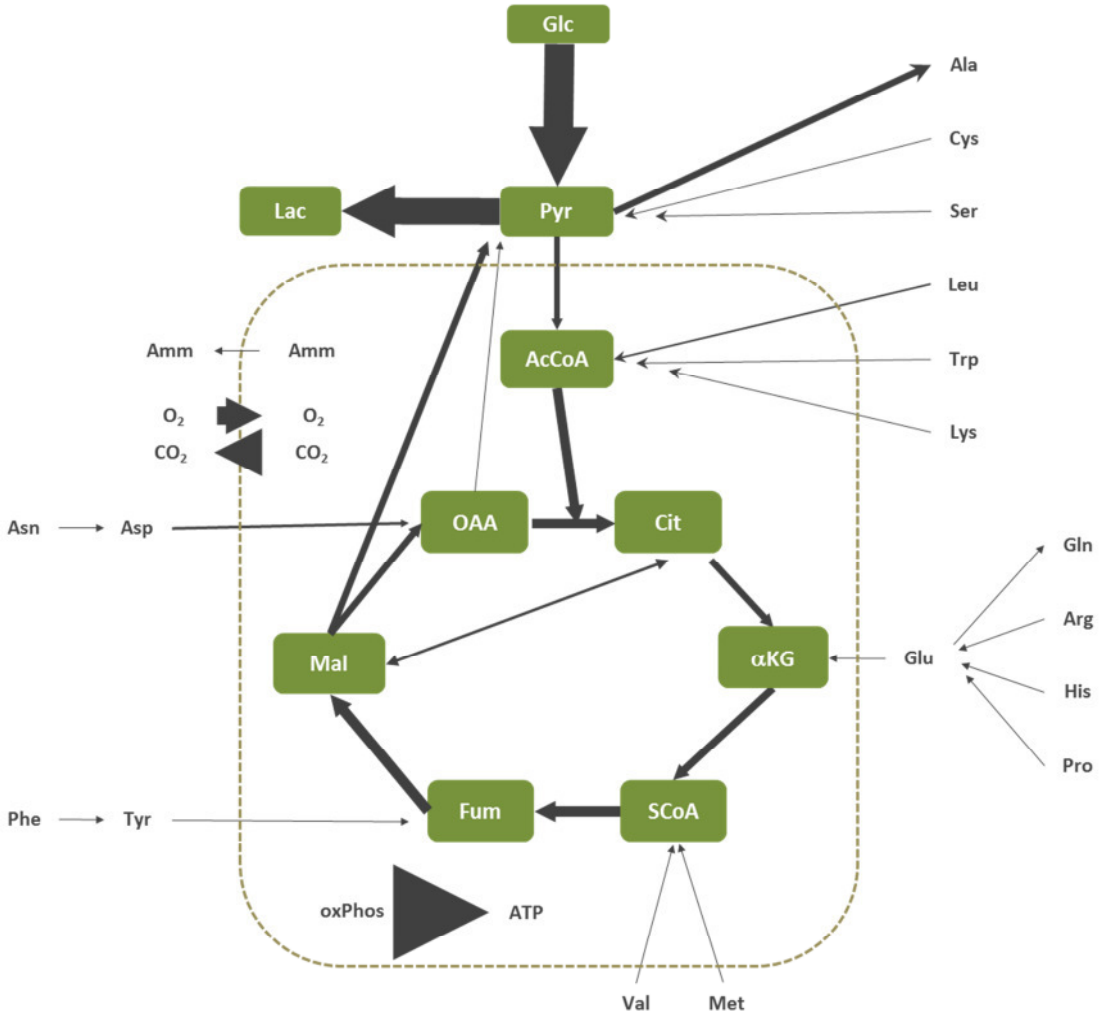

Figure 4.1.7: Overview of flux distribution as found for CR.pIX cells. Only selected fluxes are shown. Thereby, arrow sizes correspond to rate values for this reaction as calculated with metabolic flux analysis (scenario 2). The dashed line indicates the mitochondrial membrane. For amino acids, catabolic and anabolic rates are given (not uptake or release rates).

Analyzing the development of extracellular metabolite concentrations raised the question whether there are significant differences between both cultivation systems (STR and Wave bioreactor). However, a thorough statistical analysis including all relevant errors (measurement error, technical repetitions and inter-experimental variability) showed no statistically significant differences. The statistical analyses also suggested that with measurement errors above 10%, a minimum of four independent biological replication experiments are needed. Comparing two systems with less experiments thus might indicate trends, but might not be a proof for actual differences.

In more detail, the metabolism of CR.pIX cells was analyzed using MFA. Figure 4.1.7 summarizes the identified flux distribution for CR.pIX cells grown in a STR. As a basis, biomass composition of CR and CR.pIX cells was determined, and showed to resemble compositions found for other cells. Also, general CR.pIX cell metabolism resembled metabolism found for other immortalized cell lines with high glycolysis rates leading mostly to lactate and alanine. Glutaminolysis was practically not present, and required glutamine for biomass formation was even recruited from glutamate. These findings could be confirmed by enzyme activity measurements and, in addition, glutamine-free cultures. The TCA feeding function of glutaminolysis was compensated by uptake and catabolism of other amino acids, e.g. asparagine/aspartate and leucine.

The performed studies on growth and metabolism of CR and CR.pIX cells showed that they grow with competitive specific growth rates to competitive cell concentrations. Thus, a use for vaccine production in large scale is possible (assuming that virus productivity is competitive as well). Also, high cell density cultivations using fed-batach or perfusion strategies are promising in order to exploit the full potential of CR.pIX cells and improve process yields. Moreover, characterization of biomass as well as cell metabolism provides a basis for more thorough studies, including dynamic modelling of growth and probably virus production.

4.2 MVA experiments

CR and CR.pIX cells were designed for the production of MVA or MVA-based vectors. Their suitability for this purpose had been shown before this project started [18, 19]. Therefore, this chapter will only shortly summarize experiments that were done to optimize infection parameters. In addition, propagation of MVAwt and recombinant MVA strains with gene inserts of fluorescent markers is shown. Achieved titers and yields of the different virus strains were compared to each other (section 4.2.1). To follow the infection status of a cell during infection, the recombinant virus strain MVAegfp was used and a flow cytometric method for this purpose was established (section 4.2.2). Finally, studies on the effects of virus infection at low and high cell concentrations are shown. Here, cell physiology (cell cycle and apoptosis) assays were performed in parallel. Obtained results on those experiments are summarized and discussed in section 4.2.3. This chapter contains results of two student projects and preliminary experiments that have been published in 2009 [19, 85, 216].

4.2.1 Seed virus production and small-scale experiments

4.2.1.1 Seed viruses

Using the starting material obtained within cooperation projects with ProBioGen or the LMU Munich (Table 3.3), working seed material was prepared for the different MVA strains used in this project (Table 4.2.1).

Table 4.2.1: Working seed viruses from different MVA strains that were prepared and used.

Virus strain	Date prepared	Prepared from	Harvest time [hpi]	Titer [viruses/mL]
MVAwt	15.02.08	MVAwt ProBioGen ($5.0x10^7$ pfu/mL)	48	$1.8x10^7$
	03.07.09	MVAwt ProBioGen ($2.0x10^7$ viruses/mL)	50	$3.72x10^7$
MVAmCherry	25.05.10	MVAmCherry LMU ($1.0x10^8$ viruses/mL)	42	$0.9x10^6$
	25.05.10		24	$1.0x10^7$
MVAegfp	29.11.10	MVAegfp LMU ($1.0x10^8$ viruses/mL)	31	$4.6x10^7$
	06.12.10		29	$1.7x10^7$

CR or CR.pIX cells were infected with the respective starting material (moi=0.05) and harvested after the indicated time points. Seed virus titers were measured after processing the harvest (3x freeze-thaw, sonication, centrifugation).

All obtained master seeds were harvested from either CR.pIX (MVAwt) or CEF cultures (MVAmCherry and MVAegfp). Based on literature and scouting experiments (data not shown), it was decided that an adaptation to CR or CR.pIX cells over several passages is not required. Therefore, working seed virus was harvested after the first passage in CR.pIX cells. All harvests showed a virus titer of about $1x10^7$ viruses/mL and could thus be used as seed viruses for all following experiments.

4.2.1.2 Optimization of infection parameters

Small-scale experiments in T-flasks or shaker flasks were performed to evaluate i) the suitability of CR and CR.pIX cells for MVA production, ii) the best ratio between growth medium CD-U2 and virus production medium medium CD-VP4, and iii) optimal infection conditions like moi (only done for MVAegfp as this had been done previously for MVAwt [18, 19]).

CR vs CR.pIX

Early in the project, comparisons were done in order to evaluate the suitability of CR and CR.pIX cells for MVA propagation. Earlier experiments had shown lower titers for CR cells when using serum-free media AEM and MegaVir [19]. After switching the system to chemically-defined media for cell growth and virus infection (CD-U2 and CD-VP4, respectively), this finding was confirmed. Infection of CR cells resulted in titers of approximately $5x10^6$ viruses/mL (average of two independent experiments), whereby $7x10^7$ viruses/mL were yielded in average when using CR.pIX cells. These results confirmed that the medium did not affect the tendency towards reduced titers in CR cells, but supported the hypothesis that the pIX gene present in CR.pIX cells positively affects virus propagation. A model explaining this effect in conjunction with the finding that pIX expressing cells show higher sensitivity towards the pathogen-associated presence of dsRNA has been proposed by Jordan et al. [18]. According to the authors, the pIX protein might activate heat shock protein 90 (Hsp90) so that Hsp90 forms a complex with Hsp70. Thus, the pool of free Hsp70 would be reduced, leaving fewer Hsp70 molecules available to interact with the co-chaperone $P58^{IPK}$. As a result, fewer $P58^{IPK}$ would be available to inhibit the anti-viral acting protein kinase R (PKR), a sensor for dsRNA in anti-viral defense pathways of the cell [217]. However, proteins expressed by MVA can counteract the elevated anti-viral state of the host cell. The hypothesis would explain increased titers achieved by pIX-expressing cells via activation of chaperones as long as the virus can neutralize PKR. The experiments described in the following were therefore mainly done with CR.pIX cells.

Implementation of CD-U2/CD-VP4

At the beginning of the project, two serum-free media were used: AEM as growth medium and MegaVir as virus production medium, used in a 1:1 mixture in the infection phase. Later, chemically-defined media especially for the CR.pIX cells were designed and thus could also be used for this project. With this switch, several parameters had to be re-analyzed. The ratio between growth and infection medium was, for example, re-tested with MVAegfp (Figure 4.2.1). Virus production medium was used to induce aggregate formation (mainly triggered by a high osmolality, which is approximately 450 mOsm/kg in CD-VP4 medium in contrast to approximately 300 mOsm/kg in CD-U2 medium). Aggregate formation, however, impairs cell counting and process monitoring during the infection phase. Therefore, it was tested whether other ratios of CD-U2:CD-VP4 would also allow to obtain high virus yields. Also, this would mean less dilution of the cell suspension so that higher cell concentrations could be infected.

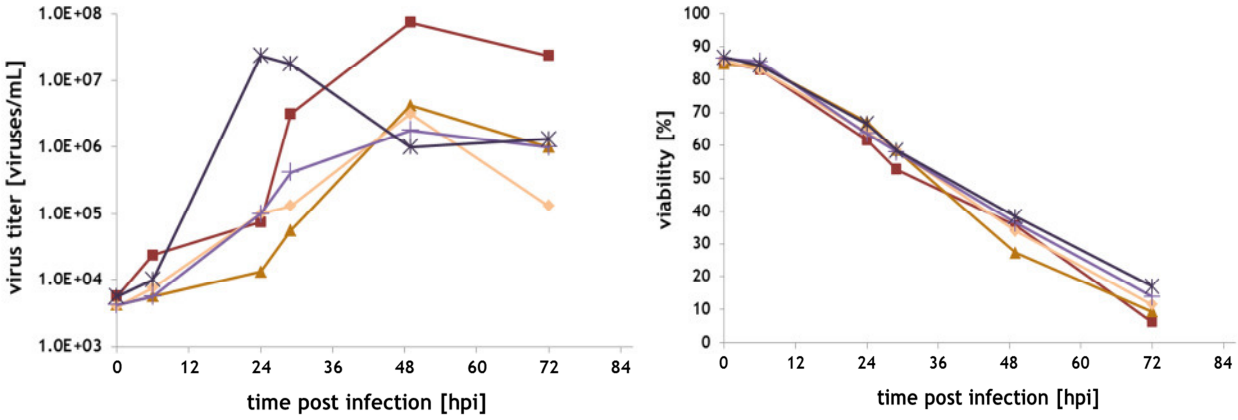

Figure 4.2.1: Propagation of MVAegfp in CR.pIX cells, which were cultivated in CD-U2 medium and infected in mixtures of CD-U2:CD-VP4. Dark violet (✱): 3:1 ratio, violet (+): 2:1 ratio, red (■): 1:1 ratio, orange (▲): 1:2 ratio, light orange (◆): 1:3 ratio. Left: Virus titer, right: Cell viability. Adapted from [216].

Using reduced volumes of CD-VP4 (3:1 ratio or 2:1 ratio instead of 1:1 ratio of CD-U2/CD-VP4), did not result in higher or at least similar titers. Interestingly, with a 3:1 ratio, a faster increase in virus titer was observed, probably due to better cell fitness in the hours after infection. However, a lower final titer was reached in comparison to the 1:1 ratio. Using more CD-VP4 (1:2 ratio or 1:3 ratio of CD-U2/CD-VP4) resulted in similar virus dynamics, but also reduced titers. The use of CD-U2 and CD-VP4 in a ratio of 1:1 therefore maximized virus yields.

Regarding cell aggregation, no difference could be observed for all tested ratios so that there was also no advantage for cell counting when using lower amounts of CD-VP4. For this reason, in all following figures, cell concentrations are not shown as cell counts

cannot be interpreted. Measurement of cell viability is also impaired after infection, but at least indicated a successful infection of the respective cell culture. As seen in Figure 4.2.1, viability drops instantaneous after virus infection and reaches 30–50% at 48 hpi. At this time, maximum titers were measured (with the exception of the 3:1 culture mentioned above). Afterwards, virus titers decreased. Harvesting would thus be optimal in a small window around 48 hpi.

Moi optimization

Upon switch towards MVA production in chemically-defined media, the dependence of virus yields on moi was re-analyzed. Earlier experiments showed an optimal moi of 0.05 for CR.pIX cells infected in AEM/MegaVir with MVAwt. For infection of CR.pIX cells in CD-U2/CD-VP4 with MVAegfp, five different moi between 0.001 and 1.0 were tested (Figure 4.2.2).

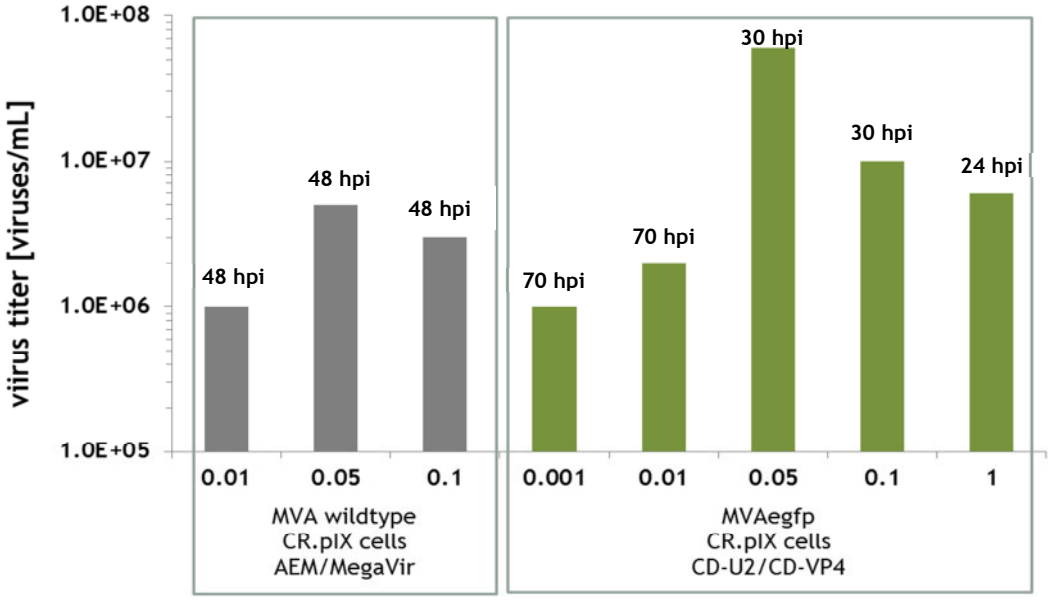

Figure 4.2.2: Maximum MVA titers at different multiplicities of infection (moi). Left bars (grey): CR.pIX cells infected with MVAwt in serum-free media (AEM/MegaVir), right bars (green): CR.pIX infected with MVAegfp in chemically-defined media (CD-U2/CD-VP4).

A moi of 0.05 yielded highest titers for this setting as well. Time points of maximum yield changed with the moi. Using moi lower than 0.05, highest yields were measured 72 hpi. Using a high moi (1.0), highest titer was achieved already 24 hpi. With moi of 0.01 and 0.05, highest virus titers could be measured between 29 and 48 hpi, consistent with the virus dynamics curves of Figure 4.2.1. Finally, a moi of 0.05 was chosen as standard moi for all subsequent experiments.

Comparison between MVAwt, MVAegfp and MVAmCherry

In order to facilitate monitoring of the infection status of host cells during cultivation, recombinant MVA strains that are genetically modified with fluorescent markers were used. MVAmcherry and MVAegfp were tested for this purpose. Overall, three different virus strains were used in this project and their propagation in CR.pIX cells was compared considering virus titers and virus dynamics. Taking together all experiments with CR.pIX cells where standard parameters were used (moi=0.05, CD-U2/CD-VP4 medium, CCI of $2x10^6$ cells/mL after 1:1 dilution of cell suspension with virus production medium), titers and time courses can be summarized as shown in Figure 4.2.3.

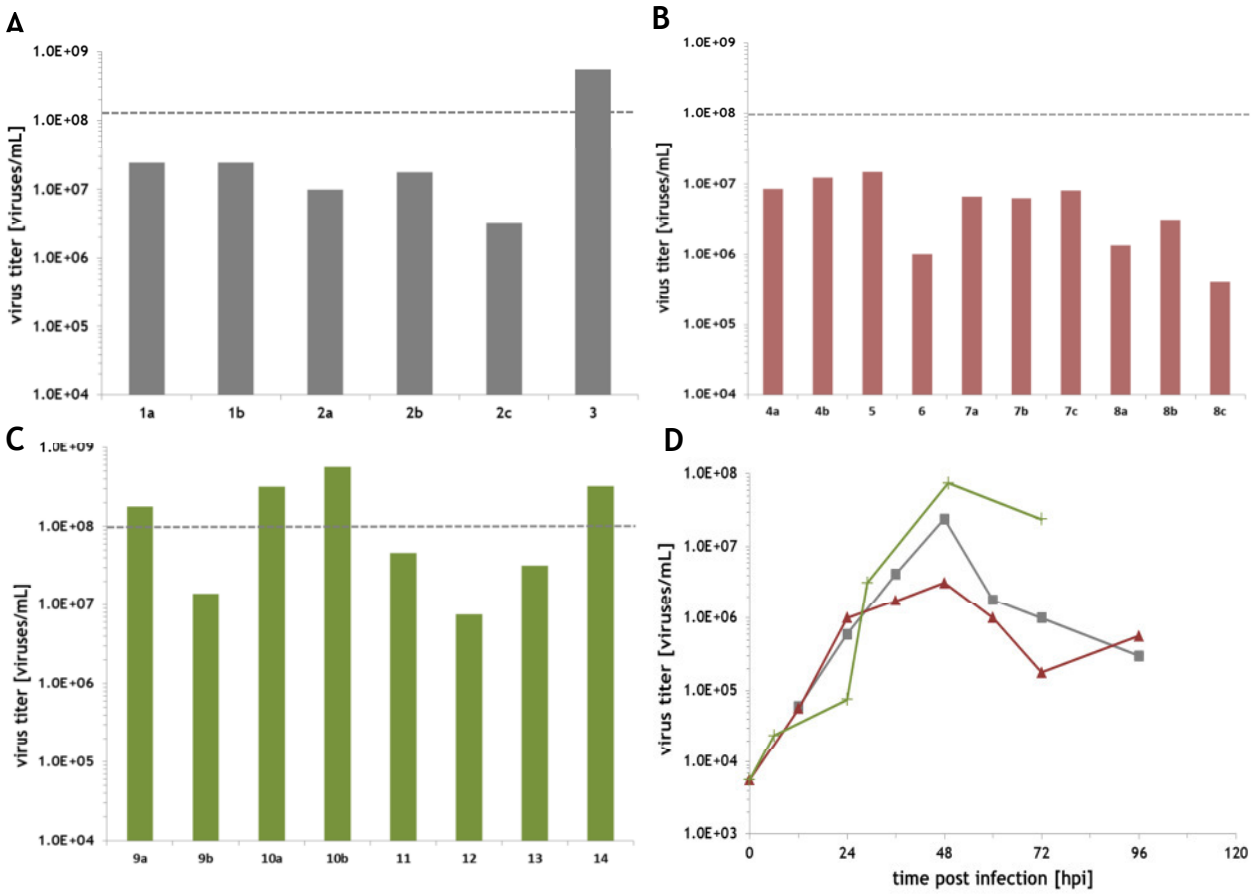

Figure 4.2.3: Maximum titers from CR.pIX infection experiments in shaker flasks using MVAwt (A), MVAmCherry (B) and MVAegfp (C). Experiments that are the basis of the shown values are numbered in order to be able to distinguish biological replica and parallel cultures. Small letters indicate that more than one flask was used in the respective experiment. Only experiments that were performed using standard infection parameters and chemically-defined media (moi=0.05, CCI=$2x10^6$ cells/mL, 1:1 ratio CD-U2/CD-VP4) are shown. D: Representative time courses of virus titers for MVAwt: grey (■), MVAmCherry: red (▲) and MVAegfp: green (+). Dashed lines indicate the benchmark of $1x10^8$ viruses/mL.

Comparing the virus titers that were achieved with the three virus strains, it is obvious that MVAwt and MVAegfp overall showed a high similarity in terms of titers and virus

dynamics. A benchmark of $1x10^8$ viruses/mL was reached for some experiments using these strains. This value is defined as benchmark due to two reasons. First, one dose of a smallpox vaccine or of a recombinant vaccine based on MVA as a vector, usually contains this amount of virus. Second, other expression systems that are used for the production of MVA supported virus titers at this concentration. In several publications, titers between $0.1x10^8$ and $10x10^8$ viruses/mL have been reported for CEF cells - the gold standard for vaccinia virus and, in particular, MVA propagation [111, 218]. Also BHK-21 or DF-1 cells, that have been shown to replicate MVA, did not produce higher titers [34, 115]. With maximum titers between $1x10^7$ and $1x10^8$ viruses/mL, CR.pIX cells can thus be considered as competitive host cells for MVA production.

The insertion of egfp into the viral genome did not impair or affect virus dynamics. MVAmCherry also showed similar dynamics, but slightly lower titers throughout the experiments. Due to difficulties with the analysis of mCherry in the available flow cytometer, and the higher titers that were obtained, MVAegfp was used for analyses of the infection status of a cell culture.

Infection at high CCI

To increase virus yields from one batch production, an increase of CCI is usually considered. Accordingly, this approach was evaluated in several small-scale experiments. However, achievable cell concentrations in a batch cultivation are limited. As shown in Table 4.1.3, a CR.pIX batch culture in shaker flasks can result in maximum cell concentrations of $0.5–1.1x10^7$ cells/mL. Due to the 1:1 dilution that is done at time of infection with CD-VP4 medium, the maximum CCI that can be tested in a batch infection experiment is approximately 0.3–0.6 cells/mL. Another probable limitation is the so-called cell density effect which has been described for several virus/host cell systems (see chapter 2.1.4.2). Figure 4.2.4 summarizes infection experiments with standard and higher CCI in conjunction with obtained maximum virus titers and cell-specific virus yields. Cell concentrations before dilution with production medium are given to indicate at which time point of cell growth the cells were infected so that the indicated standard CCI is $4x10^6$ cells/mL (which is $2x10^6$ cells/mL directly after addition of CD-VP4, referred to as standard CCI in following sections).

With increasing CCI, maximum titers slightly decreased from approximately $1x10^8$ to approximately $1x10^7$ viruses/mL: the average titer for low CCI ($4.4–5.6x10^6$ cells/mL, n=4) was $27.0x10^7$ viruses/mL; medium CCI ($6.6–6.9x10^6$ cells/mL, n=3) resulted in an average titer of $4.3x10^7$ viruses/mL, and high CCI ($8.0–8.5x10^6$ cells/mL, n=5) yielded $1.6x10^7$ viruses/mL in average. Thereby, it has to be noticed that low, medium and high

CCI experiments were not performed in the same, but biologically independent experiments, so that a trend due to different pre-cultures or titrations can be excluded.

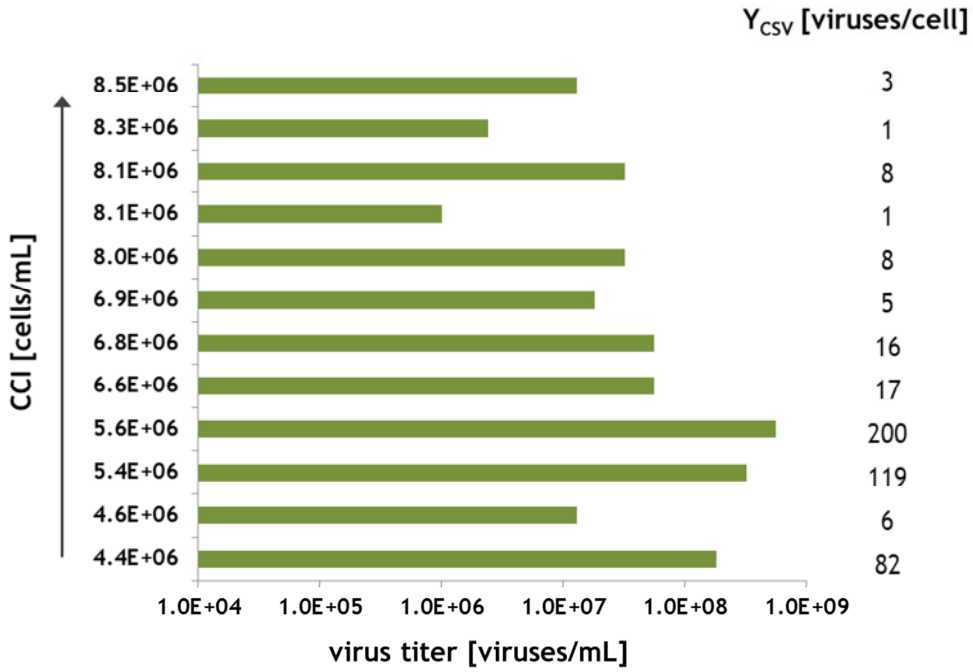

Figure 4.2.4: Maximum virus titers and cell-specific virus yields from MVA infection experiments using different CCI. CR.pIX cells were grown until different CCI and then infected with MVAegfp (moi 0.05, CD-U2/CD-VP4). Cell concentrations directly before dilution with CD-VP4 are given (y-axis).

However, obvious variations in titers make it difficult to draw valid conclusions. For example, measured titers for high CCI experiments with about $8x10^6$ cells/mL ranged between $1.0x10^6$ and $3.2x10^7$ viruses/mL. Still, the trend is clear: CCI below $5\text{-}6x10^6$ cells/mL result in higher virus titers. Similar results were obtained previously by Jordan et al. [161]. Here, CCI between $0.5x10^6$ and $2.5x10^6$ cells/mL were tested (after dilution with virus production medium). No titer decrease was observed up to these CCI. Thus, one might conclude that the critical CCI above which virus propagation is impaired, is above $5x10^6$ cells/mL (before dilution). This corresponds to the late exponential phase of CR.pIX cells grown in shaker flasks or STR. Regarding cell-specific virus yields (Y_{CSV}), the trend suggesting a cell density effect becomes more obvious. One has to note that Y_{CSV} can only be calculated based on cell concentrations measured directly before infection as cell aggregation impedes accurate cell counting after infection. Slight increases in cell concentrations which can occur during the infection phase are thus not included in the calculation. Average Y_{CSV} achieved with low CCI ($4.4\text{–}5.6x10^6$ cells/mL, n=4) was 101 viruses/cell. Medium CCI ($6.6\text{–}6.9x10^6$ cells/mL, n=3) resulted in an average yield of 13 viruses/cell and high CCI ($8.0\text{–}8.5x10^6$ cells/mL,

n=5) yielded 4 viruses/cell in average – this corresponds to only 4% of the high CCI yield. Data on MVA yields with increasing CCI are not available in literature. However, a comparison to baculovirus (produced with SF9 cells) and adenovirus (produced with HEK293 cells) can be made. In those studies, increases in CCI from $1x10^6$ cells/mL to around $4x10^6$ cells/mL resulted in yield decreases from 172 to 2 viruses/cell for baculovirus and 8300 to around 1500 viruses/cell for adenovirus [20, 21]. Only for influenza virus produced on HEK293 cells, a yield increase was observed (64 to 223 viruses/cell), and only a CCI of $6x10^6$ cells/mL resulted in a decreased yield of 139 viruses/mL [42].

The negative correlation of CCI and virus titers was described before as cell density effect. One of many reasons to explain the reduction of cell-specific virus yields with increasing CCI is a low cell fitness (apoptotic cells or cells in G0 cell cycles phase). Therefore, cell physiology analyses (by flow cytometry) were done in parallel for the experiments described above. For clarity, the obtained results will be shown and discussed after the establishment of those methods is described in chapter 4.2.4.

The yield of 1–200 infectious virus particles per cell might sound rather low. Yields reported by Carroll and Moss from infection experiments with CEF and BHK-21, two cell lines suitable for MVA production, are, however, in the same range [112]. They found approximately 500 viruses/cell for CEF and 40 viruses/cell for BHK-21 cultures. Yields reported by Drexler et al. are even lower with 20 viruses/cell for CEF cultures and 2 viruses/cell for BHK-21 cultures [34]. It has to be noted that adherent cells in 6well plates were used in those experiments so that a one-to-one comparison to the suspension process used in this work cannot be made. Generally, titers as well as yields seem to be competitive when using CR.pIX cells.

4.2.2 Production in bioreactor systems

Suspension cells provide the advantage of better scalability towards production processes in bioreactors compared to adherent cell cultures. MVA is usually grown in adherent cell cultures (CEF, MRC-5) an thus, literature on bioreactor experiments is not available. During the project, scale-up of cultures to lab-scale bioreactors was evaluated. For each modification, i.e. new media (CD-U2/CD-VP4) and new virus strain (MVAegfp), a STR run was performed. Also, the Wave bioreactor system was tested as a production system. However, due to several problems with either medium ageing or titration, only four cultivations out of nine runs in total remained for analysis. Obtained data from these four runs are shown in Figure 4.2.5 (in conjunction with one representative shaker flask experiment).

With $1x10^7$–$1x10^8$ viruses/mL, similar maximum titers as in small-scale cultures could be achieved in bioreactor experiments. Wave and STR cultivations with MVAwt in AEM/MegaVir showed similar time courses with a maximum titer reached approximately 48 hpi as also seen for shaker flask experiments. For MVAegfp cultivations in CD-U2/CD-VP4 medium, similar titers were reached until 48 hpi compared to shaker flask cultivations. However, in STR, a further titer increase was observed until 72 hpi or even 120 hpi, which was not observed in shaker flask experiments using MVAegfp in CD-U2/CD-VP4 medium. Thus, propagation of MVA in STR cultures seems to be retarded, though the reason is not clear and more evidence could not be found. However, stirring might actively affect virus spread and virus replication in STR. If the retardation is caused by low levels of convection and poor mixing, a faster increase of titers and thus better space-time yields could proabably be achieved by using higher rpm. This remains to be tested in further experiments. Generally, STR and Wave bioreactor runs showed that the MVA production process using CR.pIX cells is easily scalable which is a huge advantage compared to adherent cell cultures.

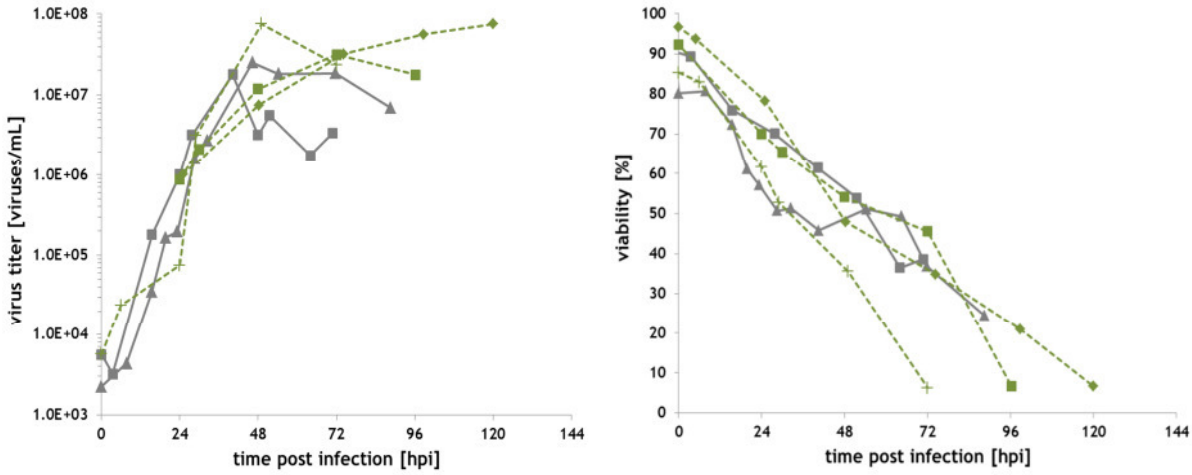

Figure 4.2.5: MVA infection experiments in STR (■,◆), Wave (▲) bioreactor and shaker flask (+). To illustrate scalability of the MVA production process, cultivations with MVA wildtype (grey) and MVAegfp (green) were performed as well as cultivations in AEM/MegaVir (solid lines) and CD-U2/CD-VP4 (dashed lines) medium. Left: Virus titers, right: Cell viabilities.

Titers in the range of $1x10^7$–$1x10^8$ viruses/mL were achieved throughout the project with MVAwt and MVAegfp (see Figure 4.2.3 to 4.2.5). Titers thereby varied to about 1 log scale even when repeating an experiment (with same parameters). Virus dynamics, however, were mostly consistent. Such variation in titers was also found by Jordan et al. who observed differences in maximum virus titers of 1 log scale [161]. Though, variability of maximum titers might be a bigger issue in uncontrolled shaker flasks as under the controlled environment of bioreactors. Three factors are likely to induce the

observed variabilities. First of all, biological variability when using the same set of parameters, but different pre-cultures, may have the biggest effect. For growth experiments, this has been shown and discussed in chapter 4.1.3.2. In virus infection experiments, a complex biological system – the virus – is added to another complex biological system, a host cell population. It is therefore likely that variability is even bigger in infection experiments than in growth experiments. This biological variability, however, can hardly be reduced and has to be accepted in virus production. A second possibility is that the used medium steadily changes during storage, so-called medium ageing. With this, slight changes in composition, salt concentration or availability of trace elements might occur that are difficult to analyze. Although we could not find a systematic correlation between lower titer experiments and older medium, this effect cannot be ruled out completely.

Variability in results might also occur due to a sub-optimal read-out of the experiments – in this case sub-optimal virus titer detection methods. Virus titers are measured via $TCID_{50}$ assay using cells, two antibody staining steps and a staining with a peroxide-inducible staining solution. Often, it was difficult to distinguish between background staining and dim staining of an infected cell. Read-out of this method is $\pm$ 0.15 log scales. Repeated titration of samples, however, showed that a measurement error of 0.5 log scales often occurs, i.e. the range of a measured titer then is $1.0 \pm 0.5 \times 10^8$ (see Appendix A13)). Assuming that the variability between experiments is not related to the cultivation system, but mainly depends on the chosen assay, an option to measure the infection status of cells by a different method was to monitor egfp accumulation in cells infected with MVAegfp. Although such alternative assays might not replace an $TCID_{50}$ measurements, a better characterization of the progression of the infection should be achieved. In addition, a correlation between infection status and virus titer can be investigated. Two methods to monitor cell physiology before and after infection were tested. The next two sections show the selection and establishment of both methods as well as results from these studies.

4.2.3 Monitoring the infection status

With the $TCID_{50}$ assay, a method was available which is error-prone and time-consuming (at least three days from sampling to virus titer). An alternative method to follow infection in the cell culture was therefore established. One option was the use of MVAegfp, which enables direct detection of intracellular virus replication by flow cytometry. After scouting experiments to optimize sample processing, fixation with paraformaldehyde, and analysis (procedure summarized in Appendix A9), infection

experiments were analyzed with this assay. First, time courses were monitored in shaker flask cultures infected with standard parameters and MVAegfp. Figure 4.2.6 shows flow cytometry histograms and microscopic pictures obtained between 0 to 48 hpi, showing infection progression in the cell culture.

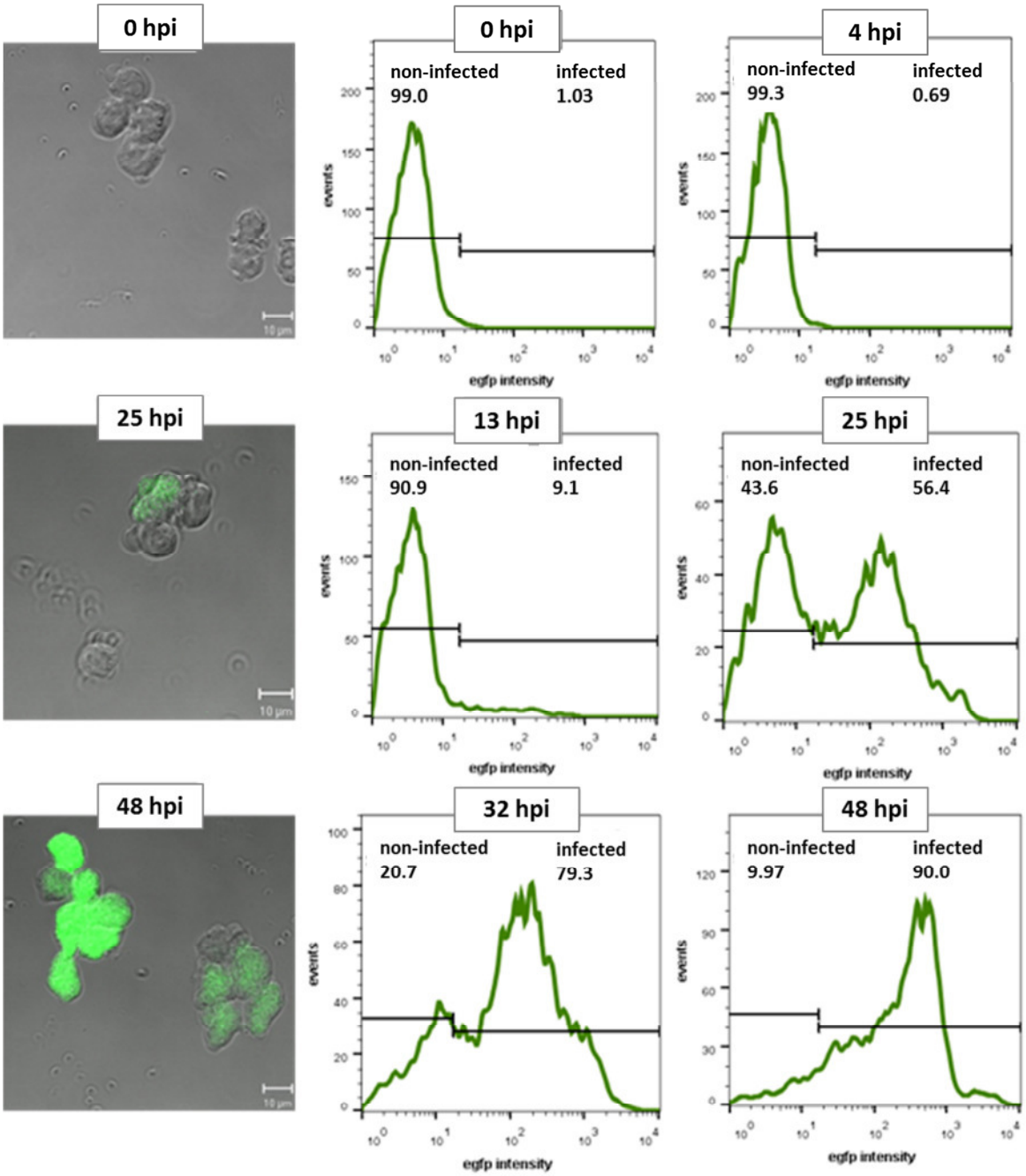

Figure 4.2.6: Egfp intensity (measured by flow cytometry in FL1 channel) during infection of CR.pIX cells with MVAegfp. Cells were cultured in shaker flasks and infected using standard parameters. Left: Pictures taken with a laser scanning microscope at 0 hpi (top), 25 hpi (middle) and 48 hpi (bottom). White bars indicate a size of 10 µm. Right: Egfp intensities as measured by flow cytometry during indicated time points. Sampling and gating procedure (based on 0 hpi sample as control) was done as described in Appendix A9. With this, the population can be divided in two sub-populations, non-infected and infected cells. Percentage values of these two populations are given within the histograms. Adapted from [216].

In the obtained histograms, one can clearly distinguish between infected and non-infected cells, having different intensities in green fluorescence. At 13 hpi, 9.1% of the cells were measured as infected and at 24 hpi more than half of the cells (56.4%) were infected. At 48 hpi, the time point of maximum virus titer, 90.0% were infected. The microscopic picture taken at the same time confirms this finding. Also for influenza virus, around 90% infected cells were reached in maximum [219]. However, this high percentage of infected cells was reached significantly earlier for influenza virus - at 6 hpi. This correlates with the generally faster spread of influenza virus as will be seen in chapter 4.3.

Most significant changes in the infection status occurred between 13 and 25 hpi. Also, the time interval between 4 hpi and 13 hpi was of interest in order to eventually identify the eclipse period of MVA, i.e. the time between infection and release of first progeny viruses. To resolve this, samples of two infected cultures were taken in short intervals (Figure 4.2.7).

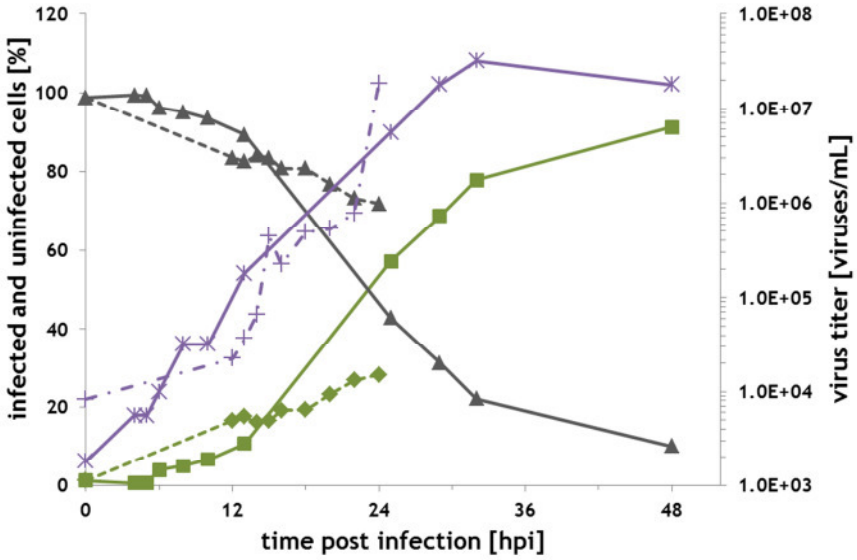

Figure 4.2.7: Time courses of percentage of infected cells (green), non-infected cells (grey) and virus titer (violet) during infection of CR.pIX cells in shaker flasks. Two independent experiments are shown (represented by solid and dashed lines, respectively). Adapted from [216].

The first increase in infection status was observed 6 hpi (to 4%) with a further increase to 13% until 13% in average. From this, one might deduce an eclipse period of 6 hpi. However, for vaccinia virus, an eclipse time of only 1.5–4 h has been shown as for example by Schweneker et al. who used HEK293 cells and an egfp expressing MVA strain [220]. As only few cells will be infected by single viruses at this time, it is possible that the flow cytometric method to measure egfp intensity is not sensitive enough to detect infected cells at this very early time point after infection. Nevertheless, 6 hpi, a steady increase in the number of infected cells was measured. In one experiment, this increase

was more or less linear. In the second experiment, an exponential increase was observed between 6 and 30 hpi.

Slightly later than the increase of egfp positive cells, an increase in titer was observed 6–8 hpi (assuming that the small increase from $3x10^3$ to $8x10^3$ viruses/mL before is not significant). As a secondary infection (progeny viruses infecting new cells) can only occur after approximately 10 hpi (from virus entry to virus release and again virus entry), the late detected titer might be a result of the higher limit of detection for the $TCID_{50}$ assay. Also, one has to note that one cannot infer from these results that first progeny viruses are released between 6 and 8 hpi as virus titers have been determined from whole lysate and thus intracellular virions were detected as well. In general, however, time courses of percentages of infected cells and virus titers are similar (of course in different scales).

In addition to shaker flask experiments, cultivations in STR were analyzed by measuring the infection status to find an indication for the late and slow titer increase observed in STR before (see Figure 4.2.5). In the first run, flow cytometry histograms were obtained that showed an altered distribution compared to histograms obtained from shaker flask experiments. Generally, the STR cell population showed only low infection status and the median values of both populations (infected and non-infected) were considerably lower than for shaker flask cultures. This might indicate that cells did transcribe and translate lower amounts of viral genes so that fewer egfp proteins accumulated in the cytoplasm. Also, bleaching of egfp cannot be ruled out so that lower egfp intensities per cell were measured. (Shaker flasks are positioned in a closed and dark incubator so that bleaching is more unlikely.) This was tested with a second STR run, using same parameters, but with aluminium foil wrapped around the reactor in order to avoid egfp bleaching.

Using this set-up, more infected cells were visible 48 hpi (87% instead of 30%). Unfortunately, samples taken at 72 hpi could not be analyzed due to the low number of cells that were obtained after sample processing. Nevertheless, 96 hpi a clear difference was observed: 76% infected cells in absence of light, 44% without coverage. These data might indicate that egfp bleaching has been avoided by wrapping the STR in aluminium foil and thus higher egfp intensities could be measured. Measured virus titers were slightly lower between 24 and 96 hpi for the covered STR. In maximum, $3.0x10^7$ viruses/mL were obtained in the uncovered STR. At the same time point, only $0.3x10^7$ viruses/mL were measured in the covered STR. At 96 hpi the difference between both values was reduced ($0.7x10^7$ and $1.1x10^7$ viruses/mL), and 120 hpi the virus titer in the covered STR reached $3.0x10^7$ viruses/mL as well. Egfp bleaching cannot explain those lower titers and the delay in titer increase that were observed in the

covered STR. The only explanation for an effect of light on the actual number of viral particles that can be measured would be toxicity of the accumulated egfp for cells.

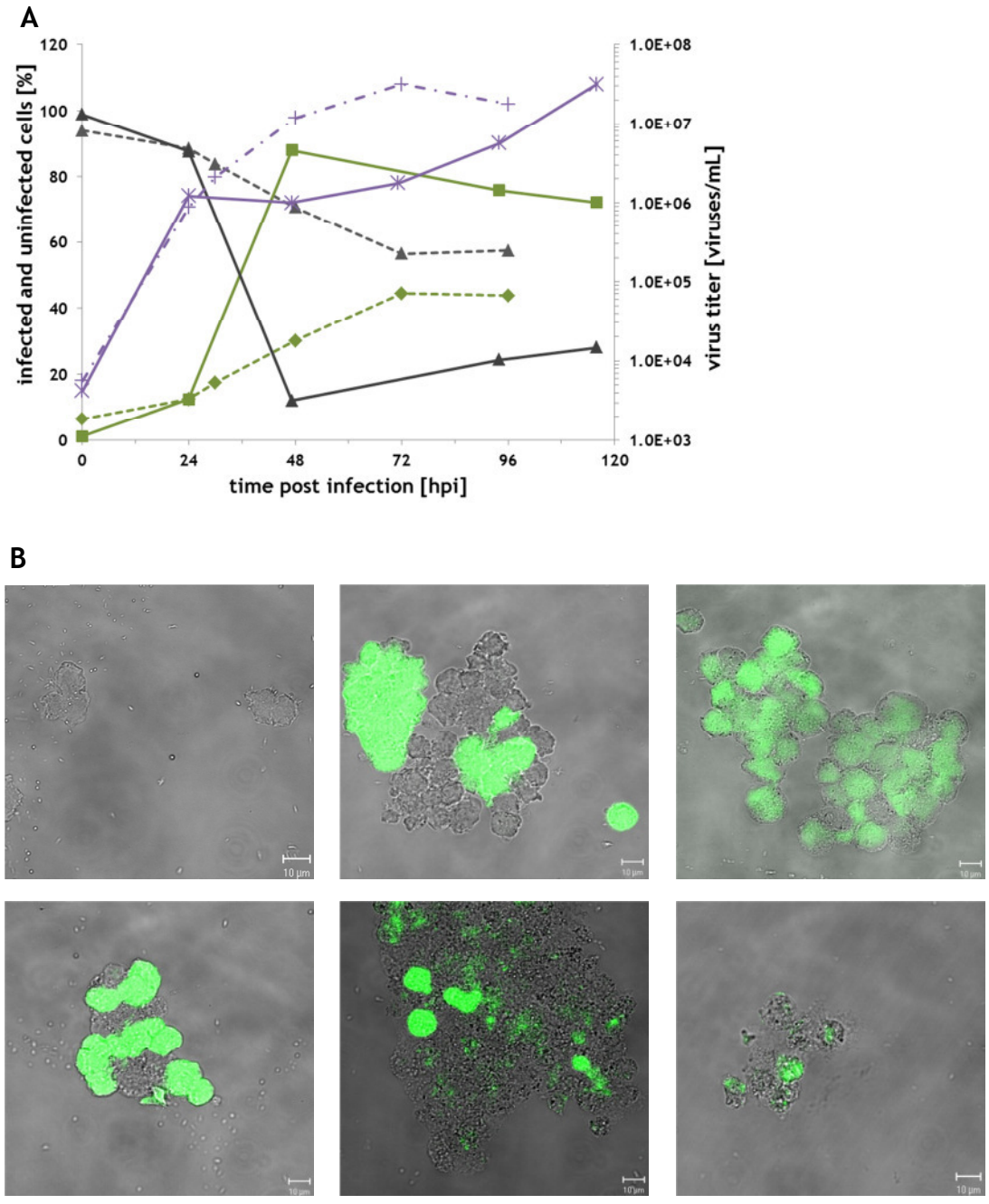

Figure 4.2.8: Infection of CR.pIX cells with MVAegfp in STR. A: Time courses of percentage of infected cells (green), non-infected cells (grey) and measured virus titer (violet) during infection of CR.pIX cells in STR reactor. Dashed lines show cultivation under normal room illumination and daylight. Solid lines show cultivation in a STR wrapped in aluminium foil and thus, in the absence of light. B: Photographs taken with a laser-scanning microscope from samples of the STR run in absence of light. Top row: 0 hpi, 24 hpi, 48 hpi samples; bottom row: 72 hpi, 94 hpi and 116 hpi samples. The white bar indicates a size of 10 µm. Adapted from [216].

A higher amount of accumulated egfp could result in a higher number of dead cells and thus less producer cells for MVA. However, the observations from this experiment are

rather the contrary. One can see in microscopic pictures that egfp positive cells are intact until 72 hpi in the STR with coverage. Afterwards, cells lysed and only skeletal structures were left. This might explain the slow rise in titer between 72 and 120 hpi, which could be caused by lysing cells only producing some more progeny virus particles. For a more profound understanding of this observation or the counter-evidence that lower titers are only measurement artefacts, more experiments are needed.

One initial question was whether the infection status correlates with titer and whether this assay could then replace the $TCID_{50}$ assay. Although initial results from shaker flask experiments were promising (see Figure 4.2.7), STR cultivations showed no clear correlation. To use egfp intensity of infected cells for titer estimation or mesaurement, an assay using also sample dilutions as in $TCID_{50}$ assay could help. A follow-up project already confirmed for influenza virus and MVA samples that this might be a more promising approach in order to reduce measurement error of the $TCID_{50}$ assay. Also, this would overcome subjectivity of $TCID_{50}$ assay that is analyzed via microscopy analyses by an operator.

Experiments with high CCI were analyzed as well with egfp intensity measurement in order to identify a difference between low and high CCI cultivations. Those experiments will be presented and discussed in conjunction with measurements of cell cycle and apoptotic status in the following sub-section.

4.2.4 Cell physiology during infection at low and high cell concentrations

To follow cell physiology of CR.pIX cells during infection with MVA in parallel to infection status, several assays were considered. Evaluating cell cycle phase distribution via propidiumiodide staining had already been done for cell cultures not infected with MVA and was thus maintained for infection experiments. However, it was expectable that measured signals from host cell DNA superimpose signal from viral DNA.

It is known that cells often undergo apoptosis in order to evade virus propagation in tissue or cell culture [84]. Studies with MVA have shown as well a slight, but visible onset of apoptosis upon infection [221, 222]. Therefore, it was of interest to measure apoptosis in conjunction with cell cycle analysis in order to characterize the cell population before and after infection at standard and high CCI. Many options, however, are available to detect apoptosis as reviewed in [223]. Among these, detection of caspases by specific anti-caspase antibodies or by using pancaspase inhibitors (e.g. FITC-VAD-FMK), is a common approach which had already be used for monitoring MDCK

cells infected with influenza virus and CEF cells infected with vaccinia viruses [111, 182, 222]. As this seemed to be a robust method, it was tested whether it can also be used to monitor apoptosis induction in CR.pIX cells infected with MVA. However, first results obtained with this assay were inconsistent. Therefore, a second assay had to be established. As DNA fragmentation was also used as apoptosis marker for vaccinia virus and MVA experiments [111], the TUNEL assay [219, 224] was tested for its applicability to CR.pIX cells infected with MVA. First results were promising, but a parallel DNA concentration measurement showed that dsDNA of MVA makes up for around 15% of total DNA present in one sample, varying with duration of the infection (data not shown). This might be problematic because fragmented DNA from MVA genomes or genome parts on the one hand, and fragmented DNA from apoptotic cells on the other hand are indistinguishable by the TUNEL assay. A consistent correlation of signal and apoptotic cells could thus not be generated and the approach using the TUNEL assay was not followed further.

Early apoptosis can be detected by staining cells with annexin V, a protein with high affinity towards phosphatidylserine (PS), a component of the cellular membrane. Annexin V can only bind to PS in case the PS has flipped to the outer side of the plasma membrane, which is an early signal of the apoptotis. Cells showing annexin V binding thus can be defined to be apoptotic. In this work, the GuavaNexin Kit was tested and used. It combines PE-coupled annexin V (as a marker for early apoptotic cells) with 7-AAD, a molecule intercalating into the viral DNA if membranes are permeabilized. Thus, three populations should be distinguishable applying both stainings to one sample: viable cells (negative for annexin V and 7-AAD), early apoptotic cells (positive for annexin V, but not for 7-AAD) and late apoptotic cells or necrotic cells (positive for annexin V and 7-AAD). After some preliminary tests with this widely used assay kit, a procedure could be established to measure apoptotic and necrotic CR.pIX cells before and after infection (also see section 4.2.3 and A4.5).

In the following, an infection experiment using CR.pIX cells in shaker flasks is described and discussed where the apoptosis/necrosis assay (GuavaNexin kit), cell cycle analysis and ViCell measurement (trypan blue staining) were analyzed in parallel. A comparison of the obtained results cell is shown in Figure 4.2.9.

One way is to directly compare the measured percentages of each fraction (Figure 4.2.9A). No correlation between the measured fractions were clearly visible when looking at percentages. Until 48 hpi, late apoptotic and necrotic cells showed higher or similar percentages as dead cells measured by ViCell (trypan blue staining). After 48 hpi, the picture changed and more tryan blue positive cells were measured. Finally, at 120 hpi, 70% of all cells were measured as dead using the ViCell device, whereas only

30% were detected as late apoptotic or necrotic. Even when summing up necrotic, early apoptotic and late apoptotic fraction, only 35% were reached. Assuming that i) damaged cells lysed during sample preparation and ii) several dead cells were present in dimers or clusters and thus excluded from cytometer analysis, the lower percentages of non-viable cells measured by the annexin V assay might be explained. The fractions of subG0G1 cells as detected by propidiumiodide staining did not correlate with the other two assay results as well. Again, percentages were lower than measured by the ViCell method. Comparing measured percentages, one has to consider that dead cell fractions detected with the ViCell device are directly measured from samples. For determination of subG0G1 fractions and apoptotic or necrotic fraction, however, samples were processed before analysis, and, due to necessary gatings, only a part of the sample will be assigned to apoptotic or necrotic status.

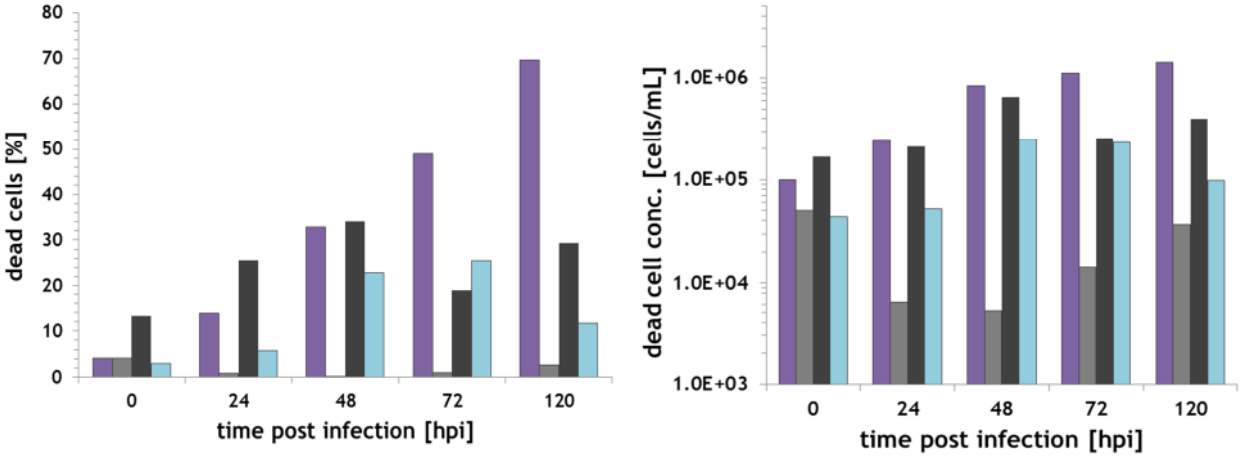

Figure 4.2.9: Non-viable cell concentrations as detected by ViCell counting, cell cycle analysis and apoptosis analysis. The following populations are shown: dead cells by ViCellXR (purple), early apoptotic cells detected by GuavaNexin assay (grey), late apoptotic and necrotic cells detected by GuavaNexin assay (black) and subG0G1 cells detected by cell cycle analysis using propidiumiodide staining (light blue). Left: percentage of dead cells as measured. Right: dead cell concentrations in [cells/mL] estaimated from sample volume and cell concentration.
CR.pIX cells were infected with MVAegfp in shaker flasks and standard infection parameters (moi=0.05, CCI=2x10^6 cells/mL).

A second approach is to estimate cell concentrations of each flow cytometer fraction in retrospect. The flow cytometer counts numbers of cells (events) of each population and thus, the respective populations can also be given as cell count and therefore as cell concentration (with the known volume of original sample used for flow cytometer assays, Figure 4.2.9B). Again, cells that are damaged at time of sampling might undergo cell lysis while samples are prepared for flow cytometric measurement. Although only as few and as mild sample processing steps as possible were chosen, this could affect corrected flow cytometry data. Using cell counts and thus cell concentrations, the picture changes slightly. Again, concentrations of subG0G1 cells were lower than trypan

blue positive cells. Throughout the infection, cell cycle analysis (subG0G1 cells) detected 1.5–2.5-fold lower concentrations of dead cells than the ViCell measurement. Nevertheless, the difference between late apoptotic and necrotic cells and trypan blue stained cells is reduced when compared using concentrations. Until 48 hpi, values were nearly identical and only later the amount of late apoptotic and necrotic cells decreased in comparison. Again, an explanation could be the loss of damaged cells during sample processing and gating.

Overall, the comparisons show that each assay or method provides only a specific measure for the percentage or concentration of non-viable cells in cell culture. As different characteristics of non-viable cells are detected by the different assays, results are not identical, and the used methods cannot substitute each other. Figure 4.2.9 also shows one finding that could be confirmed in more experiments: the percentage (and concentration) of early apoptotic cells during MVA infection is rather low. In maximum, 3% of cells were detected to be annexin V positive (120 hpi), but 7-AAD negative. Earlier during infection, even values of only 1–2% were found. In fact, fractions of late apoptotic and necrotic cells (double-positive) were substantially higher (in maximum 33% at the end of the infection phase, 120 hpi). This, however, must not mean that cells did undergo apoptosis as they all could possibly be necrotic. The assay using annexin V can thus be applied to detect early apoptotic cells, but showed that MVA induces apoptosis in only small levels as is supported by data of related studies [111, 221].

Coming back to infection experiments at high CCI (see chapter 4.2.1.2), it was of particular interest to investigate whether cell physiology is impaired at late times during cell growth, and whether infected cultures can be differentiated from non-infected cultures via flow cytometry. For this experiment, CR.pIX cells were grown to $4.6x10^6$ cells/mL (low concentration) and $8.0x10^6$ cells/mL (high concentration) and were then infected with MVAegfp (moi=0.05). After addition of CD-VP4 medium, resulting cell concentrations at 0 hpi were measured as $2.3x10^6$ cells/mL and $3.6x10^6$ cells/mL, respectively. Controls and samples for cell cycle and apoptosis measurement were taken directly before infection and throughout the virus production phase. In order to be able to distinguish between effects from “normal” cell death due to addition of virus production medium and effects from virus infection, mock-infected cultures (treated as infected cultures but without addition of seed virus) were done in parallel (for normal and high CCI each, scheme see Figure 4.2.10). In addition, infection status and virus titers were measured in order to gain a full picture of cell physiology. For both CCI, two shaker flasks were operated in parallel. Presented results will be averages of both parallel cultures.

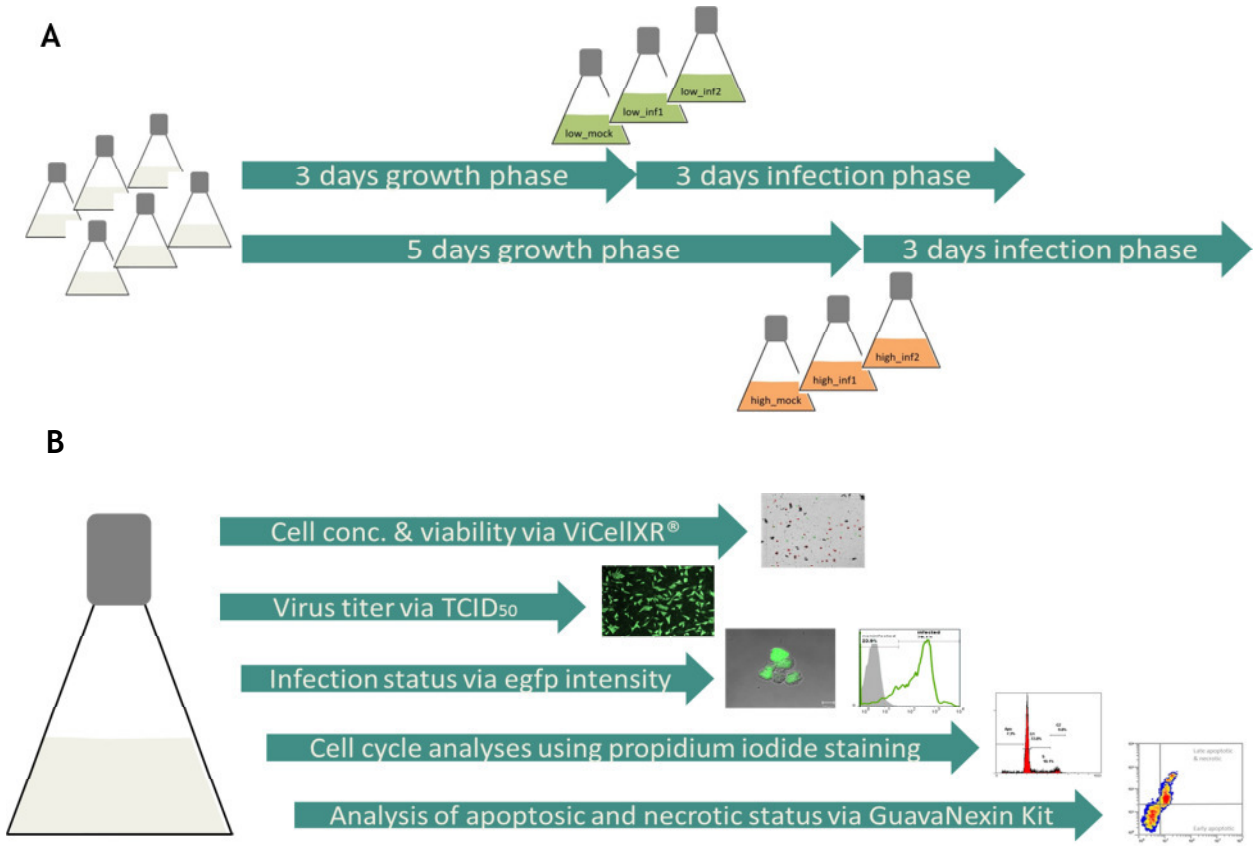

Figure 4.2.10: A: Experimental set-up for comparison of cell populations infected at standard CCI ($2.3x10^6$ cells/mL, after addition of CD-VP4 medium, infected after 3 days of cell growth) and higher CCI ($3.6x10^6$ cells/mL, after addition of CD-VP4 medium, infected after 5 days of growth). For each condition, two shaker flasks were used. In addition, one mock infection was prepared. B: After infection, different methods were used to follow MVA infection and cell physiology for 120 h.

Time courses of cell concentrations and viabilities showed that infection induced cell death, whereas mock-infected cultures remained at 70% viability until 120 hpi (Figure 4.2.11A and B). The observed viability loss in these cultures can be ascribed to cell clustering (dense aggreagtes with approximately 10–50 cells each) and thus limited nutrient and oxygen supply in CD-VP4 medium. Also, the pH in shaker flask cultivations dropped with time which can impede cell viability. However, the difference to infected cultures was clear so that it can be presumed that differences between mock-infected and infected cultures regarding apoptosis or cell cycle status must be visible. Results of those assays can be seen in Table 4.2.2.

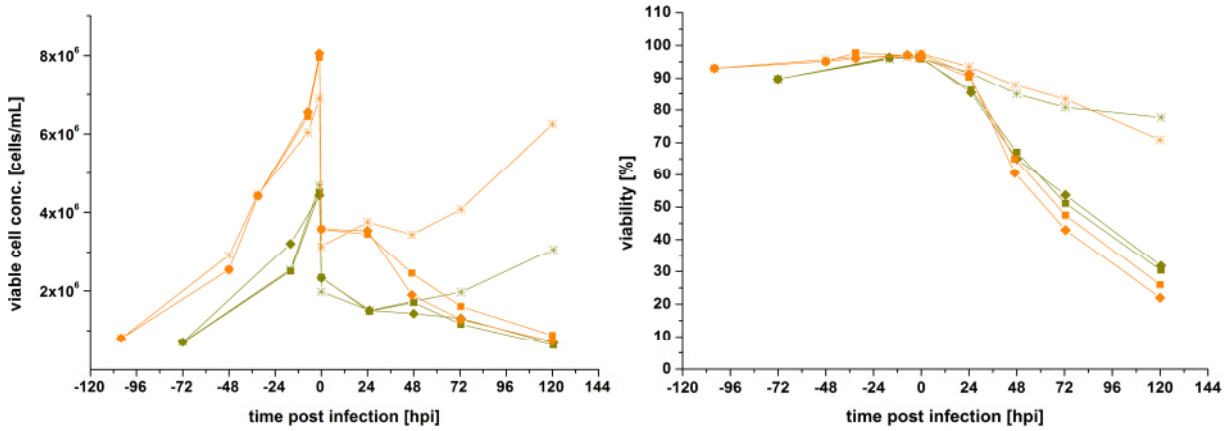

Figure 4.2.11: Time courses of viable cell concentation (left) and viability as measured by ViCell device (right) in CR.pIX cultures at low CCI (green) and high CCI (orange). Two infected cultures (■,◆) and one mock-infected culture (∗) were monitored for each CCI. CR.pIX cells were infected using moi=0.05 and infected in a 1:1 mixture of CD-U2 and CD-VP4 medium.

Regarding the cell cycle distribution, mock-infected and infected cultures did not differ at time of infection, showing that starting conditions were similar for all cultures. Two thirds of cells were in G0G1 phase and only a very low amount of 2–3% of cells were measured as subG0G1 phase cells having an incomplete genome. Also, the difference between cultures infected at low or high CCI was not significant at time of infection, although their growth phase was 3 and 5 days, respectively. Comparing mock-infected and infected cultures, a difference becomes visible at 48 hpi. The fraction of subG0G1 phase cells was about 10-fold the starting value in infected cultures, whereas for mock-infected cultures this fraction was only 8.0% (low CCI: 21.2%). In addition, the fraction of infected cells in G0G1 phase decreased to 42.3% (low CCI) and 38.3% (high CCI), respectively. As mentioned above, S phase cell population was measured in higher amounts after infection. This can be assigned most likely to G0G1 phase cells containing viral genomes or genome parts and G2M phase cells with a partly fragmented genome. Although this assay is not fully able to specifically distinguish a distinct population, infection progress can be followed. Interestingly, although starting with the same distributions, mock-infected cells of low and high CCI cultures also differed 48 hpi. At high cell concentrations, the fraction of subG0G1 cells was twice as high as at low cell concentrations. Infected cultures at both CCI were again similar to each other, indicating that infection and infection dynamics are comparable in both cultures.

With the apoptosis/necrosis assay (GuavaNexin kit), lower percentages of viable cells were measured at time of infection for high CCI cultures. Higher apoptotic or necrotic percentages were, however, not detetcted. Instead, the percentage of debris was increased. The viability of cultures after 5 day cell growth thus seems to be slightly impaired which cannot be seen with trypan blue exclusion methods as the ViCell

excludes debris from counting. With cell cycle analysis, these slight differences could not be detected. At low CCI, the apoptotic and necrotic status did increase significantly after infection. 37.1% of measured cells were assigned to be late apoptotic or necrotic 48 hpi, whereas only 9.9% of mock-infected cells were found in these populations. Noteably, around one half of all cells were debris in low CCI cultures. Looking at high CCI cultures, less cell debris were found, but higher percentages of viable cells. However, if excluding debris from low CCI cells in retrospective, similar distributions between low and high CCI do result.

Table 4.2.2: Cell cycle distribution, apoptotic and infection status of CR.pIX cells infected or mock-infected at high and low CCI.

Fraction of cell population [%]	mock low CCI	low CCI	mock high CCI	high CCI
0 hpi				
subG0G1*	2.3	2.7	2.8	2.6
G0G1*	74.2	74.1	75.3	74.6
S*	13.6	13.7	11.4	11.5
G2M*	9.5	9.1	10.0	11.0
viable#	81.1	76.8	62.9	67.1
early apoptotic#	3.9	4.2	3.2	2.6
late apoptotic/ necrotic#	11.4	15.4	11.0	10.1
infected (egfp positive)$	1.0	1.5	0.6	0.5
48 hpi				
subG0G1*	8.0	21.2	15.4	20.8
G0G1*	72.8	42.3	66.7	38.3
S*	11.1	21.5	10.8	22.4
G2M*	7.8	13.3	6.7	15.6
viable#	46.8	22.9	87.0	71.7
early apoptotic#	1.7	0.3	1.7	0.7
late apoptotic/ necrotic#	9.9	37.1	8.1	7.8
infected (egfp positive)$	0.1	45.0	0.2	46.9

*results from cell cycle analysis (propidiumiodide staining)
#results from measurement of apoptotic/necrotic status (GuavaNexin staining)
$results from measurement of egfp intensity

Overall, cell physiology analyses showed slightly more damaged cells at high CCI (after 5 days growth). Although higher percentages of viable cells were measured for those cultures with the annexin V assay (87.0% at 48 hpi), this must not imply higher cell fitness, but presumably only higher rates of cell lysis. In this experiment, infection status was not different in high CCI cultures. At 48 hpi around 45% of cells were infected in all cell cultures. Also, titers did not differ clearly: $1x10^8$ viruses/mL were produced in low CCI cultures, $4x10^8$ viruses/mL at high CCI. This resulted in cell-specific yields of 75

viruses/cell (low CCI) compared to 140 viruses/cell (high CCI). Repetition experiments of this set-up could not confirm higher titers at high CCI, but resulted in equal titers. Thus, cell-specific yields were then lower for infections above $4x10^6$ cells/mL (see also Figure 4.2.4).

Main outcome of these experiments is that a cell density effect seems to be present, although it was not as clearly observable as for influenza virus (see chapter 4.3.2.2). Slight differences in cell physiology were visible with a presumably higher degree of cell lysis at high CCI. Experiments should be repeated in controlled bioreactors in order to exclude effects of low pH. Although sometimes difficult to interpret, analyses of cell cycle and apoptotic status can complement usual cell counting methods and could show differences in mock-infected and infected cultures due to MVA replication.

4.2.5 Chapter summary and outlook

With the obtained results, recommendations regarding optimal parameters for cell growth and infection phase can be made, so that the process scheme shown in the background section (see Figure 2.11) can be filled with details (Figure 4.2.12).

With the switch to chemically-defined proliferation and production medium (CD-U2 and CD-VP4, respectively), some parameters like moi and ratio of both media had to be re-tested for MVA. Thereby, same conditions as for the serum-free medium combination AEM and MegaVir were found to support highest titers. One difficulty of monitoring the process when using virus production medium is cell aggregate induction. However, MVA titers were higher when adding CD-VP4 in a 1:1 ratio and thus, this limitation had to be accepted. After finishing this project, an adapted MVA strain was described that seems to have improved release characteristics [225]. Using this strain it was shown that percentage of virus particles in the supernatant is higher and aggregate induction is not as crucial as with MVAwt. This in future might facilitate the process itself as no medium has to be added during the cultivation, and might simplify monitoring. Throughout the project, three MVA strains were used. Wildtype MVA as well as recombinants strains (MVAmcherry and MVAegfp) were propagated in CR.pIX cells. Similar virus dynamics and maximum virus titers between $1x10^7$ and $5x10^8$ were observed showing that inserting genes coding for those fluorescent proteins does not impair MVA spread. Overall, virus titers that were achieved are competitive with the common host systems eggs, CEF or BHK-21 cells [3, 111, 112]. Using a more rigorous sonification method (with a sonicator, not a sonication waterbath) could be more efficient and thus, even more active virus

particles might be harvested. Scaling up the process it was shown that similar titers can be achieved in STR and Wave bioreactors compared to shaker flask experiments.

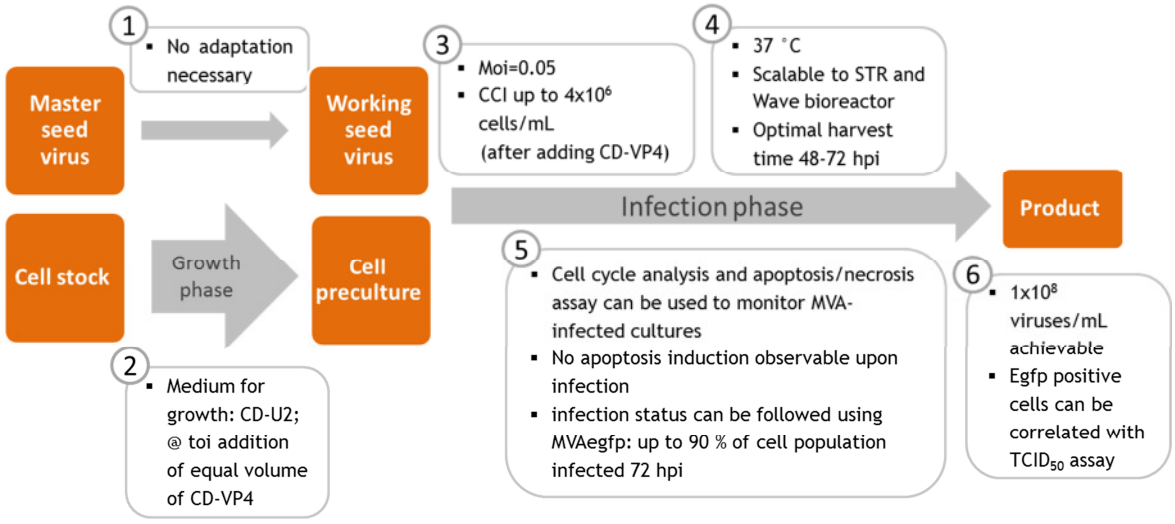

Figure 4.2.12: Results that have been obtained by optimization experiments and cell physiology analyses of CR.pIX cells infected with MVA.

Using the MVAegfp strain, infection status of the cell population could be followed with two main outcomes. First, in some experiments only half or two thirds of the cell population seem to be infected, whereas in other cultivations up to 90% of the cells were infected at about 48 hpi. Although no correlation with infection parameters or cell fitness could be identified, there seems to be potential for optimization. Second, the percentage of egfp positive cells could not be correlated directly with virus titers obtained from $TCID_{50}$ assay. More effort will be needed to replace the $TCID_{50}$ assay. Potentially, flow cytometry with the MVAegfp strain can be used for titration, but presumably dilution series will also be needed.

Finally, studies regarding a probable cell density effect were done in combination with the measurement of cell physiology. Cell cycle analysis did not reveal striking differences when using standard CCI ($2x10^6$ cells/mL after dilution with CD-VP4) or slightly higher CCI ($4x10^6$ cells/mL). However, cell lysis rates were found to be increased when cells were infected at high cell concentrations (grown for 5 days). Comparing virus yields, however, there is a trend towards reduced cell-specific virus yields at CCI above $4x10^6$ cells/mL. Although no metabolites were found to be depleted even when cells were infected late in the exponential phase, it is likely that one or several medium components are limiting virus spread. In conjuction with higher cell lysis levels, this might explain the cell density effect. Early apoptotic cells, however, were not observed for the cell population upon infection. To get clarity and definitely exclude the possibility of apoptosis induction, other caspase antibodies should be tested for immunhistological analysis of infected cell cultures.

4.3 Production of human influenza virus

In this work, the potential of CR and CR.pIX cells as substrates for influenza virus production was evaluated. Therefore, experiments on influenza virus propagation were carried out using the reference strain A/PR/8 (H1N1) and using one cold-adapted influenza A strain (A/Singapore, H1N1) as well as one cold-adapted influenza B strain (B/Vienna). Adaptation of seed viruses to CR cells was carried out first. Then, optimal infection parameters were established before conducting several experiments addressing four main questions:

- Optimal infection parameters
- Performance of CR and CR.pIX cells in comparison
- Cell density effect
- Virus titers and cell-specific virus yields achieved in comparison to other established processes

In section 4.3.1, the results for infection experiments using the reference strain A/PR/8 will be shown. In the second section (4.3.2), results on cold-adapted influenza virus strains A/Singapore and B/Vienna will be described and discussed. Some results have been either published or were either part of supervised student projects, theses or are based on experience gained within these thesis projects [46, 226-228].

4.3.1 Propagation of reference influenza virus strain A/PR/8

For production of inactivated virus vaccines, the A/PR/8 strain is commonly used as a backbone for the generation of reassortant master and working seeds. As the virus in this case is inactivated after production, the $TCID_{50}$ titer is not highly relevant, but rather the HA value is used to characterize the process batch quantity. Therefore, in experments with the A/PR/8 strain to evaluate the potential of CR and CR.pIX cells as host cell line for inactivated vaccine production, HA values are mostly shown and discussed.

4.3.1.1 Adaptation to CR cells

An adaptation of seed viruses to the respective host cell line can result in faster virus spread and higher titers as the entry of influenza viruses is dependent on binding host-

specific receptors and on endosomal pH which is also considered to be host-specific [229-231]. To achieve this, the MDCK-adapted A/PR/8 seed virus was passaged several times in CR cells grown in CD-U2 medium. The first passage was infected with a moi of 0.001, whereas the next passages were always infected using 1 mL of the previous passage (CCI was always $2x10^6$ cells/mL; $1x10^{-6}$ units trypsin/cell were added). Passaging was done as soon as the HA value exceeded 0.5 log HAU/100 µL, and the viability of the cells dropped below 90%. During the adaptation process (which was performed twice), several samples were taken to subsequently analyze the increase of HA values and $TCID_{50}$ titers (Figure 4.3.1).

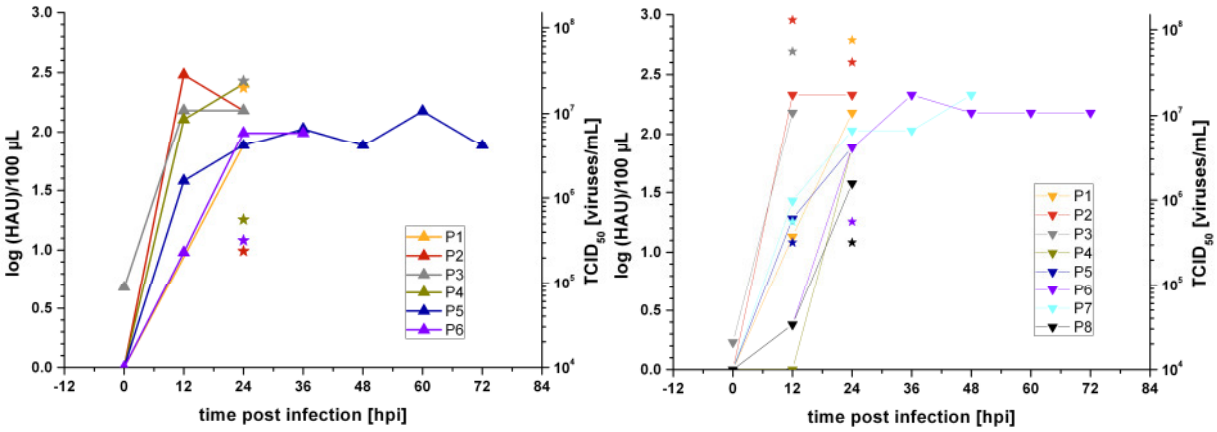

Figure 4.3.1: HA values (▲) and $TCID_{50}$ titers (★) during adaptation of A/PR/8 virus strain to CR cells (left and right: repetition of same adaptation experiment). Starting with MDCK-adapted seed virus, CR cells cultured in CD-U2 medium were infected with moi=0.001 and addition of $1x10^{-6}$ units trypsin/cell. After reaching an HA value of >0.5 log HAU/100 µL, the next CR culture was inoculated with 1 mL of previous culture. Overall, virus was passaged 6–8 times in CR cells, indicated as P1–P6 or P1–P8, respectively. Adapted from [226].

The adaptation of the A/PR/8 strain showed HA value and $TCID_{50}$ titer increases from the 1st to the 3rd passage. Also, the HA value increase occurred faster with every passage so that in the 3rd passage an HA value of ~ 2.0 log HAU/100 µL could be obtained at 12 hpi. After the 3rd passage, in both adaptations, the HA values and $TCID_{50}$ titers decreased substantially. Most likely, this was due to the very high moi which was present beginning from the 2nd passage (calculated in retrospective for example moi=10 and 40 at passage 2, moi=1 and 10 at passage 3). Infection at high moi for influenza virus is described to lead to accumulation of defective interfering particles that inhibit the potential of the whole virus population to replicate efficiently and thus titers (especially active virus titers) decrease [232]. In retrospect, the moi should have been adjusted for every single passage so that constantly low moi are used to infect a new cell population. As this would, however, be a highly laborious procedure, because titers have to be determined before the next passage is started, we decided to repeat the first passage (where moi was set to 0.001) and harvest at 16 hpi and 24 hpi to obtain a

seed virus with high HA values and high $TCID_{50}$ titers. With this, adequate titers of $1.5x10^8$ viruses/mL at 16 hpi and a slightly lower titer of $6.6x10^7$ viruses/mL at 24 hpi were achieved. Both harvests were stored at -80°C as seed virus for further experiments with the A/PR/8 strain.

4.3.1.2 Infection parameters

Several parameters can influence the infection process. Besides quality of the seed virus as well as the virus strain and the host cell line itself, these are moi, trypsin activity at time of infection, process temperature, process strategy (whether a medium exchange is performed or not) and the CCI. Some of these parameters are known to be virus strain-specific, others are process related and have been tested for A/PR/8 propagation in CR and CR.pIX cells (Figure 4.3.2).

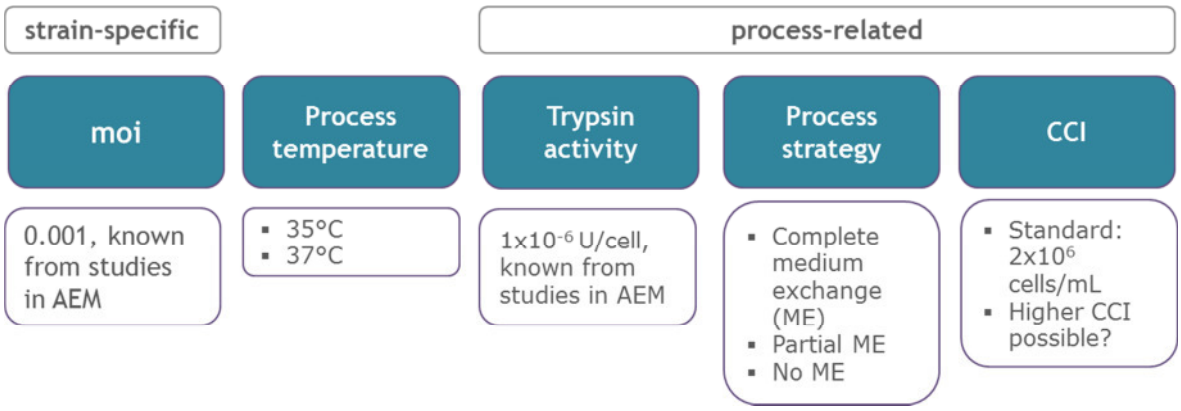

Figure 4.3.2: Infection parameters tested with the A/PR/8 strain.

At the beginning of the project, when serum-free AEM was used as proliferation medium as well as for infection with influenza virus, the infection parameters trypsin activity and moi were already optimized for the production of the A/PR/8 virus strain [19]. After switching to CD-U2 medium, these two parameters were not tested again for propagation of A/PR/8 as they are considered to be mostly virus strain and host cell line-specific. Eventually, high protein concentrations in the medium might inhibit trypsin activity. However, CD-U2 medium only contains IGF as a protein in very low amounts and thus, this was not assumed to play a role. Therefore, for all infection experiments with the A/PR/8 strain, $1x10^{-6}$ trypsin units/cell, a moi of 0.001, and a CCI of $2x10^6$ cells/mL were used if not indicated otherwise.

In most influenza virus vaccine production processes that are described, temperature is decreased to 33–35°C at time of infection [5]. At these temperatures, virus particles and cells are considered to be more stable. Figure 4.3.3. shows, however, that a

temperature reduction from 37°C to 35°C is favorable for the propagation of A/PR/8 virus strain in CR cells. A difference between both settings was neither observable for virus dynamics (constant HA values reached at 24–36 hpi for both), nor for maximum HA values (1.9–2.0 log HAU/100 µL). Therefore, a temperature of 37°C was used for all A/PR/8 experiments.

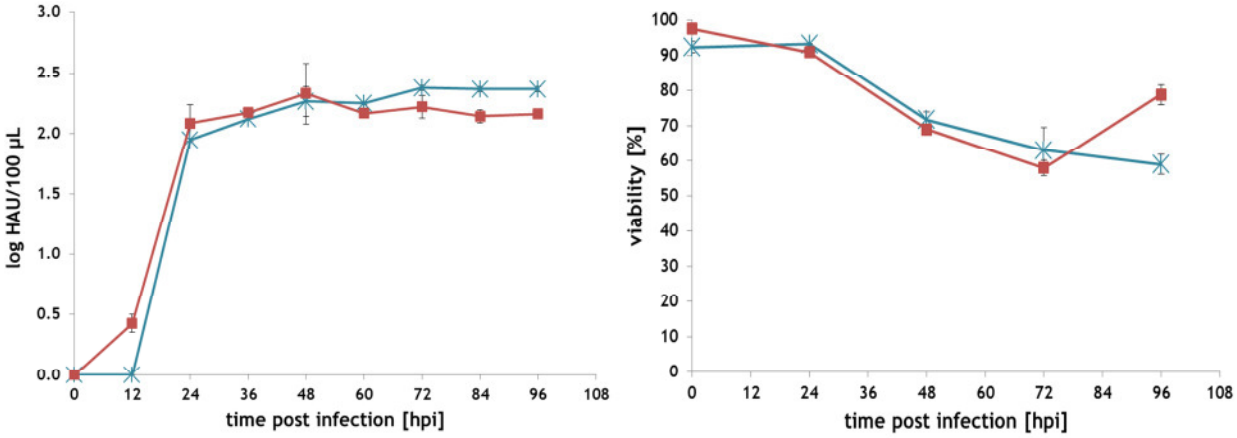

Figure 4.3.3: Propagation of influenza virus strain A/PR/8 in CR cells at 35°C (blue, ✳) and 37°C (red, ■). HA values (left) as well as cell viabilities (right) are shown. CR cells were cultured in CD-U2 medium and infected at a CCI of $2x10^6$ cells/mL in shaker flasks. Means and standard deviations of three parallel flasks are given.

The second tested parameter was the process strategy. A medium exchange or a medium feed could avoid nutrient limitations or prevent negative effects of inhibiting substances accumumulating during the cell growth phase. However, medium feeds and, in particular, medium exchange would result in a more complex process and thus its necessity should be evaluated beforehand. Three different strategies were compared when infecting CR and CR.pIX cells with the A/PR/8 strain. The first strategy was infection without any medium addition or exchange, in a second approach, half of the culture medium was exchanged by centrifugation of the cells and re-suspension in fresh CD-U2 medium, and a third approach was to completely re-suspend the cells in fresh medium (Figure 4.3.4). For both cell lines, no titer increase was observed with a medium replacement at time of infection. For all strategies tested, similar dynamics and a similar maximum (and stable) HA value were observed. From this, we concluded that a process without any medium exchange is possible in this system. For other host cell systems it has been shown that a medium exchange is needed – either in order to remove serum at time of infection which inhibits virus propagation as usually done for adherent cells [156], or to rescue HA values as observed for human CAP cells [15]. The unnecessary medium exchange when using CR or CR.pIX cells substantially simplifies a suspension process at industrial scales and is thus a desirable outcome.

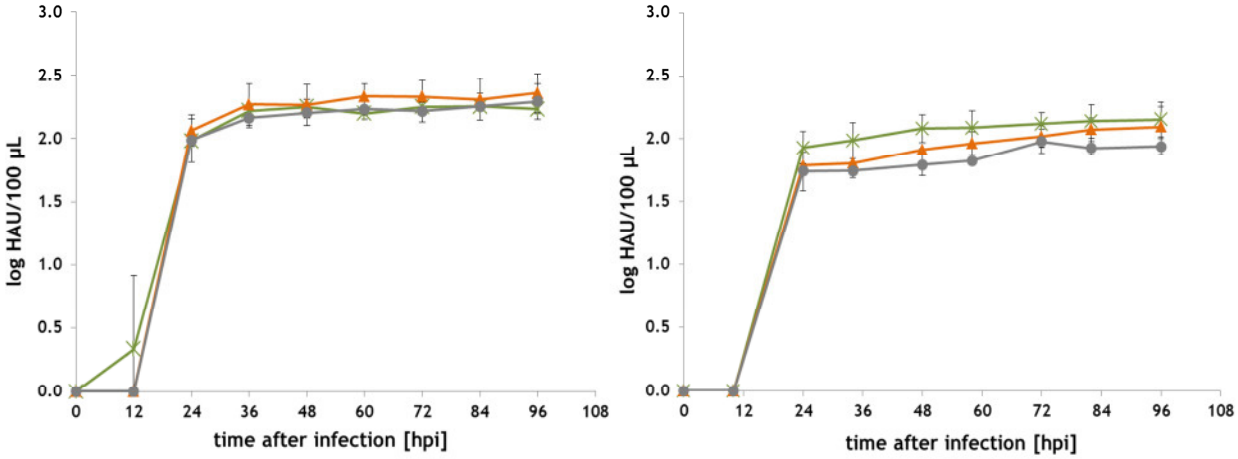

Figure 4.3.4: Optimization of process strategy at time of infection. Full medium exchange (grey, ●), medium exchange of half of the culture (orange, ▲) and no medium exchange (green, ✳) were tested for infection of CR (left) and CR.pIX (right) cells with influenza virus A/PR/8 strain. Means and standard deviations of 3 parallel flasks are shown.

It has to be noted that these experiments were all done with a CCI of $2x10^6$ cells/mL. From growth experiments (see section 4.1.2) it was known that the cells are in early exponential phase at this cell concentration (usually achieved 48–72 h after inoculation). However, CR and CR.pIX cells can be cultivated up to $10x10^6$ cells/mL in a batch process (see Figure 4.1.1 and 4.2.1), and thus it was investigated whether infection at higher cell concentrations (that means later in growth phase) does result in higher titers. As more producer cells would be in the reactor, one could expect that more virus particles are produced. On the other hand, the so called cell density effect has been described for several processes using adenovirus, baculovirus and influenza virus [42, 67, 117-119]. These studies demonstrated that above a certain CCI, the virus titer might increase in comparison to lower CCI, but the cell-specific virus productivity drops substantially. All studies related to this topic indicate that the reasons for the cell density effect are highly dependent on the production system (mainly virus species, host cell line and medium) and thus cannot be generalized. Explanations for this effect include depletion of nutrients or accumulation of inhibiting substances [119]. Also, activity or availability of host cell factors required for virus replication may change with the cell cycle [21] or with metabolic shifts [21, 117] at higher cell densities.

As this effect cannot be generalized, a test whether a critical CCI above which productivity descreases exists for the used production system was necessary. Therefore, CR cells were infected at standard CCI ($2x10^6$ cells/mL) and at higher CCI ($3x10^6$ or $6x10^6$ cells/mL). Maximum HA values and the cell-specific yield Y_{CSP} (based on total particle concentration) that were achieved within these experiments are summarized in Table 4.3.1.

Table 4.3.1: Maximum HA values and cell-specific yields from experiments using standard CCI and higher CCI.

	CCI [cells/mL]	Maximum Xv post infection [cells/mL]	Max. HA value [log HAU/100 µL]	Y_{CSP} [virus particles/cell]
Exp. 1	$1.6x10^6$	$1.6x10^6$	2.34	2022
Exp. 1	$3.8x10^6$	$3.8x10^6$	2.29	1073
Exp. 1	$6.3x10^6$	$6.3x10^6$	2.66	1536
Exp. 2	$6.6x10^6$	$7.1x10^6$	1.63	125
Exp. 3	$6.1x10^6$	$6.3x10^6$	2.80	2128

CR cells were infected in shaker flasks using standard infection parameters. Exp.1, Exp. 2 and Exp. 3 are independent experiments where different CCI were used.

As can be seen from these results, the HA values when using higher CCI slightly increased in average. An increase of CCI to $3.8x10^6$ cells/mL (72 h after inoculation) did not result in different HA or cell-specific yields. Only when using 6.3–$7.1x10^6$ cells/mL a slightly higher HA value could be detected (however, for one experiment (Exp. 2), a very low HA value of 1.63 log HAU/100 µL was measured). Looking at Y_{CSP}, it is not clear whether a cell density effect is present at cell concentrations above $4x10^6$ cells/mL. Specific yields in average were slightly reduced, but due to the low value of exp. 2, no definite conclusions are possible. The low pH which can occur especially at high cell concentrations in shaker flasks, might affect virus propagation. Therefore, bioreactor experiments with different CCI were done with one LAIV strain (see section 4.3.2).

4.3.1.3 Performance of CR and CR.pIX cells

As observable in Figure 4.3.4 and in previous studies using the AEM medium [19], differences in maximum HA values can be found for CR and CR.pIX cells lines when comparing all infection experiments with the A/PR/8 strain that were run with standard parameters (Figure 4.3.5). For CR cells, an increase in HA value was detectable at 12 hpi and leveled off at 24 hpi. With CR.pIX cells, HA values increased and reached a plateau slightly later at 24 hpi and 36 hpi, respectively. Also, there was a clear tendency of higher HA values when infecting CR cells. Values between 2.0 and 2.4 log HAU/100µL were achieved with CR cells while CR.pIX cell experiments always resulted in lower values between 1.5 and 2.1 log HAU/100 µL. The same trend was observable for $TCID_{50}$ titers. With CR cells, $2.5x10^8 \pm 2.1x10^8$ viruses/mL were achieved in average (n=5), whereas titers obtained with CR.pIX cells were 1 log lower ($3.7x10^7 \pm 2.7x10^7$ viruses/mL, n=3).

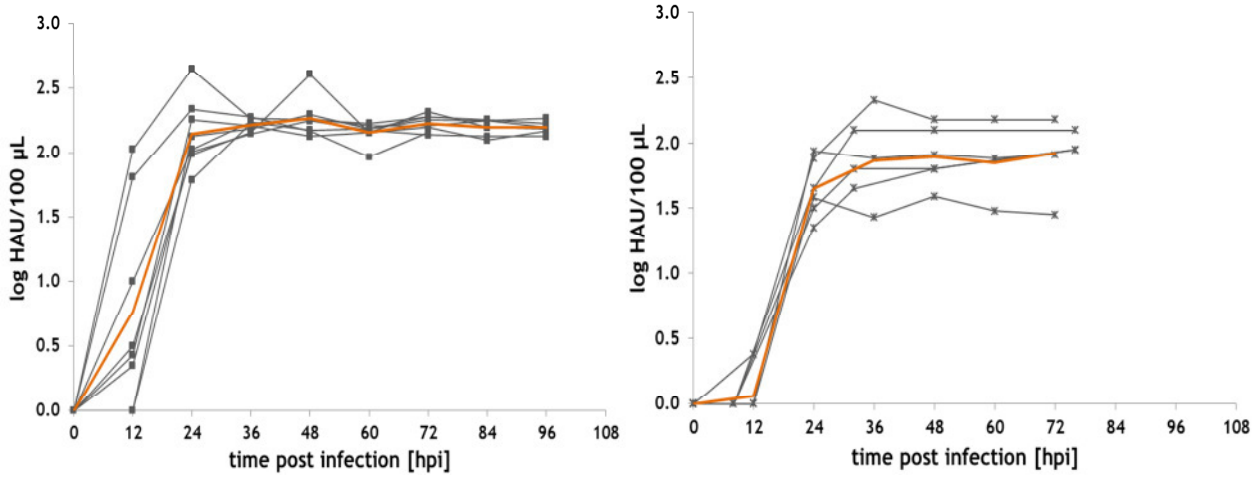

Figure 4.3.5: Summary of all experiments where CR (left) or CR.pIX (right) cells were infected with the A/PR/8 strain using standard infection parameters. All experiments were done in shaker flasks. Orange line: mean HA values from all experiments.

This was an interesting finding as both cell lines only differ in the pIX gene, which is inserted in the genome of CR.pIX cells. A mechanism, how the pIX protein might affect the propagation of influenza viruses within the cell might be as follows: As seen above, for vaccinia virus and MVA co-chaperone $p58^{IPK}$ and Hsp90 seem to play a major role [18, 233]. In contrast to that, influenza viruses have been shown to recruit Hsp70, and thereby recruit anti-viral defense pathways [217]. Expression of the pIX protein presumably leads to a complex formation between Hsp70 and Hsp90 [234]. Thus, the interplay of influenza virus with Hsp70 might be disturbed. This would explain the negative effect of present pIX protein in influenza virus infection experiments. However, one can only speculate about these relationships. For evidence, the reaction of influenza-infected CR and CR.pIX cells regarding heat shock proteins needs to be studied in more detail on a molecular basis.

4.3.1.4 HA values and cell-specific virus yields in context with established processes

The presented results demonstrate that CR and CR.pIX cells can produce influenza virus to high titers in shaker flasks. For the reference strain A/PR/8, $TCID_{50}$ titers of up to $3x10^8$ viruses/mL were achieved, which is in a similar range (10^7 to 10^9 viruses/mL) reported for other cell lines [5, 144, 235]. The achieved HA values are about 2.0 log HA units/100 µL which is about 10-fold lower than those normally obtained with conventional cells (MDCK or Vero cells) or new candidate cell lines (HEK293, PER.C6). Mostly, these are reported to propagate the A/PR/8 influenza virus strain to 3.0-3.6 log HA units/100 µL [5, 13, 42, 235]. Generally, CR and CR.pIX cells seem to

generate competitive $TCID_{50}$ titers, but lower HA values than established cell lines. Further studies should investigate the reason for obtaining comparatively low HA values. Macromolecular studies about the abundance of HA proteins on the surface of virus particles being produced by avian cells therefore could be interesting. However, CR and CR.pIX cells might be used for the manufacturing of live-attenuated virus vaccines where only active virus titers determine yield and dose formulation. It is also possible to use them not only for propagation of human, but also avian influenza virus strains as the presence of α2,3 and α2,6 sialic acid residues on cellular receptors could be demonstrated [236]. The next section characterizes the propagation of LAIV strains that we tested to evaluate the potential of CR and CR.pIX cells as substrates for live virus vaccine manufacturing.

4.3.2 Propagation of cold-adapted virus strains

Analogous to the A/PR/8 strain, the *ca* virus strains A/Singapore, B/Vienna and B/Switzerland (see Table 3.3) were adapted to the avian host cell lines. For these experiments, CR.pIX cells were used as they are the industrially more relevant cell line. In addition to high titer seed viruses, a minimum of passages was aimed at to exclude the risk of back-mutations that could lead to loss of temperature-sensitivity or cold-adaptation. After two (A/Singapore) and three (B/Vienna) passages, seed viruses with acceptable titers were obtained. Adaptation of A/Switzerland was not successful which was assigned to the very low activity of the starting material ($5x10^4$ pfu/mL).
Two A/Singapore *ca* seed viruses were filled and stored at -80°C for subsequent experiments, one harvested 24 hpi with a titer of $1.7x10^6$ viruses/mL and one harvested 28 hpi with a titer of $2.3x10^6$ viruses/mL. Harvests for B/Vienna seed viruses were taken 30 hpi and 34 hpi with titers of $0.6x10^6$ and $1.1x10^6$ viruses/mL, respectively.

4.3.2.1 Infection parameters

Some infection parameters are strain-specific (see Figure 4.3.6) so that they had to be optimized for LAIV strains. Process strategy was not optimized again. As already announced, the parameter CCI was examined in more detail using the A/Singapore strain propagated in bioreactors so that this parameter will be revisited in section 4.3.2.3.

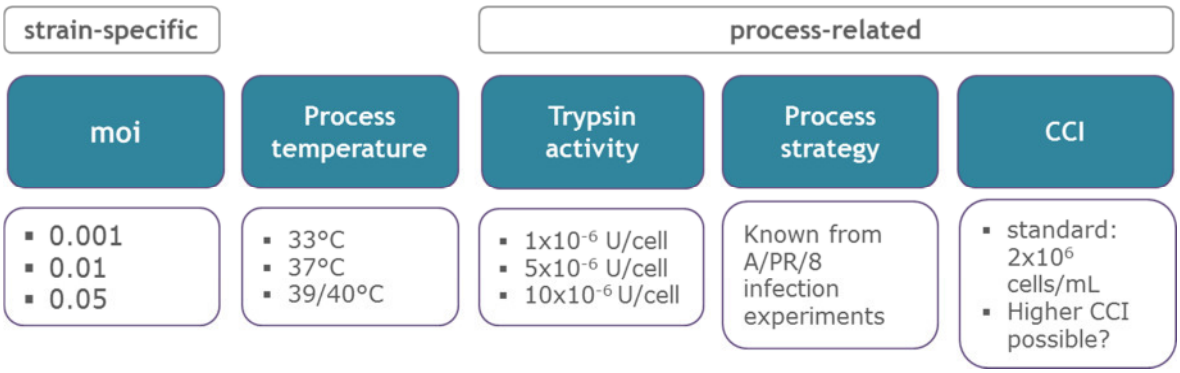

Figure 4.3.6: Infection parameters that have been tested with the cold-adapted A/Singapore strain. In the boxes at the bottom tested parameters are given.

Propagation of ca strains is usually done at 33°C so that all experiments in this section were performed at this temperature (after infection) if not indicated otherwise. However, *ca* strains that could be used for production of a live-attenuated vaccine, must have a temperature-sensitive and cold-adapted phenotype in order to be considered safe for use in human vaccination. These strains should show a reduced propagation at temperatures above 33°C. Considering this, control experiments were conducted with both *ca* strains also at 37°C and 40°C before and after adaptation to CR.pIX cells (Table 4.3.2).

Table 4.3.2: Temperature sensitivity of A/Singapore and B/Vienna strains in CR.pIX cells.

Maximum $TCID_{50}$ titers [viruses/mL][a]	33°C	37°C	40°C
Before adaptation to CR.pIX cells[b]			
A/Singapore	$1.3x10^8$	0	-[c]
B/Vienna	$1.8x10^5$	0	-
After adaptation to CR.pIX cells			
A/Singapore	$2.4x10^8$	$1.8x10^6$	0
B/Vienna	$3.2x10^6$	0	-

[a]maximum titers of CR.pIX cells infected in T-flasks at a CCI of $2x10^6$ cells/mL and with $1x10^{-6}$ units trypsin per cell [U/cell]
[b]Vero-adapted seed virus
[c]not determined

The B strain was highly sensitive to non-permissive temperature as no viral activity was determined at 37°C, obviating experiments at 40°C. The titer of A/Singapore was reduced about 2.6 log at 37°C compared to 33°C. At 40°C, no active particles were detected. This reduction is not as clear as for the B strain, but sufficient as the replication deficiency must be obvious only at 39 or 40°C for A strains [237]. Other studies have demonstrated a titer reduction of 2 log units at 37°C compared to the titer at 33°C [238] for the master donor strain B/AnnArbor/1/66 strain [239]. A similar decrease was also observed here. Testing the temperature sensitivity before and after

adaptation to CR.pIX cells (restricted to 2–3 passages) confirmed the temperature-sensitive phenotype. Both *ca* strains were pheno- and genotypically characterized for patent registration before reassortment and adaptation to CR.pIX cells [240], and it was shown that both cold-adapted strains carry several mutations compared to the wild type strains. For the A/Singapore strain there were 13 mutations with eight of them coding for an amino acid exchange. For the B/Vienna strain five mutations were detected by sequencing with three of them coding for an amino acid exchange. Sequencing of both strains could be of interest for follow-up studies considering mutations that occur during adaptation to the host cell line CR.pIX and considering the presence of mutations that might be connected with the temperature-sensitive phenotype [139, 239, 241].
Generally, the results indicate that both working virus seeds exhibit the expected temperature sensitivity.

It is known that for optimal influenza virus replication, trypsin addition is crucial. The optimal trypsin activity depends on the cell line (depending on proteases that are secreted), the medium (protein content), and also the virus strain [242]. Additionally, the trypsin activity was expected to be slightly reduced at 33°C [243]. Therefore, this infection parameter had to be tested for *ca* strains. As a reduction of trypsin activity was expected, we tested higher trypsin acitivites than the usually used $1x10^{-6}$ units/cell (Figure 4.3.7).

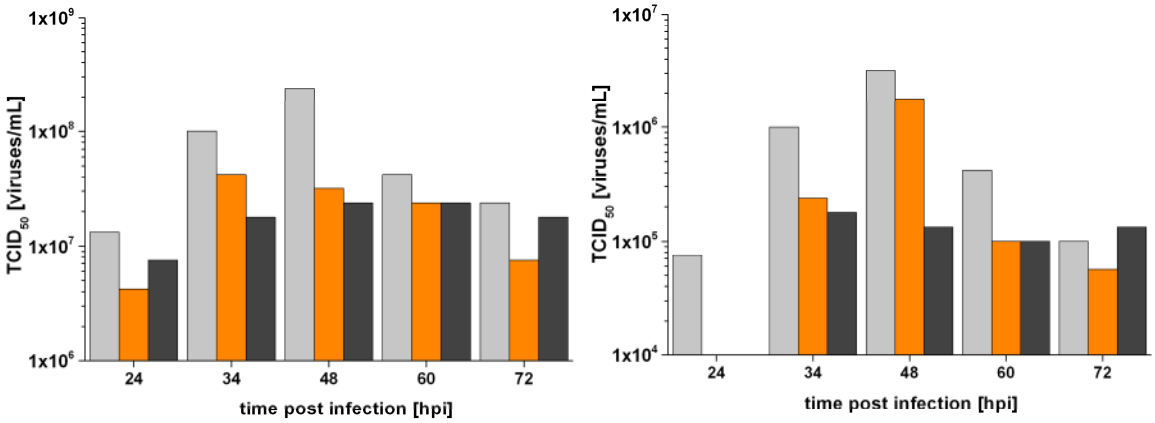

Figure 4.3.7: Optimization of trypsin activity used for the infection of CR.pIX cells with LAIV strains A/Singapore (A) and B/Vienna (B). Tested trypsin activities were $1x10^{-6}$ units/cell (grey), $5x10^{-6}$ units/cell (orange) and $10x10^{-6}$ units/cell (black). Cells were infected in T-flasks at a CCI of $2x10^6$ cells/mL, moi=0.001 and without applying a medium exchange.

When using $1x10^{-6}$ units/cell (standard concentration for A/PR/8 propagation), maximum $TCID_{50}$ titers were measured between 34 and 48 hpi. An increase of the trypsin activity to $5x10^{-6}$ units/cell or even $10x10^{-6}$ units/cell reduced the titers of

A/Singapore and B/Vienna. Infections without trypsin addition did not produce any infectious virus particles. Thus, without further adaptation of this parameter, $1x10^{-6}$ units trypsin per cell was found optimal for replication of A/Singapore ($2.4x10^{8}$ viruses/mL) and B/Vienna ($3.2x10^{6}$ viruses/mL). As trypsin activity is known to be a sensitive parameter that interacts with others, other groups have applied a Design of Experiments (DoE) approach to find the optimal concentration [153]. It is therefore possible that more extensive studies could result in a slightly different trypsin activity optimum. However, it seems that the reduced temperature of 33°C did not have a significant effect on the optimal trypsin concentration, and the chosen trypsin concentration supported acceptable titers.

4.3.2.2 Cell density effect in bioreactor cultivations

Whether the *ca* strains can be produced in bioreactors is an important test towards suitability of LAIV strain production for seasonal or pandemic vaccines in CR.pIX suspension cells. Focusing on the A/Singapore strain, experiments in a 1 L benchtop stirred tank bioreactor system were performed to test the scale-up potential.

Table 4.3.3: STR cultivations performed with the influenza strain A/Singapore.

	CCI_4_1	CCI_4_2	CCI_6_1	CCI_6_2	CCI_8_1	CCI_8_2
CCI [viable cells/mL]	$4.2x10^{6}$	$4.1x10^{6}$	$6.5x10^{6}$	$6.1x10^{6}$	$7.4x10^{6}$	$8.0x10^{6}$
Trypsin activity [units/cell]	$10x10^{-6}$	$1x10^{-6}$	$1x10^{-6}$	$1x10^{-6}$	$10x10^{-6}$	$10x10^{-6}$
Feed	-	-	-	-	-	200 mL

CR.pIX cell cultures were infected at different CCI and trypsin activities. Upon infection, the temperature was reduced to 33°C for virus propagation.

The cell density effect was evaluated by varying the CCI with the aim to identify the highest CCI that can be used without reduction of cell-specific productivity. One problem for infection at high CCI could be the release and accumulation of trypsin inhibitors during the growth phase. It was therefore also tested if a higher trypsin activity or a medium feed at high CCI can rescue productivity. Six bioreactor runs were performed with infections at approximately $4x10^{6}$ cells/mL (three days batch growth), $6x10^{6}$ cells/mL (five days batch growth) and $8x10^{6}$ cells/mL (six days batch growth) (Figure 4.3.8). Cell concentrations together with added trypsin and medium are summarized in Table 4.3.3.

At the lowest CCI ($4x10^{6}$ cells/mL), cell-specific virus yields of 15 (CCI_4_1) and 19 infectious viruses/cell (CCI_4_2) were obtained. Infection of the intermediate group with a CCI of about $6x10^{6}$ cells/mL led to reduced titers ($1x10^{7}$ viruses/mL for both

cultures) compared to the lowest CCI (1x10^8 viruses/mL) and, correspondingly, reduced cell-specific yields (Y_{CSV}=1-2 viruses/cell). Using a high CCI of about 8x10^6 cells/mL resulted in titers of 8x10^6 and 6x10^7 viruses/mL, respectively, and hence also low Y_{CSV} of 6 and 2 viruses/cell, respectively. This shows that neither the titer nor the yield was rescued when applying a higher trypsin activity (10x10^{-6} units/cell) or a medium addition (200 mL) at the highest CCI. For all cultures, viability at time of infection was above 90% (Figure 4.3.8B), showing that cells were not impaired due to extension of the growth phase. Although cell-specific virus yields are afflicted with errors from cell concentration and virus titer measurement, there was a trend observable in the direction of a cell density effect at CCI above 4x10^6 cells/mL.

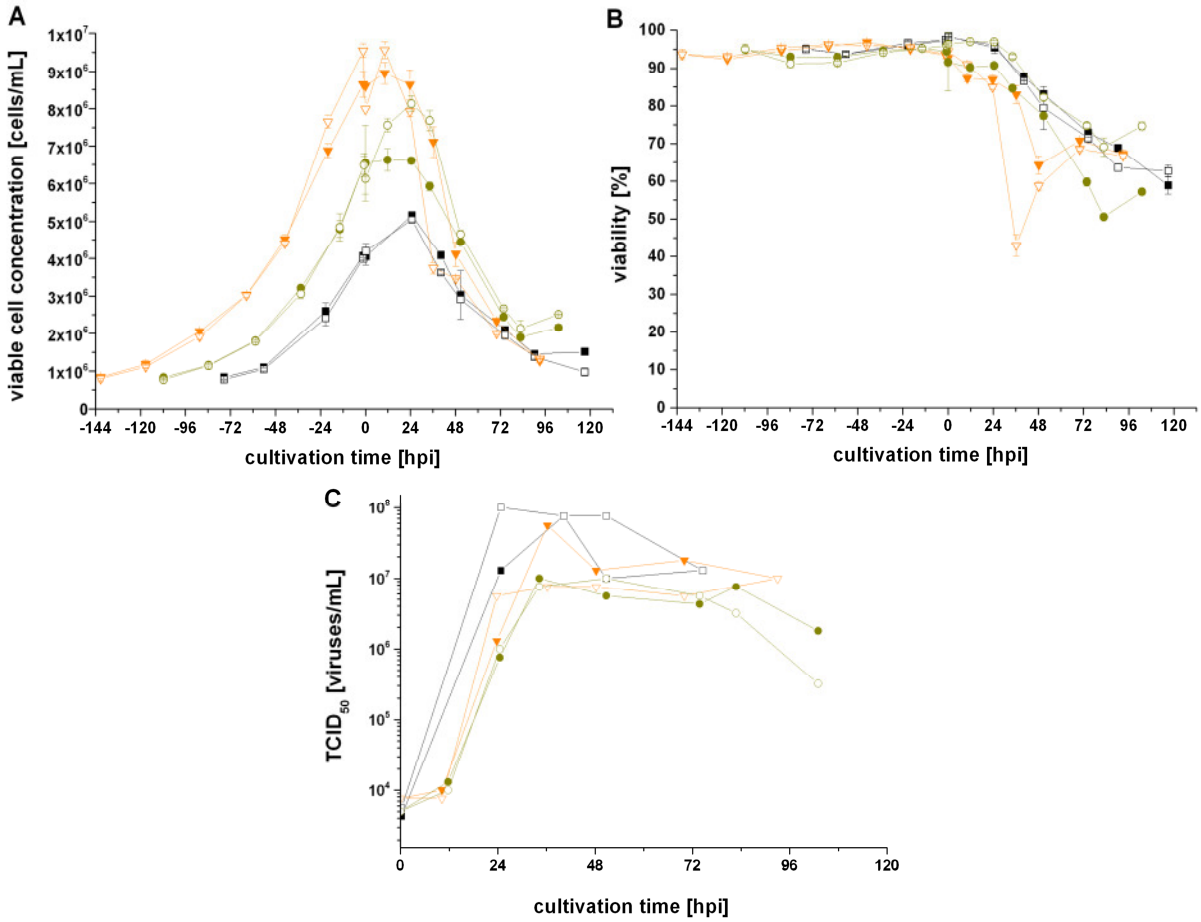

Figure 4.3.8: Infection of CR.pIX cells with the cold-adapted strain A/Singapore at different CCI (t=0 hpi). Viable cell concentrations (A), viabilities (B) and $TCID_{50}$ titers (C) of bioreactor cultivations are shown. Cells were infected with parameters summarized in Table 2: CCI_4_1 (■, black) and CCI_4_2 (□, black), CCI_6_1 (●, green) and CCI_6_2 (○, green), CCI_8_1 (▼, orange) and CCI_8_2 (▽, orange). After the cell growth phase at 37°C, bioreactor temperature was controlled at 33°C during the infection phase. Error bars for viable cell concentrations and viabilities indicate standard deviations of triplicate measurements.

A cell density effect, i.e. reduced titers and productivities at high CCI, as described for HEK293 cells and insect Sf9 cells infected with adenovirus, influenza virus and

baculovirus [20, 42, 67, 118, 119], was also observed with influenza virus-infected CR.pIX cells. At CCI above a critical concentration of $4x10^6$ cells/mL, cell-specific virus productivity decreased. The same critical cell concentration ($4x10^6$ cells/mL) was also found in studies using A/PR/8-infected HEK293 cells [42]. Influenza virus replication is known to modulate the cell cycle of host cells in order to on the one hand prevent cell to initiate cell death and on the other hand can use a running cellular machinery [244]. It was shown previously that the cell cycle fractions of a CR.pIX population at $8x10^6$ cells/mL (six days growth) do not differ significantly from the fractions at $2x10^6$ cells/mL, which corresponds to about three days growth (see Figure 4.1.2). For this reason, it was more likely that medium limitations cause for the cell density effect. Experiments with a 10-fold higher trypsin activity suggest that impaired virus propagation was not due to trypsin inhibitors released by the cells during the growth phase. Furthermore, the depletion of a common medium component also appears unlikely as a medium feed could not rescue virus titers or cell-specific productivities. Supporting this observation, neither the concentrations of the tested amino acids nor metabolites such as glucose or pyruvate appeared to be limiting (see Figure 4.1.4 for main metabolites). Still, it is probable that accumulation of other medium compounds (for example lipids, trace elements or vitamins) have an impact on virus titer. Thus, at this moment a likely speculation is that accumulation of inhibiting substances (that were not measured) cause the cell density effect. This hypothesis was currently tested in perfusion cultivations where cells were infected at very high cell concentrations. In fact, higher cell-specific virus yields of 50–600 viruses/cell were found with this system [245]. Future studies of these authors will also include modification of the medium (which was designed for proliferation and compatibility with a biphasic poxvirus production process [161]) to increase not only virus titers and productivity but also the critical CCI.

A comparison to shaker flask experiments (which resulted in a Y_{CSV} of 15–20 viruses/cell, data not shown) confirmed that scale-up to a benchtop bioreactor did not reduce virus titers or productivities at a CCI of $4x10^6$ cells/mL. From these results we concluded that a CCI of up to $4x10^6$ cells/mL can be used for virus production without the requirement for a medium exchange and, most importantly, without loss of cell-specific productivity. Shaker flask experiments were found to be highly predictive and scale-up to stirred tank bioreactors was possible without further optimization and without loss of productivity.

4.3.2.3 Virus titers and cell-specific virus yields in context with established processes

The results show that the cold-adapted strain A/Singapore can replicate to $1x10^8$ viruses/mL in a CR.pIX cell-based process. This corresponds to approximately 10,000 vaccine doses per liter reactor volume assuming that one dose contains 10^7 active virus particles (not taking into account losses during downstream processing). Romanova et al. obtained $2x10^8$ pfu/mL with the same master donor strain (A/Singapore/1/57 *ca*) using adherent Vero cells [162]. With adherent MDCK cells, titers for the related strain A/NewCaledonia/20/99 of up to 10^9 FFU/mL have been reported [152, 246-248]. Several influenza B strains were also tested in those studies and titers of 10^8 to 10^9 viruses/mL were obtained. As it is generally known that achievable titers are strain-specific, extensive optimizations normally help to maximize titers for each strain. Aggarwal et al. and George et al. have shown in their studies that high titers for B strains can be achieved after optimization of moi, microcarrier concentration, agitation rate and CCI [152, 246]. Thus, it is likely that additional optimization of CR.pIX cell-based processes (i.e. media and moi optimization) can further improve the propagation of the tested B/Vienna strain. Also, choosing CR cells for influenza propagation most likely augments titers about 1 log and thus is a vital option for a production process.

4.3.3 Chapter summary and outlook

With the obtained results, an influenza virus production process scheme with recommendations regarding optimal parameters for cell growth and infection phase can be drawn (Figure 4.3.9).

It was shown that the avian designer cell lines CR and CR.pIX did propagate influenza viruses to competitive titers in a suspension process. This was tested with the reference strain A/PR/8, usually used as backbone in the production of inactivated vaccines and with cold-adapted virus strains (A/Singapore and B/Vienna) that can be used for the production of live-attenuated influenza virus vaccines. The process is fast with peak titers already 12–24 hpi and easily scalable to industrial volumes as neither addition of microcarriers nor medium replacements are required. Though different parameters have been tested in order to maximize virus titers, HA values were not as high as for other cell lines, i.e. MDCK and HEK293 cells (around 2.0 log HAU/100 µL). Additional measures towards optimization of medium, feeding or perfusion strategy and process parameters should thus be pursued to achieve a further increase in HA values for production of inactivated influenza virus vaccines. On the other hand, achieved infectious virus titers

(via $TCID_{50}$ assay) were comparable to titers obtained from MDCK or Vero cells and thus are promising.

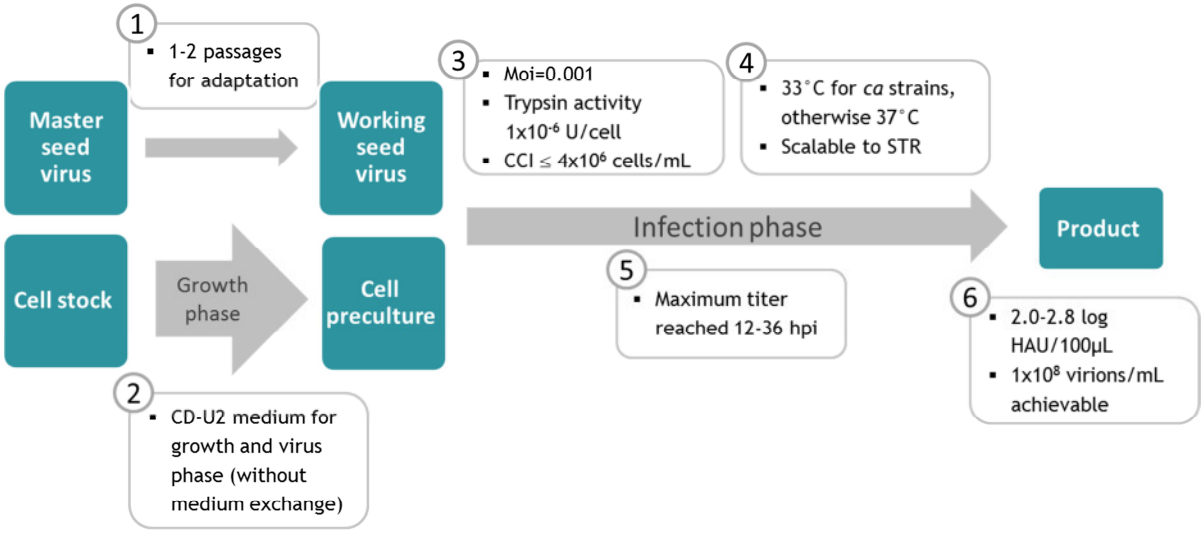

Figure 4.3.9: Optimal infection parameters that have been identified for production of influenza viruses with CR or CR.pIX cells as substrates.

Infection cell cultures at high CCI (above $4x10^6$ cells/mL) in a bioreactor resulted in slightly lower virus yields, assuming as for MVA, that somehow medium components obviate higher titers. More work is needed here in order to exploit the full potential of CR and CR.pIX suspension cells, i.e. at high cell concentrations. Also, virus titration methods should be revisited, especially for further studying live-attenuated viruses where all in process controls have to be determined via the time-consuming $TCID_{50}$ assay. Promising studies on other viruses already have shown that this is possible using flow cytometry. However, the fact that influenza virus is usually titrated on MDCK cells that allow secondary infections, make assay development in terms of reliable and robust data challenging. Nevertheless, for influenza virus a promising procedure was established during this project [228] (see Appendix A14 for schematic procedure) and will be further improved.

Generally, in this chapter it could be shown that CR and CR.pIX cells are proper host cell substrates that can be used for influenza virus vaccine manufacturing.

5 Conclusion

CR and CR.pIX cells are promising new cell substrates that can be used for production of vaccines. New host cells that might be approved for manufacturing of human vaccines, need to be characterized thoroughly. For the upstream processing, this shall assure that robust production systems are set up and that assays are at hand to monitor all crucial and all critical process parameters (cell-based or product-based). This project aimed at characterizing the upstream processing of CR (AGE1.CR®) and CR.pIX (AGE1.CR.pIX®) cells.

First, growth and metabolism during batch cultivation were characterized (chapter 4.1). Specific cell growth rates were determined to be between 0.2 h^{-1} and 0.3 h^{-1} and maximum cell concentrations of about $1x10^7$ cells/mL were achieved 5–7 days post inoculation in all tested cultivation systems. As expected for suspension cells, scalability was unproblematic.

To be able to better interpret experimental data from several bioreactor cultivations, statistical analysis comparing growth rates as well as uptake and release rates of main metabolites was performed. Therefore, method errors from method validation were taken into account in order to determine technical variances (one pre-culture, several parallel cultivations) as well as inter-experimental variances (different pre-cultures, no parallel cultivations). It could be shown that when performing the same experiment with different pre-cultures, variances in determined rates were between 7.3% and 42.1%. In parallel experiments using the same pre-cultures, such high variances were not observed, but were between 3.2% and 12.5%. Differences or heterogeneity of pre-cultures thus seem to play a major role in batch-to-batch variation.

Recording metabolite concentrations over cultivation time showed similar profiles than observed for other immortalized cell lines. However, glutamine uptake was found to be neglectable for CR and CR.pIX cells, and MFA was used to further study metabolism. Therefore, calculated exchange rates were calculated and combined with a developed metabolic network model and biomass analysis to determine a flux distribution of CR.pIX cultivated in batch mode in a STR. It was shown that CR.pIX cells do not use glutamine, but rather other amino acids like asparagine and leucine in order to fuel the TCA cycle. Whereby glutaminolysis is one of the main pathways used for many immortalized mammalian cell lines like HEK293 and CHO, it seemed to be nearly inactive for avian CR.pIX cells. This finding was supported by measurements of

maximum glutaminase and glutamine synthetase activities and by successful cultivation in glutamine-free medium. Apart from that, CR.pIX cells showed a typical overflow metabolism like other immortalized cell lines with high lactate production rates and a low connectivity between glycolysis and TCA cycle. In future, the developed network model enables more detailed metabolic studies that can help for example in medium optimization or process intensification.

After studies on cell growth and metabolism of CR and CR.pIX cells, infection experiments with attenuated vaccinia virus MVA were presented (chapter 4.2). First aim was to evaluate whether competitive titers can be achieved with CR and CR.pIX cells, when compared to primary CEF cultures which are traditionally used for propagation of MVA. Small-scale experiments as well as experiments in 1 L STR as well as 1 L Wave bioreactor showed that virus titers in a range of $1x10^7$–$1x10^8$ viruses/mL can be achieved with CR.pIX cells in chemically-defined media. Such values are competitive with titers achieved with CEF, BHK-21 cells or other avian cell substrates.
Having a suspension cell line at hand which grows to high cell concentrations, we aimed at maximized yields when infecting cell cultures late in growth phase when more cells are present. When CCI of 2–$4x10^6$ cells/mL were used, similar cell-specific virus yields were observed (6–200 viruses/mL). However, when using CCI ≥$4x10^6$ cells/mL at time of infection, virus titers did not increase further, and thus, cell-specific virus yields were lower in average (1–8 viruses/mL). Whether this was a result of impaired fitness of cells early and late in exponential growth phase was evaluated using cell cycle and apoptosis assays. Indeed, we found less apoptotic cells in flow cytometry analyzing samples from high CCI which most likely was a result of higher cell lysis rate. However, it could not be proven whether productivity loss at high cell concentrations is an effect of cell fitness or whether it might be caused by missing or interfering medium components that could not be measured.
Following infection status of cell cultures was possible by using MVAegfp, a recombinant MVA strain. Upon infection, infected cells accumulated EGFP in the cytoplasm which could be measured by green fluorescence intensity with the flow cytometer. Small-scale and bioreactor infection experiments showed that 45–90% of the cell population were infected at maximum. This might suggest that there is a potential for optimizing virus propagation in CR.pIX cell cultures. However, a recent study by Stiefel et al. with the non-attenuated western reserve strain propagated on HeLa cells observed only a low success rate (approximately 50%) of vaccinia viruses entering the cell [250]. They used the non-attenuated western reserve strain and propagated it on cells. Taking this into

account, deficient virus particles rather than productivity of CR.pIX cells might be seen as a limiting factor.
Overall, CR and CR.pIX cells are a vital option to replace CEF cultures as production system for MVA. Flow cytometric assays to follow cell physiology and infection status have been established for CR.pIX cells infected with MVAegfp. With that, successful infection can be identified during the process and harvest times can be better defined. Moreover, data for modeling approaches can be generated. Improvements on virus titration assays, for example by using flow cytometry with MVAegfp infected CR.pIX cells for read-out, will help on the one hand to increase robustness of the assay, and on the other hand to improve the turnover time of virus titer analysis.

Finally, influenza virus was propagated in CR and CR.pIX cell cultures (chapter 4.3). Optimization of infection parameters such as moi, temperature and eventual medium replacement strategies at time of infection was done using the reference strain A/PR/8/34 (H1N1). In addition, scale-up studies towards 1 L lab-scale bioreactors and high cell concentrations that support high titers and virus yields were done using live-attenuated virus strains (A and B subtype). Temperature-sensitivity of these strains was confirmed beforehand in small-scale experiments. Similar to MVA, a critical CCI of about $4x10^6$ cells/mL was found in experiments using different CCI in a bioreactor. Above this cell concentration, maximum virus titers stayed nearly constant at approximately 10^7 viruses/mL, but lower cell-specific virus yields of 1–6 viruses/cell resulted. The fact that the nearly same critical CCI was found for both virus-host cell systems might favor the hypothesis that the limitations are associated with inhibiting or missing medium components. Indeed, follow-up studies in perfusion mode showed that virus titers can be partly rescued when medium is exchanged continuously.
With the tested influenza virus strains, competitive infectious virus titers of around 10^8 viruses/mL (i.e. determined via $TCID_{50}$ assay) could be shown as compared to MDCK and Vero cells, the gold standards for influenza virus vaccine production. With 2.0–2.8 log HA units/100 µL, HA values were 0.5–1 log scales lower than those obtained with MDCK and Vero cells, but probably still sufficient in order to produce industrially relevant amounts of virus antigen.

In conclusion, the presented results show that CR and CR.pIX cells offer the possibility to develop modern and robust vaccine production processes. The fact that chemically-defined media can be used broadens the spectrum of analyses that can be done (e.g. flux analyses). It also facilitates approval of products derived with these cell lines and technology transfer to less developed countries. This work is the first to study cell-

based parameters in detail and showed susceptibility of CR and CR.pIX cells towards influenza virus. Obtained data and results on metabolism, MVA propagation and influenza propagation can serve as a basis for further research projects, but also industrial process development.

6 References

[1] Plotkin SA. History of vaccine development. New York: Springer; 2011.
[2] Fenner F, Henderson DA, Arita L, Jezek Z, Ladnyi ID. Smallpox and its eradication. Geneva: WHO; 1988.
[3] Cottingham MG, Carroll MW. Recombinant MVA vaccines: dispelling the myths. Vaccine. 2013;31:4247-51.
[4] Wareing MD, Tannock GA. Live attenuated vaccines against influenza; an historical review. Vaccine. 2001;19:3320-30.
[5] Genzel Y, Reichl U. Continuous cell lines as production system for influenza vaccines. Expert Rev Vaccines. 2009;8:1681-92.
[6] Josefsberg JO, Buckland B. Vaccine process technology. Biotechnol Bioeng. 2012;109:1443-60.
[7] Patterson S, Papagatsias T, Benlahrech A. Use of adenovirus in vaccines for HIV. Handb Exp Pharmacol. 2009:275-93.
[8] Liniger M, Zuniga A, Naim HY. Use of viral vectors for the development of vaccines. Expert Rev Vaccines. 2007;6:255-66.
[9] Osterholm MT. Preparing for the next pandemic. N Engl J Med. 2005;352:1839-42.
[10] Armstrong ME, Giesa PA, Davide JP, Redner F, Waterbury JA, Rhoad AE, Keys RD, Provost PJ, Lewis JA. Development of the formalin-inactivated hepatitis A vaccine, VAQTA from the live attenuated virus strain CR326F. J Hepatol. 1993;18 Suppl 2:S20-6.
[11] Jordan I, Sandig V. Matrix and backstage: cellular substrates for viral vaccines. Viruses. 2014;6:1672-700.
[12] Hess RD, Weber F, Watson K, Schmitt S. Regulatory, biosafety and safety challenges for novel cells as substrates for human vaccines. Vaccine. 2012;30:2715-27.
[13] Pau MG, Ophorst C, Koldijk MH, Schouten G, Mehtali M, Uytdehaag F. The human cell line PER.C6 provides a new manufacturing system for the production of influenza vaccines. Vaccine. 2001;19:2716-21.
[14] Brown SW, Mehtali M. The Avian EB66(R) Cell Line, Application to Vaccines, and Therapeutic Protein Production. PDA J Pharm Sci Technol. 2010;64:419-25.
[15] Genzel Y, Behrendt I, Rodig J, Rapp E, Kueppers C, Kochanek S, Schiedner G, Reichl U. CAP, a new human suspension cell line for influenza virus production. Appl Microbiol Biotechnol. 2013;97:111-22.
[16] Jordan I, Lohr V, Genzel Y, Reichl U, Sandig V. Elements in the Development of a Production Process for Modified Vaccinia Virus Ankara. Microorganisms. 2013;1:100-21.
[17] Sanders BP, Edo-Matas D, Custers JH, Koldijk MH, Klaren V, Turk M, Luitjens A, Bakker WA, Uytdehaag F, Goudsmit J, Lewis JA, Schuitemaker H. PER.C6 cells as a serum-free suspension cell platform for the production of high titer poliovirus: a potential low cost of goods option for world supply of inactivated poliovirus vaccine. Vaccine. 2013;31:850-6.
[18] Jordan I, Vos A, Beilfuss S, Neubert A, Breul S, Sandig V. An avian cell line designed for production of highly attenuated viruses. Vaccine. 2009;27:748-56.
[19] Lohr V, Rath A, Genzel Y, Jordan I, Sandig V, Reichl U. New avian suspension cell lines provide production of influenza virus and MVA in serum-free media: studies on growth, metabolism and virus propagation. Vaccine. 2009;27:4975-82.
[20] Carinhas N, Bernal V, Yokomizo AY, Carrondo MJ, Oliveira R, Alves PM. Baculovirus production for gene therapy: the role of cell density, multiplicity of infection and medium exchange. Appl Microbiol Biotechnol. 2009;81:1041-9.
[21] Ferreira TB, Perdigao R, Silva AC, Zhang C, Aunins JG, Carrondo MJ, Alves PM. 293 cell cycle synchronisation adenovirus vector production. Biotechnol Prog. 2009;25:235-43.

[22] Carter NJ, Curran MP. Live attenuated influenza vaccine (FluMist(R); Fluenz): a review of its use in the prevention of seasonal influenza in children and adults. Drugs. 2011;71:1591-622.
[23] Kaufmann SE. Novel Vaccination Strategies. Weinheim: Wiley-VCH; 2006.
[24] http://www.historyofvaccines.org/content/timelines/diseases-and-vaccines. Accessed 05.01.2014
[25] Global vaccine market features and trends. http://who.int/influenza_vaccines_plan/resources/session_10_kaddar.pdf. Accessed 15.01.2014
[26] Mayr A, Hochstein-Mintzel V, Stickl H. Abstammung, Eigenschaften und Verwendung des attenuierten Vaccinia-Stammes MVA. Infection. 1975;3:6-14.
[27] Meyer H, Sutter G, Mayr A. Mapping of deletions in the genome of the highly attenuated vaccinia virus MVA and their influence on virulence. J Gen Virol. 1991;72 (Pt 5):1031-8.
[28] Maassab HF, Bryant ML. The development of live attenuated cold-adapted influenza virus vaccine for humans. Rev Med Virol. 1999;9:237-44.
[29] Maassab HF, Francis T, Jr., Davenport FM, Hennessy AV, Minuse E, Anderson G. Laboratory and clinical characteristics of attenuated strains of influenza virus. Bull World Health Organ. 1969;41:589-94.
[30] Artenstein AW. Vaccines: A Biography: Springer Science+Business Media; 2010.
[31] Global pandemic influenza action plan to increase vaccine supply: WHO/IVB/06.13. http://www.who.int/csr/resources/publications/influenza/WHO_CDS_EPR_GIP_2006_1/en/index.html. Accessed 27.01.2014
[32] Perrin P, Madhusudana S, Gontier-Jallet C, Petres S, Tordo N, Merten OW. An experimental rabies vaccine produced with a new BHK-21 suspension cell culture process: use of serum-free medium and perfusion-reactor system. Vaccine. 1995;13:1244-50.
[33] Drexler I, Heller K, Wahren B, Erfle V, Sutter G. Highly attenuated modified vaccinia virus Ankara replicates in baby hamster kidney cells, a potential host for virus propagation, but not in various human transformed and primary cells. J Gen Virol. 1998;79:347-52.
[34] Merten OW, Hannoun C, Manuguerra JC, Ventre F, Petres S. Production of influenza virus in cell cultures for vaccine preparation. Adv Exp Med Biol. 1996;397:141-51.
[35] Tree JA, Richardson C, Fooks AR, Clegg JC, Looby D. Comparison of large-scale mammalian cell culture systems with egg culture for the production of influenza virus A vaccine strains. Vaccine. 2001;19:3444-50.
[36] Howard CJ, Clarke MC, Sopp P, Brownlie J. Systemic vaccination with inactivated bovine virus diarrhoea virus protects against respiratory challenge. Vet Microbiol. 1994;42:171-9.
[37] Chen Z, Xu P, Salyards GW, Harvey SB, Rada B, Fu ZF, He B. Evaluating a parainfluenza virus 5-based vaccine in a host with pre-existing immunity against parainfluenza virus 5. PLoS One. 2012;7:e50144.
[38] Barrett PN, Mundt W, Kistner O, Howard MK. Vero cell platform in vaccine production: moving towards cell culture-based viral vaccines. Expert Rev Vaccines. 2009;8:607-18.
[39] Mehtali M, Chamion-Arnaud P, Leon A. Process of manufacturing viral vaccines in suspension avian embryonic derived stem cell lines. [Patent]. 2006. WO 2006/108846 A1.
[40] Olivier S, Jacoby M, Brillon C, Bouletreau S, Mollet T, Nerriere O, Angel A, Danet S, Souttou B, Guehenneux F, Gauthier L, Berthome M, Vie H, Beltraminelli N, Mehtali M. EB66 cell line, a duck embryonic stem cell-derived substrate for the industrial production of therapeutic monoclonal antibodies with enhanced ADCC activity. MAbs. 2010;2.

[41] Le Ru A, Jacob D, Transfiguracion J, Ansorge S, Henry O, Kamen AA. Scalable production of influenza virus in HEK-293 cells for efficient vaccine manufacturing. Vaccine. 2010;28:3661-71.
[42] Cortin V, Thibault J, Jacob D, Garnier A. High-titer adenovirus vector production in 293S cell perfusion culture. Biotechnol Prog. 2004;20:858-63.
[43] Maranga L, Aunins JG, Zhou W. Characterization of changes in PER.C6 cellular metabolism during growth and propagation of a replication-deficient adenovirus vector. Biotechnol Bioeng. 2005;90:645-55.
[44] Frensing T, Heldt FS, Pflugmacher A, Behrendt I, Jordan I, Flockerzi D, Genzel Y, Reichl U. Continuous influenza virus production in cell culture shows a periodic accumulation of defective interfering particles. PLoS One. 2013;8:e72288.
[45] Lohr V, Genzel Y, Jordan I, Katinger D, Mahr S, Sandig V, Reichl U. Live attenuated influenza viruses produced in a suspension process with avian AGE1.CR.pIX cells. BMC Biotechnol. 2012;12:79.
[46] Characterization and Qualification of Cell Substrates and Other Biological Materials Used in the Production of Viral Vaccines for Infectious Disease Indications. http://www.fda.gov/downloads/BiologicsBloodVaccines/GuidanceComplianceRegulatoryInformation/Guidances/Vaccines/UCM202439.pdf. Accessed 15.01.2014
[47] Aiello L, Guilfoyle R, Huebner K, Weinmann R. Adenovirus 5 DNA sequences present and RNA sequences transcribed in transformed human embryo kidney cells (HEK-Ad-5 or 293). Virology. 1979;94:460-9.
[48] Graham FL, Smiley J, Russell WC, Nairn R. Characteristics of a human cell line transformed by DNA from human adenovirus type 5. J Gen Virol. 1977;36:59-74.
[49] Parks RJ. Adenovirus protein IX: a new look at an old protein. Mol Ther. 2005;11:19-25.
[50] Jordan I, Woods N, Whale G, Sandig V. Production of a viral-vectored vaccine candidate against tuberculosis. BioProcess International: BioProcess International; 2012. p. 46-55.
[51] Freshney R. Culture of Animal Cells. New York: Wiley-Liss, Inc.; 1994.
[52] Chu L, Robinson DK. Industrial choices for protein production by large-scale cell culture. Curr Opin Biotechnol. 2001;12:180-7.
[53] Warnock JN, Al-Rubeai M. Bioreactor systems for the production of biopharmaceuticals from animal cells. Biotechnol Appl Biochem. 2006;45:1-12.
[54] Häggström L. Cell metabolism, animal. In: Spier RE, editor. Encyclopedia of Cell Technology. edition. Volume 1. John Wiley & Sons, Inc.; 2000. chapter.
[55] Doverskog M, Ljunggren J, Ohman L, Haggstrom L. Physiology of cultured animal cells. J Biotechnol. 1997;59:103-15.
[56] Dietmair S, Timmins NE, Nielsen LK. Engineering a mammalian super producer. J Chem Technol Biotechnol. 2011;86:905-14.
[57] Ritter JB, Wahl AS, Freund S, Genzel Y, Reichl U. Metabolic effects of influenza virus infection in cultured animal cells: Intra- and extracellular metabolite profiling. BMC Syst Biol. 2010;4:61.
[58] Boghigian BA, Seth G, Kiss R, Pfeifer BA. Metabolic flux analysis and pharmaceutical production. Metab Eng. 2010;12:81-95.
[59] Quek LE, Dietmair S, Kromer JO, Nielsen LK. Metabolic flux analysis in mammalian cell culture. Metab Eng. 2010;12:161-71.
[60] Llaneras F, Pico J. An interval approach for dealing with flux distributions and elementary modes activity patterns. J Theor Biol. 2007;246:290-308.
[61] Klamt S, Saez-Rodriguez J, Gilles ED. Structural and functional analysis of cellular networks with CellNetAnalyzer. BMC Syst Biol. 2007;1:2.
[62] Stevens L. Avian Biochemistry and Molecular Biology: Cambridge University Press; 1996.
[63] Tinker DA, Brosnan JT, Herzberg GR. Interorgan metabolism of amino acids, glucose, lactate, glycerol and uric acid in the domestic fowl (Gallus domesticus). Biochem J. 1986;240:829-36.

[64] Zustiak MP, Dorai H, Betenbaugh MJ, Sauerwald TM. Controlling apoptosis to optimize yields of proteins from mammalian cells. Methods Mol Biol. 2012;801:111-23.
[65] Zhang C, Ferreira TB, Cruz PE, Alves PM, Haury M, Carrondo MJT. The importance of 293 cell cycle phase on adenovirus vector production. Enzyme and Microbial Technology. 2006;39:1328-32.
[66] Stubblefield E. Synchronization Methods for Mammalian Cell Cultures. In: Prescott DM, editor. Methods in Cell Physiology. edition. 3. New York: Academic Press; 1968. chapter 2. p. 25-44.
[67] Ibarra N, Watanabe S, Bi JX, Shuttleworth J, Al-Rubeai M. Modulation of cell cycle for enhancement of antibody productivity in perfusion culture of NS0 cells. Biotechnol Prog. 2003;19:224-8.
[68] McTaggart S, Al-Rubeai M. Relationship between cell proliferation, cell-cycle phase, and retroviral vector production in FLYRD18 human packaging cells. Biotechnol Bioeng. 2001;76:52-60.
[69] Uzbekov RE. Analysis of the cell cycle and a method employing synchronized cells for study of protein expression at various stages of the cell cycle. Biochemistry (Mosc). 2004;69:485-96.
[70] Simpson NH, Singh RP, Perani A, Goldenzon C, Al-Rubeai M. In hybridoma cultures, deprivation of any single amino acid leads to apoptotic death, which is suppressed by the expression of the bcl-2 gene. Biotechnol Bioeng. 1998;59:90-8.
[71] Everett H, McFadden G. Poxviruses and apoptosis: a time to die. Curr Opin Microbiol. 2002;5:395-402.
[72] Takizawa T, Matsukawa S, Higuchi Y, Nakamura S, Nakanishi Y, Fukuda R. Induction of programmed cell death (apoptosis) by influenza virus infection in tissue culture cells. J Gen Virol. 1993;74 (Pt 11):2347-55.
[73] Isken B, Genzel Y, Reichl U. Productivity, apoptosis, and infection dynamics of influenza A/PR/8 strains and A/PR/8-based reassortants. Vaccine. 2012;30:5253-61.
[74] Cotter TG, al-Rubeai M. Cell death (apoptosis) in cell culture systems. Trends Biotechnol. 1995;13:150-5.
[75] Vermes I, Haanen C, Reutelingsperger C. Flow cytometry of apoptotic cell death. J Immunol Methods. 2000;243:167-90.
[76] Martin SJ, Reutelingsperger CP, McGahon AJ, Rader JA, van Schie RC, LaFace DM, Green DR. Early redistribution of plasma membrane phosphatidylserine is a general feature of apoptosis regardless of the initiating stimulus: inhibition by overexpression of Bcl-2 and Abl. J Exp Med. 1995;182:1545-56.
[77] Vermes I, Haanen C, Steffens-Nakken H, Reutelingsperger C. A novel assay for apoptosis. Flow cytometric detection of phosphatidylserine expression on early apoptotic cells using fluorescein labelled Annexin V. J Immunol Methods. 1995;184:39-51.
[78] Majno G, Joris I. Apoptosis, oncosis, and necrosis. An overview of cell death. Am J Pathol. 1995;146:3-15.
[79] Hail N, Jr., Carter BZ, Konopleva M, Andreeff M. Apoptosis effector mechanisms: a requiem performed in different keys. Apoptosis. 2006;11:889-904.
[80] Arden N, Betenbaugh MJ. Life and death in mammalian cell culture: strategies for apoptosis inhibition. Trends Biotechnol. 2004;22:174-80.
[81] McLean JE, Ruck A, Shirazian A, Pooyaei-Mehr F, Zakeri ZF. Viral manipulation of cell death. Curr Pharm Des. 2008;14:198-220.
[82] Barber GN. Host defense, viruses and apoptosis. Cell Death Differ. 2001;8:113-26.
[83] Kennedy RB, Lane JM, Henderson DA, Poland GA. Smallpox and vaccinia. In: Plotkin SA, Orenstein WA, Offit PA, editors. Vaccines. edition 6: Elsevier Saunders; 2013. chapter 32.
[84] Whitbeck JC, Foo CH, Ponce de Leon M, Eisenberg RJ, Cohen GH. Vaccinia virus exhibits cell-type-dependent entry characteristics. Virology. 2009;385:383-91.

[85] Stiefel P, Schmidt FI, Dörig P, Behr P, Zambelli T, Vorholt JA, Mercer J. Cooperative Vaccinia Infection Demonstrated at the Single-Cell Level Using FluidFM. Nano Letters. 2012;12:4219-27.
[86] McFadden G. Poxvirus tropism. Nat Rev Microbiol. 2005;3:201-13.
[87] Ward BM. The longest micron; transporting poxviruses out of the cell. Cell Microbiol. 2005;7:1531-8.
[88] Smith GL, Vanderplasschen A, Law M. The formation and function of extracellular enveloped vaccinia virus. J Gen Virol. 2002;83:2915-31.
[89] Walsh SR, Dolin R. Vaccinia viruses: vaccines against smallpox and vectors against infectious diseases and tumors. Expert Rev Vaccines. 2011;10:1221-40.
[90] Willis NJ. Edward Jenner and the eradication of smallpox. Scott Med J. 1997;42:118-21.
[91] Monath TP, Caldwell JR, Mundt W, Fusco J, Johnson CS, Buller M, Liu J, Gardner B, Downing G, Blum PS, Kemp T, Nichols R, Weltzin R. ACAM2000 clonal Vero cell culture vaccinia virus (New York City Board of Health strain)--a second-generation smallpox vaccine for biological defense. Int J Infect Dis. 2004;8 Suppl 2:S31-44.
[92] Tartaglia J, Perkus ME, Taylor J, Norton EK, Audonnet JC, Cox WI, Davis SW, van der Hoeven J, Meignier B, Riviere M, et al. NYVAC: a highly attenuated strain of vaccinia virus. Virology. 1992;188:217-32.
[93] Vollmar J, Arndtz N, Eckl KM, Thomsen T, Petzold B, Mateo L, Schlereth B, Handley A, King L, Hulsemann V, Tzatzaris M, Merkl K, Wulff N, Chaplin P. Safety and immunogenicity of IMVAMUNE, a promising candidate as a third generation smallpox vaccine. Vaccine. 2006;24:2065-70.
[94] Coulibaly S, Brühl P, Mayrhofer J, Schmid K, Gerencer M, Falkner FG. The nonreplicating smallpox candidate vaccines defective vaccinia Lister (dVV-L) and modified vaccinia Ankara (MVA) elicit robust long-term protection. Virology. 2005;341:91-101.
[95] Phelps AL, Gates AJ, Hillier M, Eastaugh L, Ulaeto DO. Comparative efficacy of modified vaccinia Ankara (MVA) as a potential replacement smallpox vaccine. Vaccine. 2007;25:34-42.
[96] Altenburger W, Suter CP, Altenburger J. Partial deletion of the human host range gene in the attenuated vaccinia virus MVA. Arch Virol. 1989;105:15-27.
[97] Antoine G, Scheiflinger F, Dorner F, Falkner FG. The complete genomic sequence of the modified vaccinia Ankara strain: comparison with other orthopoxviruses. Virology. 1998;244:365-96.
[98] Sutter G, Moss B. Nonreplicating vaccinia vector efficiently expresses recombinant genes. Proc Natl Acad Sci U S A. 1992;89:10847-51.
[99] Sancho MC, Schleich S, Griffiths G, Krijnse-Locker J. The block in assembly of modified vaccinia virus Ankara in HeLa cells reveals new insights into vaccinia virus morphogenesis. J Virol. 2002;76:8318-34.
[100] Buttner M, Czerny CP, Lehner KH, Wertz K. Interferon induction in peripheral blood mononuclear leukocytes of man and farm animals by poxvirus vector candidates and some poxvirus constructs. Vet Immunol Immunopathol. 1995;46:237-50.
[101] Dorrell L, O'Callaghan CA, Britton W, Hambleton S, McMichael A, Smith GL, Rowland-Jones S, Blanchard TJ. Recombinant modified vaccinia virus Ankara efficiently restimulates human cytotoxic T lymphocytes in vitro. Vaccine. 2000;19:327-36.
[102] Jester BC, Drillien R, Ruff M, Florentz C. Using Vaccinia's innate ability to introduce DNA into mammalian cells for production of recombinant proteins. J Biotechnol. 2011;156:211-3.
[103] Goepfert PA, Elizaga ML, Sato A, Qin L, Cardinali M, Hay CM, Hural J, DeRosa SC, DeFawe OD, Tomaras GD, Montefiori DC, Xu Y, Lai L, Kalams SA, Baden LR, Frey SE, Blattner WA, Wyatt LS, Moss B, Robinson HL, National Institute of A, Infectious Diseases HIVVTN. Phase 1 safety and immunogenicity testing of DNA and recombinant modified vaccinia Ankara vaccines expressing HIV-1 virus-like particles. J Infect Dis. 2011;203:610-9.

[104] Greenough TC, Cunningham CK, Muresan P, McManus M, Persaud D, Fenton T, Barker P, Gaur A, Panicali D, Sullivan JL, Luzuriaga K, Pediatric ACTGPT. Safety and immunogenicity of recombinant poxvirus HIV-1 vaccines in young adults on highly active antiretroviral therapy. Vaccine. 2008;26:6883-93.
[105] Ibanga HB, Brookes RH, Hill PC, Owiafe PK, Fletcher HA, Lienhardt C, Hill AV, Adegbola RA, McShane H. Early clinical trials with a new tuberculosis vaccine, MVA85A, in tuberculosis-endemic countries: issues in study design. Lancet Infect Dis. 2006;6:522-8.
[106] Bejon P, Ogada E, Mwangi T, Milligan P, Lang T, Fegan G, Gilbert SC, Peshu N, Marsh K, Hill AV. Extended follow-up following a phase 2b randomized trial of the candidate malaria vaccines FP9 ME-TRAP and MVA ME-TRAP among children in Kenya. PLoS One. 2007;2:e707.
[107] Harrop R, Shingler W, Kelleher M, de Belin J, Treasure P. Cross-trial analysis of immunologic and clinical data resulting from phase I and II trials of MVA-5T4 (TroVax) in colorectal, renal, and prostate cancer patients. J Immunother. 2010;33:999-1005.
[108] Arlen PM, Pazdur M, Skarupa L, Rauckhorst M, Gulley JL. A randomized phase II study of docetaxel alone or in combination with PANVAC-V (vaccinia) and PANVAC-F (fowlpox) in patients with metastatic breast cancer (NCI 05-C-0229). Clin Breast Cancer. 2006;7:176-9.
[109] Hornemann S, Harlin O, Staib C, Kisling S, Erfle V, Kaspers B, Hacker G, Sutter G. Replication of modified vaccinia virus Ankara in primary chicken embryo fibroblasts requires expression of the interferon resistance gene E3L. J Virol. 2003;77:8394-407.
[110] Carroll MW, Moss B. Host range and cytopathogenicity of the highly attenuated MVA strain of vaccinia virus: propagation and generation of recombinant viruses in a nonhuman mammalian cell line. Virology. 1997;238:198-211.
[111] Stoker M, Macpherson I. Syrian Hamster Fibroblast Cell Line Bhk21 and Its Derivatives. Nature. 1964;203:1355-7.
[112] Mayr A. Altered Strain of the Modified Vaccinia Virus Ankara (MVA). [Patent]. 2003. US 2003/0013190 A1.
[113] Ricci PS, Schafer B, Kreil TR, Falkner FG, Holzer GW. Selection of recombinant MVA by rescue of the essential D4R gene. Virol J. 2011;8:529.
[114] Kraus B, von Fircks S, Feigl S, Koch SM, Fleischanderl D, Terler K, Dersch-Pourmojib M, Konetschny C, Grillberger L, Reiter M. Avian cell line - Technology for large scale vaccine production. BMC Proc. 2011;5 Suppl 8:P52.
[115] Bernal V, Carinhas N, Yokomizo AY, Carrondo MJ, Alves PM. Cell density effect in the baculovirus-insect cells system: a quantitative analysis of energetic metabolism. Biotechnol Bioeng. 2009;104:162-80.
[116] Bedard C, Kamen A, Tom R, Massie B. Maximization of recombinant protein yield in the insect cell/baculovirus system by one-time addition of nutrients to high-density batch cultures. Cytotechnology. 1994;15:129-38.
[117] Meghrous J, Mahmoud W, Jacob D, Chubet R, Cox M, Kamen AA. Development of a simple and high-yielding fed-batch process for the production of influenza vaccines. Vaccine. 2009;28:309-16.
[118] Petiot E, Jacob D, Lanthier S, Lohr V, Ansorge S, Kamen AA. Metabolic and kinetic analyses of influenza production in perfusion HEK293 cell culture. BMC Biotechnol. 2011;11:84.
[119] Bock A, Schulze-Horsel J, Schwarzer J, Rapp E, Genzel Y, Reichl U. High-density microcarrier cell cultures for influenza virus production. Biotechnol Prog. 2011;27:241-50.
[120] Mahy BWJ, Kangro HO. Virology Methods Manual: Academic Press Limited; 1996.
[121] Roldao A, Oliveira R, Carrondo MJ, Alves PM. Error assessment in recombinant baculovirus titration: evaluation of different methods. J Virol Methods. 2009;159:69-80.
[122] http://www.who.int/mediacentre/factsheets/fs211/en/. Accessed 08.01.2014
[123] Szucs T. The socio-economic burden of influenza. Journal of Antimicrobial Chemotherapy. 1999;44:11-5.

[124] http://www.who.int/influenza/human_animal_interface/en/. Accessed 05.01.2014
[125] Lamb RA, Krug RM. Orthomyxoviridae: the viruses and their replication. In: Knipe DM, Howley PM, Griffin DE, Lamb RA, Martin MA, Roizman B, et al., editors. Fields Virology. edition 4: Lippincott Williams & Wilkins; 2001. chapter p. 1487-531.
[126] Hilleman MR. Realities and enigmas of human viral influenza: pathogenesis, epidemiology and control. Vaccine. 2002;20:3068-87.
[127] Tong S, Li Y, Rivailler P, Conrardy C, Castillo DA, Chen LM, Recuenco S, Ellison JA, Davis CT, York IA, Turmelle AS, Moran D, Rogers S, Shi M, Tao Y, Weil MR, Tang K, Rowe LA, Sammons S, Xu X, Frace M, Lindblade KA, Cox NJ, Anderson LJ, Rupprecht CE, Donis RO. A distinct lineage of influenza A virus from bats. Proc Natl Acad Sci U S A. 2012;109:4269-74.
[128] Tong S, Zhu X, Li Y, Shi M, Zhang J, Bourgeois M, Yang H, Chen X, Recuenco S, Gomez J, Chen LM, Johnson A, Tao Y, Dreyfus C, Yu W, McBride R, Carney PJ, Gilbert AT, Chang J, Guo Z, Davis CT, Paulson JC, Stevens J, Rupprecht CE, Holmes EC, Wilson IA, Donis RO. New world bats harbor diverse influenza A viruses. PLoS Pathog. 2013;9:e1003657.
[129] Minor PD, Engelhardt OG, Wood JM, Robertson JS, Blayer S, Colegate T, Fabry L, Heldens JG, Kino Y, Kistner O, Kompier R, Makizumi K, Medema J, Mimori S, Ryan D, Schwartz R, Smith JS, Sugawara K, Trusheim H, Tsai TF, Krause R. Current challenges in implementing cell-derived influenza vaccines: implications for production and regulation, July 2007, NIBSC, Potters Bar, UK. Vaccine. 2009;27:2907-13.
[130] Osterholm MT, Kelley NS, Sommer A, Belongia EA. Efficacy and effectiveness of influenza vaccines: a systematic review and meta-analysis. Lancet Infect Dis. 2012;12:36-44.
[131] Beyer WE, Palache AM, de Jong JC, Osterhaus AD. Cold-adapted live influenza vaccine versus inactivated vaccine: systemic vaccine reactions, local and systemic antibody response, and vaccine efficacy. A meta-analysis. Vaccine. 2002;20:1340-53.
[132] Sun K, Ye J, Perez DR, Metzger DW. Seasonal FluMist vaccination induces cross-reactive T cell immunity against H1N1 (2009) influenza and secondary bacterial infections. J Immunol. 2011;186:987-93.
[133] Tosh PK, Boyce TG, Poland GA. Flu myths: dispelling the myths associated with live attenuated influenza vaccine. Mayo Clin Proc. 2008;83:77-84.
[134] Clements ML, Betts RF, Tierney EL, Murphy BR. Resistance of adults to challenge with influenza A wild-type virus after receiving live or inactivated virus vaccine. J Clin Microbiol. 1986;23:73-6.
[135] Maassab HF. Adaptation and growth characteristics of influenza virus at 25°C. Nature. 1967;213:612-4.
[136] Klimov AI, Egorov AY, Gushchina MI, Medvedeva TE, Gamble WC, Rudenko LG, Alexandrova GI, Cox NJ. Genetic stability of cold-adapted A/Leningrad/134/47/57 (H2N2) influenza virus: sequence analysis of live cold-adapted reassortant vaccine strains before and after replication in children. J Gen Virol. 1995;76 (Pt 6):1521-5.
[137] Chan W, Zhou H, Kemble G, Jin H. The cold adapted and temperature sensitive influenza A/Ann Arbor/6/60 virus, the master donor virus for live attenuated influenza vaccines, has multiple defects in replication at the restrictive temperature. Virology. 2008;380:304-11.
[138] Ghendon YZ, Polezhaev FI, Lisovskaya KV, Medvedeva TE, Alexandrova GI, Klimov AI. Recombinant cold-adapted attenuated influenza A vaccines for use in children: molecular genetic analysis of the cold-adapted donor and recombinants. Infect Immun. 1984;44:730-3.
[139] Voeten JT, Kiseleva IV, Glansbeek HL, Basten SM, Drieszen-van der Cruijsen SK, Rudenko LG, van den Bosch H, Heldens JG. Master donor viruses A/Leningrad/134/17/57 (H2N2) and B/USSR/60/69 and derived reassortants used in live attenuated influenza vaccine (LAIV) do not display neurovirulent properties in a mouse model. Arch Virol. 2010;155:1391-9.

[140] Chu C, Lugovtsev V, Golding H, Betenbaugh M, Shiloach J. Conversion of MDCK cell line to suspension culture by transfecting with human siat7e gene and its application for influenza virus production. Proc Natl Acad Sci U S A. 2009;106:14802-7.
[141] Lohr V, Genzel Y, Behrendt I, Scharfenberg K, Reichl U. A new suspension MDCK cell line cultivated in a fully defined medium in stirred-tank and wave bioreactor. Vaccine. 2009.
[142] Doroshenko A, Halperin SA. Trivalent MDCK cell culture-derived influenza vaccine Optaflu (Novartis Vaccines). Expert Rev Vaccines. 2009;8:679-88.
[143] Litwin J. The growth of Vero cells in suspension as cell-aggregates in serum-free media. Cytotechnology. 1992;10:169-74.
[144] Paillet C, Forno G, Kratje R, Etcheverrigaray M. Suspension-Vero cell cultures as a platform for viral vaccine production. Vaccine. 2009.
[145] Rott R, Orlich M, Klenk HD, Wang ML, Skehel JJ, Wiley DC. Studies on the adaptation of influenza viruses to MDCK cells. EMBO J. 1984;3:3329-32.
[146] Seitz C, Isken B, Heynisch B, Rettkowski M, Frensing T, Reichl U. Trypsin promotes efficient influenza vaccine production in MDCK cells by interfering with the antiviral host response. Appl Microbiol Biotechnol. 2012;93:601-11.
[147] Lazarowitz SG, Choppin PW. Enhancement of the infectivity of influenza A and B viruses by proteolytic cleavage of the hemagglutinin polypeptide. Virology. 1975;68:440-54.
[148] Kaverin NV, Webster RG. Impairment of multicycle influenza virus growth in Vero (WHO) cells by loss of trypsin activity. J Virol. 1995;69:2700-3.
[149] Genzel Y, Dietzsch C, Rapp E, Schwarzer J, Reichl U. MDCK and Vero cells for influenza virus vaccine production: a one-to-one comparison. submitted to J Biotechnol. 2009.
[150] Aggarwal K, Jing F, Maranga L, Liu J. Bioprocess optimization for cell culture based influenza vaccine production. Vaccine. 2011;29:3320-8.
[151] Paillet C, Forno G, Soldano N, Kratje R, Etcheverrigaray M. Statistical optimization of influenza H1N1 production from batch cultures of suspension Vero cells (sVero). Vaccine. 2011;29:7212-7.
[152] Genzel Y, König S, Reichl U. Amino acid analysis in mammalian cell culture media containing serum and high glucose concentrations by anion exchange chromatography and integrated pulsed amperometric detection. Anal Biochem. 2004;335:119-25.
[153] Buentemeyer H. Methods for Off-Line Analysis of Nutrients and Products in Mammalian Cell Culture. In: Poertner R, editor. Methods in Biotechnology. edition 2. 24. New York: Humana Press Inc.; 2007. chapter p. 253-68.
[154] Genzel Y, Olmer RM, Schäfer B, Reichl U. Wave microcarrier cultivation of MDCK cells for influenza virus production in serum containing and serum-free media. Vaccine. 2006;24:6074-87.
[155] Lohr V, Haedicke O, Genzel Y, Jordan I, Buentemeyer H, Klamt S, Reichl U. The avian cell line AGE1.CR.pIX charaterized by metabolic flux analysis. Resubmitted to BMC Biotechnology. June 2014.
[156] Janke R, Genzel Y, Wahl A, Reichl U. Rapid and sensitive microplate-based assays for measurement of key metabolic enzyme activities in mammalian cells. Accepted by Analytical Biochemistry. 2009.
[157] Wahl A, Sidorenko Y, Dauner M, Genzel Y, Reichl U. Metabolic flux model for an anchorage-dependent MDCK cell line: characteristic growth phases and minimum substrate consumption flux distribution. Biotechnol Bioeng. 2008;101:135-52.
[158] Niklas J, Schrader E, Sandig V, Noll T, Heinzle E. Quantitative characterization of metabolism and metabolic shifts during growth of the new human cell line AGE1.HN using time resolved metabolic flux analysis. Bioprocess Biosyst Eng. 2011;34:533-45.
[159] Romanova J, Katinger D, Ferko B, Vcelar B, Sereinig S, Kuznetsov O, Stukova M, Erofeeva M, Kiselev O, Katinger H, Egorov A. Live cold-adapted influenza A vaccine produced in Vero cell line. Virus Res. 2004;103:187-93.

[160] Kalbfuss B, Knochlein A, Krober T, Reichl U. Monitoring influenza virus content in vaccine production: precise assays for the quantitation of hemagglutination and neuraminidase activity. Biologicals. 2008;36:145-61.
[161] Haedicke O, Lohr V, Genzel Y, Reichl U, Klamt S. Evaluating Differences of Metabolic Performances: Statistical Methods and Their Application to Animal Cell Cultivations. Submitted to Biotechnology and Bioengineering. 2013.
[162] Rehberg M, Ritter JB, Genzel Y, Flockerzi D, Reichl U. The relation between growth phases, cell volume changes and metabolism of adherent cells during cultivation. J Biotechnol. 2013.
[163] Rothen-Rutishauser B, Kramer SD, Braun A, Gunthert M, Wunderli-Allenspach H. MDCK cell cultures as an epithelial in vitro model: cytoskeleton and tight junctions as indicators for the definition of age-related stages by confocal microscopy. Pharm Res. 1998;15:964-71.
[164] Kiehl TR, Shen D, Khattak SF, Jian Li Z, Sharfstein ST. Observations of cell size dynamics under osmotic stress. Cytometry A. 2011;79:560-9.
[165] Niklas J, Priesnitz C, Rose T, Sandig V, Heinzle E. Metabolism and metabolic burden by alpha1-antitrypsin production in human AGE1.HN cells. Metab Eng. 2013.
[166] Palomares LA, Pedroza JC, Ramirez OT. Cell size as a tool to predict the production of recombinant protein by the insect-cell baculovirus expression system. Biotechnology Letters. 2001;23:359–64.
[167] Zupke C, Stephanopoulos G. Intracellular flux analysis in hybridomas using mass balances and in vitro (13)C nmr. Biotechnol Bioeng. 1995;45:292-303.
[168] Carnicer M, Baumann K, Toplitz I, Sanchez-Ferrando F, Mattanovich D, Ferrer P, Albiol J. Macromolecular and elemental composition analysis and extracellular metabolite balances of Pichia pastoris growing at different oxygen levels. Microb Cell Fact. 2009;8:65.
[169] Xie L, Wang DI. Applications of improved stoichiometric model in medium design and fed-batch cultivation of animal cells in bioreactor. Cytotechnology. 1994;15:17-29.
[170] Gambhir A, Korke R, Lee J, Fu PC, Europa A, Hu WS. Analysis of cellular metabolism of hybridoma cells at distinct physiological states. J Biosci Bioeng. 2003;95:317-27.
[171] Bonarius HP, Hatzimanikatis V, Meesters KP, de Gooijer CD, Schmid G, Tramper J. Metabolic flux analysis of hybridoma cells in different culture media using mass balances. Biotechnol Bioeng. 1996;50:299-318.
[172] Ferrance JP, Goel A, Ataai MM. Utilization of glucose and amino acids in insect cell cultures: Quantifying the metabolic flows within the primary pathways and medium development. Biotechnol Bioeng. 1993;42:697-707.
[173] Altamirano C, Illanes A, Casablancas A, Gamez X, Cairo JJ, Godia C. Analysis of CHO cells metabolic redistribution in a glutamate-based defined medium in continuous culture. Biotechnol Prog. 2001;17:1032-41.
[174] Selvarasu S, Ho YS, Chong WP, Wong NS, Yusufi FN, Lee YY, Yap MG, Lee DY. Combined in silico modeling and metabolomics analysis to characterize fed-batch CHO cell culture. Biotechnol Bioeng. 2012;109:1415-29.
[175] Nadeau I, Sabatie J, Koehl M, Perrier M, Kamen A. Human 293 cell metabolism in low glutamine-supplied culture: interpretation of metabolic changes through metabolic flux analysis. Metab Eng. 2000;2:277-92.
[176] Sheikh K, Forster J, Nielsen LK. Modeling hybridoma cell metabolism using a generic genome-scale metabolic model of Mus musculus. Biotechnol Prog. 2005;21:112-21.
[177] Xie L, Wang DI. Fed-batch cultivation of animal cells using different medium design concepts and feeding strategies. Biotechnol Bioeng. 1994;43:1175-89.
[178] Vriezen N, van Dijken JP. Fluxes and enzyme activities in central metabolism of myeloma cells grown in chemostat culture. Biotechnol Bioeng. 1998;59:28-39.
[179] Schulze-Horsel J. Zellphysiologische Charakterisierung von Zellkulturen in der Influenza-Impfstoffproduktion [PhD thesis]. Magdeburg: Universität Magdeburg; 2011.

[180] Tey BT, Al-Rubeai M. Suppression of apoptosis in perfusion culture of Myeloma NS0 cells enhances cell growth but reduces antibody productivity. Apoptosis. 2004;9:843-52.
[181] Quesney S, Marvel J, Marc A, Gerdil C, Meignier B. Characterization of Vero cell growth and death in bioreactor with serum-containing and serum-free media. Cytotechnology. 2001;35:115-25.
[182] Slivac I, Srcek VG, Radosevic K, Kmetic I, Kniewald Z. Aujeszky's disease virus production in disposable bioreactor. J Biosci. 2006;31:363-8.
[183] Merten OW, Kierulff JV, Castignolles N, Perrin P. Evaluation of the new serum-free medium (MDSS2) for the production of different biologicals: use of various cell lines. Cytotechnology. 1994;14:47-59.
[184] Maranga L, Goochee CF. Metabolism of PER.C6 cells cultivated under fed-batch conditions at low glucose and glutamine levels. Biotechnol Bioeng. 2006;94:139-50.
[185] Shirgaonkar IZ, Lanthier S, Kamen A. Acoustic cell filter: a proven cell retention technology for perfusion of animal cell cultures. Biotechnol Adv. 2004;22:433-44.
[186] Kallel H, Jouini A, Majoul S, Rourou S. Evaluation of various serum and animal protein free media for the production of a veterinary rabies vaccine in BHK-21 cells. J Biotechnol. 2002;95:195-204.
[187] Ozturk SS, Palsson BO. Growth, metabolic, and antibody production kinetics of hybridoma cell culture: 1. Analysis of data from controlled batch reactors. Biotechnol Prog. 1991;7:471-80.
[188] Schneider M, Marison IW, von Stockar U. The importance of ammonia in mammalian cell culture. J Biotechnol. 1996;46:161-85.
[189] Slivac I, Blajic V, Radosevic K, Kniewald Z, Gaurina Srcek V. Influence of different ammonium, lactate and glutamine concentrations on CCO cell growth. Cytotechnology. 2010;62:585-94.
[190] O'Donnell-Tormey J, Nathan CF, Lanks K, DeBoer CJ, de la Harpe J. Secretion of pyruvate. An antioxidant defense of mammalian cells. J Exp Med. 1987;165:500-14.
[191] Miwa H, Fujii J, Kanno H, Taniguchi N, Aozasa K. Pyruvate secreted by human lymphoid cell lines protects cells from hydrogen peroxide mediated cell death. Free Radic Res. 2000;33:45-56.
[192] Siegwart P, Cote J, Male K, Luong JH, Perrier M, Kamen A. Adaptive control at low glucose concentration of HEK-293 cell serum-free cultures. Biotechnol Prog. 1999;15:608-16.
[193] Acosta ML, Sanchez A, Garcia F, Contreras A, Molina E. Analysis of kinetic, stoichiometry and regulation of glucose and glutamine metabolism in hybridoma batch cultures using logistic equations. Cytotechnology. 2007;54:189-200.
[194] Nagashima H, Watari A, Shinoda Y, Okamoto H, Takuma S. Application of a quality by design approach to the cell culture process of monoclonal antibody production, resulting in the establishment of a design space. J Pharm Sci. 2013;102:4274-83.
[195] Kirdar AO, Chen G, Weidner J, Rathore AS. Application of near-infrared (NIR) spectroscopy for screening of raw materials used in the cell culture medium for the production of a recombinant therapeutic protein. Biotechnol Prog. 2010;26:527-31.
[196] Arriaga EA. Determining biological noise via single cell analysis. Anal Bioanal Chem. 2009;393:73-80.
[197] Elowitz MB, Levine AJ, Siggia ED, Swain PS. Stochastic gene expression in a single cell. Science. 2002;297:1183-6.
[198] Le H, Kabbur S, Pollastrini L, Sun Z, Mills K, Johnson K, Karypis G, Hu WS. Multivariate analysis of cell culture bioprocess data--lactate consumption as process indicator. J Biotechnol. 2012;162:210-23.
[199] Goudar CT, Biener R, Konstantinov KB, Piret JM. Error propagation from prime variables into specific rates and metabolic fluxes for mammalian cells in perfusion culture. Biotechnol Prog. 2009;25:986-98.
[200] Priesnitz C, Niklas J, Rose T, Sandig V, Heinzle E. Metabolic flux rearrangement in the amino acid metabolism reduces ammonia stress in the alpha1-antitrypsin producing human AGE1.HN cell line. Metab Eng. 2012;14:128-37.

[201] Nyberg GB, Balcarcel RR, Follstad BD, Stephanopoulos G, Wang DI. Metabolism of peptide amino acids by Chinese hamster ovary cells grown in a complex medium. Biotechnol Bioeng. 1999;62:324-35.
[202] Fitzner K, Heckinger E. Sample size calculation and power analysis: a quick review. Diabetes Educ. 2010;36:701-7.
[203] Niklas J, Priesnitz C, Rose T, Sandig V, Heinzle E. Primary metabolism in the new human cell line AGE1.HN at various substrate levels: increased metabolic efficiency and alpha1-antitrypsin production at reduced pyruvate load. Appl Microbiol Biotechnol. 2012;93:1637-50.
[204] Sidorenko Y, Wahl A, Dauner M, Genzel Y, Reichl U. Comparison of metabolic flux distributions for MDCK cell growth in glutamine- and pyruvate-containing media. Biotechnol Prog. 2008;24:311-20.
[205] Glacken MW, Fleischaker RJ, Sinskey AJ. Reduction of waste product excretion via nutrient control: Possible strategies for maximizing product and cell yields on serum in cultures of mammalian cells. Biotechnol Bioeng. 1986;28:1376-89.
[206] Cruz HJ, Ferreira AS, Freitas CM, Moreira JL, Carrondo MJ. Metabolic responses to different glucose and glutamine levels in baby hamster kidney cell culture. Appl Microbiol Biotechnol. 1999;51:579-85.
[207] DeBerardinis RJ, Mancuso A, Daikhin E, Nissim I, Yudkoff M, Wehrli S, Thompson CB. Beyond aerobic glycolysis: transformed cells can engage in glutamine metabolism that exceeds the requirement for protein and nucleotide synthesis. Proc Natl Acad Sci USA. 2007;104:19345-50.
[208] Xie L, Wang DI. Material balance studies on animal cell metabolism using a stoichiometrically based reaction network. Biotechnol Bioeng. 1996;52:579-90.
[209] Sellick CA, Croxford AS, Maqsood AR, Stephens G, Westerhoff HV, Goodacre R, Dickson AJ. Metabolite profiling of recombinant CHO cells: designing tailored feeding regimes that enhance recombinant antibody production. Biotechnol Bioeng. 2011;108:3025-31.
[210] Fitzpatrick L, Jenkins HA, Butler M. Glucose and glutamine metabolism of a murine B-lymphocyte hybridoma grown in batch culture. Appl Biochem Biotechnol. 1993;43:93-116.
[211] Neermann J, Wagner R. Comparative analysis of glucose and glutamine metabolism in transformed mammalian cell lines, insect and primary liver cells. J Cell Physiol. 1996;166:152-69.
[212] Janke R, Genzel Y, Handel N, Wahl A, Reichl U. Metabolic adaptation of MDCK cells to different growth conditions: effects on catalytic activities of central metabolic enzymes. Biotechnol Bioeng. 2011;108:2691-704.
[213] Xie L, Wang DI. Energy metabolism and ATP balance in animal cell cultivation using a stoichiometrically based reaction network. Biotechnol Bioeng. 1996;52:591-601.
[214] Zamorano F, Wouwer AV, Bastin G. A detailed metabolic flux analysis of an underdetermined network of CHO cells. J Biotechnol. 2010;150:497-508.
[215] Blechert AK. Durchflusszytometrische Untersuchungen zur Replikationsdynamik von MVA in AGE1.CR.pIX-Zellen [Master thesis]. Braunschweig: TU Braunschweig; 2011.
[216] Djeljadini S. Durchflusszytometrische Untersuchungen zur Replikationsdynamik von MVA in AGE1.CR-Zellen [Bachelor thesis]. Villingen-Schwenningen: Hochschule Furtwangen; 2010.
[217] Melville MW, Tan SL, Wambach M, Song J, Morimoto RI, Katze MG. The cellular inhibitor of the PKR protein kinase, P58(IPK), is an influenza virus-activated co-chaperone that modulates heat shock protein 70 activity. J Biol Chem. 1999;274:3797-803.
[218] Carroll MW, Moss B. Poxviruses as expression vectors. Curr Opin Biotechnol. 1997;8:573-7.
[219] Jordan I, Northoff S, Thiele M, Hartmann S, Horn D, Howing K, Bernhardt H, Oehmke S, von Horsten H, Rebeski D, Hinrichsen L, Zelnik V, Mueller W, Sandig V. A

chemically defined production process for highly attenuated poxviruses. Biologicals. 2011;39:50-8.
[220] Schulze-Horsel J, Schulze M, Agalaridis G, Genzel Y, Reichl U. Infection dynamics and virus-induced apoptosis in cell culture-based influenza vaccine production-Flow cytometry and mathematical modeling. Vaccine. 2009;27:2712-22.
[221] Schweneker M, Lukassen S, Spath M, Wolferstatter M, Babel E, Brinkmann K, Wielert U, Chaplin P, Suter M, Hausmann J. The vaccinia virus O1 protein is required for sustained activation of extracellular signal-regulated kinase 1/2 and promotes viral virulence. J Virol. 2012;86:2323-36.
[222] Guerra S, Lopez-Fernandez LA, Pascual-Montano A, Najera JL, Zaballos A, Esteban M. Host response to the attenuated poxvirus vector NYVAC: upregulation of apoptotic genes and NF-kappaB-responsive genes in infected HeLa cells. J Virol. 2006;80:985-98.
[223] Chahroudi A, Garber DA, Reeves P, Liu L, Kalman D, Feinberg MB. Differences and similarities in viral life cycle progression and host cell physiology after infection of human dendritic cells with modified vaccinia virus Ankara and vaccinia virus. J Virol. 2006;80:8469-81.
[224] Archana M, Bastian, Yogesh TL, Kumaraswamy KL. Various methods available for detection of apoptotic cells--a review. Indian J Cancer. 2013;50:274-83.
[225] Peschel B, Frentzel S, Laske T, Genzel Y, Reichl U. Comparison of influenza virus yields and apoptosis-induction in an adherent and a suspension MDCK cell line. Vaccine. 2013;31:5693-9.
[226] Jordan I, Horn D, John K, Sandig V. A genotype of modified vaccinia Ankara (MVA) that facilitates replication in suspension cultures in chemically defined medium. Viruses. 2013;5:321-39.
[227] Djeljadini S. "Hochzelldichteeffekt" bei der Produktion von Influenzaviren in AGE1.CR Zellen [Student project]. Villingen-Schwenningen: Hochschule Furtwangen; 2010.
[228] Mahr S. Produktion attenuierter Influenzaviren in AGE1.CR-Zellen [Bachelor thesis]. Villingen-Schwenningen: Hochschule Furtwangen; 2010.
[229] Vazquez-Ramirez D. Development of a flow cytometry-based assay for the quantification of active viral particles [Master thesis]. Hamburg: TU Hamburg-Harburg; 2012.
[230] Roedig JV, Rapp E, Hoper D, Genzel Y, Reichl U. Impact of host cell line adaptation on quasispecies composition and glycosylation of influenza A virus hemagglutinin. PLoS One. 2011;6:e27989.
[231] Murakami S, Horimoto T, Ito M, Takano R, Katsura H, Shimojima M, Kawaoka Y. Enhanced growth of influenza vaccine seed viruses in vero cells mediated by broadening the optimal pH range for virus membrane fusion. J Virol. 2012;86:1405-10.
[232] Galloway SE, Reed ML, Russell CJ, Steinhauer DA. Influenza HA subtypes demonstrate divergent phenotypes for cleavage activation and pH of fusion: implications for host range and adaptation. PLoS Pathog. 2013;9:e1003151.
[233] Marcus PI, Ngunjiri JM, Sekellick MJ, Wang L, Lee CW. In vitro analysis of virus particle subpopulations in candidate live-attenuated influenza vaccines distinguishes effective from ineffective vaccines. J Virol. 2010;84:10974-81.
[234] Hung JJ, Chung CS, Chang W. Molecular chaperone Hsp90 is important for vaccinia virus growth in cells. J Virol. 2002;76:1379-90.
[235] Niewiarowska J, D'Halluin JC, Belin MT. Adenovirus capsid proteins interact with HSP70 proteins after penetration in human or rodent cells. Exp Cell Res. 1992;201:408-16.
[236] Feng SZ, Jiao PR, Qi WB, Fan HY, Liao M. Development and strategies of cell-culture technology for influenza vaccine. Appl Microbiol Biotechnol. 2011;89:893-902.
[237] Lohr V, Rath A, Jordan I, Sandig V, Genzel Y, Reichl U. Avian Designer Cells AGE1.CR as Candidates for MVA and Influenza Vaccine Production. In: Jenkins N, Barron N, Alves P, editors. Proceedings of the 21st Annual Meeting of the European Society for Animal Cell Technology (ESACT). Dublin, Ireland: SpringerLink; 2009. p. 615-31.

[238] Prevention and Control of Influenza: Recommendations of the Advisory Committee on Immunization Practices (ACIP).
http://www.cdc.gov/mmwr/preview/mmwrhtml/rr5408a1.htm. Accessed 27.01.2014
[239] Solorzano A, Ye J, Perez DR. Alternative live-attenuated influenza vaccines based on modifications in the polymerase genes protect against epidemic and pandemic flu. J Virol. 2010;84:4587-96.
[240] Chen Z, Aspelund A, Kemble G, Jin H. Molecular studies of temperature-sensitive replication of the cold-adapted B/Ann Arbor/1/66, the master donor virus for live attenuated influenza FluMist vaccines. Virology. 2008;380:354-62.
[241] Katinger H, Egorov A, Ferko B, Romanova J, Katinger D. Live attenuated influenza vaccine. [Patent]. 2009. PCT/EP01/11087.
[242] Kiseleva I, Su Q, Toner TJ, Szymkowiak C, Kwan WS, Rudenko L, Shaw AR, Youil R. Cell-based assay for the determination of temperature sensitive and cold adapted phenotypes of influenza viruses. J Virol Methods. 2004;116:71-8.
[243] Steinhauer DA. Role of hemagglutinin cleavage for the pathogenicity of influenza virus. Virology. 1999;258:1-20.
[244] Moskvichyov BV, Komanov EV, Ivanova GP. Study of Trypsin Thermodenaturation Process. Enzyme and Microbial Technology. 1986;8:498-502.
[245] He Y, Xu K, Keiner B, Zhou J, Czudai V, Li T, Chen Z, Liu J, Klenk HD, Shu YL, Sun B. Influenza A virus replication induces cell cycle arrest in G0/G1 phase. J Virol. 2010;84:12832-40.
[246] Genzel Y, Vogel T, Buck J, Behrendt I, Ramirez DV, Schiedner G, Jordan I, Reichl U. High cell density cultivations by alternating tangential flow (ATF) perfusion for influenza A virus production using suspension cells. Vaccine. 2014.
[247] George M, Farooq M, Dang T, Cortes B, Liu J, Maranga L. Production of cell culture (MDCK) derived live attenuated influenza vaccine (LAIV) in a fully disposable platform process. Biotechnol Bioeng. 2010;106:906-17.
[248] Liu J, Shi X, Schwartz R, Kemble G. Use of MDCK cells for production of live attenuated influenza vaccine. Vaccine. 2009.
[249] Hussain AI, Cordeiro M, Sevilla E, Liu J. Comparison of egg and high yielding MDCK cell-derived live attenuated influenza virus for commercial production of trivalent influenza vaccine: in vitro cell susceptibility and influenza virus replication kinetics in permissive and semi-permissive cells. Vaccine. 2010;28:3848-55.
[250] Stiefel P, Schmidt FI, Dorig P, Behr P, Zambelli T, Vorholt JA, Mercer J. Cooperative vaccinia infection demonstrated at the single-cell level using FluidFM. Nano Lett. 2012;12:4219-27.

Appendix

A.1 Materials and devices used in this project

Materials and devices that have been used only occasionally and that are already listed in one of the SOPs are not listed here again (e.g. chemicals needed for *in vitro* enzyme assays).

List of equipment

Device	Supplier
Autoclaves: Varioklav 75S, 135S	Thermo Scientific
Balances PG5002-S/PG12001-S/AG204/PR9620-3	Mettler-Toledo/Sartorius Stedim Biotech
Bioprofile 100Plus Analyzer	Nova Biomedical
Centrifuges: Biofuge Fresco/Strato/Nano/Primo Avanti J20 XP	Hereaus Instruments Beckman Coulter
Clean bench Herasafe/Safe 2020	Hereaus Instruments/Thermo Scientific
Confocal Laser Scanning Microscope Axiovert 100M with LSM510	Carl Zeiss AG
Culture tube rotator SC1	Stuart Scientific Bibby
Electronic single and multichannel pipettes Research (300 µL, 1200 µL)	Eppendorf
Epics XL Flow cytometer	Beckman Coulter
Flasks (glassware)	Schott
DasGip bioreactor system + equipment	DasGip AG
Digital camera	Nikon
HPLC system DX600	Dionex
Incubator Heracell T6060	Hereaus Instruments
Incubator Multitron 2 (for shaker flasks)	Infors HT
Magnetic stirrer VarioMag/IKE RET basic	Thermo Fisher Scientific/IKA
Micro pipettes Research (1, 10, 100, 200, 1000, 2500, 5000 µL)	Eppendorf AG
Microscopes: Axioskop 2/Axiovert 25/Axiovert S100	Carl Zeiss AG
Microtiter plate reader Infinite M200 NanoQuant	Tecan
Multichannel pipettes Research (10, 100, 300 µL)	Eppendorf AG
Multipette plus	Eppendorf AG
pH meter Inolab	WTW
pH probe DasGip bioreactor: 405-DPAS-SC-K85/200	Mettler-Toledo
Pipettor Pipetus	Hirschmann
pO_2 probes DasGip bioreactor: Fermprobe InPro 6100/120/T/N	Broadley James Corp. Mettler-Toledo
Sonication water bath	Merck eurolab
Thermoblock QBT/neoBlock 1	Grant/neolab
Ultrapure Water Purification System Milli-Q	Millipore

ViCell XR Cell Viability Analyzer	Beckman Coulter
Vortexer Reax Top	Heidolph
Water bath HB4 basic	IKA
Wave bioreactor system BioWave 20 SPS	Wave Biotech AG

List of consumables

Material/chemical	Purchased from
Bags for Wave bioreactor: Cultibag RM 2 L basic	Sartorius Stedim Biotech
Combitips for Multipette (5, 10 mL)	Eppendorf AG
Cryotubes PP (2 mL)	Greiner bio-one
Falcon tubes (15, 50 mL)	Greiner bio-one
Microtiter plates, 6well format	Greiner bio-one
Microtiter plates, 96well format, flat bottom	Greiner bio-one
Microtiter plates, 96well format, U bottom	Greiner bio-one
Micropipette tips (10, 200, 1000, 2500 µL)	Brand/Eppendorf AG
Pipettes Cellstar 1, 2, 5, 10, 25, 50 mL	Greiner bio-one
Reaction tubes (0.5, 1.5, 2.2 mL)	Greiner bio-one
Shaker flasks (125, 250 mL)	Corning
Sterile filter: Minisart 0.20 µm, Minisart 0.45 µm	Sartorius Stedim Biotech
Sterile membrane filter 0.22 µm	Nalgene nunc
Syringes Omnifix (5, 10, 20, 50 mL)	B.Braun
T-flasks: Cellstar 25, 75, 175 cm^2	Greiner bio-one/TPP

List of chemicals and materials

Material/chemical	Purchased or obtained from
Acetic acid	Roth, #3738.5
Acetone	Roth, #CP40.4
Aminoethylcarbozole	Sigma, #A5754
L-alanine	Sigma, #A7469
Bovine serum albumin	Sigma, #A3912
N,N-Dimethylformamide	Sigma, #D4551
Dimethylsulfoxide	Roth, # A994.1
Ethanol	Roth, #T868.2
Fetal bovine serum	Sigma, #F7524
Gentamicin	Invitrogen, #11130-036
L-glutamine	Sigma, #G8540
GuavaNexin Reagent	Millipore, #4500-0450
Hydrochloric acid	Roth, #4625.2
Hydrogen peroxide 30% with inhibitor	Sigma, #216763
Hydrogen Peroxide Assay	BioCat, #K265-200-BU
Long-R3 IGF (insulin-like growth factor)	Sigma, #91590C
Methanol	Roth, #4627.6
Paraformaldehyde	Sigma, #P6148
Potassium chloride	Merck, #1.04936.1000
Potassium hydrogen phosphate	Roth, #6875.1

Propidium iodide	Sigma, #P4170
RNAse A Type IIIA from bovine PA	Sigma, #R5125
Sodium acetate	Sigma, #S8750
Sodium carbonate	Roth, #8563.1
Sodium chloride	Roth, #9265.1
Sodium dihydrogenphosphate	Roth, #K300.2
Sodium hydrogenphosphate	Roth, #T877.1
Sodium hydroxide	Merck, #1.06482.1000
Sodium pyruvate	Sigma, #P2256
Staurosporine	Sigma, # S5921
Triton X-100	Sigma #T9284
Trypan blue	Merck, #1.11732.0025
Trypsin, porcine	Sigma, #T7409
Uric Acid Assay Kit QuantiChromTM	BioAssay Systems, #DIUA
Antibodies	
anti-influenza A/PR/8/34 H1N1 (HA serum sheep)	NIBSC, #03/242
anti-influenza A/Brisbane/59/2007 (HA serum sheep)	NIBSC, #08/112
anti-influenza B/Yamagata/16/88 (HA serum sheep)	NIBSC, #07/356
anti-rabbit IgG (H+L), HRP conjugate	Promega, #W4011 Lots: 21357802, 29303403, 22927703, 26824903, 29303401, 24947004
anti-sheep IgG from donkey, AlexaFluor 488 conjugate	Invitrogen, #A-11015
anti-vaccinia virus, from rabbit, polyclonal	Quartett, #1220100717 Lots: 294612, 272415, 273420, 294907
Culture media	
Adenovirus Expression Medium (AEM)	Fisher Scientific, #12582011 Lots: 396146, 449731
CD-U2	obtained from ProBioGen: Lot 1314T Biochrom, #F9121 Lots: T103412-0344, T103410-0698, T103410-2704, T103411-3177
CD-VP4	obtained from ProBioGen: Lots 1, 3, 1313T Biochrom, #F9127 Lots: 0295w, 0645A
DMEM high glucose (4.5 g/L)	PAA, #E15-079
GMEM	Gibco, #22100-093
HyQ SFM4 MegaVir™	HyClone, #SH30552 Lots: ASL30771, ASF29636, ATL32501
Cell lines	
AGE1.CR	ProBioGen AG
AGE1.CR.pIX	ProBioGen AG
MDCK, Madine Darby Canine Kidney, epithelial	ECACC, Cat. No. 84121903
Vero, African Green Monkey Kidney, epithelial	WHO seed, ECACC, Cat. No. 88020401

A.2 Parameters used for STR cultivations

Configuration:

Two-sided pH control by addition of CO_2 and base; temperature control; pO2 control cascade by gas flow, XO_2 (O_2 concentration in added gas) and rpm

Parameter	Set-points	Settings
Temperature	37 °C	----
DO	50%	P=0.05; T_i=600s; Cascade: minimum 0%; maximum 100%; Start cascade at XO_2=50%; factor 0.08, FlowLimit=4 sL/h; start rpm cascade at XO_2=75%, factor 0.02, limit=150 rpm
pH	7.0–7.2*	P=25; T_i=3600 s; base strength: AcBS=0.5; Deadband=0.05; MaxFlow=40 mL/h
Agitation	120 rpm	Pwr.SP=80%; DirCCW

*depending on status of cell culture, i.e. growth or infection phase

A.3 ViCell protocol “Entenzellen” and validation of the method

ViCell settings for cell counting, program “Entenzellen”:

Parameter	Settings
Minimum diameter [µm]	8
Maximum diameter [µm]	30
number of images	100
aspirate cycles	3
trypan blue mixing cycles	3
cell brightness [%]	90
cell sharpness	100
viable cell spot brightness [%]	85
viable cell spot area [%]	3
Minimum circularity	0.5
Decluster degree	high

Validation of counting CR or CR.pIX cells with this program (analysis with template “temp_vali_AR_v1.8.xlsx”):
Test system: ViCell XR, counting method „Entenzellen"; cells: CR.pIX from shaker pre-culture (150 mL), passage 95; medium: CD-U2, Charge 1314-T, from 28.01.2010

Approach

1. Upper concentration determined (n=3) from pre-culture, average: 9.17×10^6 cells/mL; defined as upper limit
2. Dilution scheme calculated (for 2 mL per concentration, independent dilutions, equidistant steps)

theoretical concentration [cells/mL]	dilution	nominal concentration by dilution of pre-culture [cells/mL]
1.00E+07	1 : 1	9.17E+06
7.50E+06	1 : 1.33	6.89E+06
5.00E+06	1 : 2	4.59E+06
2.50E+06	1 : 4	2.29E+06
1.00E+06	1 : 10	9.17E+05
7.50E+05	1 : 13.33	6.88E+05
5.00E+05	1 : 20	4.59E+05
2.50E+05	1 : 40	2.29E+05

3. First measurement series: measurement of each concentration, n=3 (in randomized order)
4. Second measurement series: measurement of upper and lower limits n=8 (upper limit: 9.17×10^6 cells/mL nominal concentration, lower limit: 0.23×10^6 cells/mL nominal concentration)
5. Analysis with validation template

Results

n=3 measurement (e.g. for reactor experiments)		n=1 measurement (e.g. for shaker flask experiments)	
standard deviation of the method, Sx0	0.008×10^6 cells/mL	standard deviation of the method, Sx0	0.024×10^6 cells/mL
relative standard deviation of the method, Vx0	**2.48 %**	relative standard deviation of the method, Vx0	**5.00 %**
coefficient of determination, R^2	0.9997	coefficient of determination, R^2	0.9985
limit of detection, LOD	0.028×10^6 cells/mL	limit of detection, LOD	0.080×10^6 cells/mL
limit of quantification, LOQ	0.084×10^6 cells/mL	limit of quantification, LOQ	0.241×10^6 cells/mL

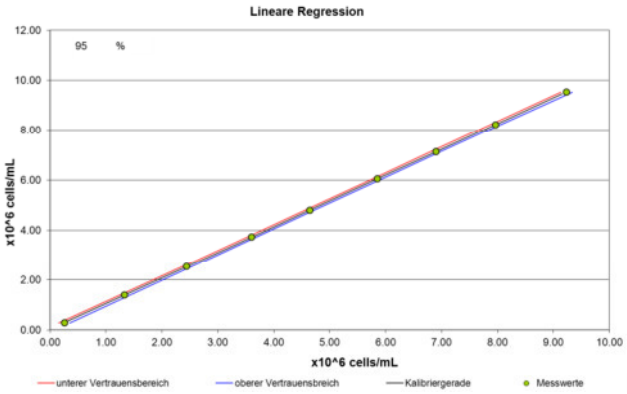

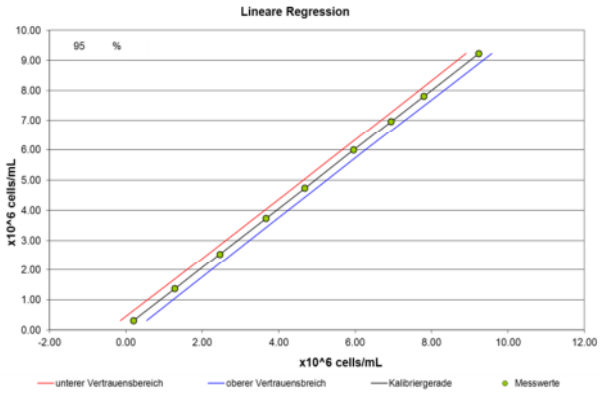

Variances were determined to be inhomogeneous over the concentration range and thus, the relative standard deviation of the method will be given as method error. Overall, error was 5.0% in maximum for precision of this cell counting method.

A.4 SOP cell cycle analysis

Document: A/03 version 1.0
Date: 07.01.2013
Author: Verena Lohr

Cell cycle analysis by propidium iodide staining of cellular DNA

1. Introduction

Eukaryotic cells pass through different cell cycle phases during growth. These phases can be distinguished either by certain marker proteins (e.g. cyclines) whose abundances differ during these phases or by measuring the DNA content which also differs with the cell cycle phases.

The following scheme shows the cell cycle phases and the corresponding DNA content (in genome copies per cell).

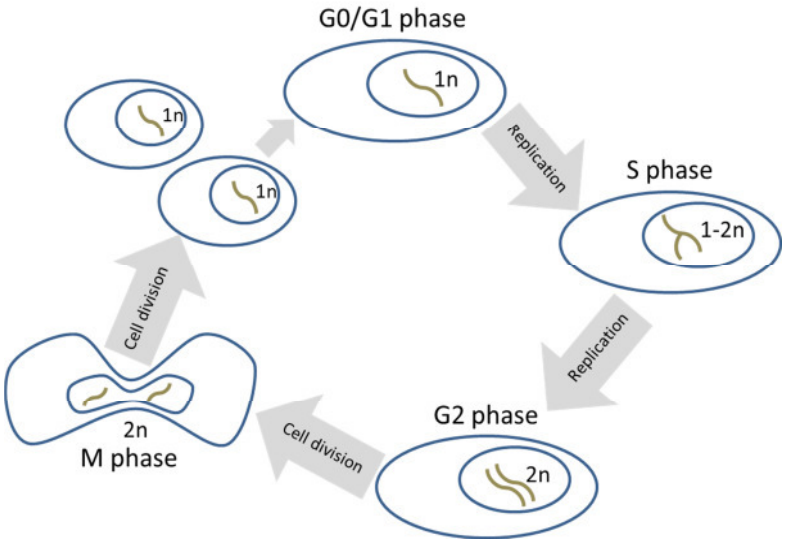

To evaluate the DNA content of a cell, the most common method is to stain the cells with propidium iodide (PI). If the plasma membranes of the cells are permeabilized before staining, PI can pass the membranes and intercalate between the nucleotides of the DNA. As it also binds to RNA, a treatment of the sample with RNase is necessary. Intercalation of PI happens with little sequence preference and with a stoichiometry of one dye per 4-5 base pairs of DNA. Due to PI's attribute to emit red light (562-588 nm) when excited with light of 488 nm wavelength, a flow cytometric or fluorescence microscopy analysis of the stained cells can be done.

2. Materials

- Cells in suspension
- ViCellXR for cell counting
- Reaction tubes (1 mL)
- Centrifuge with swing-out rotor for small tubes
- 1x trypsin solution (stored in N1.06 4 °C, prepared as described in worksheet V/02.1)
- Fetal calf serum or culture medium
- Vortex
- Rotator or tumbler for reaction tubes
- Non-sterile 15 mL tubes (Falcon)
- Micropipettes (100 µL, 1000 µL und 5000 µL), disposable tips, non-sterile
- Non-sterile phosphate buffered saline, (PBS, produced as described in SOP M/01)
- 70 % ethanol as 4.5 mL aliquots in 15 mL tubes, stored at -20 °C
- Propidium iodide stock solution 1 mg/mL in MilliQ H_2O, stored at 4 °C (Sigma-Aldrich, Nr. P4170)
- RNase A (Sigma-Aldrich, Nr. R5125, 2 mg/mL), boiled for 5 min at 80 °C to remove DNase, aliquoted in 1 mL and stored at -20 °C
- Triton X100 (Sigma-Aldrich, Nr. T9284)
- Flow cytometer tubes (Sarstedt, Nr. 55.1578, 5 mL, PP)
- Flow cytometer with 488 nm laser and a 560-590 nm bandpass filter (e.g. Epics XL from BeckmanCoulter)
- Software to evaluate flow cytometer data (Expo32 software from BeckmanCoulter or FlowJo software

3. Method

3.1 Sample preparation

Count cells from infected or non-infected cell culture with the ViCellXR device. Pipet the volume needed for $1.25x10^6$ cells in a reaction tube. Best, prepare two samples as technical replicates. Centrifuge the samples for 10 min at 500xg at 4 °C. (These centrifugation conditions are evaluated to be optimal for AGE1.CR cells, if your cells need different conditions use those; thereby make sure that all cells including dead cells are pelleted). Discard the supernatant and re-suspend the pellets in 500 µL 1x trypsin (that means pipet the pellet carefully up and down to homogenize the suspension). Incubate for 5 min at 37 °C in an incubator before stopping the reaction by adding 500 µL of serum or culture medium (again: pipet to homogenize, this is important in order to avoid having too many aggregates!). For fixation, pipet the sample slowly, drop by drop (!), into the 70 % ethanol tubes. It is crucial that the ethanol is still cold (take the tubes only immediately before using them out of the -20 °C freezer) and that the tubes are vortexed while pipetting the sample slowly into it. Do not use the highest vortex speed, but only 2/3 of the maximum speed. Label each tube appropriately and store them at -20 °C in an explosion-safe freezer. Samples should be

stored there for at least 6 h before analysis and can be stored up to one year. The best way is to fix and collect all samples from one experiment and stain and analyze them later on in one procedure.

3.2 Staining procedure

Prepare the staining solution freshly and store it at 4 °C in the dark until you need it.
Staining solution (sufficient for 10 samples):

- 9000 µL PBS
- 1000 µL RNase A
- 200 µL PI stock solution
- 10 µL Triton X-100

Centrifuge the tubes containing the cells in ethanol at 700xg for 10 min at 4 °C in a swing rotor. It is important that the samples in ethanol do not warm up in this time! Quickly discard the supernatant into a special bottle (make sure that it is labeled appropriate and take care that this ethanol-containing waste is discarded correctly) and fill each tube with 5 mL PBS. Vortex or pipet carefully to re-suspend the pellet, then centrifuge again. Discard the supernatant and add 1 mL of fresh staining solution. Homogenize by pipetting and in doing so transfer the reaction mix into reaction tubes (1.5 mL). Label all tubes and put them onto a rotator or tumbler in dark (!) for 45-60 min at 37 °C. Now the samples are ready for either analysis with a fluorescence microscope or for measurement with a flow cytometer.

3.3 Measurement & Analysis

Before working with the flow cytometer please read the instruction and (!) ask an experienced person to show you the most important things.

Start and purge the cytometer as described in the instruction (N0.11). Open the protocol “DNA_content_pIX.pro” which is saved in the account “admin”. Transfer the samples into cytometer tubes. If you know that large aggregates are still in the sample, use a filter cap to remove these aggregates. This really is important as the diameter of the flow cell is around 50 µm, which means that an aggregate of more than 4 cells can already clog the cytometer stream! Vortex each tube before putting it into the cytometer sample device. Measurement starts automatically and all necessary plots also appear automatically. It is important to measure at ”low” flow speed and that the FL3 signal is amplified in a linear way!

If necessary, adjust the “single cells” gate: it should look as in this example:

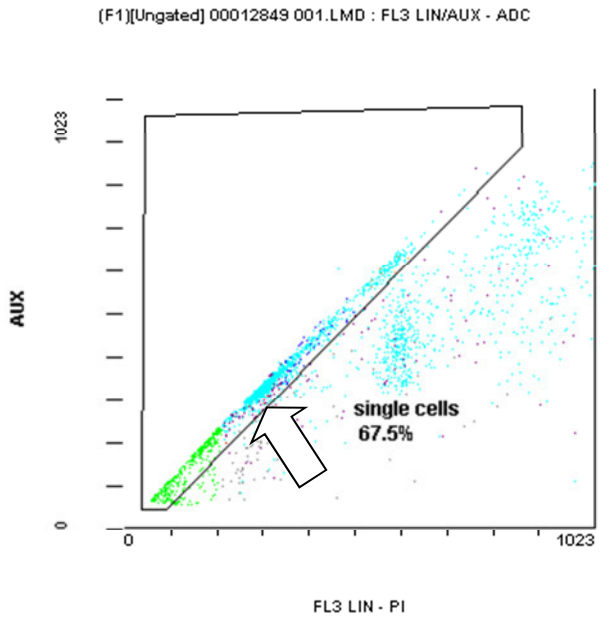

The cells which are lying beneath the gating area are aggregates (mostly “double” cells) and need to be separated from single cells as they also would be counted as a double set of chromosomes and so would distort the result. Each measurement should be documented in the “FC_data_collection.xls” file (second PC, desktop) with the protocol used and the Lmd-file which was generated. Measure all samples, purge and shut down the cytometer as described in the instruction.

For analysis, best use the FlowJo software. It might be necessary to adjust the gates for “apo or sub-G0G1”, “G0/G1”, “S” and “G2/M”. For one experiment, gates should be set to the same parameters for all samples. Best would be to take the first sample (0 h sample or an equivalent) as a template for all gate settings.

Typical histograms look like these examples:

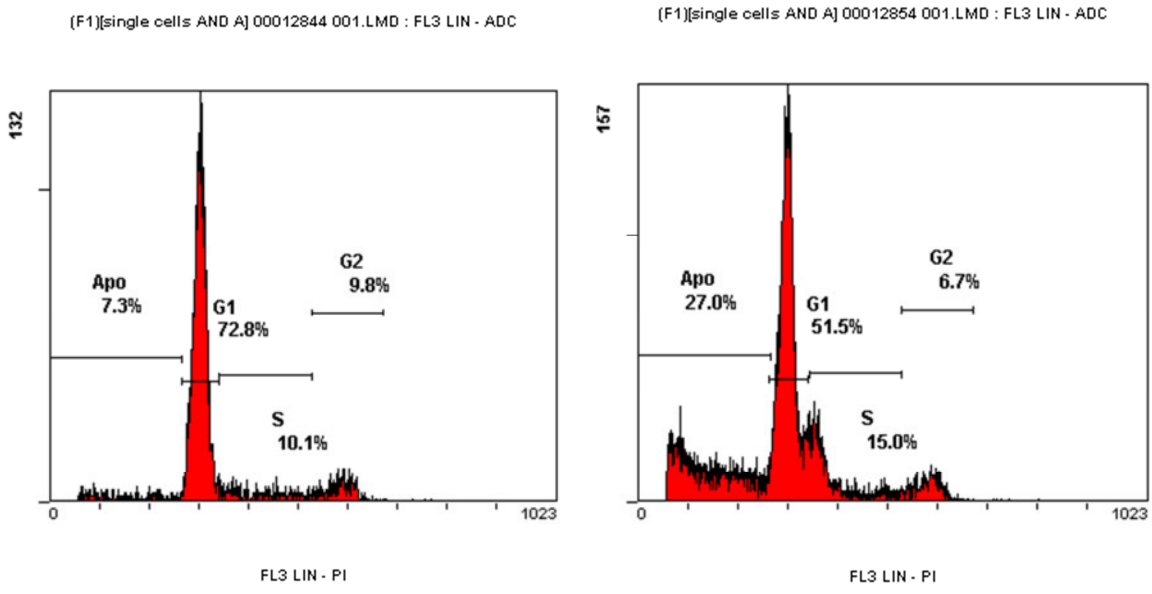

4.1.1 Points to consider

The FlowJo software also includes a cell cycle analysis tool which fits the areas G0/G1, S and G2/M using a model. Different models can be chosen. However, this only works if the cell cycle distribution does not “vary” from a very typical distribution (e.g. the left picture shown above). After virus infection, this fitting is sometimes inappropriate. Also, the sub-G0/G1 population cannot be fitted with these tools.

The apo/sub-G0G1 peak cannot be assigned definitely to apoptotic cells as all cells or even cell debris that have the same size as a typical cell and show a low PI signal are gated into this population. To really get an impression about the amount or fraction of apoptotic cells in the cell population, a specialized apoptosis assay is necessary!

Also, cell cycle distributions after infection with dsDNA viruses as MVA might lead to misinterpretations as cells with a lot of intracellular virions will have an increased DNA content. On the other hand, cells that were in G2/M phase, but now are damaged or apoptotic will first occur as S phase cells and only later as G0/G1 or sub-G0/G1 phase cells!

A.5 SOP apoptosis measurement

Document: A/04 version 1.0
Date: 18.02.2013
Author: Verena Lohr

Measurement of apoptotic and necrotic cells by GuavaNexin staining

1. Introduction

Eucaryotic cells are known to undergo apoptosis and necrosis during cell proliferation and in particular after infection with virus. The apoptotic progress is controlled by several caspases (early caspases: 8,9,10,2; late caspases 3,6,7) and comprises loss of membrane integrity, disaggregation of genomic DNA and blebbing of cells that finally leads to the formation of apoptotic bodies. The TUNEL assay that detects DNA defragmentation and is used in the BPT group cannot be used for cells that have been infected with DNA viruses (e.g. Modified Vaccinia Virus Ankara, MVA) as false-positive signals occur due to viral DNA. Therefore, a different principle needs to be applied when detecting apoptotic cells infected with such viruses. One event of early apoptosis that can be detected is the flip of the phopshoplipid molecule phosphatidylserine (PS) to the outer membrane. After this event, the membrane loses its integrity and becomes permeable. Necrotic or late apoptotic cells can therefore be stained with bigger molecules that enter the cell like trypan blue or 7-Aminoactinomycin (7-AAD). Figure 1 shows how the cell looks like in the different stages.

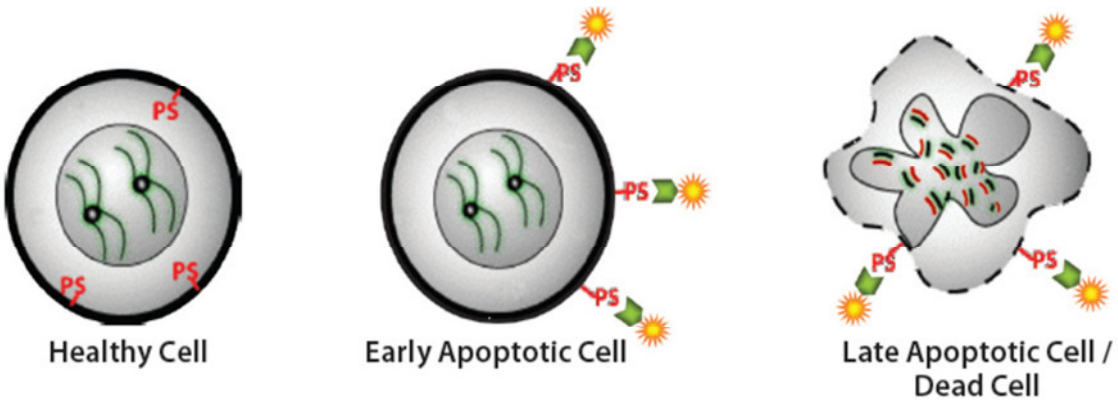

Source: Production Bulletin GuavaNexin Assay, Millipore

The protein annexin V binds to PS so that cells with PS at its outer membrane can be detected. The GuavaNexin reagent contains annexin V which is coupled with phycoerythrin (PE) leading to a red signal in the flow cytometer when annexin V is bound to a cell. To detect only early apoptotic cells it is important that the cells are not permeabilized before staining which means that no fixation in ethanol or paraformaldehyde should be done. A second marker in the GuavaNexin reagent is the molecule 7-AAD that serves (as trypan blue) as a marker for disintegrated cells that are in the stage of late apoptosis or necrosis. Overall, using the GuavaNexin Reagent, four

cell populations can be distinguished in the flow cytometer:

- Non-apoptotic (AnnV-, 7-AAD-)
- Early apoptotic (AnnV+, 7-AAD-)
- Late apoptotic/necrotic (AnnV+, 7-AAD+)
- Mostly debris (AnnV-, 7-AAD+)

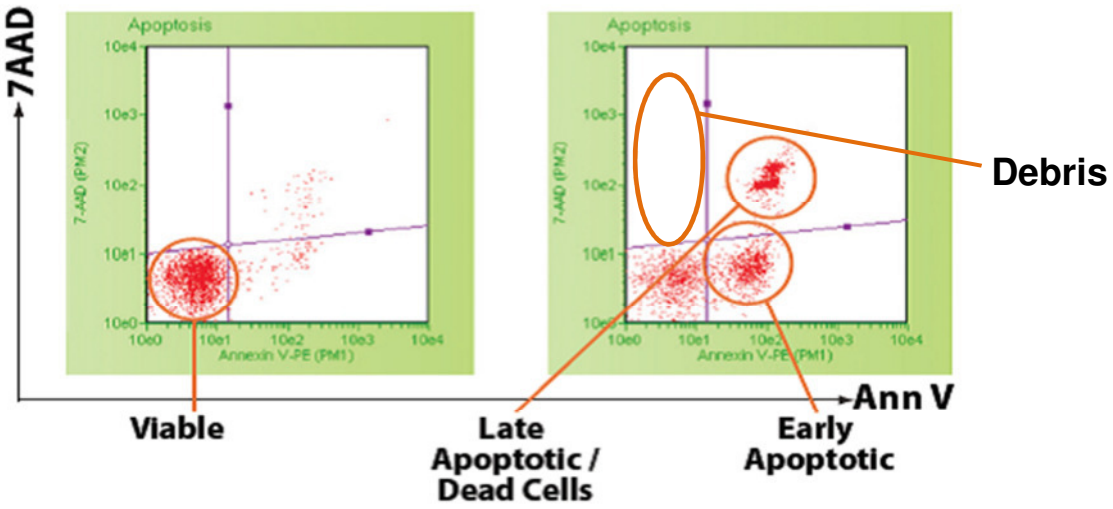

Source: Production Bulletin GuavaNexin Assay, Millipore

The 7-AAD signal (red) is detected in the flow cytometer in the FL4 channel (emission at 650-660 nm), whereas the PE signal is detected in the FL2 channel (emission at 570-580 nm).

2. Materials

- Cells in suspension
- ViCellXR for cell counting
- Reaction tubes (1 mL)
- Micropipettes (10 µL, 100 µL, 1000 µL) and disposable tips, non-sterile
- Non-sterile phosphate buffered saline, (PBS, produced as described in SOP M/01)
- 30 % (w/w) BSA solution (dissolved bovine serum albumine (BSA, Sigma, #A3912) in PBS; e.g. for 10 mL solution dissolve 3 mg of BSA in 10 mL PBS)
- GuavaNexin Reagent (Millipore, #4500-0450)
- Flow cytometer tubes (Sarstedt, Nr. 55.1578, 5 mL, PP)
- Flow cytometer with 488 nm laser and bandpass filters to detect green, red and orange fluorescence (e.g. Epics XL from BeckmanCoulter)
- Software to evaluate flow cytometer data (Expo32 software from BeckmanCoulter or FlowJo software)

3. Method

3.1 Sample preparation and staining procedure

Count cells from infected or non-infected cell culture with the ViCellXR device. Pipet the volume needed for $0.5x10^6$ cells in a reaction tube or directly into a cytometer tube. Prepare two tubes per sample with one as a "non-stained negative control". Add BSA solution, PBS and GuavaNexin to the sample as shown in the following table:

	Cell suspension	30 % BSA solution	GuavaNexin Reagent	PBS
Non-stained control	$0.5x10^6$ cells	10 % v/v of cell suspension	-	100 µL + volume nee to fill up to 500 µl
Stained sample	$0.5x10^6$ cells	10 % v/v of cell suspension	100 µL	volume needed to fil to 500 µL

Example: If your cell suspension has a **total** cell concentration of $4x10^6$ cells/mL, pipet 125 µL into a tube, add 13 µL of 30 % BSA solution, add 100 µL GuavaNexin Reagent (or 100 µL PBS for the control) and 262 µL PBS.

Do not calculate based on the viable cell concentration as you are also interested in dead cells! Only flip the mix softly as you don't want to induce apoptosis! Then, incubate for 20 min at room temperature in the dark (!!). The samples cannot be stored and need to be analyzed in the flow cytometer after exactly 20 min! Due to critical incubation and measurement time, do only stain and handle 10 samples in maximum at once.

3.2 Measurement & Analysis

Before working with the flow cytometer please read the instruction and (!) ask an experienced person to show you the most important things.

Start and purge the cytometer as described in the instruction (N0.11). For measuring AGE1.CR or AGE1.CR.pIX cells, open the protocol "compens_gfp_annexin.pro" which is saved in the account "admin". If you stained the samples in 1 mL tubes, transfer the samples into cytometer tubes. Don't use a filter cap to remove aggregates unless it is not avoidable. If large aggregates are present, better add trypsin to the sample before incubation. Also, do not vortex the tubes. Put each tube into the cytometer sample device - measurement will start automatically and all necessary plots also appear automatically. Each measurement should be documented appropriately with the protocol used and the Lmd-file that was generated. Measure all samples, purge and shut down the cytometer as described in the instruction.

For analysis, best use the FlowJo software. First, set a "monomeres" or "single cells" gate to exclude aggregates from analysis. This can be done e.g. by plotting the AUX signal vs FS signal. Monomeres should appear at the bisecting line like in this example:

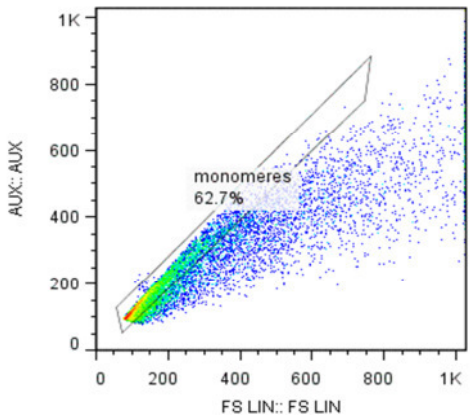

The cells which are lying beneath the gated area (with same FS signal intensity, but lower AUX values) are aggregates (mostly “double” cells) and need to be separated from single cells as they distort the result. Adjust the gates for “viable”, “early apoptotic”, “late apoptotic” and “debris”. For one experiment, gates should be set to the same parameters for all samples with the non-stained controls that were prepared and analyzed in parallel.

Typical plots could look like these examples (left: non-stained control; right: stained sample):

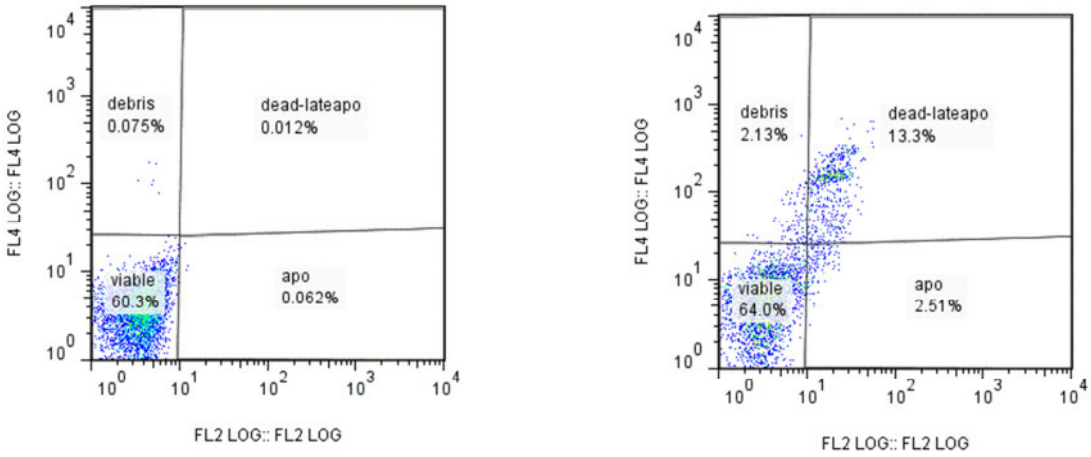

If the cells have been infected with e.g. MVA-egfp (containing and translating an egfp gene), a third fluorescent (the EGFP protein) is present besides PE and 7-AAD. The emission spectrum of EGFP overlaps with the PE spectrum and thus compensation needs to be done with the following controls:

- Non-stained non-infected
- Non-stained infected
- Stained non-infected
- Stained infected

With these controls, the percentage of false-positive FL2 emission due to EGFP fluorescence can be quantified with the help of the Epics XL compensation matrix. For the analysis of MVAegfp-infected CR or CR.pIX cells stained with GuavaNexin, this compensation has been done and checked several times and the resulting compensation matrix is saved in the protocol “compens_gfp_annexin.pro”. The following plots show how this can influence the distribution.

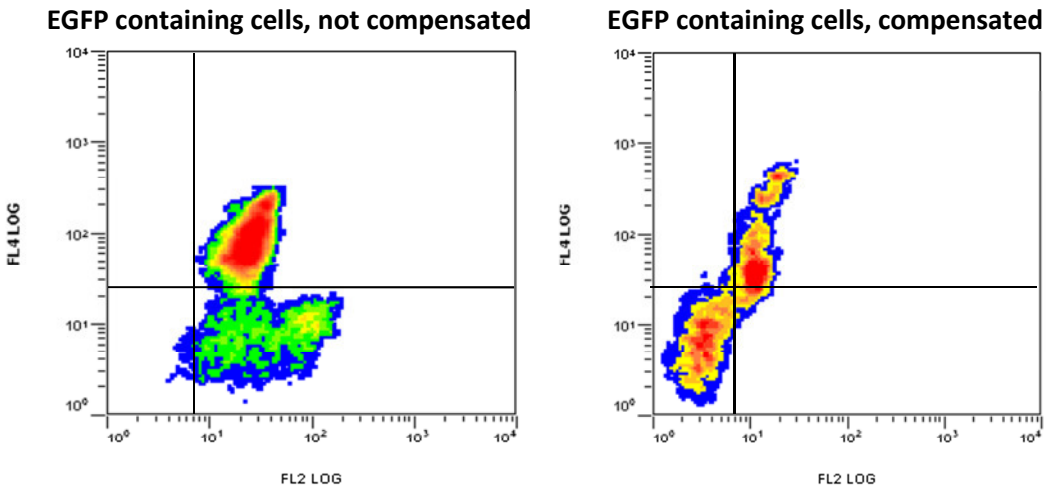

If other cells or another virus or another third fluorescent is used, the compensation has to be done again.

4.1.1 Points to consider

When setting up the assay for a new cell line, it can be helpful to perform pre-tests using apoptosis inducer molecules like staurosporine or valinomycin. With this, sensitivity of the cells towards the GuavaNexin Reagent can be tested and flow cytometer and gate settings can be checked. Also, mock infections should always be measured when setting up a new assay with infected cells.

Remember that late apoptotic and necrotic cells cannot be distinguished from each other, but appear in the same gate!

A.6 List of SOPs used in this work

SOPs from the Bioprocess Engineering group of the MPI Magdeburg that were used in this work, but have not been written for this project, are listed here.

Title	SOP number and version	Date
Metabolitbestimmung aus Zellkultur	A/02 version 1.0	07.04.2010
Pyruvate dehydrogenase (PDH) (EC 1.2.4.1)	E/06 version 1.0	07.10.2009
Pyruvate carboxylase (PC) (EC 6.4.1.1)	E/07 version 1.0	08.10.2009
Glutamine synthetase (GS) (EC 6.3.1.2)	E/08 version 1.0	08.10.2009
Glutaminase (GLNase) (EC 3.5.1.2)	E/29 version 1.0	21.11.2009
Bestimmung des $TCID_{50}$ für MVA (Modified Vaccinia Virus Ankara)	V/09 version 1.1	04.10.2011
Hemagglutination assay (HA assay)	V/05 version 2.2	20.01.2011
$TCID_{50}$ Assay	V/08 version 2.1 english	09.01.2013

A.7 Reactions included in reaction network model for metabolic flux analysis

	Uptake rates
r1, Glc	$Glc \rightarrow Glc_{cyt}$
r2, Pyr	$Pyr + 0.33\ ATP_{cyt} \rightarrow Pyr_{cyt}$
r3, O2	$O_2 \rightarrow O_{2,cyt}$
r4, Gln	$Gln + 0.33\ ATP_{cyt} \rightarrow Gln_{cyt}$
r5, Glu	$Glu + ATP_{cyt} \rightarrow Glu_{cyt}$
r6, Ala	$Ala + 0.33\ ATP_{cyt} \rightarrow Ala_{cyt}$
r7, Asp	$Asp + ATP_{cyt} \rightarrow Asp_{cyt}$
r8, Arg	$Arg + 0.33\ ATP_{cyt} \rightarrow Arg_{cyt}$
r9, Asn	$Asn + 0.33\ ATP_{cyt} \rightarrow Asn_{cyt}$
r10, Cys	$Cys + 0.33\ ATP_{cyt} \rightarrow Cys_{cyt}$
r11, Gly	$Gly + 0.33\ ATP_{cyt} \rightarrow Gly_{cyt}$
r12, His	$His + 0.33\ ATP_{cyt} \rightarrow His_{cyt}$
r13, Ile	$Ile + 0.33\ ATP_{cyt} \rightarrow Ile_{cyt}$
r14, Leu	$Leu + 0.33\ ATP_{cyt} \rightarrow Leu_{cyt}$
r15, Lys	$Lys + 0.33\ ATP_{cyt} \rightarrow Lys_{cyt}$
r16, Val	$Val + 0.33\ ATP_{cyt} \rightarrow Val_{cyt}$
r17, Met	$Met + 0.33\ ATP_{cyt} \rightarrow Met_{cyt}$
r18, Phe	$Phe + 0.33\ ATP_{cyt} \rightarrow Phe_{cyt}$
r19, Pro	$Pro + 0.33\ ATP_{cyt} \rightarrow Pro_{cyt}$
r20, Ser	$Ser + 0.33\ ATP_{cyt} \rightarrow Ser_{cyt}$
r21, Thr	$Thr + 0.33\ ATP_{cyt} \rightarrow Thr_{cyt}$
r22, Trp	$Trp + 0.33\ ATP_{cyt} \rightarrow Trp_{cyt}$
r23, Tyr	$Tyr + 0.33\ ATP_{cyt} \rightarrow Tyr_{cyt}$
	Glycolysis
r24, G6P	$Glc_{cyt} + ATP_{cyt} \rightarrow G6P_{cyt}$
r25, F6P	$G6P_{cyt} \leftrightarrow F6P_{cyt}$
r26, FBP	$F6P_{cyt} + ATP_{cyt} \leftrightarrow FBP_{cyt}$
r27, DHAP	$FBP_{cyt} \leftrightarrow GAP_{cyt} + DHAP_{cyt}$
r28, GAP	$DHAP_{cyt} \leftrightarrow GAP_{cyt}$
r29, PG	$GAP_{cyt} \leftrightarrow NADH_{cyt} + ATP_{cyt} + PG_{cyt}$
r30, PEP	$PG_{cyt} \leftrightarrow PEP_{cyt}$
r31, PEP_Pyr	$PEP_{cyt} \rightarrow Pyr_{cyt} + ATP_{cyt}$
r32, Pyr_Lac	$Pyr_{cyt} + NADH_{cyt} \leftrightarrow Lac_{cyt}$
r33, PDH	$Pyr_{mit} + CoA_{mit} \rightarrow AcCoA_{mit} + CO_{2,mit} + NADH_{mit}$
	Pentose phosphate pathway
r34, R5P	$G6P_{cyt} \rightarrow R5P_{cyt} + CO_{2,cyt} + 2\ NADPH_{cyt}$
	TCA cycle
r35, OAA	$Mal_{cyt} \leftrightarrow OAA_{cyt} + NADH_{cyt}$
r36, Cit	$AcCoA_{cyt} + OAA_{cyt} \rightarrow Cit_{cyt} + CoA_{cyt}$
r37, Fum_Mal	$Fum_{cyt} \leftrightarrow Mal_{cyt}$
r38, Cit_{mito}	$AcCoA_{mit} + OAA_{mit} \rightarrow Cit_{mit} + CoA_{mit}$
r39, OAA_{mito}	$Mal_{mit} \leftrightarrow OAA_{mit} + NADH_{mit}$

r40, Fum_Mal$_{mito}$	$Fum_{mit} \leftrightarrow Mal_{mit}$
r41, SCoA$_{mito}$	$aKG_{mit} + CoA_{mit} \rightarrow SuccCoA_{mit} + CO_{2,mit} + NADH_{mit}$
r42, Fum$_{mito}$	$SuccCoA_{mit} \leftrightarrow Fum_{mit} + CoA_{mit} + ATP_{mit} + FADH_{2,mit}$
r43, aKG$_{mito}$	$Cit_{mit} \leftrightarrow aKG_{mit} + CO_{2,mit} + NADH_{mit}$
	Anaplerosis
r44, Ana_PyrI	$Mal_{cyt} \rightarrow Pyr_{cyt} + CO_{2,cyt} + NADPH_{cyt}$
r45, Ana_PyrII	$Mal_{mit} \leftrightarrow Pyr_{mit} + CO_{2,mit} + NADPH_{mit}$
r46, PC	$Pyr_{mit} + CO_{2,mit} + ATP_{mit} \rightarrow OAA_{mit}$
	Amino acid catabolism
r47, GDH	$Glu_{mit} \leftrightarrow aKG_{mit} + Amm_{mit} + NADPH_{mit}$
r48, GS	$Gln_{cyt} \leftrightarrow Glu_{cyt} + Amm_{cyt} + ATP_{cyt}$
r49, Ala$_{cat}$	$Ala_{cyt} + aKG_{cyt} \leftrightarrow Pyr_{cyt} + Glu_{cyt}$
r50, Asn_Asp	$Asn_{cyt} \leftrightarrow Asp_{cyt} + Amm_{cyt}$
r51, His$_{cat}$	$His_{cyt} \rightarrow Glu_{cyt} + 2\ Amm_{cyt} + CO_{2,cyt}$
r52, Ile$_{cat}$	$Ile_{cyt} + aKG_{cyt} + 2\ CoA_{mit} + ATP_{mit} \rightarrow SuccCoA_{mit} + AcCoA_{mit} + Glu_{cyt} + NADH_{mit} + FADH_{2,mit}$
r53, Leu$_{cat}$	$Leu_{cyt} + aKG_{cyt} + 3\ CoA_{mit} + 2\ ATP_{mit} \rightarrow 3\ AcCoA_{mit} + Glu_{cyt} + NADH_{mit} + FADH_{2,mit}$
r54, Lys$_{cat}$	$Lys_{cyt} + 2\ aKG_{cyt} + 2\ CoA_{mit} + NADPH_{cyt} \rightarrow 2\ AcCoA_{mit} + 2\ Glu_{cyt} + 2\ CO_{2,mit} + 2\ NADH_{cyt} + 2\ NADH_{mit} + FADH_{2,mit}$
r55, Met$_{cat}$	$Met_{cyt} + Ser_{cyt} + CoA_{mit} + 3\ ATP_{cyt} + ATP_{mit} \rightarrow Cys_{cyt} + SuccCoA_{mit} + Amm_{cyt} + NADH_{mit} + CO_{2,cyt}$
r56, Phe$_{cat}$	$Phe_{cyt} + O_{2,cyt} + NADPH_{cyt} \rightarrow Tyr_{cyt}$
r57, Pro$_{cat}$	$Pro_{cyt} \leftrightarrow Glu_{cyt} + 2\ NADH_{cyt}$
r58, Thr$_{cat}$	$Thr_{cyt} \rightarrow Pyr_{mit} + Amm_{mit} + CO_{2,mit} + NADH_{cyt} + NADH_{mit} + FADH_{2,mit}$
r59, Trp$_{cat}$	$Trp_{cyt} + 2\ CoA_{mit} + 3\ O_{2,cyt} + NADPH_{cyt} \rightarrow Ala_{cyt} + 2\ AcCoA_{mit} + Amm_{cyt} + 2\ CO_{2,mit} + 2\ CO_{2,cyt} + NADH_{cyt} + 2\ NADH_{mit} + FADH_{2,mit}$
r60, Val$_{cat}$	$Val_{cyt} + aKG_{cyt} + CoA_{mit} + ATP_{mit} \rightarrow SuccCoA_{mit} + Glu_{cyt} + CO_{2,cyt} + 3\ NADH_{mit} + FADH_{2,mit}$
r61, Tyr$_{cat}$	$Tyr_{cyt} + aKG_{cyt} + 2\ CoA_{cyt} + 2\ O_{2,cyt} \rightarrow Fum_{cyt} + 2\ AcCoA_{cyt} + Glu_{cyt} + CO_{2,cyt}$
r62, Ser$_{cat}$	$Ser_{cyt} \leftrightarrow Pyr_{cyt} + Amm_{cyt}$
r63, Cys$_{cat}$	$Cys_{cyt} + aKG_{cyt} + O_{2,cyt} \rightarrow Pyr_{cyt} + Glu_{cyt}$
r64, Asp$_{cat}$	$Asp_{cyt} + aKG_{mit} \leftrightarrow Glu_{cyt} + OAA_{mit}$
r65, Arg$_{cat}$	$Arg_{cyt} + aKG_{cyt} \rightarrow 2\ Glu_{cyt} + Urea_{cyt} + NADH_{cyt}$
	MTHF & uric acid synthesis
r66, MTHF_I	$Ser_{cyt} + THF_{cyt} \rightarrow Gly_{cyt} + MTHF_{cyt}$
r67, MTHF_II	$Gly_{cyt} + THF_{cyt} \rightarrow NADH_{cyt} + CO_{2,cyt} + Amm_{cyt} + MTHF_{cyt}$
r68, UricAcid	$Asp_{cyt} + 2\ Gln_{cyt} + Gly_{cyt} + 2\ MTHF_{cyt} + 7\ ATP_{cyt} + CO_{2,cyt} \rightarrow UricAcid_{cyt} + Fum_{cyt} + 2\ Glu_{cyt} + 2\ THF_{cyt}$
	Lipid synthesis
r69, CH$_{Lip}$	$18\ AcCoA_{cyt} + 18\ ATP_{cyt} + 11\ O_{2,cyt} + 27\ NADPH_{cyt} \rightarrow CH + 18\ CoA_{cyt} + 9\ CO_{2,cyt}$
r70, PC$_{Lip}$	$GAP_{cyt} + Ser_{cyt} + 27.6\ ATP_{cyt} + 17.6\ AcCoA_{cyt} + 4\ MTHF_{cyt} + 2\ NADH_{cyt} + 31.2\ NADPH_{cyt} \rightarrow PC + 17.6\ CoA_{cyt} + 4\ THF_{cyt}$
r71, PE$_{Lip}$	$GAP_{cyt} + Ser_{cyt} + 18.6\ ATP_{cyt} + 17.6\ AcCoA_{cyt} + MTHF_{cyt} + 2\ NADH_{cyt} + 31.2\ NADPH_{cyt} \rightarrow PE + 17.6\ CoA_{cyt} + THF_{cyt}$
r72, PS$_{Lip}$	$GAP_{cyt} + Ser_{cyt} + 18.6\ ATP_{cyt} + 17.6\ AcCoA_{cyt} + 2\ MTHF_{cyt} + 2\ NADH_{cyt} + 31.2\ NADPH_{cyt} \rightarrow PS + 17.6\ CoA_{cyt} + 2\ THF_{cyt}$
r73, PGL$_{Lip}$	$2\ GAP_{cyt} + 17.6\ ATP_{cyt} + 17.6\ AcCoA_{cyt} + 4\ NADH_{cyt} + 31.2\ NADPH_{cyt} \rightarrow PGL + 17.6\ CoA_{cyt}$
r74, PI$_{Lip}$	$GAP_{cyt} + G6P_{cyt} + 17.6\ ATP_{cyt} + 17.6\ AcCoA_{cyt} + 2\ NADH_{cyt} + 31.2\ NADPH_{cyt} \rightarrow PI + 17.6\ CoA_{cyt}$

r75, SM_{Lip}	2 Ser_{cyt} + 27.8 ATP_{cyt} + 16.8 $AcCoA_{cyt}$ + 3 $MTHF_{cyt}$ + 2 $NADH_{cyt}$ + 29.6 $NADPH_{cyt}$ → SM + 16.8 CoA_{cyt} + 3 THF_{cyt}
r76, DPG_{Lip}	3 GAP_{cyt} + 35.2 ATP_{cyt} + 35.2 $AcCoA_{cyt}$ + 6 $NADH_{cyt}$ + 62.4 $NADPH_{cyt}$ → DPG + 35.2 CoA_{cyt}
	Release rates
r77, ATP_{main}	ATP_{cyt} → maintenance
r78, Lac_{out}	Lac_{cyt} → Lac
r79, Ala_{out}	Ala_{cyt} → Ala
r80, $UricAcid_{out}$	Uric $acid_{cyt}$ → Uric acid
r81, $Urea_{out}$	$Urea_{cyt}$ → Urea
r82, Amm_{out}	Amm_{cyt} → Amm
r83, $CO_{2\ out}$	$CO_{2,cyt}$ → CO_2
r84, Pyr_{out}	Pyr_{cyt} → Pyr
	Transport reactions, oxidative phosphorylation
r85, $NADH_{cyt,trans}$	$NADH_{cyt}$ ↔ $NADH_{mit}$
r86, ATP_{trans}	ATP_{cyt} ↔ ATP_{mitt}
r87, $CO_{2\ trans}$	$CO_{2,cyt}$ ↔ $CO_{2,mit}$
r88, MAL_{trans}	Mal_{cyt} + Cit_{mit} ↔ Mal_{mit} + Cit_{cyt}
r89, Glu_{trans}	Glu_{cyt} ↔ Glu_{mit}
r90, Pyr_{trans}	Pyr_{cyt} ↔ Pyr_{mit}
r91, aKG_{trans}	aKG_{cyt} ↔ aKG_{mit}
r92, Amm_{trans}	Amm_{cyt} ↔ Amm_{mit}
r93, $FADH_{ox}$	$O_{2,cyt}$ + 2 $FADH_{2,mit}$ → 3 ATP_{mit}
r94, $NADH_{mit,trans}$	$NADH_{mit}$ ↔ $NADPH_{mit}$
r95, $NADH_{ox}$	$O_{2,cyt}$ + 2 $NADH_{mit}$ → 5 ATP_{mit}
r96, $NADH_{cyt,trans}$	$NADH_{cyt}$ ↔ $NADPH_{cyt}$
	Synthesis of macromolecules and biomass
97, μ	0.552 proteins + 0.263 carbohydrates + 0.131 lipids + 0.023 DNA + 0.031 RNA → biomass

Proteins [1g] = 955.79 Asp_{cyt} + 1344.29 Ala_{cyt} + 543.16 Gln_{cyt} + + 817.99 Glu_{cyt} + 1024.72 Arg_{cyt} + 362.10 Asn_{cyt} + 19.61 Cys_{cyt} + 913.16 Gly_{cyt} + 271.58 His_{cyt} + 240.54 Ile_{cyt} + 588.41 Leu_{cyt} + 724.21 Lys_{cyt} + 191.97 Val_{cyt} + 114.57 Met_{cyt} + 201.91 Phe_{cyt} + 205.97 Pro_{cyt} + 247.44 Ser_{cyt} + 202.07 Thr_{cyt} + 21.17 Trp_{cyt} + 61.87 Tyr_{cyt} + 24046.3 ATP_{cyt}

Lipids [1g] = 181 CH + 661.4 PC + 250.3 PE + 90.9 PI + 24.9 PS + 12.6 PGL + 81.4 SM + 26.8 DPG

DNA [1g] = 3009 $R5P_{cyt}$ + 3912 Asp_{cyt} + 5717 Gln_{cyt} + -2106 $NADH_{cyt}$ + 1505 Gly_{cyt} + 22569 ATP_{cyt} + 903 $NADH_{mit}$ + -2407 Mal_{cyt} + 903 $NADPH_{cyt}$ + -5717 Glu_{cyt} + 5417 $MTHF_{cyt}$ + -5417 THF_{cyt}

RNA [1g] = 3020 $R5P_{cyt}$ + 3606 ATP_{cyt} + 6316 Gln_{cyt} + 293 $O_{2,cyt}$ + -2435 $NADH_{cyt}$ + 1477 Gly_{cyt} + 22614 ATP_{cyt} + 586 $NADH_{mit}$ + -2069 Mal_{cyt} + -2954 $NADPH_{cyt}$ + -6316 Glu_{cyt} + 4431 $MTHF_{cyt}$ + -4431 THF_{cyt}

Carbohydrates [1g] = 6172.8 $G6P_{cyt}$ + 21605 ATP_{cyt}

A.8 Information about strain MVAegfp

Excerpts from "Formblatt GA", filed for registration of studies with MVAegfp at the MPI Magdeburg

2.1 Zweck und Zielsetzung

Das Modifizierte Vacciniavirus Ankara (MVA) ist ein attenuiertes Vacciniavirus, das aufgrund seiner immunstimulierenden Eigenschaften als Pocken- und Vektorimpfstoff verwendet werden kann. Daher ist die Untersuchung der Vermehrung von MVA interessant, vor allem in potentiellen Produktionszelllinien. Die Analytik mit einem fluoreszenzmarkierten Virus erleichtert den Nachweis des Virus in der Wirtszelle. Für diese Untersuchungen soll ein rekombinantes MVA verwendet werden, welches das Markerprotein GFP trägt, wessen Gensequenz mittels homologer Rekombination unter Kontrolle des Vacciniavirus Promoters PmH5 in die Deletion Site III des MVA-Genoms inseriert wurde (MVA-GFP).

GFP
GFP steht fuer Green Fluorescent Protein, welches aus der Qualle *Aequorea victoria* isoliert wurde und seitdem häufig als Markerprotein verwendet wird (Shimomura, O. et al. (1962); J Cell Comp Physiol 59:223-239).

2.2 Ursprung des MVA-GFP

Die Zielgensequenz von GFP wurde unter Kontrolle des Vacciniavirus-spezifischen Promoters PmH5 in das MVA-Transferplasmid pIII-PmH5-gfp (Sutter & Moss PNAS 1992, Staib Biotechniques 2000, Hornemann J Virol. 2003) eingesetzt, mit dessen Hilfe eine Insertion der GFP-Zielgensequenz in das MVA-Genom erfolgte. Das Plasmid enthält die MVA-Gensequenzen Flank III-1 und Flank III-2, welche die Insertion des Zielgens in die Stelle der Deletion III im MVA-Genom (Meyer J Gen Virol 1991) ermöglicht.
Das Markergen wurde mit Hilfe des generierten Plasmids (s. o.) durch homologe Rekombination im MVA-Genom inseriert. Dazu wurden Hühnerembryofibroblasten (HEF) oder Hamsternieren-Zellen (BHK-21) mit der Plasmid-DNA transfiziert und gleichzeitig mit nicht-rekombinantem MVA infiziert. Durch Sichtung der GFP-Expression im Fluoreszenzmikroskop konnten rekombinante MVA, die das GFP-Zielgen stabil in ihr Genom integriert haben, in Zellkulturpassagen auf HEF klonal isoliert werden. Die so gewonnenen rekombinanten MVA wurden auf HEF amplifiziert und einer molekularbiologischen Qualitätskontrolle unterzogen (Test auf Expression des Zielgens und genetische Stabilität). Eine Kultur des in HEF generierten MVA-GFP, bereitgestellt durch das Institut für Infektionsmedizin und Zoonosen an der Ludwig-Maximimilians-Universtät München soll genutzt werden, um die geplanten Arbeiten am Max-Planck-Institut in Magdeburg durchzuführen.

Zur Konstruktion der MVA-Vektorplasmide wurden Escherichia coli Stämme, wie K12 und Derivate, verwendet, die die Kriterien für die Risikogruppe 1 erfüllen (Liste risikobewerteter Spender- und Empfängerorganismen für gentechnische Arbeiten (BVL 78/2009/4) der ZKBS).

MVA ist ein hoch attenuiertes, replikationsdefizientes Vacciniavirus, welches in die Risikogruppe 1 eingestuft wurde (Liste risikobewerteter Spender- und Empfängerorganismen für gentechnische Arbeiten (BVL 78/2009/4) der ZKBS).

Dies gilt auch für rekombinante MVA, die Reportergene bzw. Strukturgene enthalten, die die Vermehrungsfähigkeit von MVA in vom Menschen stammenden Zellen nicht wiederherstellen (Stellungnahme der ZKBS vom Juni 2002 Az. 6790-10-74).

Die Gensequenz von GFP wurde aus dem käuflich erwerbbaren Plasmid pEGFP präpariert (Fa. Clontech, Heidelberg, Germany). Bei GFP handelt es sich um ein Fluoreszenzprotein, das als inertes Markierungsprotein bei unterschiedlichsten Organismen hervorragend charakterisiert ist. Es kann daher mit großer Sicherheit davon ausgegangen werden, dass GFP keinen Einfluss auf die Vermehrungsfähigkeit von MVA haben wird.

A.9 SOP infection status measurement

Document: A/05 version 1.0
Date: 14.04.2014
Author: Verena Lohr

Flow cytometric measurement of cells infected with MVAegfp

1. Introduction

Modified Vaccinia Virus Ankara (MVA) is a large dsDNA virus suitable to carry a considerable amount of foreign antigens in its genome. Commonly, the site of insertion is Deletion Site III, one of the six large parts that are not existent in MVA compared to its ancestor vaccinia virus. However, also for research with MVA recombinant strains are often produced using marker genes such as GFP. When MVA then infects a cell and transcription and translation of the viral genome starts, the marker gene is translated as well. As MVA replicates in the cytoplasm of the cell, the produced protein then usually accumulates in the cytoplasm (schematically shown in Figure 1). Thus, infected cells will show elevated marker protein content in the cytoplasm, whereas uninfected cells do not.

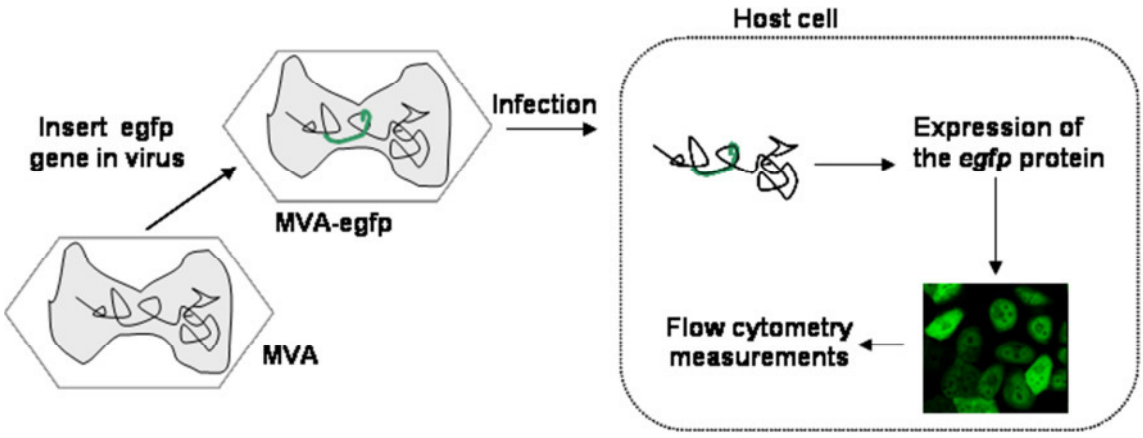

Figure 1: Schematic representation of egfp expression in a recombinant MVA strain that can be used to follow the infection status in an infected cell population.

With this, by detection of intracellular protein, infected and uninfected cells can be distinguished and thus, one can get information about the infection status of a cell population. In case the marker protein is a fluorophor, e.g. GFP, this can be done by flow cytometric analysis. To prevent diffusion out of the cell from the rather small GFP protein, cellular and viral proteins need to be fixed in the cell before analysis. Then, the flow cytometric measurement can directly follow.
This procedure describes how infection status of AGE1.CR.pIX suspension cells is determined when infected with MVAegfp, a recombinant MVA strain with an egfp gene insertion in deletion III (construction by G. Sutter, LMU München). However, with small adaptations it should be transferable to other recombinant strains with a fluorophor as

marker protein and other cells than AGE1.CR.pIX.

2. Materials

- Cells in suspension
- ViCellXR for cell counting
- Reaction tubes (2,2 mL)
- Centrifuge with swing-out rotor for small tubes
- 1x trypsin solution (stored in N1.06 4 °C, prepared as described in worksheet V/02.1)
- Fetal calf serum or culture medium
- Vortex
- Micropipettes (100 µL, 1000 µL), disposable tips, non-sterile
- Non-sterile phosphate buffered saline, (PBS, produced as described in SOP M/01)
- Paraformaldehyde solution (2 %), **caution: harmful!**
- Flow cytometer tubes (Sarstedt, Nr. 55.1578, 5 mL, PP)
- Flow cytometer with 488 nm laser and a fluorescence channel of 505-545 nm (e.g. Epics XL from BeckmanCoulter)
- Software to evaluate flow cytometer data (Expo32 software from BeckmanCoulter or FlowJo software)

3. Method

3.1 Sample preparation and staining procedure

Count cells from infected or non-infected cell culture with the ViCellXR device. Pipet the volume needed for $1.0x10^6$ cells in a 2.2 mL reaction tube. Calculate the required volume of cell suspension based on total cell concentration and slightly round up the volume. Add an equal volume of 2 % paraformaldehyde solution to the sample. Mix gently and store at 4 °C (best is to place them lying) for at least 1 h, but 24 h in maximum. This offers the opportunity to measure samples from two days together. Make sure not to store them longer than 24 h as then the EGFP intensity drops and results might be falsified.

After the incubation time centrifuge the samples at 500xg for 10 min, re-suspend the cell pellet in PBS (500 µL is sufficient) and re-do this washing step. After having washed the cells three times, leave the sample in PBS until measurement at the flow cytometer.

3.2 Measurement & Analysis

Before working with the flow cytometer please read the instruction and (!) ask an experienced person to show you the most important things.

Start and purge the cytometer as described in the instruction (N0.11). For measuring AGE1.CR or AGE1.CR.pIX cells, open the protocol “MVAegfp.pro” which is saved in the account “admin”. Transfer the samples into cytometer tubes. Don’t use a filter cap

to remove aggregates unless it is not avoidable. If large aggregates are present, better add trypsin to the sample before incubation. Put each tube into the cytometer sample device - measurement will start automatically and all necessary plots also appear automatically. Each measurement should be documented appropriately with the protocol used and the Lmd-file that was generated. Measure all samples, purge and shut down the cytometer as described in the instruction.

For analysis, best use the FlowJo software. First, set a “monomeres” or “single cells” gate to exclude aggregates from analysis. This can be done e.g. by plotting the AUX signal vs FS signal. An examplary histogram can be seen in the SOP A/03 about cell cycle measurement via propidium staining and flow cytometric analysis.

The EGFP intensity is followed in the FL1 channel (green fluorescence). Adjust the gates for “uninfected” and “infected” cells using a mock-infected sample or a sample taken at 0 h post infection. At this time point, no EGFP signal is visible. For one experiment, gates should be set to the same parameters for all samples. Typical plots could look like the examples in Figure 2.

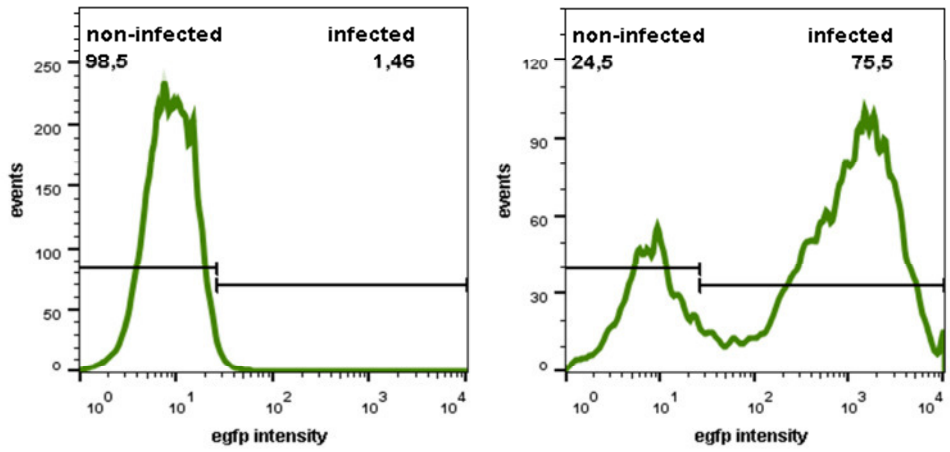

Figure 2: EGFP intensity histogram derived from measurement of a AGE1.CR.pIX cell culture infected with MVAegfp and measured 0 h post infection (left) and 72 h post infection (right). Analysis was done using FlowJo software (version 10).

4.1.1 Points to consider

At late time points after infection, it might be that a considerable amount of infected cells is already damaged. During fixation and washing steps, these cells might lyse. This might result in a decrease in percentage of infected cells.

A.10 Long-term passaging of CR and CR.pIX cells in AEM

Long-term monitoring of viable cell concentrations (left graph) and viabilities (right graph) during passaging of cells in AEM. Passages 34–45 are shown for CR cells (black), passages 34–70 are shown for CR.pIX cells (red). Passaging was always done twice a week, thus after 3 days and after 4 days for every subsequent passage so that values are alternately slightly higher and lower.

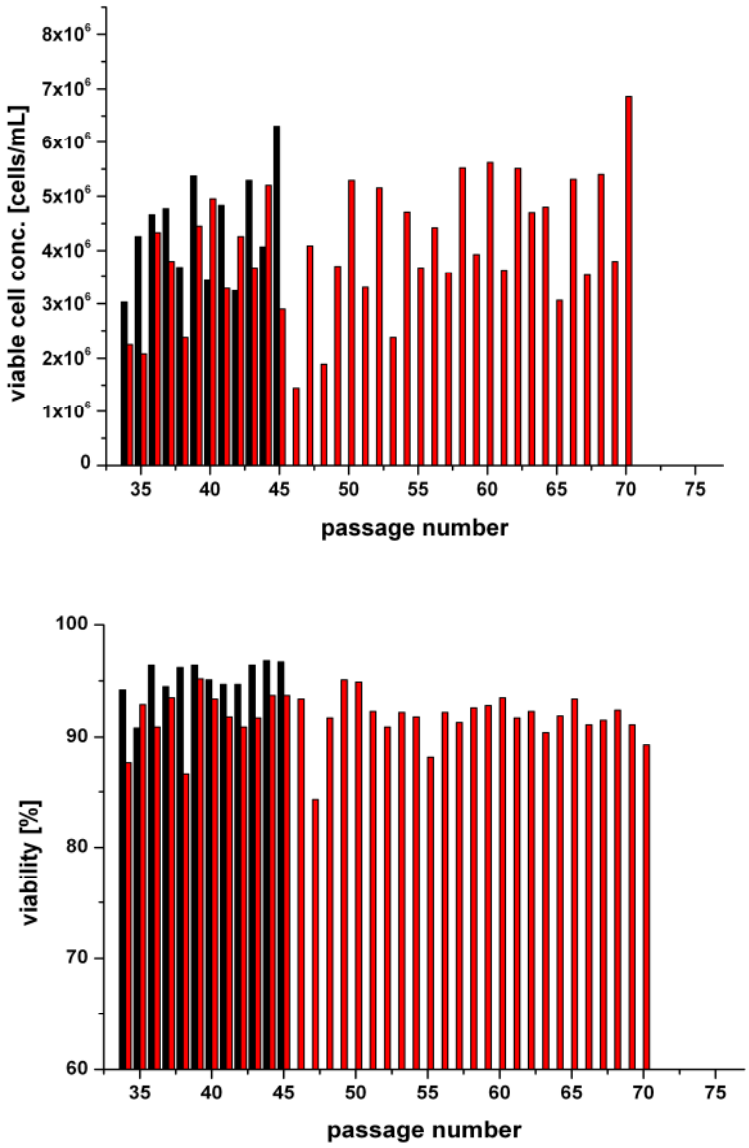

Graph adapted from:
Mahr S. Produktion attenuierter Influenzaviren in AGE1.CR-Zellen [Bachelor thesis]. Villingen-Schwenningen: Hochschule Furtwangen; 2010.

A.11 Long-term passaging of CR and CR.pIX cells in CD-U2 medium

Long-term monitoring of viable cell concentrations (left graph) and viabilities (right graph) during passaging of cells in CD-U2. Passages 34–76 are shown for CR cells (black), passages 34–77 are shown for CR.pIX cells (red). Passaging was always done twice a week, thus after 3 days and after 4 days for every subsequent passage so that values are alternately slightly higher and lower.

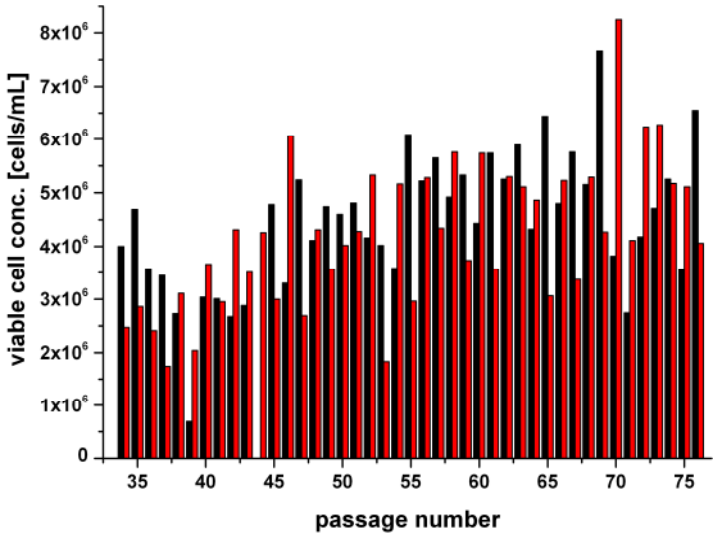

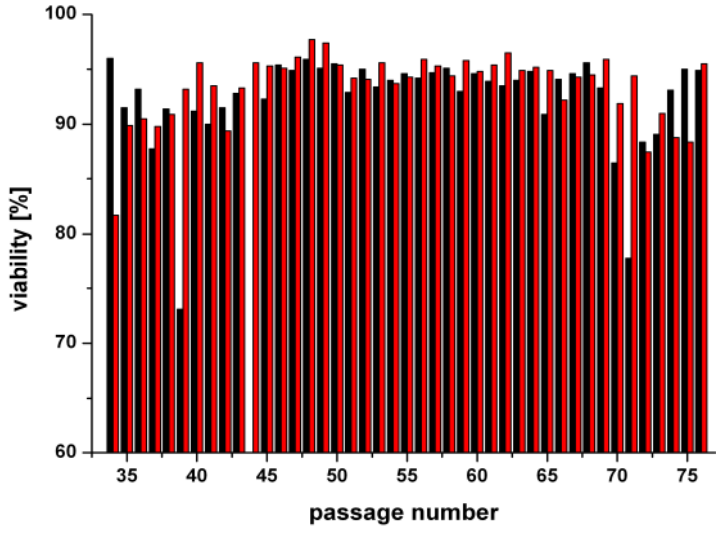

Graph adapted from:
Mahr S. Produktion attenuierter Influenzaviren in AGE1.CR-Zellen [Bachelor thesis]. Villingen-Schwenningen: Hochschule Furtwangen; 2010.

A.12 Calculated flux ranges and fluxes determined by Metabolic Flux Analysis

Calculated rate ranges (scenario 1; by FVA) or rates (scenario 2; by MFA) for CR.pIX cells cultured in stirred tank reactors. Values in italics indicate fluxes that have been measured. All fluxes are given in [µmol/gDW/h].

Reaction	Scenario 1	Scenario 2	Reaction	Scenario 1	Scenario 2
	Uptake rates			**Amino acid catabolism**	
r1	*200.42-222.05*	*211.24*	r47	-22.56-23.25	-3.16
r2	*29.39-30.96*	*30.18*	r48	-8.39-(-8.10)	-8.26
r3	54.43-450.10	230.41	r49	-47.13-(-36.73)	-41.25
r4	*0.00-0.10*	*0.00*	r50	5.58-22.62	19.03
r5	*0.33-2.43*	*1.42*	r51	0.00-0.77	0.09
r6	*0.00-0.00*	*0.00*	r52	0.00-8.77	4.70
r7	*14.52-20.99*	*18.12*	r53	0.00-6.50	2.63
r8	*7.16-12.74*	*7.22*	r54	0.00-0.54	0.62
r9	*8.58-25.56*	*21.99*	r55	1.31-5.21	3.35
r10	0.00-0.00	0.00	r56	0.00-1.97	0.58
r11	*0.00-9.53*	*5.08*	r57	-1.43-(-1.30)	-1.41
r12	*1.96-2.72*	*2.06*	r58	0.00-3.73	1.32
r13	*1.86-10.63*	*6.57*	r59	0.00-0.39	0.01
r14	*4.69-11.19*	*7.35*	r60	0.00-5.67	2.90
r15	*5.22-5.76*	*5.88*	r61	0.00-3.63	0.49
r16	*1.48-7.15*	*4.39*	r62	-17.98-7.62	-2.81
r17	*2.19-6.10*	*4.25*	r63	0.00-3.91	2.04
r18	*1.56-3.53*	*2.15*	r64	-13.80-37.46	30.95
r19	*0.00-0.10*	*0.00*	r65	0.00-5.58	0.01
r20	*0.00-16.66*	*10.59*		**MTHF & uric acid synthesis**	
r21	*1.56-5.29*	*2.90*	r66	3.74-8.70	6.03
r22	*1.31-1.70*	*1.33*	r67	0.40-5.17	2.94
r23	*0.00-3.62*	*1.89*	r68	0.00-0.00	0.00
	Glycolysis			**Lipid synthesis**	
r24	200.42-222.05	211.24	r69	0.31-0.32	0.31
r25	176.32-198.49	187.51	r70	1.14-1.16	1.14
r26	176.32-198.49	187.51	r71	0.43-0.44	0.43
r27	176.32-198.49	187.51	r72	0.043-0.044	0.043
r28	176.32-198.49	187.51	r73	0.021-0.022	0.022
r29	350.66-395.04	373.07	r74	0.156-0.160	0.157
r30	350.66-395.04	373.07	r75	0.140-0.143	0.141

r31	350.66-395.04	373.07
r32	288.82-306.39	297.61
r33	53.08-150.33	102.04
Pentose phosphate pathway		
r34	2.13-2.18	2.15
TCA cycle		
r35	-41.91-(33.71)	-40.28
r36	-41.91-(-33.71)	-40.28
r37	0.00-3.63	0.49
r38	60.67-176.63	115.90
r39	-1845.84-159.43	84.95
r40	18.15-156.79	79.70
r41	16.82-137.13	68.75
r42	18.15-156.79	79.70
r43	18.76-142.93	75.62
Anaplerosis		
r44	1.57-5.20	2.07
r45	14.72-2036.34	35.03
r46	0.00-1996.42	0.00
r76	0.046-0.047	0.046
Release rates		
r77	0.00-1996.42	965.79
r78	*288.82-306.39*	*297.61*
r79	*26.73-36.50*	*30.81*
r80	*0.00-0.00*	*0.00*
r81	0.00-5.58	0.01
r82	*11.70-13.56*	*12.60*
r83	140.29-492.32	300.87
r84	*0.00-0.00*	*0.00*
Transport reactions, oxidative phosphorylation		
r85	-70.43-19.72	-30.19
r86	81.69-2102.95	1087.58
r87	-466.50-(-126.43)	-284.04
r88	-41.91-(-33.71)	-40.28
r89	-22.56-23.25	-3.16
r90	14.01-113.28	65.69
r91	-47.13-(-1.59)	-27.24
r92	-25.12-18.83	1.84
r93	9.08-91.19	45.94
r94	-2055.10-(-2.61)	-31.87
r95	40.77-341.05	177.25
r96	62.66-68.51	65.51
Biomass synthesis		
r97	0.0131-0.0134	0.0132

A.13 Validation $TCID_{50}$ MVA

Virus material: Seed virus MVAwt from infection of CR.pIX cells in a shaker flask (AEM/MegaVir medium), harvested 50 hpi

Inter-assay variation:
Titration by operator A, n=6, independent assay batches (i.e. different Vero cell culture, fresh staining solution each time)

titration no.	determined virus titer [viruses/mL]
1	$1.8x10^7$
2	$7.5x10^7$
3	$1.0x10^7$
4	$3.2x10^7$
5	$7.5x10^7$
6	$1.3x10^7$
average and standard deviation [viruses/mL]	$3.7 \pm 3.0x10^7$

Inter-operator variation:
Titration by operator A, B and C, n=3 each, one assay batch (i.e. same Vero cell pre-culture, same fresh staining solution), but independent handling and counting

	operator A	operator B	operator C	overall
titration no.	determined virus titer [viruses/mL]	determined virus titer [viruses/mL]	determined virus titer [viruses/mL]	
1	$1.0x10^7$	$0.75x10^7$	$0.42x10^7$	
2	$1.8x10^7$	$0.56x10^7$	$0.56x10^7$	
3	$1.0x10^7$	$0.75x10^7$	$0.42x10^7$	
average titer and standard deviation [viruses/mL]	$1.27 \pm 0.46x10^7$	$0.69 \pm 0.11x10^7$	$0.47 \pm 0.08x10^7$	$0.81 \pm 0.41x10^7$

With a variance analysis (α=0.05), the parameter “operator” was determined to have a significant effect on the titer measurement.

A.14 Approach to determine influenza virus titers by flow cytometry

To determine virus titers by flow cytometry, MDCK cells were seeded in 24 multiptiter plates (MTPs) and infected in these MTPs with mostly 1:2 dilutions of the virus sample. Shortly after virus addition to the cells, serum is added in order to prevent secondary infections in the cell population. After 18-24 h, cells are harvested into a 96well MTP, fixed, washed, and stained with influenza strain-specific antibody as well as fluorescent-conjugated secondary antibody. Analysis then is done with the flo cytometer resulting in influenza virus positive and negative cells. Virus titers [green fluorescent units/mL] can then be calculated from the gained percentages (see bottom graphic as example).

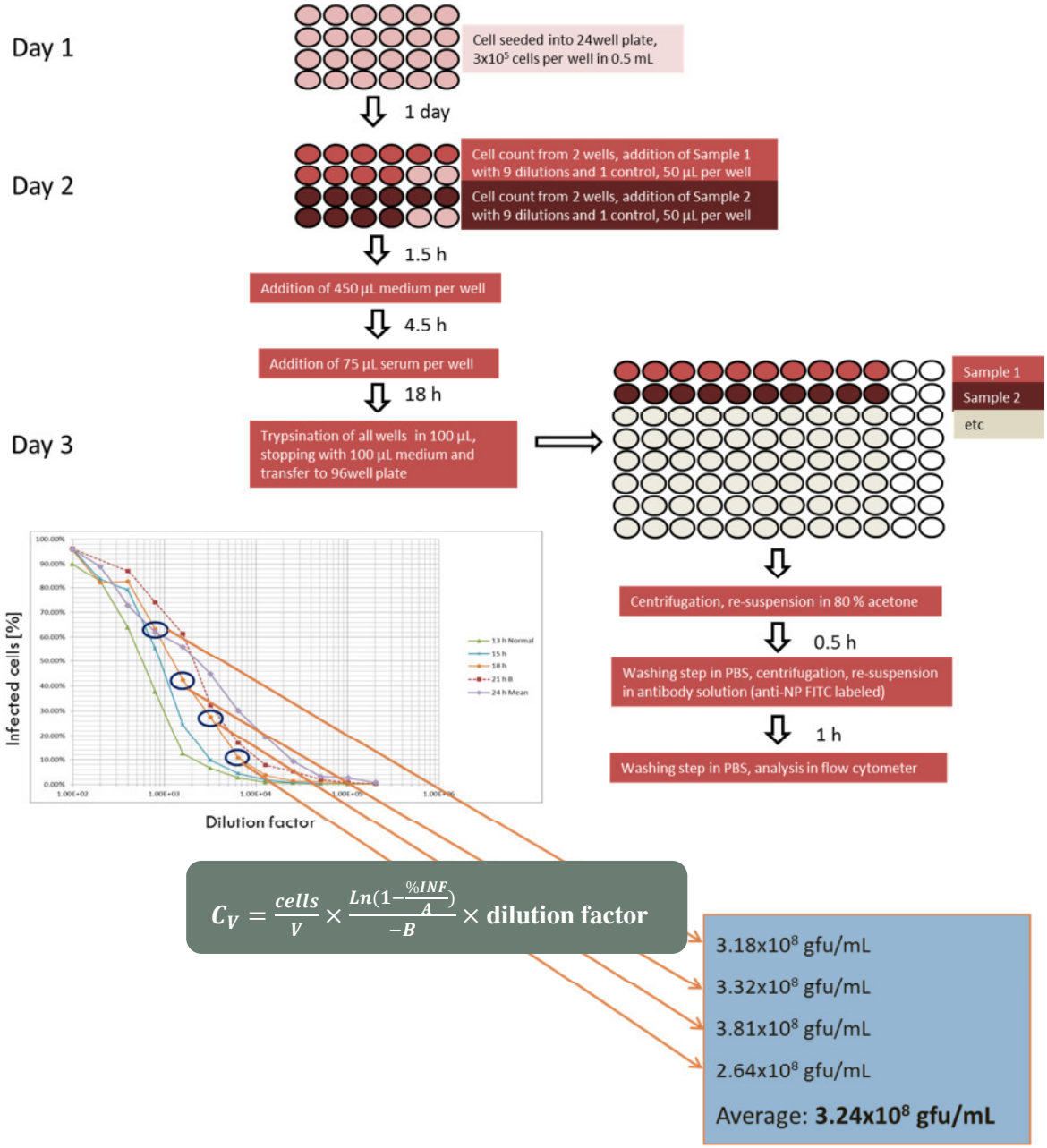

List of own publications

Lohr V*, Hädicke O*, Genzel Y, Jordan I, Klamt S, Reichl U. “The avian cell line AGE1.CR.pIX characterized by metabolic flux analysis”. Revisions submitted to BMC Biotechnology June 2014.

Jordan I, Lohr V, Genzel Y, Reichl U, Sandig V. 2013. “Elements in the development of a production process for Modified Vaccinia Virus Ankara”. Microorganisms 1(1):100-121.

Hädicke O*, Lohr V*, Genzel Y, Reichl U, Klamt S. 2013. “A statistical framework to evaluate the significance of variations in metabolic rates in cell culture processes”. Biotechnology and Bioengineering 110(10):2633-2642.

Lohr V, Genzel Y, Jordan I, Katinger D, Mahr S, Sandig V, Reichl U. 2012. “Live attenuated influenza viruses produced in a suspension process with avian AGE1.CR.pIX cells”. BMC Biotechnology 12:79.

Petiot E, Jacob D, Lanthier S, Lohr V, Ansorge S, Kamen AA. 2011. “Metabolic and kinetic analyses of influenza production in perfusion HEK293 cell culture”. BMC Biotechnology 11:48.

Rödig J, Rapp E, Djeljadini S, Lohr V, Genzel Y, Jordan I, Sandig V, Reichl U. 2011. „Impact of Influenza Virus Adaptation Status on HA N-Glycosylation Patterns in Cell Culture-Based Vaccine Production”. Journal of Carbohydrate Chemistry 30(4-6): 281-290.

Lohr V, Genzel Y, Behrendt I, Scharfenberg K, Reichl U. 2010. “A new MDCK suspension line cultivated in a fully defined medium in stirred-tank and wave bioreactor”. Vaccine 28:6256-6264.

Lohr V, Rath A, Jordan I, Sandig V, Genzel Y, Reichl U. 2009. “Avian designer cells AGE1.CR as candidates for MVA and influenza vaccine production”. In Jenkins N (ed.): Proceedings of the 21st Annual Meeting of the European Society for Animal Cell Technology (ESACT), Dublin, Ireland. Springer Science + Business Media B.V.

Lohr V*, Rath A*, Genzel Y, Jordan I, Sandig V, Reichl U. 2009. “New avian suspension cell lines provide production of influenza virus and MVA in serum-free media: Studies on growth, metabolism and virus propagation”. Vaccine 27: 4975-4982.

*shared first

Talks

Lohr V, Genzel Y, Jordan I, Sandig V, Reichl U. "Metabolism and cell physiology of avian designer cells during MVA production". Talk at the Dechema Jahrestagung der Biotechnologen, Mannheim. September 2009.

Lohr V, Rath A, Jordan I, Sandig V, Genzel Y, Reichl U. "Avian designer cells AGE1.CR: Possible candidates for MVA and influenza vaccine production?". 21st ESACT Meeting, Dublin, June 2009.

Rath A, Lohr V, Genzel Y, Schwarzer J, Sandig V, Jordan I, Reichl U. „Influenza and modified vaccinia virus Ankara (MVA) production in avian designer cells". Talk at the European Bioperspectives, Hannover. October 2008.

Poster

Lohr V, Genzel Y, Katinger D, Jordan I, Sandig V, Reichl U. "Live attenuated influenza virus production in batch high cell density cultivation of suspension AGE1.CR.pIX cells". Poster at the Vaccine Technology IV, Albufeira, Portugal. May 2012.

Lohr V, Hädicke O, Genzel Y, Klamt S, Jordan I, Sandig V, Reichl U. "Comparative metabolic flux analyses of cultivations with novel avian designer cell lines used for vaccine production". Poster at the Cell Culture Engineering XIII, Scottsdale, USA. April 2012.

Lohr V, Blechert AK, Genzel Y, Jordan I, Reichl U. „Charakterisierung von AGE1.CR.pIX Hochzelldichte-kultivierungen zur Produktion von Vacciniaviren". Poster at the GVC/DECHEMA Vortrags- und Diskussionstagung – Biopharmazeutische Produktion, Freiburg, Germany, May 2012.

Lohr V, Blechert AK, Djeljadini S, Genzel Y, Reichl U. "Production of GFP expressing Modified Vaccinia Virus Ankara in Avian Cell cultures: Monitoring Infection and Cell Physiology by Flow Cytometry". 22nd ESACT Meeting, Vienna, May 2011.

Lohr V, Genzel Y, Jordan I, Sandig V, Reichl U. "Characterization of avian designer cells as substrates for MVA production". Poster at the 21st ESACT Meeting, Dublin. June 2009.

Lohr V, Rath A, Genzel Y, Jordan I, Sandig V, Reichl U. "Metabolism of avian designer cells during influenza and MVA production". Poster at the Vaccine Technology II, Albufeira, Portugal. June 2008.

List of supervised projects

Master theses

Vazquez-Ramirez, D. “Development of a flow cytometry-based assay for the quantification of active viral particles”. TU Hamburg-Harburg, 2012.

Blechert, A.-K. „Durchflusszytometrische Untersuchungen zur Replikationsdynamik von MVA in AGE1.CR.pIX-Zellen“. TU Braunschweig, 2011.

Bachelor theses

Mahr, S. „Produktion attenuierter Influenzaviren in AGE1.CR-Zellen“. Hochschule Furtwangen, Villingen-Schwenningen, 2010.

Djeljadini, S. „Durchflusszytometrische Untersuchungen zur Replikationsdynamik von MVA in AGE1.CR-Zellen“. Hochschule Furtwangen, Villingen-Schwenningen, 2010.

Internships/student projects

Díaz Míron, J. E. Z. „Virus quantification via flow cytometry: method development and validation”. Veracruz Institute of Technology, 2012.

Djeljadini, S. "Hochzelldichteeffekt bei der Produktion von Influenzaviren in AGE1.CR Zellen“. Hochschule Furtwangen, Villingen-Schwenningen, 2010.